

Site Characterisation of LNAPL - Contaminated Fractured - Rock Aquifer

by

Modreck Gomo

Student no: 2006113035

A dissertation submitted to meet the requirements for the degree of

Magister Scientiae

at the

Institute for Groundwater Studies

Faculty of Natural- and Agricultural Sciences

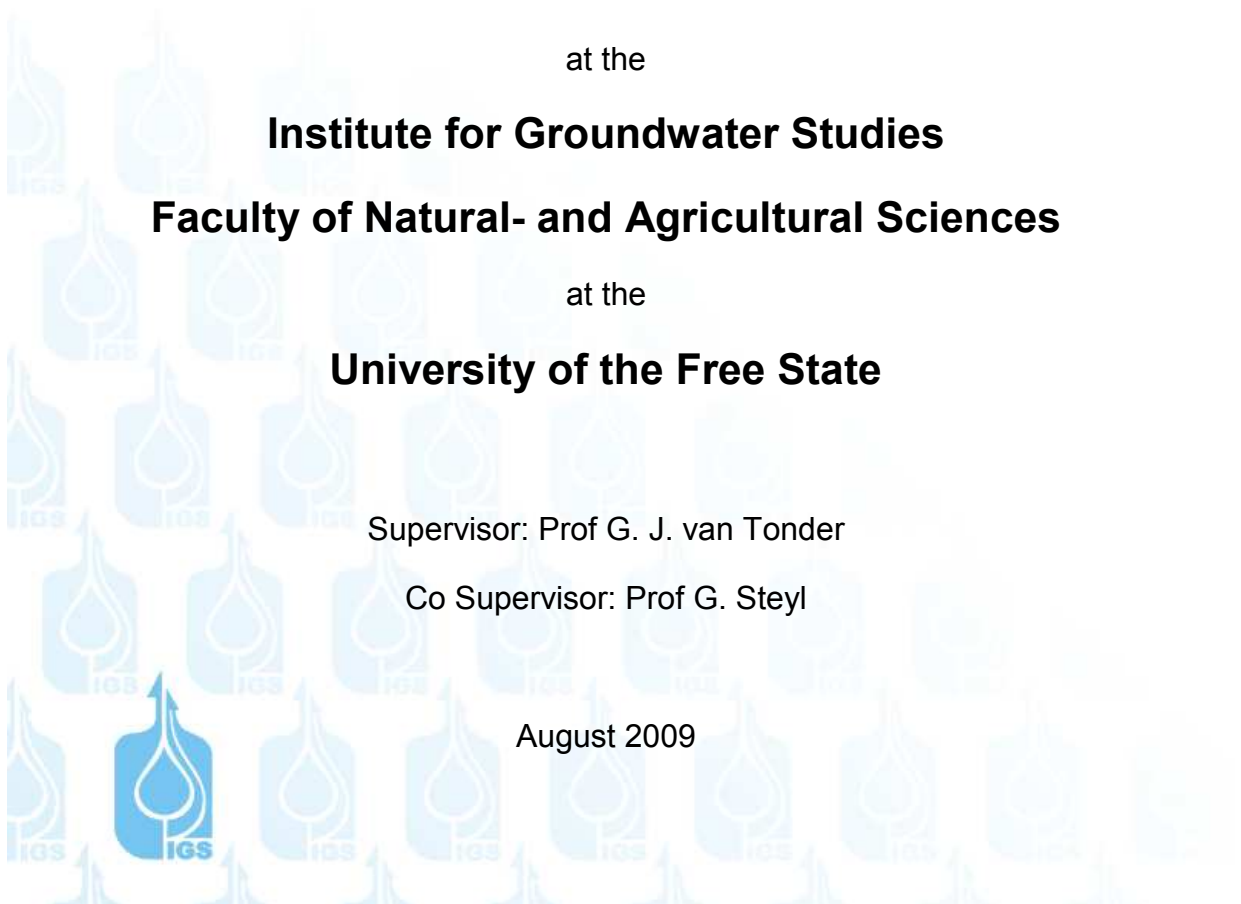
at the

University of the Free State

Supervisor: Prof G. J. van Tonder

Co Supervisor: Prof G. Steyl

August 2009



Declaration

I, Modreck Gomo declare that; this thesis hereby submitted by me for the Master of Science Geohydrology degree in the Faculty of Natural and Agricultural Sciences, Institute of Groundwater Studies at the University of the Free State is my own independent work. The work has not been previously submitted by me or anyone at another university. I furthermore cede the copyright of the thesis in favour of the University of the Free State.

Acknowledgments

I would like to express my sincere thanks to Dr A.P. Jennifer and Dr B.H Usher for all their support and academic guidance. Special thanks also go to my academic supervisor Prof G. J. van Tonder and co - supervisor Dr G. Steyl for their technical and academic guidance. Technical assistance and support in various forms from **all** IGS staff members is greatly appreciated. The study could have been impossible without technical field assistance from Jamie. L. Bothwell, Kevin. H. Vermaak and Stephen. N.T Fonkem. Special acknowledgments are also given to Geo Pollution Cape Technology (GPCT) consulting company in particular Samuel Mörr for permission to use their site and reports.

This thesis emanated from a Water Research Commission (WRC) funded project entitled **“Field investigation to study the fate and transport of light non - aqueous phase liquids (LNAPLs) in groundwater”**. Sincere thanks are given to WRC for financing this project.

Special mention also goes to my friend Ntomboxolo Louw for her encouragements and support during the study period. Lastly but certainly not least, I thank my family for their prayers and encouragements.

Keywords

Bedding plane fracture

Borehole geophysical characterisation

Chemical characterisation

Contaminated site characterisation

Geohydrological tools

Hydraulic characterisation

Karoo fractured rock aquifer

Light - Non Aqueous Phase Liquids (LNAPLs)

Preferential flow path

Contents

CONTENTS.....	I
FIGURES.....	VI
LIST OF ACRONYMS	XII
CHEMICAL SYMBOLS.....	XIV
LIST OF PARAMETERS AND THEIR UNITS	XV
1 INTRODUCTION.....	1
1.1 BACKGROUND	1
1.2 AIMS AND OBJECTIVES.....	3
1.2.1 <i>Data Collection Strategy</i>	3
1.3 SITE CHARACTERISATION OVERVIEW	4
1.3.1 <i>Contaminated Site Characterisation</i>	4
1.3.2 <i>Phases of Site Characterization</i>	6
1.3.3 <i>Beaufort West Study Area Site Characterisation Summary</i>	7
1.4 THESIS OUTLINE	9
1.5 SUMMARY OF CHAPTER 1	9
2 LNAPL PETROLEUM HYDROCARBON CONTAMINATION	10
2.1 LNAPL PROPERTIES.....	10
2.2 POTENTIAL SOURCES OF LNAPL	13
2.2.1 <i>South African Petroleum Industry</i>	13
2.2.1.1 Petroleum Manufactures.....	13
2.2.1.2 Petroleum Downstream Markets.....	16
2.2.1.2.1 Service Stations and Storage Depots.....	16
2.2.1.3 Transportation of Petroleum Products	18
2.3 LNAPL MIGRATION IN THE SUBSURFACE.....	21
2.3.1 <i>LNAPL Migration in the Vadose Zone</i>	21
2.3.2 <i>LNAPL Migration in the Saturated Porous Media</i>	22
2.3.3 <i>LNAPL Migration in the Fractured Media</i>	23
2.4 SUMMARY OF CHAPTER 2.....	26
3 SITE PRELIMINARY INVESTIGATIONS	27

3.1	SITE DESCRIPTION.....	27
3.1.1	<i>Climate</i>	28
3.1.2	<i>Geology</i>	29
3.1.3	<i>Geohydrology</i>	33
3.1.3.1	Historical Groundwater Data.....	34
3.2	DESKTOP STUDY	36
3.2.1	<i>Site History</i>	37
3.3	SITE SURVEY (WALKOVER).....	37
3.4	INITIAL CONCEPTUAL MODEL	38
3.5	HYDROCENSUS.....	39
3.6	SUMMARY OF CHAPTER 3.....	42
4	GEOLOGIC CHARACTERISATION	43
4.1	CORE DRILLING	44
4.1.1	<i>Core Geological Logs</i>	45
4.1.1.1	MW6 Core Geological Log.....	45
4.1.1.2	MW8 Core Geological Log.....	48
4.1.1.3	Core Logs Correlation	49
4.2	PERCUSSION DRILLING	51
4.2.1	<i>Percussion Geological Logs</i>	52
4.2.1.1	MW5 Percussion Geological Log.....	52
4.2.1.2	MW7 Percussion Geological Log.....	53
4.2.2	<i>Borehole Construction</i>	54
4.3	CORE AND PERCUSSION LOGS COMPARISON	56
4.4	SUMMARY OF CHAPTER 4	60
5	BOREHOLE GEOPHYSICS CHARACTERISATION	62
5.1	ELECTRICAL CONDUCTIVITY (EC) LOGGING.....	62
5.1.1	<i>EC Logging in Contaminated Private Boreholes</i>	63
5.1.2	<i>EC Logging in newly Drilled Boreholes</i>	64
5.1.2.1	EC Logging in MW5 and MW6 Boreholes.....	64
5.1.2.2	EC Logging in MW7 and MW8 Boreholes.....	65
5.2	COMBINED BOREHOLE GEOPHYSICS	66
5.2.1	<i>Brief Description of the used Boreholes Geophysics Tools</i>	66
5.2.2	<i>MW6 Logging</i>	67

5.2.2.1	Bedding Plane Fracture Feature between 18.5 - 19 mbgl	68
5.2.2.2	Fracture Feature in Sandstone Formation at 31.5 mbgl	70
5.2.3	<i>MW7 Logging</i>	71
5.2.3.1	Horizontal Bedding Plane Fracture Feature at 24.5 mbgl.....	71
5.2.3.2	Horizontal Bedding Plane Fracture Feature at 33 - 34 mbgl.....	73
5.2.4	<i>MW8 Logging</i>	74
5.2.4.1	Horizontal Bedding Plane Fracture Feature at 24.5 mbgl.....	74
5.3	SUMMARY OF CHAPTER 5.....	76
6	HYDRAULIC CHARACTERISATION.....	77
6.1	CHALLENGES FACED DURING AQUIFER TESTING	77
6.2	AQUIFER TEST BOREHOLE SELECTION	80
6.3	SLUG TESTS.....	81
6.4	PUMP TEST	83
6.4.1	<i>Pump Test 1</i>	83
6.4.2	<i>Pump Test 2</i>	87
6.4.3	<i>Pump Test 3</i>	88
6.5	TRACER TESTS.....	89
6.5.1	<i>Tracer Injection Test</i>	90
6.5.2	<i>Point Dilution Test</i>	91
6.5.3	<i>Radial Convergent Tests</i>	94
6.5.3.1	Radial Convergent Test 1	94
6.5.3.1.1	Tracer Decay Measurements in PW5 Injection Borehole	95
6.5.3.1.2	Tracer Breakthrough Measurements in PW2 Observation Borehole	98
6.5.3.1.3	Tracer Breakthrough Measurements in RW2 Abstraction Borehole	98
6.5.3.2	Radial Convergent Test 2	100
6.5.3.2.1	Tracer Decay Measurements in MW7 Injection Borehole	102
6.5.3.2.2	Tracer Breakthrough Measurements in MW8 Abstraction Borehole.....	104
6.5.3.2.2.1	EC Tracer Breakthrough Measurements in MW8 Abstraction Borehole.....	104
6.5.3.2.2.2	Bromide Tracer Breakthrough Measurements in MW8 Abstraction Borehole.....	105
6.5.3.2.2.3	Comparison between EC and Bromide Tracer Breakthrough.....	107
6.6	SUMMARY OF CHAPTER 6.....	108

7	CHEMICAL CHARACTERISATION.....	109
7.1	SAMPLING	109
7.2	SAMPLE ANALYSIS	111
7.2.1	<i>Organic Chemistry</i>	<i>112</i>
7.2.1.1	Distribution of LNAPL Contaminants at the Study Area	112
7.2.1.2	Evidence of LNAPL Biodegradation at the Study Area.....	117
7.2.1.3	Soil Vapor Surveys	122
7.2.1.4	Site Laboratory (Lab) Kit.....	123
7.2.1.4.1	Site Laboratory Analysis for Hydrocensus Boreholes	124
7.2.1.4.2	Correlation between Site and Reference Laboratory results	126
7.2.2	<i>Inorganic Chemistry</i>	<i>129</i>
7.3	SUMMARY OF CHAPTER 7	133
8	SITE CONCEPTUAL MODEL	135
8.1	GEOLOGICAL COMPONENT	135
8.2	HYDRAULIC PARAMETERS	136
8.2.1	<i>Groundwater Levels.....</i>	<i>136</i>
8.2.2	<i>Recharge</i>	<i>137</i>
8.2.3	<i>Aquifer and Transport Parameters</i>	<i>138</i>
8.3	LNAPL MIGRATION AND DISTRIBUTION	138
8.4	SUMMARY OF CHAPTER 8	140
9	CONCLUSIONS AND RECOMMENDATIONS.....	141
9.1	CONCLUSIONS	141
9.1.1	<i>Findings about the Study Area</i>	<i>141</i>
9.1.2	<i>Conclusions for Site Characterisation of LNAPL - Contaminated Fractured - Rock Aquifers</i>	<i>142</i>
9.2	RECOMMENDATIONS	143
9.2.1	<i>Basic steps to follow after site characterisation</i>	<i>144</i>
9.2.2	<i>Recommended Remedial Options.....</i>	<i>145</i>
9.2.3	<i>Challenges encountered with Site Characterisation Tools.....</i>	<i>145</i>
10	REFERENCES	147
11	APPENDICES.....	154

APPENDIX 1 GEOHYDROLOGICAL INFORMATION OBTAINED FROM THE HYDROCENSUS CARRIED OUT IN THE BEAUFORT WEST STUDY AREA.	154
APPENDIX 2 BOREHOLE GEOPHYSICS LOGS.....	155
<i>MW6 Logging</i>	155
Acoustic Viewer (AV).....	155
Full Wave Sonic (FWS)	157
Conventional Logging (Gamma, Resistivity and Spontaneous Potential)	158
<i>MW7 Logging</i>	160
Acoustic Viewer (AV).....	160
Full Wave Sonic (FWS)	162
<i>Conventional Logging (Gamma, Resistivity and Spontaneous Potential)</i>	163
<i>MW8 Logging</i>	165
Acoustic Viewer (AV).....	165
Full Wave Sonic (FWS)	167
APPENDIX 3 SLUG TEST PROCEDURE	168
APPENDIX 4 POINT DILUTION TRACER TEST PROCEDURE	169
APPENDIX 5 RADIAL CONVERGENCE TRACER TEST PROCEDURE.....	170
APPENDIX 6 EC PROFILES FOR RW1, RW2, PW2 AND PW5 BOREHOLES.....	172
APPENDIX 7 RECHARGE ESTIMATION	173
ABSTRACT	174
OPSOMMING	175

Figures

Figure 1-1 Location of the study area in Beaufort West (Western Cape Province of South Africa).	1
Figure 2-1 Location of major petroleum production and refinery facilities in South Africa (Taken from <i>google maps</i> , 2009).	14
Figure 2-2 Capacities of the South African fuel production and refinery facilities from 1992 - 2005.	15
Figure 2-3 Typical petroleum UST installed at the study area's service stations (Taken during the fieldwork).	18
Figure 2-4 Example of a leaking petroleum pipeline (Taken from <i>pacificenvironment</i> , 2009)..	19
Figure 2-5 Overturned petrol tanker on fire (Taken from <i>sabcnews</i> , 2003).	20
Figure 2-6 LNAPL phases in the unsaturated zone (Taken from Huling and Weaver, 1991)...22	
Figure 2-7 Simple conceptual model of LNAPL migration in the subsurface (Adapted from Mercer and Cohen, 1990).	23
Figure 2-8 Conceptualised LNAPL movement in a typical Karoo fractured aquifer.	25
Figure 3-1 Location of the potential LNAPL sources, contaminated and uncontaminated boreholes at the Beaufort West study area (Western Cape Province of South Africa).	27
Figure 3-2 Average temperature and rainfall distribution for Beaufort West.	28
Figure 3-3 Examples of bedrock vertical fractures and horizontal bedding planes (Taken from <i>earthscienceworld</i> , 2009)	29
Figure 3-4 Rose joints from field data collected within 30 km of Beaufort West (Taken from Campbell, 1980).	30
Figure 3-5 Sandstone boulders from core drillings on the study area (Taken during the field work).	31
Figure 3-6 Simplified geological map of South Africa (Taken from <i>geoscience</i> , 2009).	32
Figure 3-7 River sand deposits from 0 - 3 mbgl on the study area (Taken during the field work).	33
Figure 3-8 Monitored water levels in the Beaufort West study area (Taken from Nabee, 2007).	35
Figure 3-9 Location of potential LNAPL sources and boreholes with monitored water levels (2002 - 2007) at the Beaufort West study area.	35
Figure 3-10 Initial conceptualised LNAPL contaminant migration at the study area (Taken from Van Biljon and Hassan, 2003).	39

Figure 3-11 Location of the existing and hydrocensus boreholes on the Beaufort West study area.....	40
Figure 3-12 Groundwater use activities in the Beaufort West study area.	41
Figure 4-1 Location of newly drilled boreholes in relation to the contaminated boreholes and potential LNAPL sources on the Beaufort West study area.....	43
Figure 4-2 Core drilling equipment used at the Beaufort West study area (Taken during the field work).....	44
Figure 4-3 MW6 core geological log and EC log.....	46
Figure 4-4 Fractured sandstone between 9 - 10 mbgl in MW6 core borehole (Taken during the field work).....	47
Figure 4-5 Fractured sandstone at 31.5 mbgl in MW6 core borehole (Taken during the field work).....	47
Figure 4-6 MW8 core geological log and EC log.....	48
Figure 4-7 Subvertical fracture intersected at 8.9 mbgl in MW8 core borehole (Taken during the field work).....	49
Figure 4-8 Vertical fracture intersected from 10.7 - 11.5 mbgl in MW8 core borehole (Taken during field work).....	49
Figure 4-9 Core geological log correlation between MW6 and MW8 core boreholes.	50
Figure 4-10 Air rotary percussion drilling equipment used at the study area (Taken during the field work).....	51
Figure 4-11 MW5 geological log and EC log.....	52
Figure 4-12 MW7 geological log and EC log.....	53
Figure 4-13 MW5 and MW7 borehole construction schematic.	55
Figure 4-14 Steel metal casing and locking cap placed on MW5 borehole (Taken during the field work).....	56
Figure 4-15 Geological log correlations between MW6 (Core) and MW5 (Percussion) boreholes.	57
Figure 4-16 Geological log correlations between MW8 (Core) and MW7 (Percussion) boreholes.	58
Figure 4-17 Typical drilling cuttings from the Beaufort West study area (Taken during the field work).....	59
Figure 5-1 EC profile in PW2 and PW5 private boreholes.	63
Figure 5-2 EC profiling in MW5 (Percussion) and MW6 (Core) boreholes.	64
Figure 5-3 EC profiling in MW7 and MW8 boreholes and MW8 core geological log.....	65

Figure 5-4 Gamma, Resistivity and SP logs from 15 - 20 mbgl in MW6 core borehole.	68
Figure 5-5 AV and FWS images from 15 - 20 mbgl in MW6 core borehole.	69
Figure 5-6 FWS and conventional logs from 28 - 33 mbgl in MW5 borehole.	70
Figure 5-7 FWS and AV images from 20 - 25 mbgl in MW7 borehole.	71
Figure 5-8 Gamma, Resistivity and SP logs from 20 -25 mbgl in MW7 borehole.	72
Figure 5-9 AV image from 30 - 35 mbgl in MW7 borehole.	73
Figure 5-10 Gamma, SP and Resistivity logs from 30 -35 mbgl in MW7 borehole.	74
Figure 5-11 AV image between 20 - 25 mbgl in MW8 core borehole.	74
Figure 5-12 FWS image between 20 - 25 mbgl in MW8 core borehole.	75
Figure 6-1 Location of the boreholes used for aquifer testing in the Beaufort West study area.	77
Figure 6-2 Contaminated pumping equipment on PW5 private borehole (Taken during the fieldwork).	78
Figure 6-3 Recovering water level during slug test in RW1 (Instead of receding).	79
Figure 6-4 Taking out a pump from PW5 borehole prior to the aquifer tests (Taken during the field work).	80
Figure 6-5 Location of boreholes used for pump test 1 in the Beaufort West study area.	84
Figure 6-6 Late time Cooper Jacob fit on RW1 pumping well drawdown.	85
Figure 6-7 Water level rise during recovery against t^* in RW1 borehole.	85
Figure 6-8 Location of the boreholes used for pump test 2 and 3 in the Beaufort West study area.	87
Figure 6-9 Late time Cooper Jacob fit on MW8 pumping borehole drawdown.	88
Figure 6-10 Location of the boreholes used for tracer testing in the Beaufort West study area.	89
Figure 6-11 EC tracer breakthrough measurements in pumping RW2 borehole.	90
Figure 6-12 Set up of point dilution tracer test equipment on PW5 private borehole.	91
Figure 6-13 EC measurements for point dilution tracer test in PW5 borehole.	92
Figure 6-14 Standardized EC concentration for point dilution tracer test in PW5 borehole.	93
Figure 6-15 EC measurements for radial convergent tracer test in PW5 injection borehole. ...	96
Figure 6-16 Standardized EC concentration for radial convergent tracer test in PW5 borehole.	96
Figure 6-17 EC tracer breakthrough measurements in PW2 observation borehole.	98

Figure 6-18 Small flow through cell used for EC measurement at abstraction boreholes during radial convergent tracer tests at the Beaufort West study area (Taken during the field work).....	99
Figure 6-19 EC tracer breakthrough measurements in abstraction borehole RW2.....	100
Figure 6-20 Schematic equipment set up for radial convergent test 2 between MW7 and MW8 boreholes.	102
Figure 6-21 EC measurements for radial convergent tracer test in MW7 injection borehole.	102
Figure 6-22 Standardized EC concentration for radial convergent tracer test in MW7 injection borehole.....	103
Figure 6-23 EC tracer breakthrough measurements in MW8 observation borehole.	104
Figure 6-24 Bromide tracer breakthrough measurements in MW8 abstraction borehole.....	105
Figure 6-25 Best fit between the model and measured bromide tracer breakthrough concentration in MW8 abstraction borehole.....	106
Figure 6-26 Comparison between EC and bromide tracer breakthrough measurements in MW 8 abstraction borehole.....	107
Figure 7-1 Location of sampled boreholes on the Beaufort West study area in relation to the potential LNAPL sources.....	110
Figure 7-2 Specific steel sampling bailer used for sampling in RW1, RW2, PW5 and PW2 boreholes (Taken during the field work).....	111
Figure 7-3 Percentage proportions of LNAPLs detected in contaminated boreholes at the Beaufort West study area.....	113
Figure 7-4: BTEX concentration in LNAPL contaminated boreholes.	115
Figure 7-5 Inferred groundwater flow direction under assumed natural conditions in the Beaufort West study area.....	116
Figure 7-6 MTBE, TAME and Naphthalene concentrations in LNAPL contaminated boreholes.	117
Figure 7-7 Percentage proportions of Fe (II), Mn, NO ₃ - N and SO ₄ in uncontaminated boreholes.....	118
Figure 7-8 Percentage proportions of Fe (II), Mn, NO ₃ - N and SO ₄ in contaminated boreholes.	120
Figure 7-9 Oxidation Reduction Potential in contaminated and uncontaminated boreholes.	121
Figure 7-10 VOC concentration measured during the drilling of MW5 percussion borehole and geological log for MW5.....	123
Figure 7-11 UVF-3100 Site Lab analytical test kit (Taken from <i>site-lab</i> , 2009).....	124

Figure 7-12 Site Lab TPH and BTEX concentrations detected in hydrocensus boreholes. ...	125
Figure 7-13 Boreholes sampled for assessing the applicability of the Site lab kit.....	126
Figure 7-14 TPH correlation between Site and Reference laboratory concentrations.	127
Figure 7-15 BTEX correlation between Site and Reference laboratory concentrations.	127
Figure 7-16 Piper diagram showing the study area water chemistry.....	129
Figure 7-17 Durov diagram showing the study area water chemistry.....	130
Figure 7-18 Stiff diagrams showing the study area water chemistry.	131
Figure 7-19 Total hardness for the Beaufort West study area groundwater.	133
Figure 8-1 Beaufort West study area geological conceptualization.....	135
Figure 8-2 Correlation between topography and water level on the Beaufort West study area.	136
Figure 8-3 Inferred groundwater flow direction under assumed natural conditions in the Beaufort West study area (This same Figure has been used in section 7.2.1.1 as Figure 7- 5).	137
Figure 8-4 Conceptual model of LNAPL source loading, movement and migration at the Beaufort West study area. Red arrows indicate the downward migration of both free and dissolved LNAPL phases through vertical and subvertical fractures in the vadose and saturated zones. Blue arrows indicate the conceptualised movement of dissolved LNAPL along the bedding plane fractures at sandstone/mudstone and sandstone/shale contact areas.....	140
Figure 0-1 Flow through cell used for tracer injection at the study area (Taken during the field Photos).	169
Figure 0-2 Pumping out injected tracer after the tracer tests (Taken during the field work)...	171

Tables

Table 2-1 Estimated number of fuel service stations in South Africa (2007).	17
Table 2-2 Estimated number of fuel storage depots in South Africa.	17
Table 4-1 Drilling achievements and failures at the Beaufort West study area.	60
Table 6-1 Slug test results.	82
Table 6-2 Aquifer parameters estimated using RPTSOLV from pump test 1.	86
Table 6-3 Aquifer parameters estimated using RPTSOLV from pump test 2.	88
Table 6-4 Darcy velocity estimated from point dilution test 1.	94
Table 6-5 Estimated Darcy velocity under forced gradient from radial convergent tracer test 1.	97
Table 6-6 Mass transport parameter estimates from the TRACER programme (Riemann, 2002).	106
Table 6-7 Estimated mass transport parameters from the tracer tests.	108
Table 7-1 Sampling depths.	110
Table 7-2 Vapor pressure and solubility of selected LNAPL compounds.....	114
Table 7-3 Concentration of Fe (II), Mn, NO ₃ - N and SO ₄ in uncontaminated boreholes.	119
Table 7-4 Concentration of Fe (II), Mn, NO ₃ - N and SO ₄ in contaminated boreholes.....	120

List of acronyms

API	American Petroleum Institute
AV	Acoustic Viewer
BP	British Petroleum
BTEX	Benzene Toluene Ethylbenzene Xylene
COP	Crude Oil Pipeline
DJP	Durban Johannesburg Pipeline
DNAPLs	Dense Non - Aqueous Phase Liquids
DWAF	Department of Water Affairs and Forestry
DWP	Durban Witwatersrand Pipeline
EC	Electrical Conductivity
EDRO	Extended Diesel Range Organics
<i>EIA</i>	Environmental Information Administration
FWS	Full Wave Sonic
GH	Geohydrology
GPT	Geo Pollution Technology
GRO	Gasoline Range Organics
IGS	Institute of Groundwater Studies
Lab	Laboratory
LNAPLs	Light Non - Aqueous Phase Liquids
LPG	Liquefied Petroleum Gas
MCL	Maximum Contamination Level
MNA	Monitored Natural Attenuation

MTBE	Methyl Tert - Butyl Ether
NO₃ - N	Nitrate as nitrogen
ORP	Oxidation Reduction Potential
PID	Photo Ionic Detector
RMSE	Root Mean Square Error
SSTL	Site-Specific Targets Levels
<i>SAFLII</i>	Southern African Legal Information Institute
SATS	South African Transport Services
SAWQG	South African Water Quality Guidelines
SSTL	Site-Specific Targets Levels
SP	Spontaneous Potential
Sr	Residual saturation
TAME	Tertiary Amyl Methyl Ether
TLC	Temperature Level Conductivity
TPH	Total Petroleum Hydrocarbon
US EPA	United States Environmental Protection Agency
USSs	Underground Storage Systems
USTs	Underground Storage Tanks
UVF	Ultraviolet Fluorescence
VOC	Volatile Organic Carbon
WRC	Water Research Commission

Chemical symbols

Br	Bromide
Ca	Calcium
Cl	Chloride
CO₃	Carbonate
Fe (II)	Ferrous iron
HCO₃	Bicarbonate
K	Potassium
Mg	Magnesium
Mn	Manganese
Na	Sodium
N	Nitrogen
NO₃	Nitrates
Si	Silica
SO₄	Sulphates

List of parameters and their units

Abstraction rate	l/s
Capillary pressure	m
Concentration	ppb, $\mu\text{g/l}$ or mg/l
Darcy velocity	m/day
Dispersion	m
Distance	m
Electrical conductivity	mS/m
Elevation	mamsl
Density	kg/m^3
Gamma count	cps
Hydraulic conductivity	m/day
Interfacial tension	J/m^2
Mass	kg
Recharge	%
Petroleum production/refinery capacity	bbl/d
Resistance	ohms
Saturation	%
Seepage velocity	m/day
Solubility	mg/l
Spontaneous potential	mV
Time	min and day
Transmissivity	m^2/day
Total dissolved solids	mg/l
Vapor pressure	mmHg

Viscosity	kg/(ms)
Volatile Organic Carbons	ppm
Water level	mbgl

1 Introduction

1.1 Background

Light Non - Aqueous Phase Liquids (LNAPLs), in particular those that are released from petroleum product accidental spillages and leakages from Underground Storage Systems (USSs) continue to pose a threat of contaminating groundwater. The need for a detailed site characterisation on LNAPL contaminated fractured rock aquifers, with the objective of providing valuable information prior to remediation exercises and improvement of knowledge was the core motivation for this study. The study describes the application of various geohydrological tools to characterise an LNAPL contaminated fractured rock aquifer located in Beaufort West (Western Cape Province of South Africa, Figure 1-1). Contaminated site characterisation is an important step towards aquifer remediation planning, designs and implementation. In the case of LNAPL contamination, site characterisation enables evaluating the potential impacts from a contaminant release and development of efficient remedial plans.

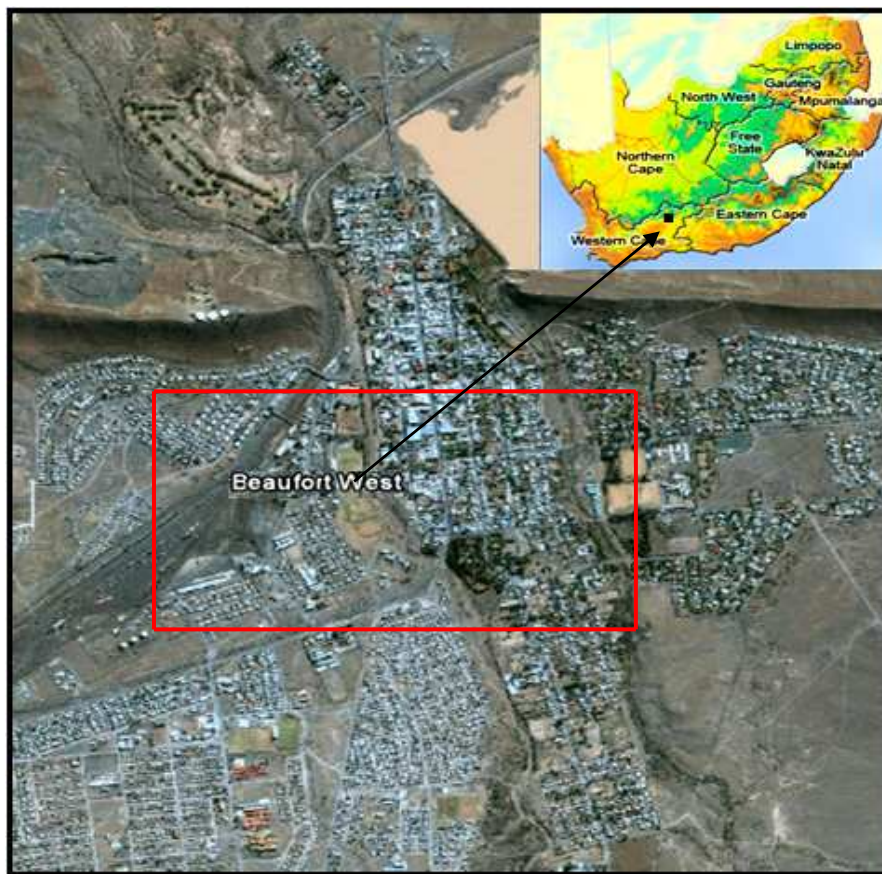


Figure 1-1 Location of the study area in Beaufort West (Western Cape Province of South Africa).

The history of the LNAPL contamination at the Beaufort West study area (see the enclosed area, Figure 1-1) dates back to the early 1980's accidental spills and leakages. These accidental spills and leakages are believed to have been released by an Underground Storage Tank (UST), which is located at a retail service station (Van Biljon, 2002). Initial site investigations by the Geo Pollution Technology Cape (GPT) consulting company were prompted when some private borehole owners reported pumping free phase petroleum product of diesel and petrol. Diesel and petrol free phase product were also detected and collected during the field investigations. Some of the private boreholes are contaminated with both free and dissolved phase of the petroleum products and the local population has been adversely affected (this was observed by the author). For instance, 6 m of free phase petrol product was detected on top of water in private borehole PW12 rendering the borehole polluted as the water is no longer suitable for its intended purpose (vegetable gardening). The need for a social scientist to give proper counseling to the affected people cannot be overemphasized and was recommended after the hydrocensus exercise.

Field investigations were designed to define and determine properties of fractured preferential flow paths responsible for the LNAPL transportation in a typical Karoo fractured rock aquifer. During the field tests, geohydrological tools were utilized so as to compliment one another, thus the use of the term site characterisation complementary tools. Drilling explorations and borehole geophysics were valuable for geological subsurface investigations, in particular the location of fractures which are often associated with high hydraulic conductive flow zones. Aquifer tests to determine the hydraulic and mass transport parameters for the preferential flow paths were of paramount importance, considering the influence of the parameters on the movement and fate of LNAPLs. Groundwater sampling was performed on both private and newly drilled boreholes for organic and inorganic contaminants, this was important in order to determine the distribution of LNAPL on the study area.

The application of complementary geohydrological tools for characterising an LNAPL contaminated fractured rock aquifer has great potential to optimize site understanding. The Beaufort West study area is characterised by a stressed aquifer system as a result of abstractions on municipal and private boreholes. In this stressed groundwater system, pumping effects are mobilizing the LNAPLs and further accelerating contaminant migration.

Some of the findings of this MSc thesis are built on the assumption that the four identified potential LNAPL sources are the only ones contributing to groundwater contamination in the Beaufort West study area.

1.2 Aims and Objectives

The study aims to characterise an LNAPL contaminated fractured rock aquifer through the use of existing geohydrological field and laboratory techniques. To achieve this aim, the following specific objectives were performed:

- Desktop study covering contamination history, local and regional hydrogeology.
- Site survey (Walkover and Visual inspection).
- Hydrocensus in the vicinity of potential LNAPL sources.
- Geological characterisation.
- Borehole geophysics characterisation.
- Hydraulic characterisation.
- Chemical characterisation.

1.2.1 Data Collection Strategy

In this thesis, the following work was outsourced (work which was not performed individually by the MSc student):

Site survey

- Dr A.P. Jennifer, Dr B.H. Usher, Modreck Gomo [Water Research Commission (WRC) LNAPL project] and Samuel Mörr [Geo Pollution Technology (GPT)].

Hydrocensus

- Personnel hired by the WRC LNAPL project.

Geological characterisation

- Drilling - Willir Drilling Company
- Geological logging - Modreck Gomo (WRC LNAPL project) and Jamie. L. Bothwell (WRC Bulk flow project).

Borehole geophysics characterisation

- Borehole geophysics logging - Personnel and equipment hired from Department of Water Affairs and Forestry (DWAF).

Hydraulic characterisation

- Slug testing - Modreck Gomo and Kevin. H. Vermaak (WRC LNAPL project).
- Pump testing - Modreck Gomo, Kevin. H. Vermaak (WRC LNAPL project) and Jamie. L. Bothwell (WRC Bulk flow project).
- Tracer testing - Modreck Gomo and Kevin. H. Vermaak (WRC LNAPL project).

Chemical characterisation

- Inorganic chemistry analysis - Institute of Groundwater Studies (IGS) laboratory.
- Organic chemistry analysis - Eurofins Analytico (Netherlands based laboratory).

1.3 Site Characterisation Overview

Site characterisation is an important facet of geohydrological investigations which is used to develop a site conceptual model. It provides an important understanding for predicting future site behavior. The prediction of future site behavior is based on the observed features and processes governing the groundwater flow and contamination migration at the site. Groundwater site characterization has two major components; assessment of the groundwater flow system and assessment of the contamination in the ground water.

1.3.1 Contaminated Site Characterisation

In the context of groundwater contamination, site characterisation aims to obtain fundamental data which is needed to describe the subsurface flow pathways, distribution of contaminants and fluid flow properties. According to US EPA (1991), during site characterisation emphasis is often placed on the assessment of contamination in the ground water which mainly involves groundwater quality monitoring. US EPA (2001) gives a detailed discussion on the "State - of - the - Practice of Characterisation and Remediation of Contaminated Ground Water at Fractured Rock Sites". Based on site characterisation results, the initial conceptual model is continuously upgraded. This evolving conceptual model should reflect the most likely

distribution of contaminants as well as the hydrogeologic features and transport processes controlling the contaminant distribution.

US EPA (2004) documented guidelines on the “Site Characterisation Technologies for DNAPL Investigations”. The guidelines are intended to help managers at sites with potential or confirmed DNAPL contamination to identify suitable characterisation technologies and screening the technologies for potential application. A Manual for Site Assessment at DNAPL contaminated sites in South Africa was also developed to provide guidance for site owners and investigators on the available technologies and cost - effective assessment methodologies (Gebrekristos *et al*, 2007). The manual discuss in detail tools and approaches for locating and characterizing DNAPL contamination in the South African geohydrological setting. It is upon such a background on site characterisation technologies that there was need to investigate and assess the applicability of various geohydrological tools to characterise an LNAPL contaminated fractured rock aquifer located in Beaufort West.

It is important to highlight that the level and details of a site characterisation exercise is largely dependent on the characterisation objectives, available technologies and practical economic constrains. In other words, there are no specific procedures or steps which can be recommended because it is site specific and depended on various factors. The site characterisation tools and technologies utilized differ from one site to the other. Despite the main objective of contaminated site characterisation being to collect data for site remediation designs, planning and subsequently implementation, what prompt site investigations is usually different.

Take for instance in this study, investigations at the Beaufort West site was only prompted when free phase petroleum products on top of water were detected in some private boreholes. This current study is different from other investigations which are started because a potential contamination source exists, even before affecting the receptors. A good example for the second scenario is petrol spill from a road transport tanker. Using these two scenarios as an example, the approach of site characterisation in terms of goals, steps, tools and technologies is going to be different. Based on this argument, it is difficult for the author to include any case studies in which the current site characterisation steps and tools have been applied. In this study site characterisation was conducted in the following phases.

1.3.2 Phases of Site Characterization

Phase 1 involves a review of site the history, contaminant properties, and local/regional studies. This review should include the following aspects (API, 1989):

- Information on storage, transportation, use, monitoring, and disposal of LNAPLs at the site.
- Locations, volumes, and timing of any known LNAPL releases.
- Locations of underground piping, structures and utilities which might influence the LNAPL flow.
- Regional or local geologic and hydrogeologic studies, soil surveys, climatic data, and pertinent maps or historic photographs of the site.
- Preliminary information available from the literature concerning pertinent contaminant transport and fate parameters for the site - specific contaminants.

A site **survey (Walkover and Visual inspection)** is then carried out as part of phase 1 to verify and confirm data collected during the desktop study and review of the site history. An initial conceptual model for groundwater flow, contaminant transportation and fate in the subsurface is then developed based on this information. The initial conceptual model, despite being at times flawed, provides a basis for field investigations (phase 2). The conceptual model can be confirmed or rejected and or improved as detailed information is unveiled during the investigation.

Phase 2 involves detailed field investigations, this can include drillings, borehole geophysics, sampling for water quality analyses and aquifer tests depending on the available capacity for the investigation. The closure of phase 2 is a conceptual model which must reflect the most likely distribution of contaminants as well as the transport pathways and processes controlling LNAPL migration and distribution. This makes it possible to consider both the current and future contaminant impacts under different remediation scenarios (US EPA, 2001).

Site characterization plays an important role in evaluating the potential impacts from a contaminant release and development of efficient remedial plans. A major challenge in the application of site characterization technologies is to locate the significant fractures and apply technologies in a way such that measurements properly reflect the in - situ conditions (US EPA, 2001). In other words, priority should be given to the identification of major fractures which are chiefly responsible for the groundwater and contaminant conveyance.

1.3.3 Beaufort West Study Area Site Characterisation Summary

Characterisation of the Beaufort West study area was conducted in two phases. A brief summary of the work is given below.

Phase 1

1. Desktop Study

A review of the site contaminant history was conducted; this included potential LNAPL sources at the site and the affected receptors. Historical groundwater levels and quality were obtained from old Geohydrology (GH) reports as part of the regional and local geohydrological review. Old GH maps were also utilized to identify the location of intrusions among other geological features of great implications to groundwater and contamination flow in the study area.

2. Site Survey (Walkover and Visual inspection)

This was conducted to verify the validity of the information collected during the desktop study. Emphasis was placed on the selection of drilling positions and aquifer test boreholes from the existing private monitoring boreholes.

3. Initial Conceptual Model

This was constructed based on all the data collected from the desktop study and site survey.

Phase 2

1. Hydrocensus

The hydrocensus exercise was conducted as an extended hydrocensus after the previous work by GPT. The main objective was to assess the impact and extend of the LNAPL contamination on the groundwater users located in the vicinity of conceptualised LNAPL sources. The hydrocensus played an important role in plume delineation and planning for the field tests.

2. Geologic Characterisation

Two percussion and four core boreholes were drilled. The core and percussion geological logs were compared. Location of the major fractures and possible fracture orientations was observed from the core geological logs. Weathered and bedding plane zones were also identified.

3. Borehole Geophysics Characterisation

Borehole geophysics was conducted in newly drilled boreholes. Electrical conductivity (EC) profiling was conducted to locate hydraulically conductive zones associated with the biodegradation of LNAPLs in the aquifer. Full Wave Sonic (FWS) and Acoustic Viewer (AV) images were obtained to enable the measurement of fracture depth, orientation, dip, and apparent aperture where possible. Conventional borehole geophysics logging; Gamma, Spontaneous Potential (SP) and Resistivity logs were also obtained to characterise the subsurface. During the borehole geophysics characterisation, emphasis was placed on the identification of hydraulically conductive fractures.

4. Hydraulic Characterisation

Eight slug and three pump tests were carried out in the newly drilled and existing contaminated private boreholes to determine aquifer hydraulic parameters, in particular fracture and matrix transmissivity. A single point dilution and two radial convergent tracer tests were also conducted to estimate mass transport parameters specifically: Darcy velocity (forced and natural), seepage velocity and kinematic porosity.

5. Chemical Characterisation

Organic and inorganic chemical water analyses were conducted for the Beaufort West study area. Dissolved hydrocarbon compound analysis was carried out using site laboratory field screening kit (Site Lab) and overseas reference laboratory. Volatile Organic Carbons (VOCs) were also measured during the air percussion drilling using a Photo Ionization Detector (PID).

6. Site Conceptual Model

Was developed through updating the initial conceptual model based on the entire field data collected.

1.4 Thesis Outline

Chapter 1: Introduction

Chapter 2: LNAPL Petroleum Hydrocarbon Contamination

Chapter 3: Site Preliminary Investigations

Chapter 4: Geologic Characterisation

Chapter 5: Borehole Geophysics Characterisation

Chapter 6: Hydraulic Characterisation

Chapter 7: Chemical Characterisation

Chapter 8: Site Conceptual Model

1.5 Summary of Chapter 1

The chapter gives the background information leading to this MSc thesis on characterising an LNAPL contaminated fractured rock aquifer in the Beaufort West study area. An overview and outline of the LNAPL site characterisation is given, with emphasis being placed on the application of various complimentary geohydrological tools to optimize site understanding. Optimum understanding of contaminated sites is important for undertaking remediation exercises and other safety measures which might be necessary to protect the environment and public from health hazards. The next Chapter details the review of literature on LNAPL properties, migration in different mediums and activities in the South African petroleum industry which has the potential to contaminate groundwater.

2 LNAPL Petroleum Hydrocarbon Contamination

2.1 LNAPL Properties

By definition, LNAPLs are less dense liquids than water. They do not readily mix with water; however they are composed of other molecules of organic origin which are slightly soluble in water. Examples of common LNAPL petroleum products include petrol, paraffin, diesel, and jet fuel. The LNAPL properties and the nature of the hosting subsurface determine to a greater extent the migration and distribution of the contaminants. A brief summary of the LNAPL properties that influence flow at **pore scale** migration is given in this section. For detailed explanations and measurement of these properties reference is hereby made to (Mercer and Cohen, 1990) and (Cohen and Mercer, 1993) respectively. LNAPL released into the subsurface can exist and move in the following distinct phases (Cohen *et al*, 1996):

- Vaporised phase.
- Residual entrapped LNAPLs in soil pores.
- Dissolved compounds in water (Dissolved phase).
- Free immiscible phase floating on top of water (Free phase).

Properties playing an important role in the pore scale migration of LNAPLs include:

1. Density (kg/m^3)

It is defined as the mass of substance acting per unit volume. LNAPLs have densities less than water; they float on top of water as a free phase product, thus they are referred to as “light”. Their less density insures that undissolved hydrocarbons cannot penetrate significantly below the water table. Density has influence on the migration rate of LNAPLs, more importantly in the unsaturated zone where the effects of gravity are dominant. As the LNAPL density increases, the rate of migration also increases because of high gravitational force. Their light density property implies the existence of at least free LNAPL phase and dissolved among other phases which in most cases require different remediation approaches.

2. Viscosity kg/(ms)

Is the resistance of a fluid to flow and it decreases as the fluid temperature increases. Low viscosity LNAPLs offer less resistance to flow, hence are bound to travel much faster in the porous media.

3. Interfacial Tension (J/m²)

Is the surface energy at the interface of two immiscible fluids that are in contact, it results from differences of molecular attraction forces within the fluids (Bear, 1972). The property measures the stability of the interface between the two immiscible fluids. High interfacial tension would imply great stability hence more energy required to separate the fluids. In a saturated media, high interfacial tension may also imply increased potential for groundwater advection to transport free phase LNAPL as they can stick together for much of the time.

4. Wettability

Is defined as the ability of one fluid to spread or adhere to a solid surface in the presence of another immiscible fluid and has great influence on the LNAPL fluid pore distribution. In a multiphase system, the wetting fluid would preferentially wet solid surface and as a result tend to occupy smaller pore space while at the same time confining and restricting non - wetting fluid to largest interconnected pores (Newell *et al*, 1995). In the saturated fractured media, water as the wetting fluid displaces LNAPL from pore spaces thus potentially confining LNAPLs into high transmissivity fractures. The confining of LNAPLs into the high transmissivity fractures has the potential to increase LNAPL mobility, hence accelerating the contamination movement. Mercer and Cohen (1990) describe and discuss in detail the factors influencing wettability.

5. Capillary Pressure (m)

Capillary pressure is the pressure difference across the interface between the wetting and non - wetting phases. Capillary pressure is often expressed as the height of an equivalent water column. Capillary pressure generally increases with decreasing pore size, decreasing initial moisture content, and increasing interfacial tension. Capillary pressure also measures the tendency by the porous media to attract wetting fluid while repelling the non - wetting fluid.

In the unsaturated zone where LNAPLs tend to be the wetting phase against air, the strength of capillary pressure determines the amount of residual LNAPL entrapped in the soil pore spaces. The capillary pressure for the residual LNAPLs has important implications for product recovery remediation exercises through pumping. It requires extremely high gradients in excess of 1 ft/ft (0.3048 m/m) (Newell *et al*, 1995) to displace and move residual LNAPLs, thus difficult to clean.

6. Saturation and Residual Saturation (S_r)

Saturation is the relative fraction of the total pore space filled with the specific fluid and could be a saturation ratio of water or LNAPLs. The saturation level where continuous LNAPLs become discontinuous and are immobilized by the capillary forces is known as residual saturation (S_r). Residual saturation of LNAPL represents a potential source for continued groundwater contamination that is tightly held in the soil pore spaces and thus difficult to remove through cleaning remediation technologies.

7. Relative Permeability

Relative permeability is the ratio of the effective permeability of the medium to a fluid at a specified saturation and the permeability of the medium to the fluid at 100 % saturation. Values for relative permeability range between 0 and 1. Williams and Wilder (1971) explain and discusses the use of relative permeability curves to describe different types of multiphase flow regimes which may exist at any particular site.

At **field scale**, LNAPL migration is controlled by a complex combination of release factors, soil or aquifer properties and LNAPLs properties which includes (Mercer and Cohen, 1990):

- Volume of LNAPL released.
- Rate of source loading.
- LNAPL infiltration area at the release site.
- Properties of the LNAPL.
- Properties of the soil and aquifer media.
- Permeability and pore size distribution.
- Fluid and porous media relationships.
- Lithology and stratigraphy.
- Macro - scale features.

2.2 Potential Sources of LNAPL

Groundwater contamination can occur from petroleum product spills and leakages during production, transportation and or storage. Production activities could be drilling and or refinery. Petroleum products are hereby referring to Light Non - Aqueous Phase Liquid (LNAPL) such as petrol, diesel, aviation fuel and paraffin. The contamination often occurs as a point source, where the contamination can be traced back to a single origin or source. For instance, the source could be a leaking underground storage tank, accidental tanker spills and or pipeline transportation leakage. Petroleum hydrocarbon contamination can also be a non - point source pollution, in cases where disposed oils and spilled brake fluid from the motor vehicle industry are rain washed and transported by the urban runoff.

A review of the South African Petroleum industry is given below with the objective of bringing to light potential LNAPL sources and activities which can lead to groundwater contamination. The potential LNAPL sources can occur during the production, refinery, transportation and or storage of petroleum products.

2.2.1 South African Petroleum Industry

2.2.1.1 Petroleum Manufactures

The industry is composed of six main petroleum manufacturers; four of these are crude oil refineries, one is a coal to liquid conversion facility and the other is a gas to liquid conversion plant. South Africa is reported to be having the second largest petroleum refining capacity of 519 547 barrel per day (bbl/d) in Africa, surpassed by Egypt. Its refined products are sold both in the local market and also exported mainly within Southern Africa, but also in the Indian and Atlantic basin markets. Major South African petroleum refineries include; Sapref and Enref in Durban, Chevron in Cape Town, and Natref at Sasolburg (Figure 2-1). (*eia*, 2007).

Sapref is South Africa's largest crude oil refinery with 35 % of the country's refining capacity which equates to 180 000 bbl/d of crude oil or 8.5 million tons per year. Its operations include refinery in prospect, storage facilities at Durban harbor, management of a single buoy mooring where tankers offload 80 % of the country's crude oil and ships bunkering services, both on behalf of industry partners. Sapref refines crude oil to produce petroleum products for the South African market. Products include petrol, diesel, paraffin, aviation fuel, liquid petroleum gas and marine fuel oil (*sapref*, 2007).

Engen supplies about 18 % of South Africa's liquid fuel requirements through the Enref refinery in Durban. The refinery has the capacity to refine 150 000 bbl/d. Their refined products include a wide range of petrol, diesels, paraffin, jet fuel, liquefied petroleum gas (LPG), heavy fuel oil, bunker fuel oil and bitumen (*engen*, 2007). The Chevron refinery is the third largest crude oil refinery in South Africa. The refinery is situated approximately 20 km northeast of Cape Town's Central Business District in the suburb of Milnerton. According to (*eia*, 2007), Chevron has a refining capacity of 110 000 bbl/d. Total caters for South Africa's liquid fuel requirements through the Natref refinery at Sasolburg. According to (*total*, 2007) Natref has a refining capacity of about 108 500 bbl/d. Figure 2-1 shows the location of major petroleum production in South African and refinery facilities.

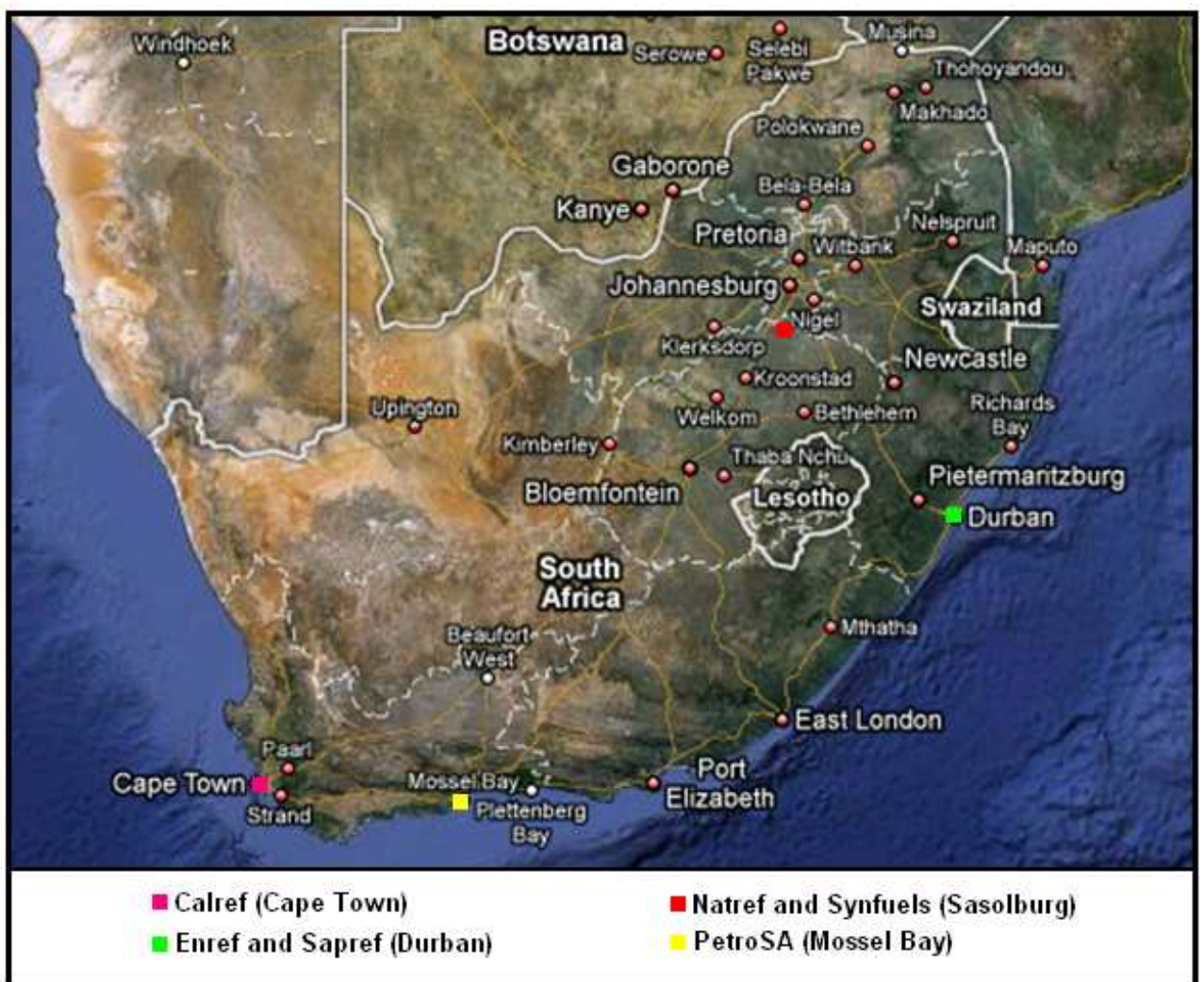


Figure 2-1 Location of major petroleum production and refinery facilities in South Africa (Taken from *google maps*, 2009).

Sasol, the world's largest manufacturer of oil from coal, maintains the coal liquefaction plants located at Secunda (oil) and Sasolburg (petrochemicals). Sasol caters for the South African petroleum industry requirements through their highly developed synthetic fuels produced by coal to liquid conversion processes. Sasol Synfuels has an operating capacity of 150 000 bbl/d. State owned PetroSA began synthetic fuel production in 1993. PetroSA converts the gas into a variety of liquid fuels including motor gasoline, distillates, kerosene, alcohols and LPG with an operation capacity of 50 000 bbl/d. (*eia*, 2007). Figure 2-2 shows some of the trend in capacities of the South African petroleum production facilities.

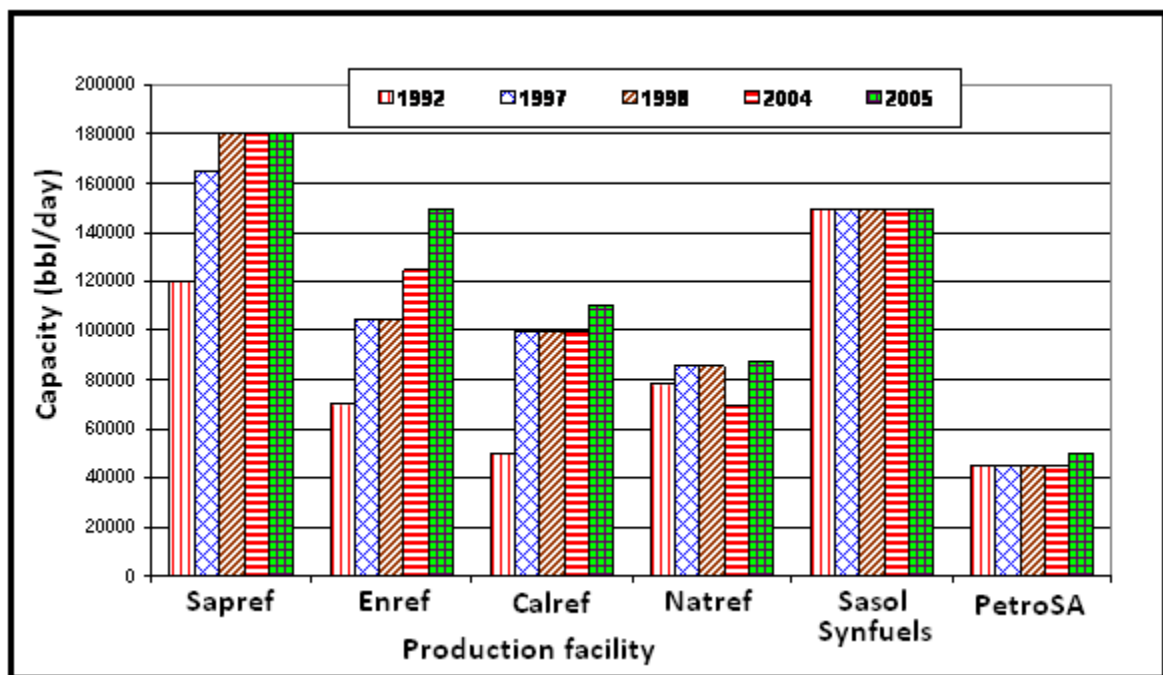


Figure 2-2 Capacities of the South African fuel production and refinery facilities from 1992 - 2005.

Sources: Sasol Facts 2007., *sapref*, 2007., *engen*, 2007., *saflii*, 2007 and *eia*, 2007.

These production capacity figures reflect a continued increase in the production of petroleum products. The increased production capacity implies increased need for storage and transportation. It is usually during the transportation and storage petroleum products where accidental spillages and leakages are bound to occur. Accidental spillages and leakages have the potential to cause groundwater contamination once the spilled petroleum product finds a preferential flow path towards the water table.

2.2.1.2 Petroleum Downstream Markets

The downstream markets involve wholesale, retail marketing and distribution of the petroleum products. This is mainly achieved through the use of storage depots and retailing service stations. Multinational companies, including British Petroleum (BP), Shell, Caltex (Chevron Texaco), Engen, and Total, are the major participants in South Africa's downstream petroleum markets. Several domestic firms are also involved, these includes Naledi Petroleum and Afric Oil.

2.2.1.2.1 Service Stations and Storage Depots

Engen is the largest marketer of petroleum products in South Africa and has about 27 % market share with about 1 400 service stations in South Africa (*engen*, 2007). Their products include a wide range of petrol, diesels, paraffin, jet fuel, liquid petroleum gas (LPG), heavy fuel oil, bunker fuel oil and bitumen. According to Sasol Facts (2007), Sasol Oil market fuels are blended at Secunda and are refined through its 63.6 % share in Sasolburg's Natref refinery. Sasol oil's products include petrol, diesel, jet fuel, illuminating paraffin, fuel oils, bitumen and lubricants. These products are marketed and distributed through its 390 service stations established since January 2004. (Sasol Facts, 2007).

Caltex is a joint venture between two of the world's major oil companies, Chevron Corporation and Texaco. Caltex controls a network of approximately 1 000 service stations and a total of 31 storage depots in South Africa. BP Southern Africa is in control of about 790 BP branded service stations, 26 depots and other distribution sites. BP Southern Africa's distribution sites include three coastal installations. Shell has a total of about 800 branded service stations and 40 storage depots. (*shell*, 2007 and *saflii*, 2007).

Total's marketing assets includes 688 branded service stations, with a network of depots and a fleet of road tankers. The company manufactures and sells a full range of petroleum products including lubricants, greases, kerosene, jet fuel and liquid petroleum gas (*total*, 2007). Table 2-1 and 2-2 gives a summary of the estimated number of fuel service stations and storage depots in South Africa respectively. Jet fuel is stored in mobile dispensers at the airports, and is owned by the Johannesburg, Cape Town and Durban international Airports. These mobile dispensers are owned by a consortium of the six major oil companies. (*saflii*, 2007).

Table 2-1 Estimated number of fuel service stations in South Africa (2007).

Company	Estimated number of fuel service stations
BP SA	790
Caltex (Chevron)	1 000
Engen	1 400
Sasol Oil	390
Shell Oil SA	800
Total Oil SA	688
Total	5 068

Sources: Sasol Facts 2007., *total*, 2007., *shell*, 2007 and *saflii*, 2007.

Table 2-2 Estimated number of fuel storage depots in South Africa.

	Number of fuel storage depots		
Company	Owned	Guest	Total
BP SA	11	14	25
Caltex (Chevron)	20	11	31
Engen	13	9	22
Sasol Oil	2	23	25
Shell Oil SA	13	17	30
Total Oil SA	13	13	26
Total	72	87	159

Sources: *total*, 2007 and *saflii*, 2007.

Petroleum product retail service stations' arrangement in most cases consists of dispenser pumps supplied by USTs (Figure 2-3). According to US EPA (2003), petroleum product leakages from USTs are a worldwide phenomenon as many of them have either leaked or are currently leaking.



Figure 2-3 Typical petroleum UST installed at the study area's service stations (Taken during the fieldwork).

It was estimated in the early 1990s that there were about 50 000 USTs being used in South Africa (Charman, 2003). It is important to highlight that not all of the 50 000 USTs were installed at service stations and storage depots. However the magnitude of the impact from USTs installed at service station is more likely to be enormous, because of the huge quantities of fuel they handle and store. The remainder of the USTs is installed at farms, garages and transport yards. In other words, the USTs deserve special mention and attention especially considering that the LNAPL contamination on the Beaufort West study area is from USTs installed at retail service stations.

2.2.1.3 Transportation of Petroleum Products

In the early 1960's the state - owned South African Transport Services (SATS) commenced the construction of a 12 inch diameter pipeline intended to convey refined petroleum product from Durban to Johannesburg. The pipeline, which become known as the Durban Johannesburg Pipeline (DJP) was commissioned in 1965. In order to accommodate the steady growth inland demand for fuel products, the DJP was in 1972, extended to Pretoria West Waltloo and Benoni from Alrode and to Klerksdorp via Potchefstroom from Sasolburg. The government also decided to accumulate crude oil reserves in disused coalmines in the inland area at Ogies and at farm tanks throughout South Africa. To this end an 18 inch diameter Crude Oil Pipeline (COP) was commissioned in 1969. When Natref was commissioned in

1971, the COP was also used to convey the inland refinery's crude oil requirements. After the commissioning of Natref in 1971, a pipeline was constructed from Natref to Johannesburg airport in 1973 for the conveyance of jet fuel. (*saflii*, 2007).

The growth in demand for refined oil product in the inland market resulted in the DJP becoming capacity constrained. In 1978, SATS commissioned the Durban Witwatersrand Pipeline (DWP). This 16 inch white oil pipeline from Durban to Alrode via Ladysmith, Volksrust and Secunda and from Secunda to Witbank via Kendal was intended to augment the DJP's capacity in order to meet the inland growing demand for white fuels. The DJP has 11 terminals where the refined products are removed and transported by road or rail to the relevant depots or service stations (*saflii*, 2007). Petroleum product leakages can occur along these transporting pipes such that they can become a continuous point source of contamination. Figure 2-4 shows an example of a leaking petroleum pipeline (*pacificenvironment*, 2009). A number of petroleum product accidental spillages and leakages events in Durban from 1998 - 2004 have been given in Appendix 1 (*groundwork*, 2009).



Figure 2-4 Example of a leaking petroleum pipeline (Taken from *pacificenvironment*, 2009).

As evident in Figure 2-4, the leaking free phase petroleum product is already floating on the surface water. Considering the ground and surface water interaction processes in particular recharge and base flow, some of the petroleum product will eventually find their way into the saturated zone. In other words the existence of petroleum transporting pipelines is a threat to

both surface and groundwater resources as they are bound to leak as a result of ageing and bursts among other factors.

After pipeline transportation, long - haul rail is the second most cost - effective means of transporting refined product to the inland region. Once on the inland, petroleum product transportation is achieved through long - haul road transport services. Road transportation of petroleum products in South Africa is provided by a number of third parties to which the oil companies have outsourced the service. The third party transportation services are complimented by the oil companies' owned fleets (*saflii*, 2007). Petroleum product accidental spillages are bound to occur during road and rail transportation, for example Figure 2-5 shows an accidental petrol spillage from a tanker, carrying about 35 000 liters of petrol (*sabcnews*, 2003). Once an accidental spill has occurred some of the spilled petroleum product has the potential to cause groundwater contamination.



Figure 2-5 Overturned petrol tanker on fire (Taken from *sabcnews*, 2003).

2.3 LNAPL Migration in the Subsurface

Groundwater constitutes of the vadose or unsaturated, capillary fringe and saturated zones which are all prone to various forms of LNAPL contamination. Groundwater dictionary by IGS of South Africa describes the three groundwater zones in the following manner:

1. Unsaturated/Vadose Zone

Is defined as the zone between the earth's surface and the water table, this may include the capillary fringe. Water in this zone is generally under less pressure than atmospheric pressure. The voids in the unsaturated zone may contain water and air or other gases. Most groundwater recharge passes through this zone. The nature and thickness of this zone has great influence on the amount of contaminants reaching the water table. High clay content in the unsaturated zone has the potential to retard and reduce contaminant migration towards the water table.

2. Capillary Fringe

The zone in which water naturally occurs in contact with, but rising above the water table. The rise above the water table is caused by tensional forces in the soil pore spaces, sediment and rock material. In fine grained material the capillary rise may amount to 2 - 3 m, but only measures a couple of centimeters in coarser grained material.

3. Saturated Zone

Is that part of the earth's crust beneath the water table or piezometric surface in which all voids, large and small, are filled with water under pressure greater than atmospheric. The saturated zone is the groundwater.

2.3.1 LNAPL Migration in the Vadose Zone

On introduction into the subsurface, LNAPLs will migrate as a distinct phase downward through the unsaturated zone under the influence of gravity. Because of less density, LNAPLs travels much slower as compared to DNAPLs under the influence of gravity. The vertical migration will also be accompanied to some extent by the lateral spreading because of the effect of capillary forces. The advective groundwater effect also promotes the lateral spreading, thus in an ideal porous and homogeneous media the LNAPL plume is bound to follow groundwater flow direction. In the unsaturated zone, the LNAPL contaminant can exist

in all four distinct phases (Huling and Weaver, 1991). Figure 2-6 shows the possible existence all four LNAPL phases; gas, free, dissolved phases and residual entrapped LNAPLs in the soil pores.

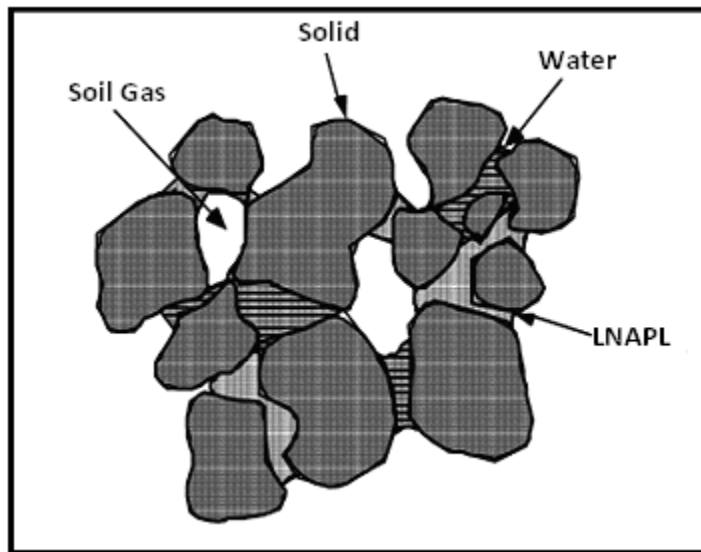


Figure 2-6 LNAPL phases in the unsaturated zone (Taken from Huling and Weaver, 1991).

As the LNAPL descend through the unsaturated zone, the free phase volume decreases because the immobile LNAPL is left behind in the soil column as residual entrapped LNAPLs in the pore spaces. This entrapment of residual LNAPL is due to the surface tension effects which are a function of grain structure, texture and size among other factors. In general, the migration of LNAPL may also be limited by physical barriers such as low permeability layers (Brost and DeVaul, 2000). This fact seems to suggest that various permeability materials exhibit different retention capacities for LNAPLs. In addition to the migration of the non-aqueous phase, some of the LNAPL may volatilize and form a gaseous envelope of organic vapor extending beyond the main zone of contamination (Abriola, 1989).

2.3.2 LNAPL Migration in the Saturated Porous Media

On reaching the water table, the LNAPL behavior is chiefly dependent on its lighter density property and will spread laterally along the capillary fringe forming a lens or pancake. It may also depress natural groundwater levels during the lateral spreading. During interaction with the advective flowing groundwater, soluble components may dissolve to form a contaminant plume (Figure 2-7). The dissolved LNAPL phase can then migrate under the influence hydraulic gradients present in the aquifer (Newell *et al*, 1995). It is important to highlight that both natural and artificial gradients has great potential to mobilize LNAPL contaminants. On

the Beaufort West study area, artificial gradients from abstraction on private and municipal boreholes are conceptualised to be mobilizing the LNAPL contamination.

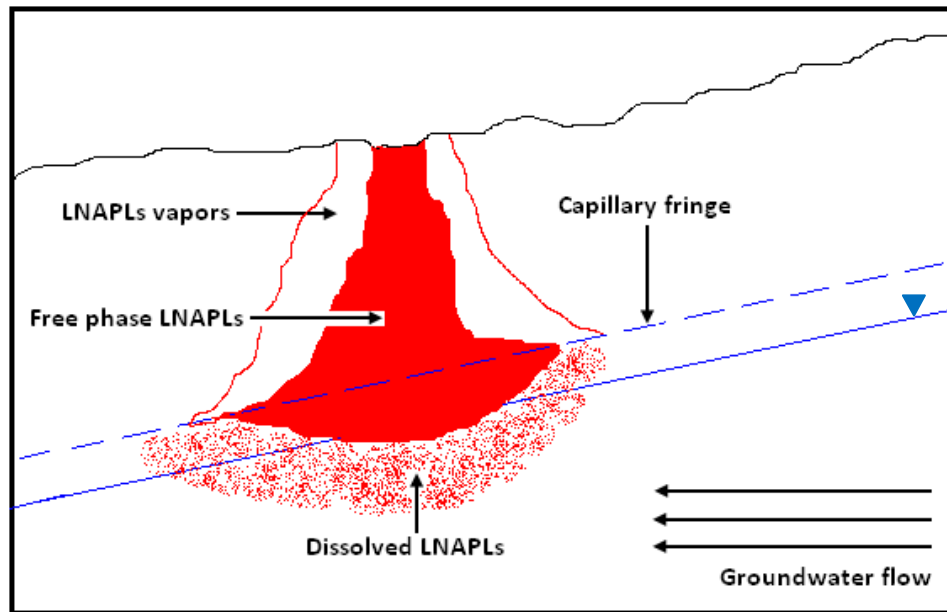


Figure 2-7 Simple conceptual model of LNAPL migration in the subsurface (Adapted from Mercer and Cohen, 1990).

Accumulated LNAPLs at or near the water table are subject to “smearing” as a result of changes in the water table elevation due to seasonal changes and or abstraction regimes. Seasonal changes could be due to recharge or discharge or tidal influence close to coastal environments. Mobile LNAPL floating above the water saturated zone will move vertically as the groundwater elevation fluctuates. As the water table rises or falls, LNAPLs will be retained in the soil pores, leaving behind a residual LNAPL “smear zone”. If smearing occurs during a decline in the groundwater elevations, residual free phase LNAPLs may be trapped below the water table as groundwater elevations rise (Newell *et al*, 1995). Entrapment of the free phase LNAPLs below the water table elevations can lead to a wrong impression that the free phase contaminant has depleted, only for it to reappear as water levels falls.

2.3.3 LNAPL Migration in the Fractured Media

The behavior of LNAPL within a fractured rock media is a function of the properties of the immiscible fluid, geometry of the fracture network, rock matrix properties, and the groundwater flow regime. In other words, the LNAPL behavior is completely different in fractured rocks as compared to porous media. According to US EPA (2001), fractured rock sites are among the most complex because of their considerable geologic heterogeneity and the nature of fluid flow

and contaminant transport through fractured media. Complex geology poses a great challenge to site characterization.

Hardisty *et al* (2004) noted the potential of relatively small volumes of LNAPL within vertical and sub - vertical fractures to produce significant LNAPL pressure heads. Significant LNAPL pressure heads can result in the pronounced LNAPL penetration into the saturated zone and such penetration can be significantly deeper than predicted by porous medium models. Once the LNAPL reaches the groundwater surface, its accumulated weight will begin to depress the LNAPL - water interface within the fracture. In a water wet system, LNAPL will enter a given fracture only if the LNAPL - water capillary pressure (P_c) at the fracture entrance is greater than the fracture entry pressure P_e . Considering the fracture as two parallel plates of aperture b , the fracture entry pressure can be described as a capillary phenomenon, and is expressed with the following equation (Kueper and McWhorter, 1991).

$$P_e = \frac{2\sigma \cos \phi}{b}$$

Equation 1

Where; σ is the interfacial tension between LNAPL and water, and ϕ is the interface contact angle through the wetting phase. At the water table, where the water fluid pressure P_w equals zero, the capillary pressure is equal to the LNAPL fluid pressure at the interface and is proportional to the connected vertical height of LNAPL within the fracture (h_l). This pressure is balanced by the buoyancy of the LNAPL provided by the penetration beneath the groundwater surface, and the entry pressure of the fracture as shown in equation 2 below (Hardisty *et al*. 1998).

$$h_l \rho_l g = h_l \rho_w g + \frac{2\sigma \cos \phi}{b}$$

Equation 2

Advection plays an important role in both groundwater and LNAPL flow through the fractured aquifer system. Groundwater flow in a fractured aquifer is mainly dependent on; fracture density, orientation, effective aperture width and nature of the matrix. Mercer and Spalding (1991) noted the tendency of the LNAPL to be transported in the same general direction as the groundwater. Fetter (2001) also reported the dissolved LNAPLs travelling at the same rate with

average linear groundwater velocity. In other words, groundwater advection plays an important role in driving the LNAPL contamination in fractured rock aquifers.

In the fractured rock aquifers, dip and fracture orientations have great influence on the rate of LNAPL migration. These fracture features have the potential to move contamination up or across the gradient. The fracture dip and orientations also have important implications for detailed LNAPL site characterisation. Hardisty *et al* (2004) highlighted the need to consider the possible existence of the LNAPL contamination both below the historical groundwater levels and sometimes significantly up - gradient or cross - gradient of the source when placing monitoring wells. Figure 2-8 shows a conceptualised migration of LNAPLs in a typical Karoo fractured rock aquifer. In a typical Karoo fractured rock aquifer, the majority fluid flow occurs in the fractured preferential flow paths with matrix diffusion also contributing immensely to the LNAPL migration and distribution.

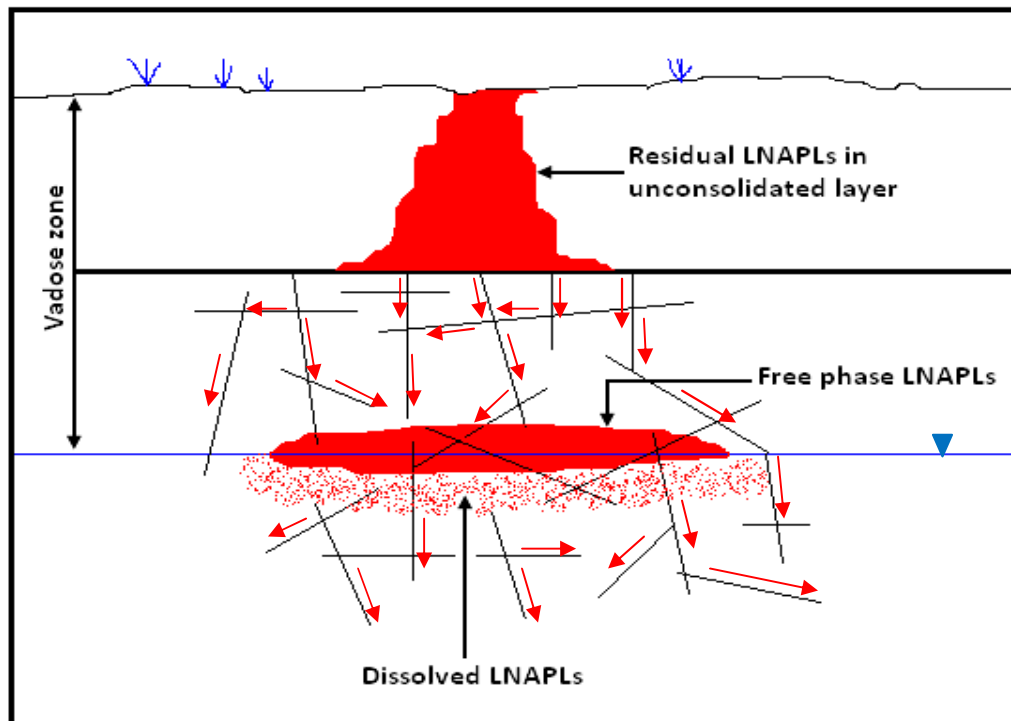


Figure 2-8 Conceptualised LNAPL movement in a typical Karoo fractured aquifer.

The nature and properties of the rock matrix also plays an important role in the movement of groundwater water and contaminants through the fractured rock aquifer. The study area is dominated by coarse grained sandstone which is characterised by high primary porosity and permeability. Though fractures serve to convey the bulk of groundwater fluids, matrix diffusion has strong implications for dissolved LNAPL contamination distribution. The existence of

chemical concentration gradients between the fractures and the rock matrix will result in mass transfer of contaminants from the flowing groundwater in the fractures into the relatively immobile groundwater in the rock matrix (Feenstra *et al*, 1984). Due to the matrix diffusion effect the contamination concentrations in the fracture preferential flow path are bound to diminish rapidly into the matrix resulting in the contaminant plume moving at slower rate than groundwater. It is also possible for the dissolved LNAPLs in the matrix to diffuse back into the fracture preferential flow path once the concentration gradient reverses, posing great challenges for contamination flushing through remedial action.

It's imperative to determine the rock matrix properties when characterising the LNAPL contaminated fractured rock aquifers given the value of the property in understanding matrix and fracture interactions. However for this thesis, due to limited resources and time span needed, rock matrix properties experiments were not conducted. For the detailed experiment to determine rock matrix porosity readers are referred to Feenstra *et al* (1984).

2.4 Summary of Chapter 2

In summary, Chapter 2 gives a review of literature on the LNAPL properties which are important because of their great influence on the behavior of LNAPLs in the earth's subsurface. A review of the South African petroleum industry is also given with the objective of bringing to light potential LNAPL sources and activities which can lead to groundwater contamination during the production, refinery, transportation and storage of petroleum products. Another important aspect addressed as part of the literature review is the migration process of LNAPL in the subsurface environment with emphasis being placed in the fractured media migration. More emphasis was placed on LNAPL migration in the fractured rock media taking into consideration that the study area is characterised by a typical Karoo fractured rock aquifer. The next Chapter documents preliminary investigations which were conducted on the Beaufort West study area.

3 Site Preliminary Investigations

3.1 Site Description

The study area is located in Beaufort West town, which is situated in the Western Cape Province of South Africa. Figure 3-1 shows the study area and positions of contaminated and uncontaminated private boreholes. The map also shows the location of the main potential LNAPL sources at the Beaufort West study area.

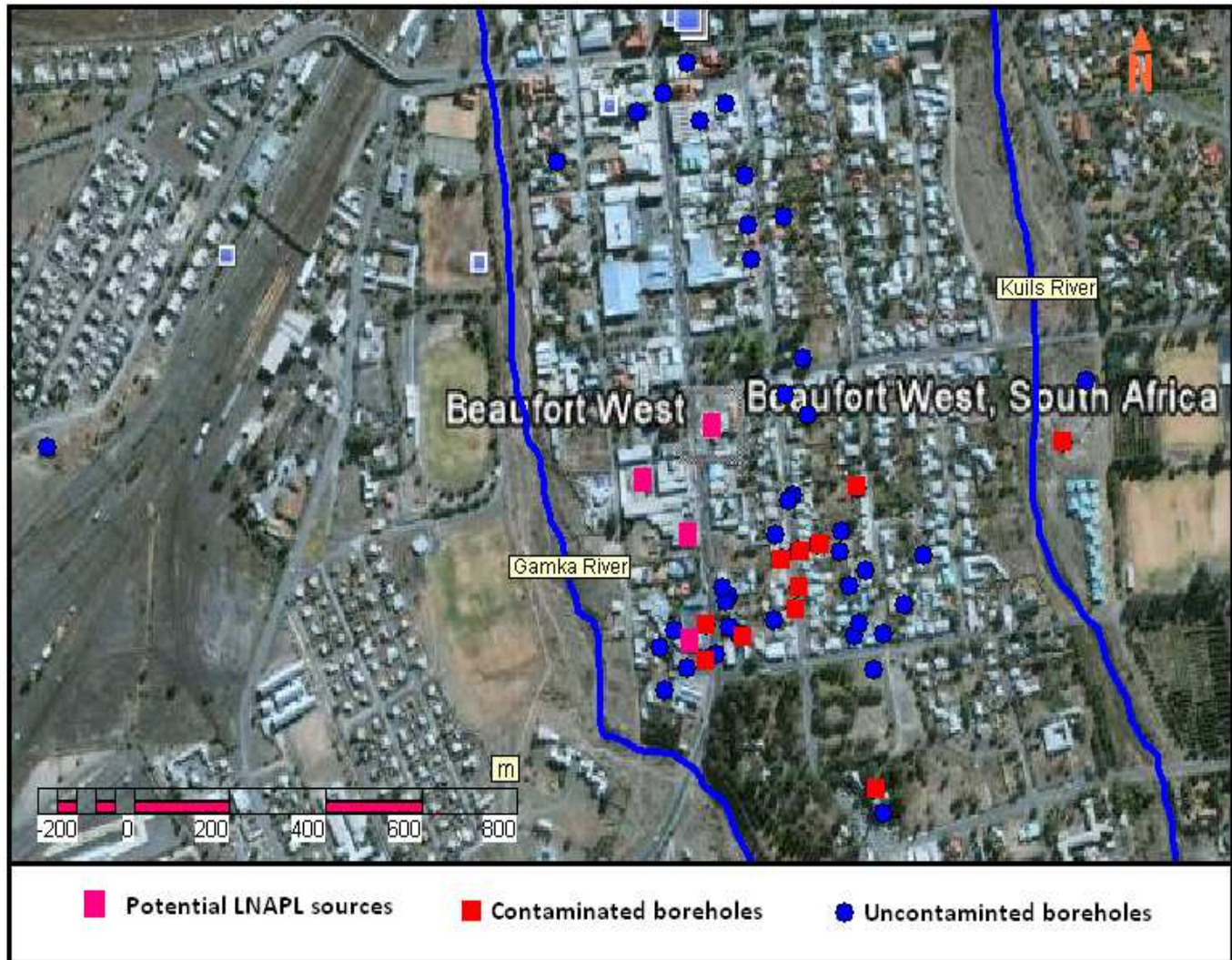


Figure 3-1 Location of the potential LNAPL sources, contaminated and uncontaminated boreholes at the Beaufort West study area (Western Cape Province of South Africa).

3.1.1 Climate

Beaufort West is generally characterised by arid to semi - arid climate with long periods of insignificant rainfall amount. The area is generally dry, receiving on average about 230 mm rainfall per year. Figure 3-2 shows the average monthly temperature and rainfall distributions for Beaufort West from 1960 -1990 (*weathersa*, 2008). Summer daily maximum temperatures may rise above 40 °C and winter temperatures can fall below freezing point. Snow often covers the Nuweveld Mountains in mid - winter. Evaporation rates at the study area are in the order of 2000 mm/year.

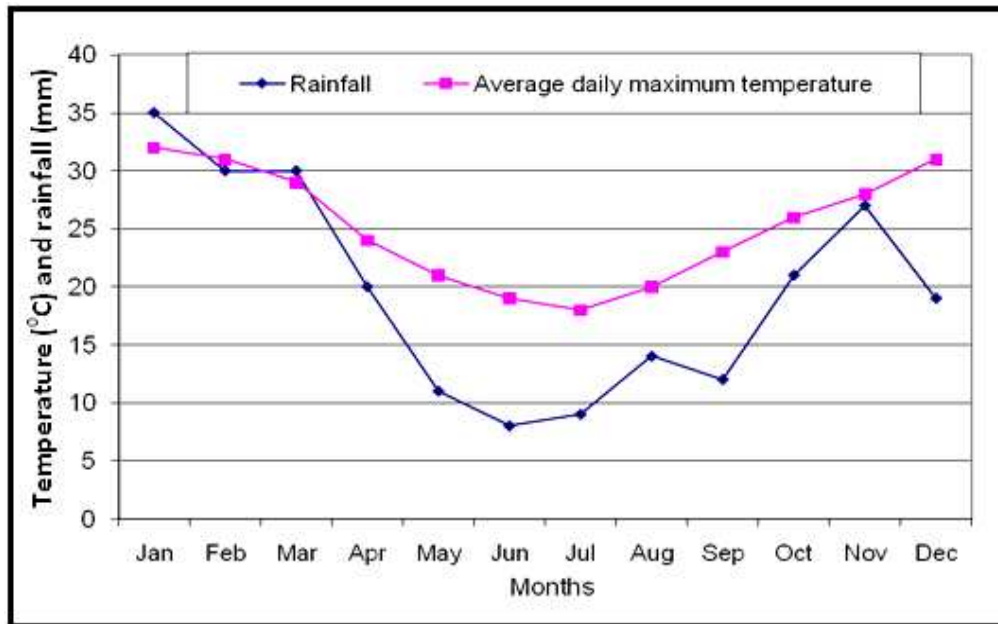


Figure 3-2 Average temperature and rainfall distribution for Beaufort West.

The study area is characterized by a generally flat topography which drains into a south to south east and to south west direction. Typical trellis drainage pattern which is mainly attributed to the underlying sedimentary formations and generally flat topography dominates the study area. The study area is bounded by Gamka and Kuils seasonal rivers which are about 1 km apart. Gamka River is largely activated by the spillway overflow from the Gamka Dam. Gamka River which drains the Nuweveld Mountains is a tributary of the Dwyka - Gouritz system, a major drainage of the Great Karoo. The vegetation in the vicinity of the study area reflects the general aridity and insolation associated with high temperatures. Mesembs and other succulents are the dominant plant types. Hardy acacia is mostly confined to runoff

channels and drainage systems, with the resistant white steak grass being the most common representation of its species.

3.1.2 Geology

The study area falls under Beaufort group of the main Karoo Supergroup. The Karoo super group mainly constitute of sandstone, mudstone, shale and siltstone sedimentary rocks. The sandstones of the southern Karoo basin have extremely low primary porosity and permeability (Woodford and Chevallier, 2002). Teekloof formation dominated by the red mudstone characterizes the Adelaide Subgroup in the study area. The Beaufort Group (Adelaide Sub - group) sediments are highly indurated with appreciable chlorite and sericite, these includes carbonates, iron oxides, calcite, feldspar and quartz.

The Adelaide Subgroup attains a maximum thickness of about 5000 m in the southeast, which decreases rapidly to about 800 m in the center of the Karoo Basin and thereafter more gradually to around 100 - 200 m in the extreme north. In the southern and central parts of the basin, the Adelaide Subgroup consist of alternating bluish - grey, greenish - grey or grayish red - mudrock and grey, very fine to medium grained, lithofeldspathic sandstone. In the northern part of the basin, coarse to very coarse sandstone, or even gluestone, are also common in the Normandien formation (Woodford and Chevallier, 2002). The sediments of the lower part of Beaufort Group (Adelaide Sub - group) within the general area of the study site comprises of a sequence of shale, mudstone, and sandstone. The sandstones vary in colour from yellowish - green and grayish blue to purple (Campbell, 1980).

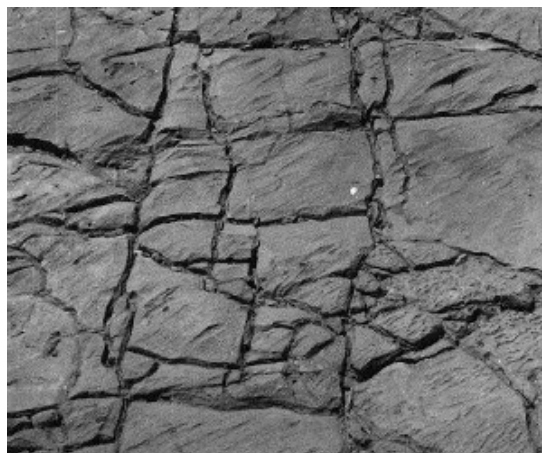


Figure 3-3 Examples of bedrock vertical and horizontal bedding plane fractures (Taken from *science.jrank*, 2009)

The sediments are well jointed and fractured, horizontal to sub - horizontal in altitude; highly variable in thickness and extend. Bedding plane and vertical joints are common in the sandier facies, whereas siltstone - mudstone facies are dominated by a more irregular fracture pattern with random orientation and curvilinear joint planes. Figure 3-3 shows examples of bedrock vertical fractures and horizontal bedding planes.

The joints are recognized as dominant with the best developed and most frequently occurring being the striking between $N 25^{\circ}$ and $N 30^{\circ} W$ in Beaufort West (Campbell, 1980). A directional frequency diagram (Figure 3-4) shows the dominant joint sets that strike between $150^{\circ} - 160^{\circ}$ and $330^{\circ} - 340^{\circ}$.

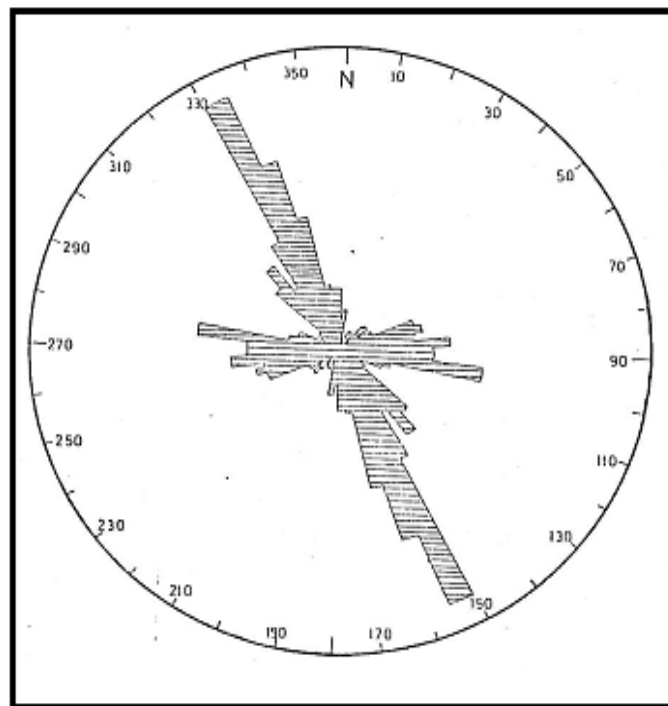


Figure 3-4 Rose joints from field data collected within 30 km of Beaufort West (Taken from Campbell, 1980).

The existence of joints and fractures present great potential for contaminant transportation as they are usually associated with high transmissivity. In high transmissivity fractures and bedding planes, advection transportation is most likely to be the dominant mass transport process considering that the bulk of groundwater flow occurs in the fractures. The contribution of fracture flow to advective mass transportation process is also dependent on other fracture features and properties. Regionally the dolerite is intrusive at all levels of the sedimentary sequence but is most prominently displayed as transgressive sheets on sills. The dolerite

intrudes most preferentially at sandstone - siltstone contacts and within sandstones following bedding planes and joints. The intrusion is presumed to have been injected during the episode of igneous activity which brought close to a Karoo deposition at the end of the Jurassic period (Campbell, 1980). Sills are usually discordant, causing relative displacement of stratification and are often intruded at the same stratigraphic levels as sandstone units, preferentially along the upper and lower sandstone - siltstone contacts. On the other hand, the dolerite dykes generally trend northerly or sometimes in easterly directions. Two sets of joints in the country rock are associated with the dolerite dykes, one parallel to the dyke margin and the other perpendicular to it (Vandoolaeghe, 1978). It was evident from the core geological logs (Figure 3-5) that the uppermost layer of the study area is characterized by the unconsolidated river depositional material.



Figure 3-5 Sandstone boulders from core drillings on the study area (Taken during the field work).

According to Woodford and Chevallier (2002), quaternary deposits are a major characteristic along main rivers of the Karoo basin. Deposits on the bed of braided streams consist mainly of coarse sediments, conglomerates and patches of finer material on their banks. Meandering streams on the other hand deposit mainly fine - grained sand, mudstone and siltstone with little or no conglomerates (Visser, 1989). These deposits mainly constitute of gravels, comprising of well - rounded cobbles and boulders which are sometimes cemented by calcrete. The thickness of the quaternary deposits varies where fine sediments dominate the unsaturated zone. Volatized LNAPLs are of great concern considering the potential for increased diffusion in fine grained sediments. The underlying consolidated material on the study area comprises of shale and sandstone which are typical Karoo Supergroup attributes.

Figure 3-6 shows the location of the Karoo basin on a simplified geological map of South African.

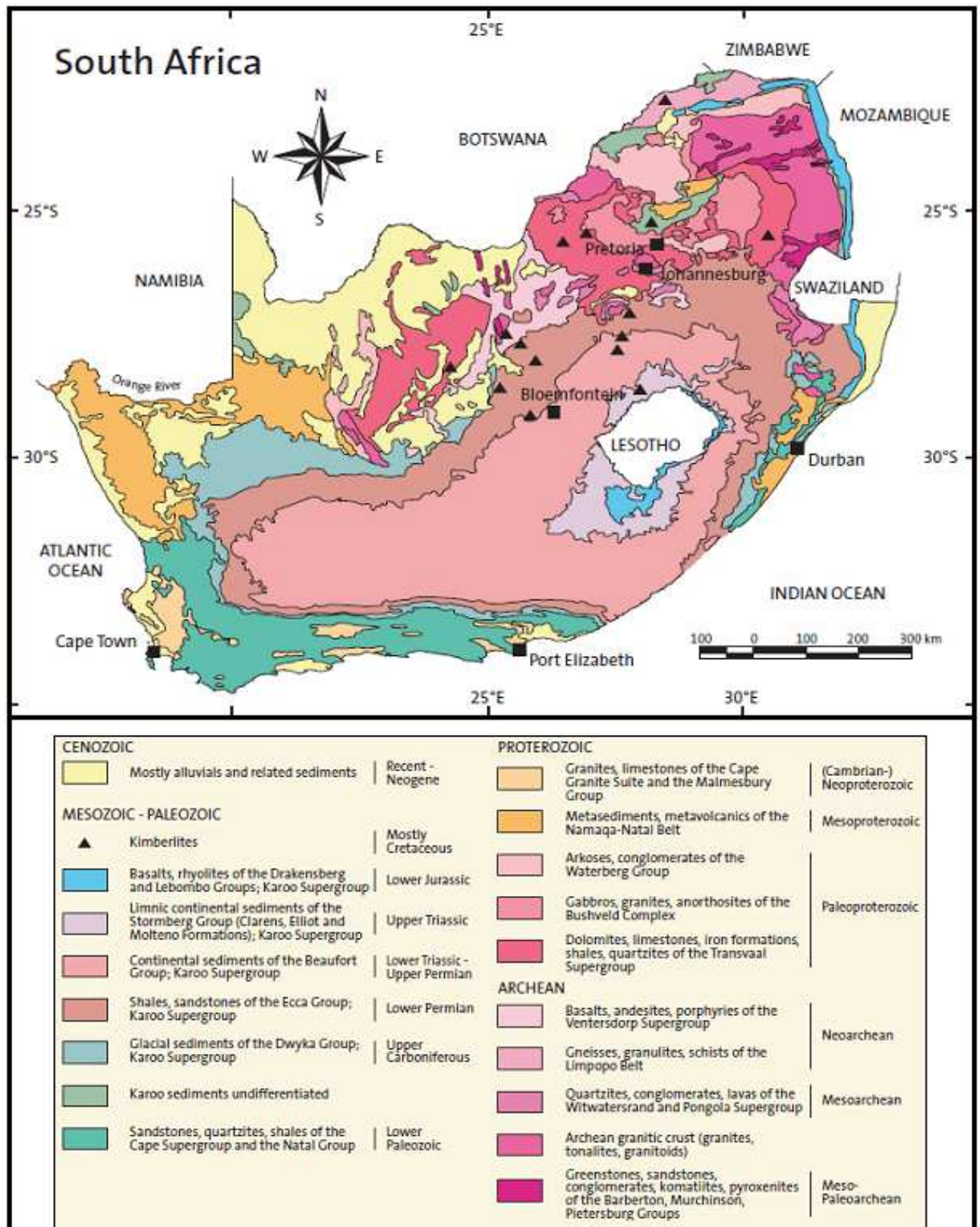


Figure 3-6 Simplified geological map of South Africa (Taken from *geoscience*, 2009).

Alluvial deposits dominate the study area's flood plains with much of the deposits being concentrated along valleys and stream courses of Gamka and Kuils rivers. The nature of these deposits has important implications for recharge and contaminant movement through the unsaturated zone. Boulder alluvium composed primarily of dolerite and metamorphosed sedimentary rocks are found along banks and flood zones of the Gamka River on the upstream of the Gamka dam. Most boulders accumulate in the orders of 1 - 3 meters below ground level (mbgl) in thickness (Campbell, 1980). Thick unsaturated alluvial deposits have great potential to facilitate diffusion of the VOCs. In such environments, precautionary measures has to be taken during air percussion drilling to asses and measure the VOC levels, in order to avoid incidence of fire. The result from the core geological logs (Figure 3-7) confirms the presence of alluvium deposits on the study area where a thickness of 3 m river sand was observed.



Figure 3-7 River sand deposits from 0 - 3 mbgl on the study area (Taken during the field work).

3.1.3 Geohydrology

The study area is characterised by a typical Karoo fractured rock aquifer occurring within the Karoo Super group and is the most extensive type of aquifer present in South Africa. Fractured rock aquifers are essential as they present preferential flow path which play an important role in both groundwater flow for abstraction purposes. However fractured preferential flow paths also present opportunities for accelerated contaminant migration.

According to Botha *et al* (1998), a major characteristic of the Karoo Supergroup which consists mainly of sandstones, mudstone, shale and siltstone is their low permeability. The storage capacities of Karoo formations are limited and as a result the matrix becomes a storage reservoir supplying the fractures which serves as the main conduit for groundwater flow. Vegter and Foster (1992) noted that the porosity of Karoo sediments appears higher close to the surface and this has implications for both groundwater yield and contamination flow in the

catchment. The high porosity sediments are important as they present potential for high recharge along major rivers of the Karoo basin. High recharge waters also have important implications for LNAPL biodegradation as they aid in replenishing groundwater oxygen which serve as the first electron acceptor during microbial consumption of organic hydrocarbon. Through dilution, recharge greatly contributes to natural attenuation of contaminants. In contrary, high recharge rates can also enhance contaminant migration through smearing and mobilization.

Regionally ubiquitous bodies which intruded the sediments cause induration of the contact sediments of the horst rock. This phenomenon leads the formation of a baked zone which when exposed to erosion by groundwater movement becomes water bearing and hydraulically conductive. It is the existence of such hydraulically conductive zones that might have facilitated and accelerated LNAPL migration in the Beaufort West study area.

In contrast the thickness and associated induration of the sill intrusions are considerably large and this result in the contact zones near the sill intrusions being thoroughly metamorphosed. In other words the potential of sill contact area being highly permeable and hydraulically conductive is substantially reduced. Good groundwater storage properties of low transmissivity are however sometimes provided by the clayey product of the dolerite weathering. The main recharge zone for Beaufort West is located at the piedmont of the Nuweveld escarpment. In this recharge zone, boreholes sited near drainage channels showed the most rapid rise in groundwater levels after local rains (Campbell, 1980).

3.1.3.1 Historical Groundwater Data

The regional hydraulic gradient is directed north to south, with the gradient being high in all localities. Figure 3-8 shows monitored groundwater levels from 2001 - 2007 by GPT at the Beaufort West study area. Figure 3-9 shows the potential LNAPL sources and the location of boreholes in which the water levels was monitored from 2001 - 2007. The exhibited fluctuating trend can be attributed to rise and fall of the water table during dry and wet periods respectively. It is however important to point out that the degree of fluctuations is possibly a function of rainfall amounts and intensities. Campbell (1980) observed a similar trend in the vicinity of Beaufort West town. Exceptional rise in water levels occurring along the Nuweveld escarpment were observed after abnormal rains between December 1975 and March 1976. This exceptional rise in water levels was explained and linked to main recharge zone located at the piedmont of the Nuweveld escarpment.

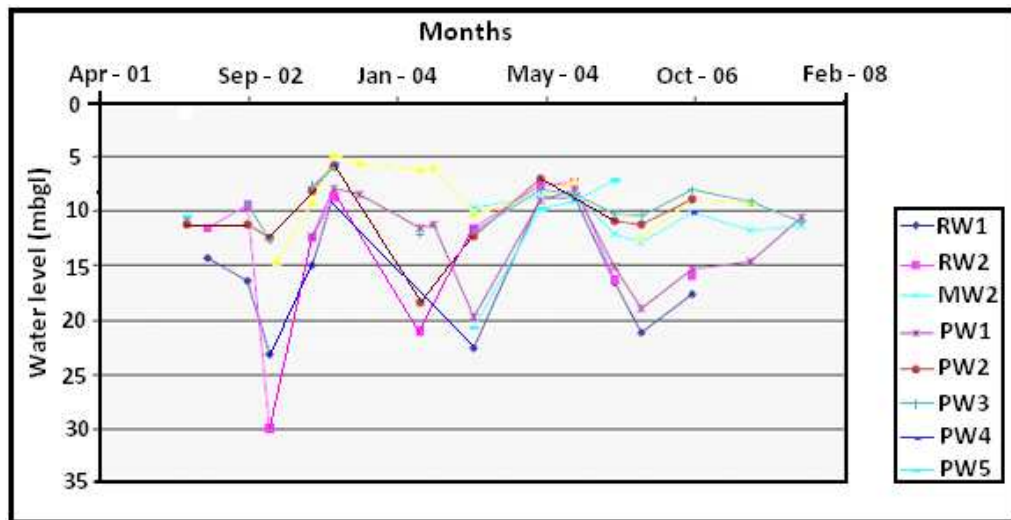


Figure 3-8 Monitored water levels in the Beaufort West study area (Taken from Nabee, 2007).

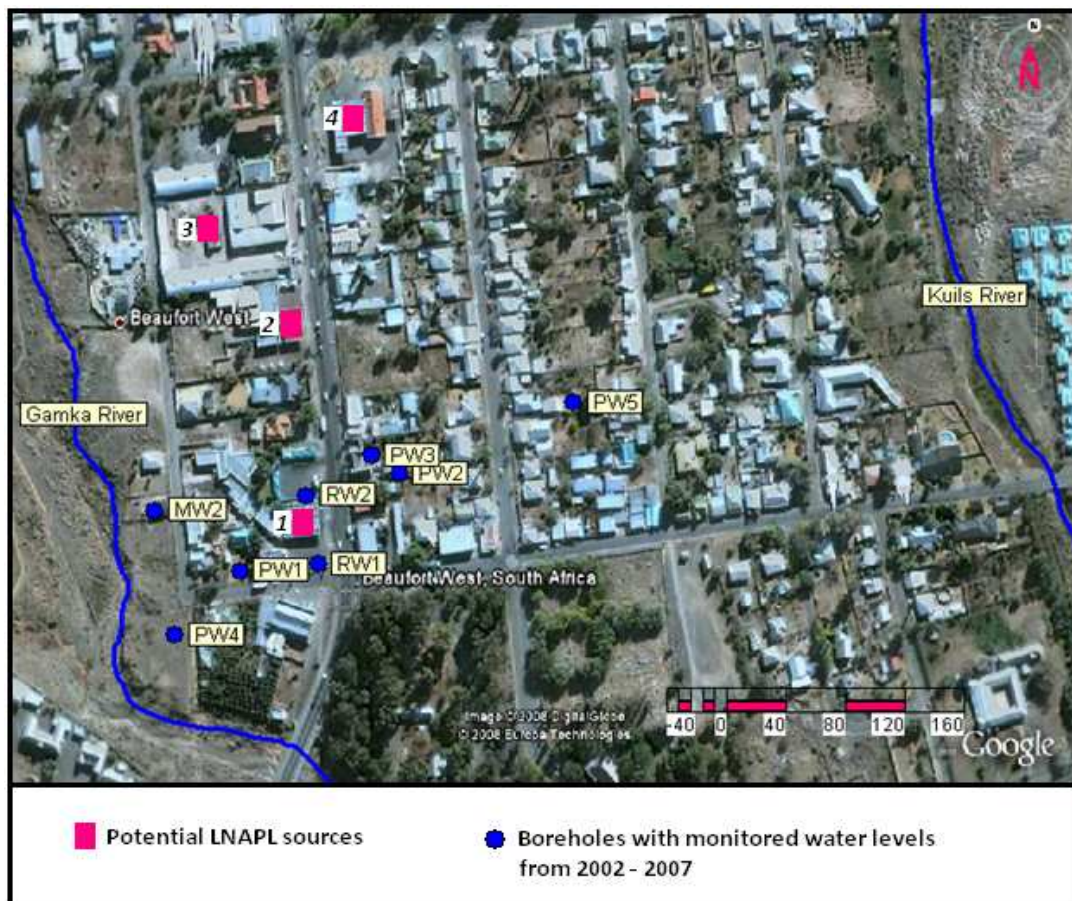


Figure 3-9 Location of potential LNAPL sources and boreholes with monitored water levels (2002 - 2007) at the Beaufort West study area.

Based on the pump tests carried during the same period (Campbell, 1980), the aquifer was categorized as a semi - confined to confined and highly anisotropic. The effects of increased abstraction during the dry seasons contributing to different degree of water level fluctuation cannot be ruled out. Increased abstraction rates during the dry seasons are an important factor considering the large number of groundwater users identified in the study area during the hydrocensus. Fluctuations in the groundwater levels as indicated on Figure 3-9, has the potential to cause vertical smearing and entrapment of LNAPLs in the event of a quick rise of water levels.

According to (Vandoolaeghe, 1978), the quality of groundwater in Beaufort West is highly variable. Total Dissolved Solids (TDS) ranges from 45 mg/l in Gamka river area north of Beaufort West to a value of 7500 mg/l in high infiltration areas covered with alluvial and surface limestone deposits. Groundwater quality generally deteriorates with increasing distance from the Nuweveld Mountains recharge zone. The water near the Nuweveld escarpment is generally regarded to be fresh (< 150 mS/m). Regionally the classic hydrochemical trend of water is from calcium bicarbonate (CaHCO_3) - sodium bicarbonate (NaHCO_3) types to mixed facies to sodium sulphate (NaSO_4) - sodium chloride (NaCl) types (Campbell, 1980).

3.2 Desktop Study

The exercise comprised of a detailed search of the available historical and current records, maps to identify the potential on and off - site LNAPL sources, pathways and receptors of contamination. A well conducted desktop study enables future investigations in a cost effective and an efficient manner. During the desktop study, past geophysics and geohydrological information (1970 - 1980) was obtained from old GH reports. These old GH reports were obtained from the DWAF's library in Pretoria with the assistance of Eddie Van Wyk. Old Beaufort West geohydrological and geological maps were provided by Professor Van Tonder of the IGS. Old GH reports and geological maps played an important role in showing regional geological distributions and location of intrusions in the vicinity of the Beaufort West study area. Also realised from the old GH maps is the location of various boreholes which were sited during geophysical investigations in Beaufort West (Vandoolaeghe, 1978).

3.2.1 Site History

Site history data was obtained courtesy of GPT consulting company currently working at the site. The site consists of petroleum product service stations as the main potential LNAPL sources. Other potential sources of LNAPLs include motor vehicle dealership, general stores, garages, workshops and transport yards where USSs are usually located. Underground Storage Systems are a major source of soil and groundwater contamination. The United States EPA in 1988 acknowledged USSs as one of the five major threats to groundwater quality (Bedient, 1994).

LNAPL contaminants at the study site are believed to have been released by an accidental petroleum spill around 1983 or 1984 and leakages from an UST at a service station. Free phase petroleum products were detected in a number of private boreholes and as a result the boreholes are contaminated with both free and dissolved phases. The contamination has adversely affected some of the Beaufort West groundwater users; some of the residents have stopped using their boreholes. Groundwater use activities mostly affected include gardening, swimming pools and domestic purposes.

It is worth mentioning that the desktop study revealed important information which had strong bearing on the planning and preparation of the site survey and subsequent field work. From the previous work done on the site, it was noted that some of the previous drilling attempts had failed because the drill bit got stuck after the borehole wall had collapsed. During planning of the fieldwork, the driller was requested to bring long casings to avert such dangers. From the old GH reports and maps, possible dolerite and sill intrusion positions in the vicinity of Beaufort West study area were also revealed. These intrusions have the potential to generate groundwater bearing and transmitting fractures at contact areas with the horst sedimentary deposits, but at the same time they can also facilitate quick movements of contaminant.

3.3 Site survey (Walkover)

A site survey is a process of confirming the information gathered during the desktop study. This involves physical walking on and around the site. This helps to reveal any features such as structures, tanks, pipe work which may suggest possible sources and pathways of contamination. The activity is important for planning and decision making prior to the actual field work. The survey on the Beaufort West study area enabled achievement of the following aspects:

- Selection of private boreholes to be used during the field tests and taking measures to prevent contaminant mobilization during tests.
- Identification of boreholes with free phase product. This was important considering that all boreholes having free phase product are most likely to be intersecting the preferential fracture flow path connected to the LNAPL sources. It was therefore important for these boreholes to be part of the field investigation.
- Identification of other potential LNAPL sources such as motor vehicle garages and transport yards on the study area. This was more important because previous investigations had mainly concentrated on the LNAPL source number 1.
- The need for a hydrocensus to assess the plume migration and affected groundwater use activities was prompted and established during the site survey. This was after the free phase petrol product was reported in a previously unmonitored private borehole.
- Identification of the drilling positions for the planned field investigation was done during the site survey.
- Assessment of the private borehole owner's willingness to assist in the investigation and their time of availability. Appointments were conveniently arranged in advance. In essence, more production time was unveiled and the working environment was well secured for both the personnel and equipment.
- Four main potential sources of LNAPL contamination at petroleum products service stations were identified during the site survey. Numbers 1 to 4 will be used throughout this thesis to refer to these potential LNAPL sources.

3.4 Initial Conceptual Model

Based on the desktop study and previous work done on the Beaufort West study area, the aquifer was conceptualized as a typical Karoo fractured rock aquifer, with transport occurring primarily in the high transmissivity fractured sandstone. The bulk of the groundwater is being stored in the low transmissivity sedimentary deposits matrix. The aquifer system is artificially stressed due to the abstraction on private and municipal boreholes leading to mobilization of the LNAPLs. As a result the contamination was conceptualised to be migrating up and across gradient (Figure 3-10).

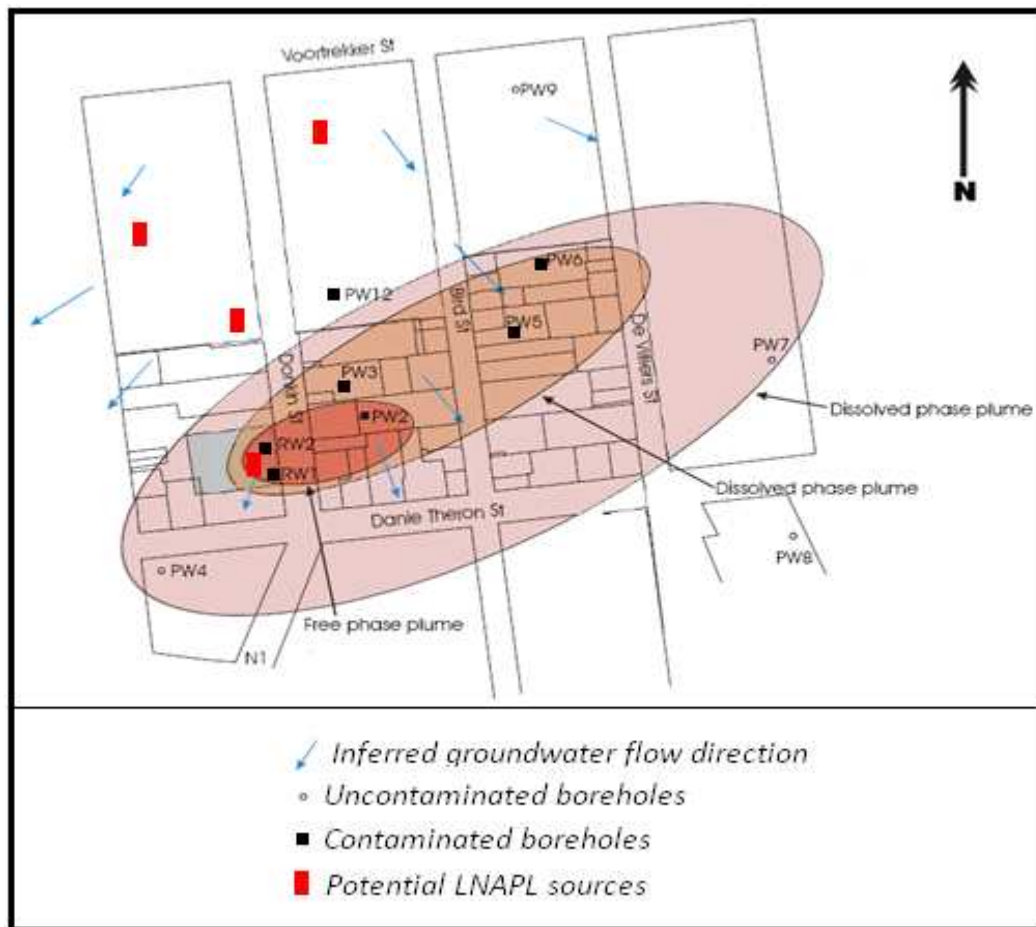


Figure 3-10 Initial conceptualised LNAPL contaminant migration at the study area (Taken from Van Biljon and Hassan, 2003).

Previous drilling results indicated the existence of fractured zones which are potential preferential flow pathways to LNAPL contaminants. Depicted on the initial conceptual model are the potential LNAPL sources which were identified during the site survey. It is also conceptualised that these are the only LNAPL sources causing groundwater contamination in the Beaufort West study area.

3.5 Hydrocensus

The hydrocensus was carried out in October 2008 to identify and characterise the groundwater use activities in the vicinity of the four identified main potential LNAPL sources (Figure 3-10). The exercise was carried out as an extended hydrocensus, considering that some of the groundwater users had already been identified during previous investigations by the GPT consulting company. It is also important to highlight that the hydrocensus was carried out in the main conceptualized direction (North to north east) of the contaminant migration as

understood from desktop study and site survey. A total of 22 boreholes were identified during the hydrocensus exercise adding to 20 already identified private boreholes by GPT.

Figure 3-11 shows the existing monitoring boreholes and those identified during the hydrocensus on the Beaufort West study area.

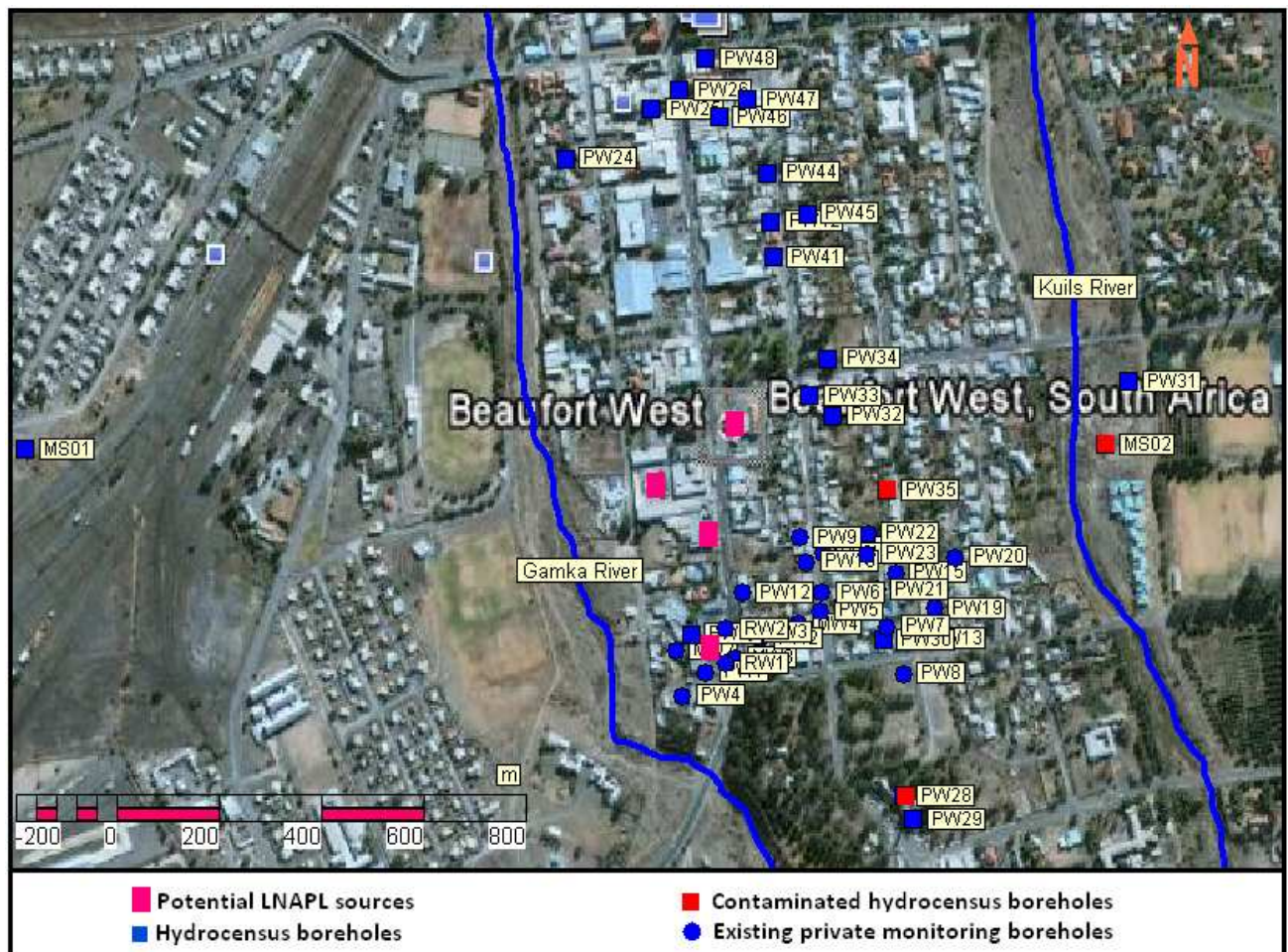


Figure 3-11 Location of the existing and hydrocensus boreholes on the Beaufort West study area.

The initial hydrocensus by GPT was triggered after some private boreholes located to the north and north east of the conceptualised LNAPL source reported pumping of free petroleum products from their boreholes. The initial hydrocensus covered a radius of about 500 m from the conceptualised contamination source. The current hydrocensus increased the radius of coverage to about 1.3 km from the potential contamination sources. Two municipal boreholes (MSO1 and MSO2) were also sampled during the hydrocensus, considering their value as part of Beaufort West town water supply system. MSO2 borehole which is located on the east side of Kuils River (Figure 3-11) was found to be contaminated with dissolved LNAPLs, which

implies that the contamination crossed the Kuils River. Such an observation highly suggests the existence of preferential pathways underneath the Kuils River. Organic chemistry results for the boreholes sampled during hydrocensus have been placed under chemical characterisation, see section 7.21. Geohydrological data collected during the hydrocensus is placed in Appendix 1.

The hydrocensus results indicate that gardening dominate the groundwater use activities, accounting for more than 57 % of the groundwater use activities. The remainder is shared between irrigation, domestic and on swimming pools (Figure 3-12).

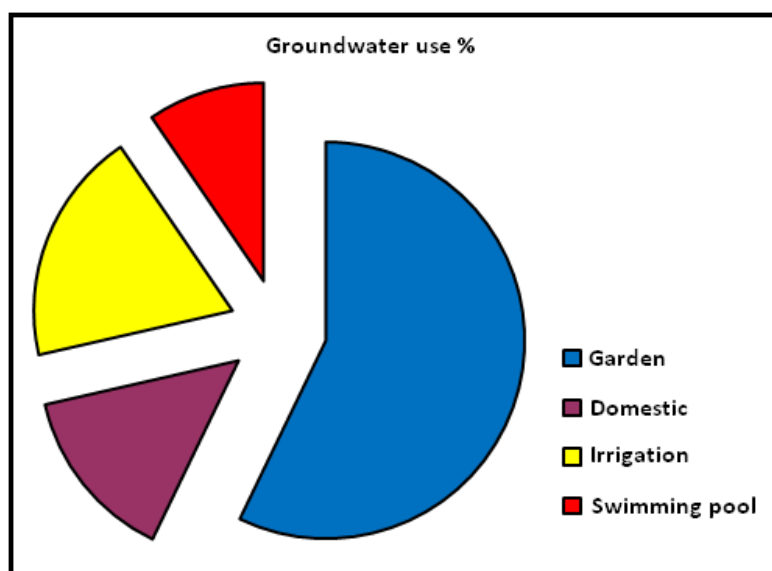


Figure 3-12 Groundwater use activities in the Beaufort West study area.

The groundwater use findings are in line with previous GPT results in which most boreholes were reported to be supplying water for gardening, with few being used for domestic purposes. Some of the gardens are no longer operational as the water is contaminated with both free and dissolved phase. For instance at borehole PW5 the owner had to abandon the gardening as the water is contaminated with free and dissolved phases of diesel product. With some people still using the water for domestic and swimming purposes, the risk to human health is a cause of concern.

In general the uptake of hydrocarbons in animal or human tissue is governed by similar principles to other lipophilic substances. Adsorption occurs through respiratory surfaces of the gastrointestinal tract and external surfaces, with the hydrocarbons generally being deposited in the lipid - rich tissues. Benzene is the most significant LNAPL compound with a high health

risk considering its carcinogenic effects. It was very sad to note how the local population in particular boreholes owners had been affected by the contamination; abandoned gardens, uncertain health effects for those who have been using the water, uncertainty about when the problem will be resolved among other observable effects. The need for a social scientist was and is still imperative to give counseling to the affected people, and is given as one of the study recommendations.

3.6 Summary of Chapter 3

In summary, Chapter 3 gives details on the preliminary investigations that were conducted prior to field tests and how they played a pivotal role in planning for the field tests. Old Geohydrology reports and GPT consulting reports contributed most to the desktop study. The desktop study captured information on the contaminant history, local and regional geology and geohydrology of the Beaufort West study area. A site survey was conducted following the desktop study and it prompted the need for a hydrocensus after free phase of petrol product was detected in a previously unmonitored borehole. The hydrocensus which was conducted in the vicinity of potential LNAPL sources to assess the groundwater use activities and extend of the contamination proved helpful in identifying drilling positions and boreholes to use for aquifer tests. Based on the information collected during the preliminary investigations, initial site conceptual model was then developed to kick start the field work. The next Chapter describes the geologic characterisation which was achieved through core and percussion drilling explorations.

4 Geologic Characterisation

Geological characterisation of the subsurface was achieved through drilling log analysis and visual observations made during the drilling. A total of 4 core and 2 percussion boreholes (Figure 4-1) were drilled on the Beaufort West study area as part of the LNAPLs project. The siting of the drilling positions was conducted by a contaminant geohydrology expert. During drilling, a PID was used to detect and measure VOCs and the environment was deemed safe for work.

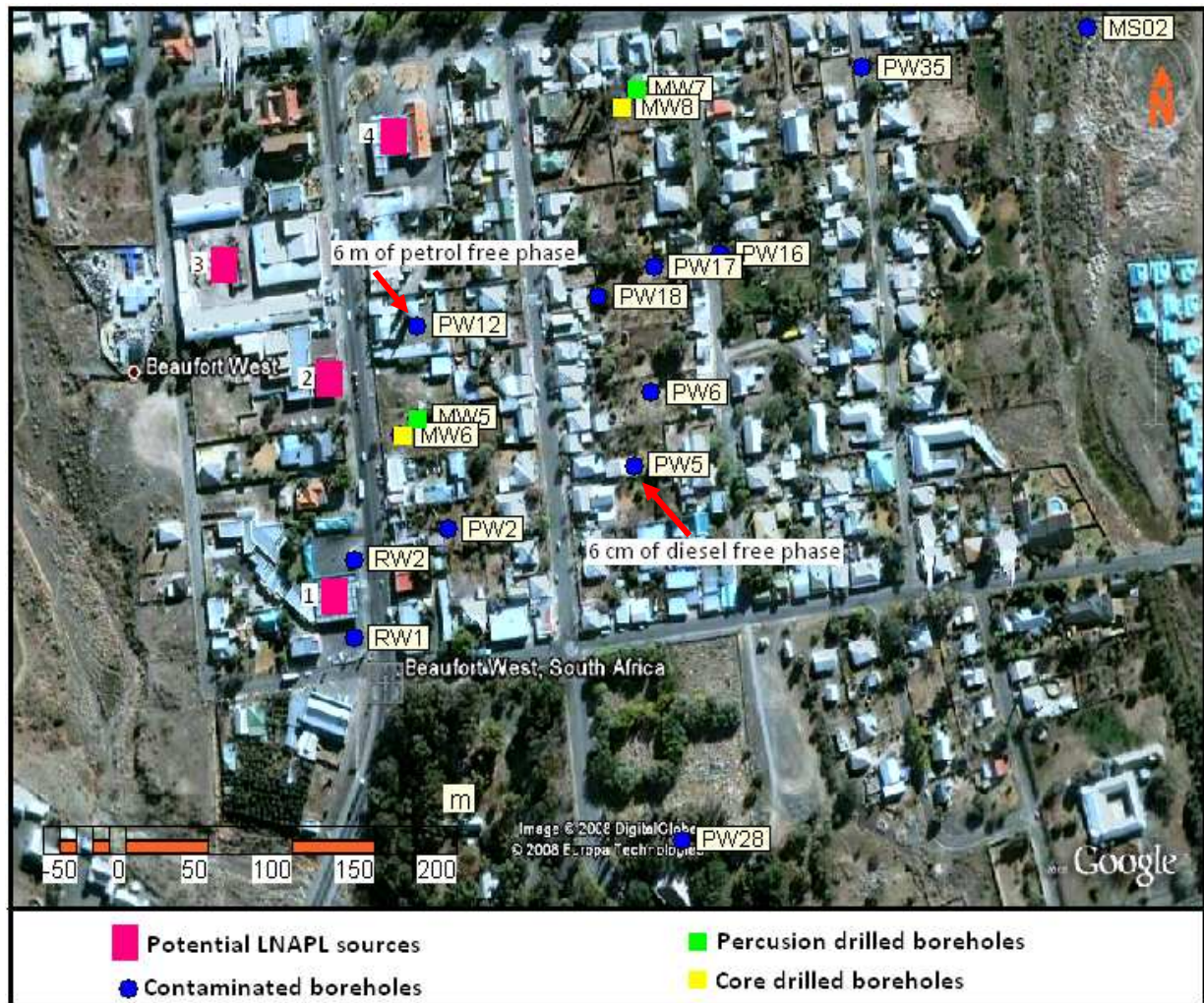


Figure 4-1 Location of newly drilled boreholes in relation to the contaminated boreholes and potential LNAPL sources on the Beaufort West study area.

Drilling was also conducted with the idea of using the new boreholes for downhole geophysical logging and aquifer testing. The aim of the drilling exercise was to compare the conventional percussion drilling to core drilling. The comparison was carried out to assess the applicability

of various geohydrological techniques as complimentary tools for characterising an LNAPL contaminated fractured rock aquifer. Comparison and discussion of geological logs and other observable features during the two drilling techniques were also conducted. The comparison helped to determine how these methods can be used most effectively, separately or in combination, to maximize information about lithology and fracture location in a fractured rock aquifer. The geological logs and observed fracture features were then cross correlated with borehole geophysics to maximize subsurface understanding.

4.1 Core Drilling

Core drilling is an effective tool where detailed structural geologic analysis is necessary to identify and quantify contaminant migration pathways (Bunker, 1998). Structural and lithologic information obtained from oriented cores provide an understanding of migration pathways, more importantly with regard to fracture networks which are hydraulically very conductive. Core drilling technology is widely used in the petroleum, mining exploration and engineering geology construction industries, but can also yield valuable information for groundwater exploration and contamination studies.



Figure 4-2 Core drilling equipment used at the Beaufort West study area (Taken during the field work).

Core drilling equipment (Figure 4-2) involves use the of a core barrel, attached at the bottom of a string of rods, which is rotated and advanced through the soil or rock to obtain a core sample of the material. Water or drill fluid is used to cool the cutting bit and to carry cuttings to the surface. The cutting bits are usually constructed of steel with carbide inserts or with impregnated diamonds. To retrieve a core cut with a conventional core barrel, the entire string of drill rods must be removed from the hole. The wire line of the core barrel has an inner barrel which holds the core that can be pulled up through the drill rods thereby eliminating the need to remove the entire string of drill rods.

Core drilling presents the opportunity to view and assess fracture orientations in situ while at the same time allowing sampling of solid core for laboratory matrix and porosity measurements. With a maximum of core recovery, it is possible to determine the dip and strike of fractures. It is however difficult in some cases to distinguish between natural and drilling induced fractures, especially in geological rocks of high cleavage (for instance in shale formation). Despite the valuable and superior results from core drilling, it is a costly exercise and requires well skilled and experienced drillers for maximum core recovery. Tire'n, *et al* (1999) highlighted one of the main challenges of the core drilling as the tediousness involved in orienting of the core, more importantly in fractured rocks where it is difficult to restore the core rendering orienting almost impossible. This challenge has great implications to the use of core drilling as part of fractured rock characterisation given that the main goal is to view and asses fracture orientations in situ.

Additional information can however be obtained through the use of a borehole camera to analyse core drilled wall. The borehole camera can be used in conjunction and or compared with core logged data to optimize subsurface geological understanding. In most cases, percussion drilling and coring are often followed by borehole geophysics logging to maximise information on the fractured zones (US EPA, 2001). As part of this study, 2 core boreholes (MW6 and MW8) were drilled. During the drilling exercise, geological logging and core sampling were performed in most cases accompanied by photos.

4.1.1 Core Geological Logs

4.1.1.1 MW6 Core Geological Log

Figure 4-3 shows MW6 geological core log. From the geological log, it is evident that the uppermost layer of the Beaufort West study area is characterised by a thin layer of river sand

underlain by sandstone boulders which are part of the river sequence deposition. This is expected considering that the study area is located in the Karoo basin where quaternary deposits are a major characteristic along rivers. It is important to highlight that this river depositional sequence characteristic occupying the top unconsolidated layer was observed in both percussion and core geological logs. The underlying consolidated material comprises of sandstone interlayered with mudstone and shale formations which are typical Karoo Supergroup attributes.

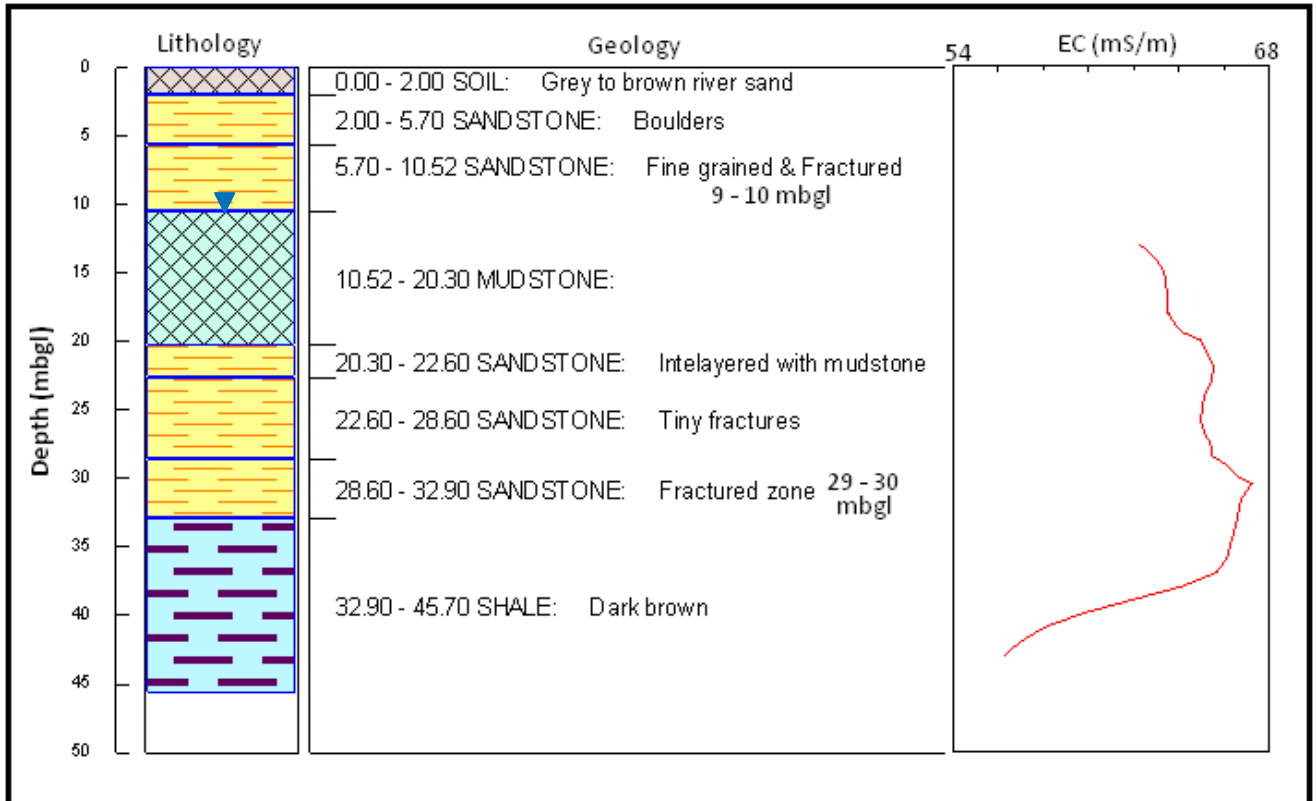


Figure 4-3 MW6 core geological log and EC log.

Observed features on MW6 core geological log (Figure 4-3) include; vertical to subvertical fractures intersected from 9 - 10 mbgl and at 31.5 mbgl as depicted on Figure 4-4 and 4-5 respectively. The fractured zone between 9 -10 mbgl lies in the sandstone formation and was intersected in the unsaturated zone. The influence of the fracture intersected between 9 - 10 mbgl is difficult to evaluate using EC logging considering that it's located in the unsaturated zone. The identified fracture at 31.5 mbgl correlates closely to the EC logging (Figure 4-3) where a peak anomaly of 67.3 mS/m was also observed at 31.5 mbgl. The fracture intersected at 31.5 mbgl (Figure 4-5) in MW6 core hole can be inferred to be one of the preferential flow

pathways. In this situation, the fracture is possibly conveying contaminated groundwater or naturally high TDS groundwater as indicated by elevated EC.



Figure 4-4 Fractured sandstone between 9 - 10 mbgl in MW6 core borehole (Taken during the field work).



Figure 4-5 Fractured sandstone at 31.5 mbgl in MW6 core borehole (Taken during the field work).

4.1.1.2 MW8 Core Geological Log

Figure 4-6 shows MW8 core geological log. Of particular interest on MW8 geological log besides the quaternary depositional sequence observed in all the logs is the location of fractured zones at 8.9 mbgl (Figure 4-7) and 10.7 - 11.5 mbgl (Figure 4-8). The first subvertical fracture intersected at 8.9 mbgl is located in the consolidated mudstone formation of the unsaturated zone (Figure 4-7). Despite this subvertical fracture feature being intersected in the unsaturated zone (Figure 4-7). Despite this subvertical fracture feature being intersected in the unsaturated zone, it still has the potential to act as a preferential flow path for both groundwater and LNAPL contamination. It can contribute immensely to aquifer recharge and also accelerated contaminant movement in the unsaturated zone towards the water table.

Another vertical fracture (Figure 4-8) in sandstone formation was identified between 10.7 - 11.5 mbgl and is still located above the measured water level of 12.6 mbgl. It is important to highlight that in both core drilled boreholes (MW6 and MW8) which are about 275 m apart, subvertical to vertical fractures were intersected in the vadose zone. These fractures are most likely responsible for conveying contaminants vertically towards the water table.

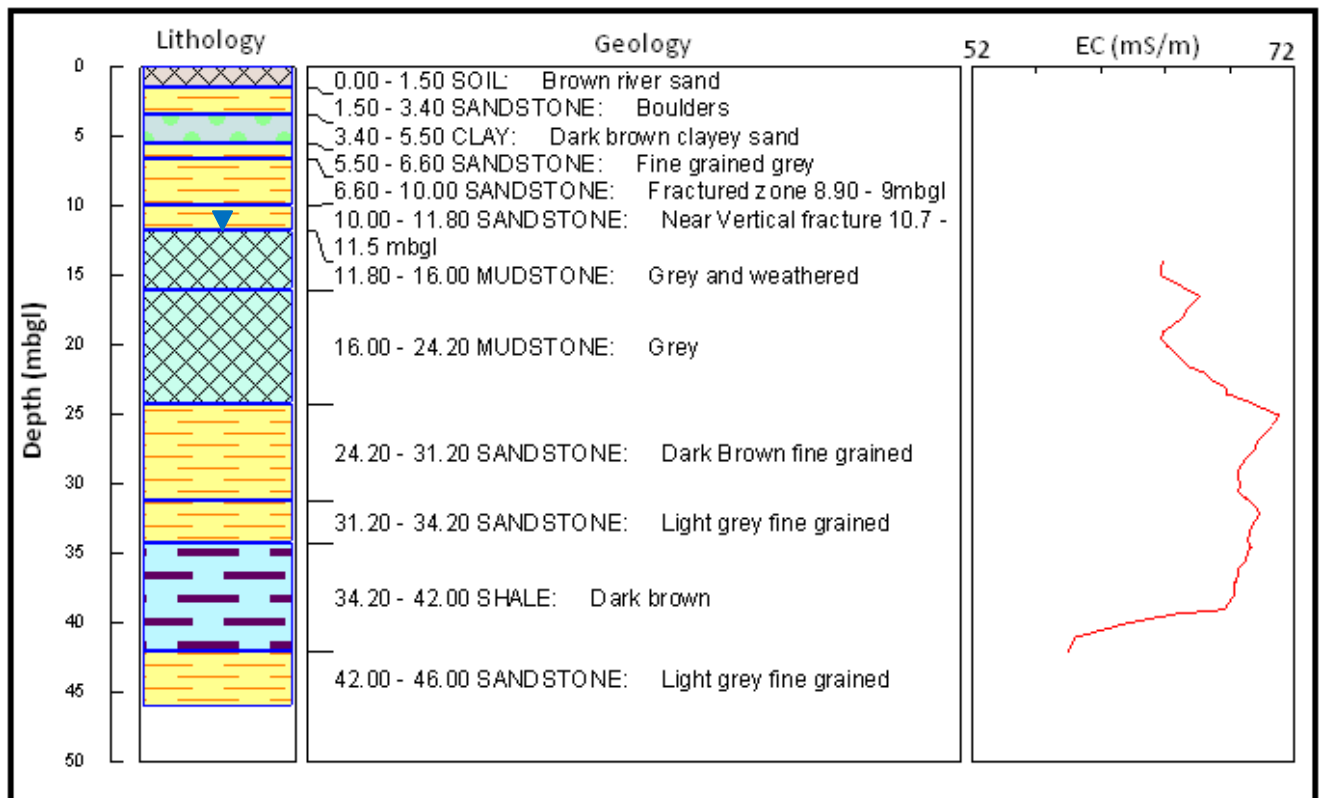


Figure 4-6 MW8 core geological log and EC log.



Figure 4-7 Subvertical fracture intersected at 8.9 mbgl in MW8 core borehole (Taken during the field work).



Figure 4-8 Vertical fracture intersected from 10.7 - 11.5 mbgl in MW8 core borehole (Taken during field work).

4.1.1.3 Core Logs Correlation

Core geological logs from MW6 and MW8 boreholes which are about 270 m apart were compared with the objective of trying to relate the observed geological formation to the depth of location and thickness. Figure 4-9 shows the lithologic correlation between MW6 and MW8

core geological logs. All the identified formations can be linked in depth between the two logs with negligible variation in sedimentary layers' thickness, which could be a function of other geological processes. The analysis is of great value in the geological characterisation of LNAPL contaminated fractured rock aquifer and will be used to define the geological conceptual model.

Based on the core drilling results, it can be concluded that river sand, sandstone interlayered with mudstone and shale formations constitute the study area subsurface lithology. Sandstone being the main constituent of the formation forms the fractured water bearing aquifer. The bulk of the fluid flow takes places in the fractures while matrix diffusion is also a significant factor. The fact that all identified formations between the two core holes (Located about 270 m apart) can be related to depth of location is good evidence to show the core drilling's ability to characterise the geological subsurface.

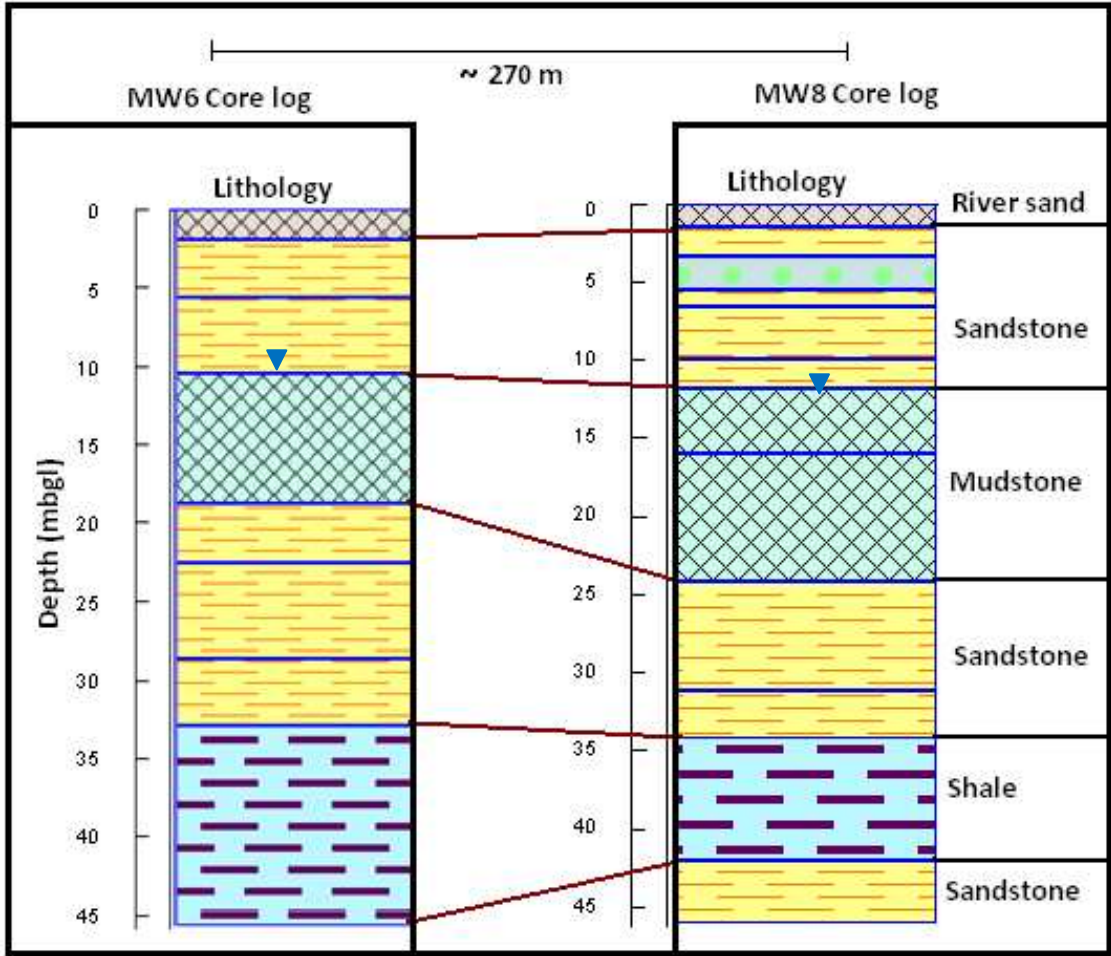


Figure 4-9 Core geological log correlation between MW6 and MW8 core boreholes.

4.2 Percussion Drilling

Traditionally percussion drilling is used to drill boreholes for groundwater abstraction. However, it can also be of insurmountable value for contaminated site investigation, in particular site characterisation and monitoring purposes. According to US EPA (2001), drilling boreholes remains the principal means of geological characterization. Because percussion drilling is generally slow and inexpensive, it contributes significantly to the reduction of site characterization cost. It is possible to obtain geological logs, but interpretation is much difficult because most of the drilling cuttings are crushed into fine soil material, making it difficult to relate to rocks of origin. Percussion drilled boreholes at the study area (Figure 4-10) were also meant to be utilized during aquifer tests and borehole geophysics. The use of newly drilled boreholes for aquifer test meant the presence of geological and borehole data to be used during aquifer test planning. There is more merit in having geological and geohydrological data for boreholes prior to the conducting of aquifer tests and borehole geophysics logging. The availability of such data enables good aquifer test planning in the selection of equipment and test depths among other aquifer tests requirements. Rotary air percussion drilling method (Figure 4-10) was used for this drilling exercise.



Figure 4-10 Air rotary percussion drilling equipment used at the study area (Taken during the field work).

With the air rotary percussion drilling method, air alone lifts the cuttings from the borehole. A large compressor provides the air which is forced into the drill pipe and escapes through small ports at the bottom of the drill bit, thereby lifting the cuttings and cooling the drill bit. The

cuttings are blown out to the top of the hole and collect at the surface around the borehole. The capacity of the compressor dictates the drilling depth and diameter. Cutting removal is a function of the air up hole velocity, which should be sufficient to lift them to the surface provided they grounded finely enough. Two percussion boreholes (MW5 and MW7) of 45 m depth were drilled, geologically logged and soil samples were also collected for VOC analysis. VOC analysis was important, especially considering the potential of compressed air percussion drilling method to volatilise the LNAPLs.

4.2.1 Percussion Geological Logs

Figure 4-11 and 4-12 shows the geological logs for MW5 and MW7 percussion boreholes respectively. Results from both logs indicate the presence of river depositional materials dominated by river sand and pebbles in the thin unconsolidated section. As expected, the underlying consolidated section is composed of sandstone, mudstone and shale which are typical Karoo Supergroup attributes.

4.2.1.1 MW5 Percussion Geological Log

Figure 4-11 shows geological log of MW5, which is a percussion dilled borehole.

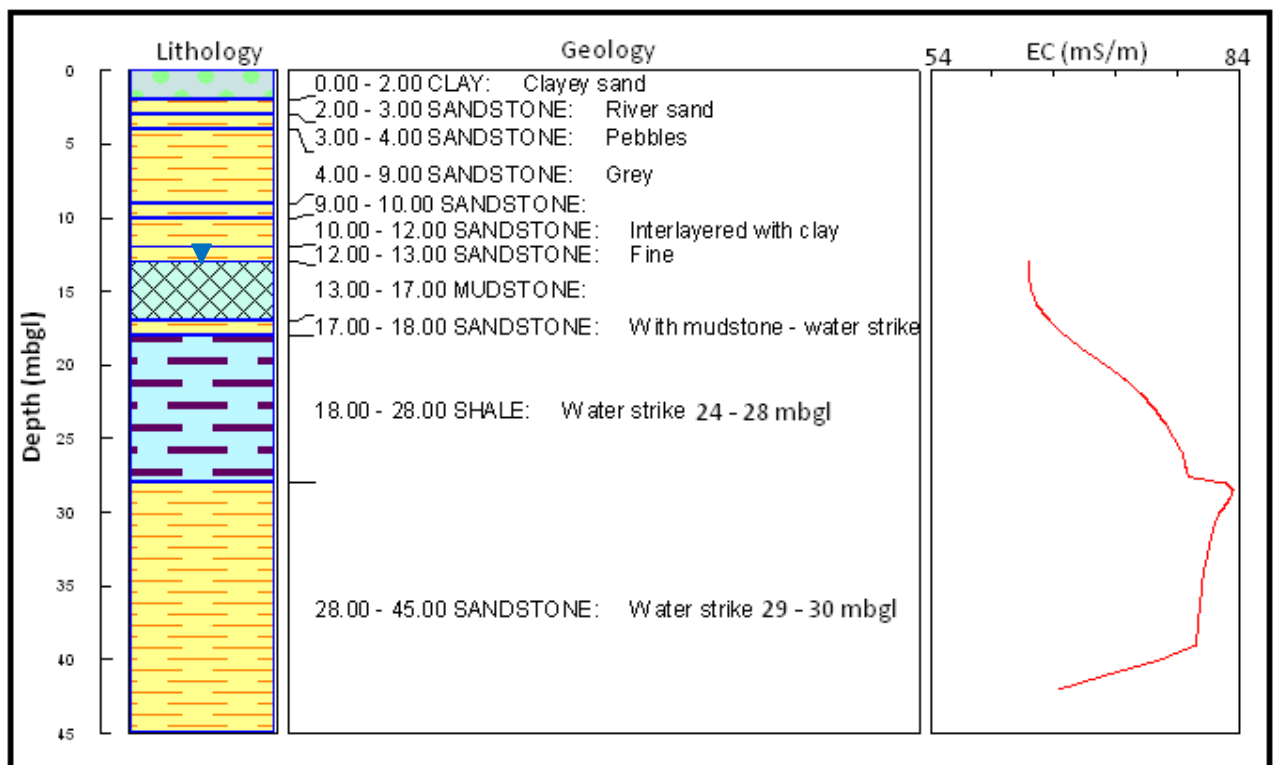


Figure 4-11 MW5 geological log and EC log.

Of particular interest on MW5 percussion geological log (Figure 4-11) is the shale and sandstone contact area at about 27.5 mbgl which is also characterised by an elevated EC of 84 mS/m. Sedimentary deposit contact areas are important for hosting bedding plane fractures that can act as a preferential flow paths to both groundwater and contamination. On the Beaufort West study area, the location of bedding plane fractures features has important implications for LNAPL migration and fate. Another shale and sandstone contact area associated with a water strike is observable on Figure 4-11 between 17 - 18 mbgl. It will be important to correlate drilling logs to borehole geophysics; such an analysis has been included in the borehole geophysics section (Chapter 5). A blow yield of < 0.1 l/s was measured on MW5 and is strong evidence to suggest that the intersected fractures are of low yields.

4.2.1.2 MW7 Percussion Geological Log

Figure 4-12 shows geological log of MW7, which is a percussion dilled borehole.

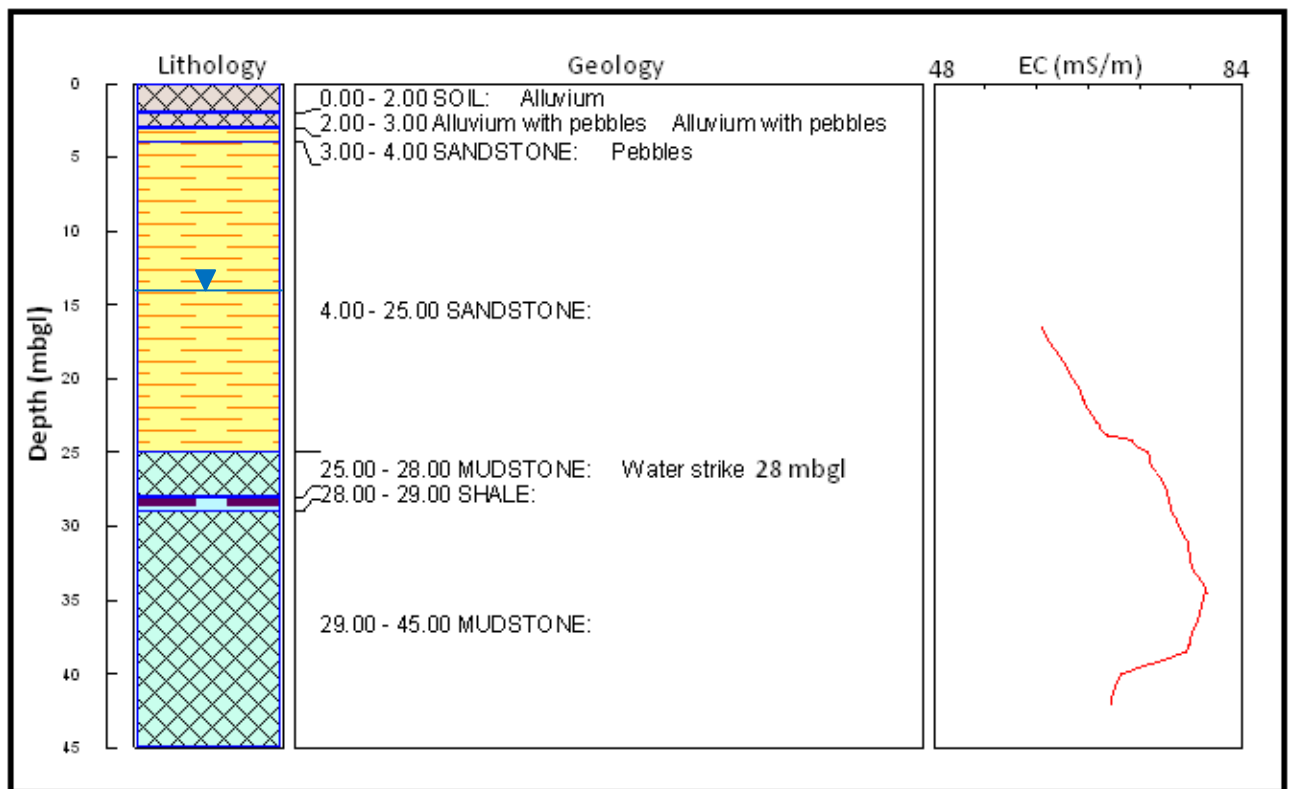


Figure 4-12 MW7 geological log and EC log.

Besides observation of the typical Karoo sedimentary depositions sequence, MW7 geological log (Figure 4-12) also shows the main water strike at 28 mbgl which is located close to the sandstone and shale contact area (25 mbgl). On average, a blow yield of 0.8 l/s was measured

suggesting the possibility of a high yielding fracture being intersected as a bedding plane fracture at a sandstone and shale contact area. It is important to note that the location of water strikes in both MW5 and MW7 percussion boreholes, between 25 - 30 mbgl are all on contact areas between sandstone and shale formation. Such an observation is strong evidence to suggest the existence of bedding plane fractures that are being intersected by the boreholes at different depths and are at different levels of connectivity as suggested by different blow yields.

4.2.2 Borehole Construction

In general, groundwater monitoring boreholes are necessary to collect precise and reliable data for understanding aquifer behavior. Important aspects of aquifer behavior include; groundwater flow directions and rates, groundwater quality and aquifer boundaries. The design and construction of test and monitoring boreholes at the study site placed some special consideration on the following aspects:

- The compatibility of construction materials with LNAPLs.
- Allowing for the collection of both free phase product and water samples.
- Technical capability and availability of the material.

Boreholes were cased at shallow unconsolidated depths where the rock was weathered and weak, and were left uncased and unscreened below these zones. Figure 4-13 shows the borehole construction schematic for MW5 and MW7 percussion drilled boreholes. On the schematic a 5.7 m steel casing was used with 3 m of perforations made on its bottom to cater for the possible rises in water levels. In all drilled boreholes water levels of at least 9 mbgl were measured during and two weeks after drilling.

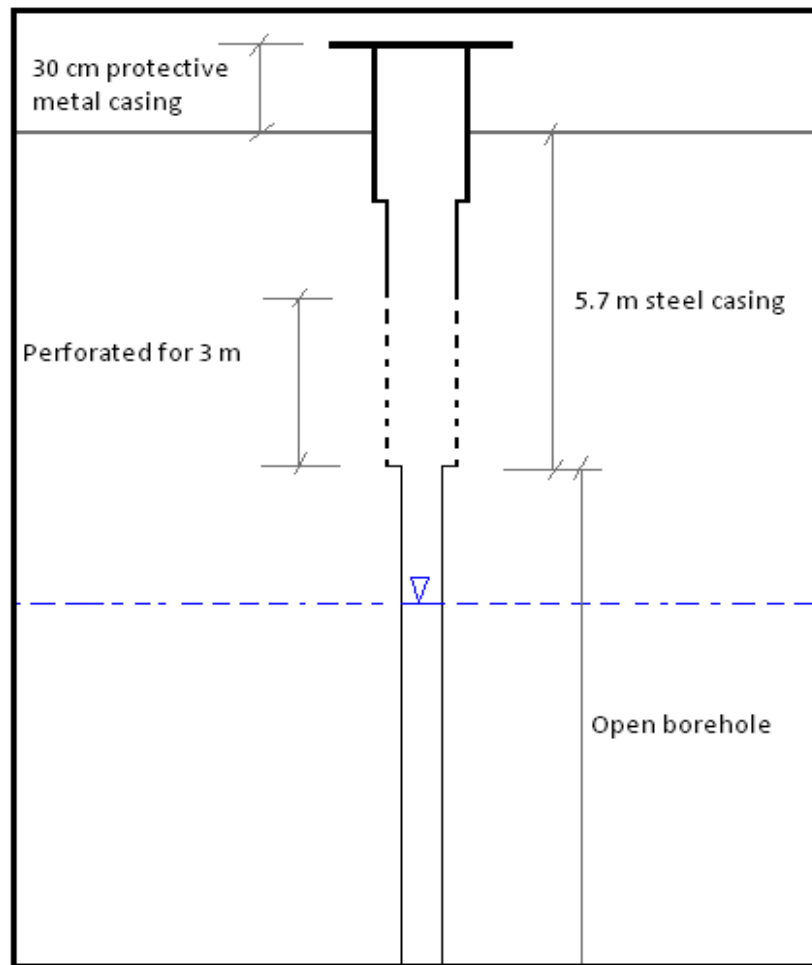


Figure 4-13 MW5 and MW7 borehole construction schematic.

Protective metal steel casing and locking caps (Figure 4-14) were installed at the two boreholes. This protection measure was put in place taking into consideration the existing public environment around these boreholes. The two boreholes (MW5 and MW7) will be used as part of the existing monitoring borehole network by the GPT consulting company working on the site.



Figure 4-14 Steel metal casing and locking cap placed on MW5 borehole (Taken during the field work).

4.3 Core and Percussion Logs Comparison

It was one of the drilling objectives to compare the core and percussion geological logs. The core drilling logs were used as the basis of comparison and correlation to assess the reliability of percussion logs. This comparison is based on geological logs logged by two MSc geohydrology students working together on each log. The lithologic correlation was based on the principle of original horizontality of sedimentary layers which state that “the sedimentary beds were originally deposited horizontally or nearly so” (GWS114, 2008). In other words observed sequence from the core logs would be expected to continue close to a horizontal manner unless tectonic processes such folding, faulting and or intrusion causes deviation from original horizontal position. As far as percussion drilling has been the principal means of geological characterization because of its low cost in comparison to coring. Other attributes besides cost were analysed and compared based on field observations.

Figure 4-15 shows a lithologic correlation between MW5 percussion and MW6 core geological logs. The boreholes are located only 4.7 m apart.

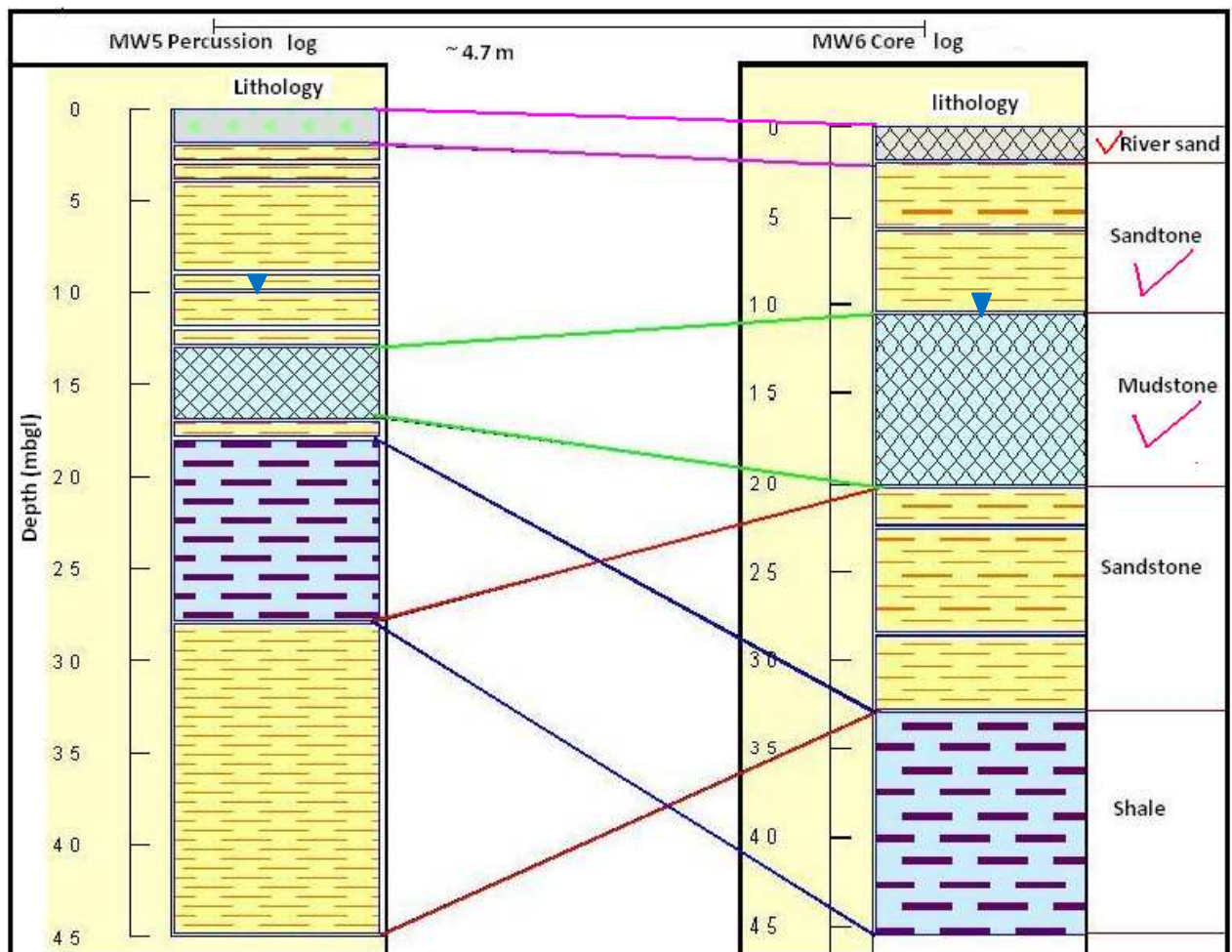


Figure 4-15 Geological log correlations between MW6 (Core) and MW5 (Percussion) boreholes.

It is evident from the correlation analysis (Figure 4-15), that only the first 3 layers (River sand, sandstone and mudstone) in that order from the top can be easily related in their depth of location between the two logs. This is despite the variation in thickness of layers, which is expected due to the subsurface heterogeneities and core losses during drilling. A rating of 60 % can be given for correct correlation of the first 3 layers out of a total of 5 (Figure 4-15). One of the main possible reasons for missing the last two layers could be the accumulation and mixing of drilling cuttings as the drilling depth increases and on hitting the first water strike. The first water strike in MW5 was at 1.7 mbgl. It is evident on Figure 4-15 that immediately after hitting the first water strike misinterpretation of formations also started to occur.

Figure 4-16 shows lithologic correlation between MW7 percussion and MW8 core geological logs. The boreholes are only 4.7 m apart.

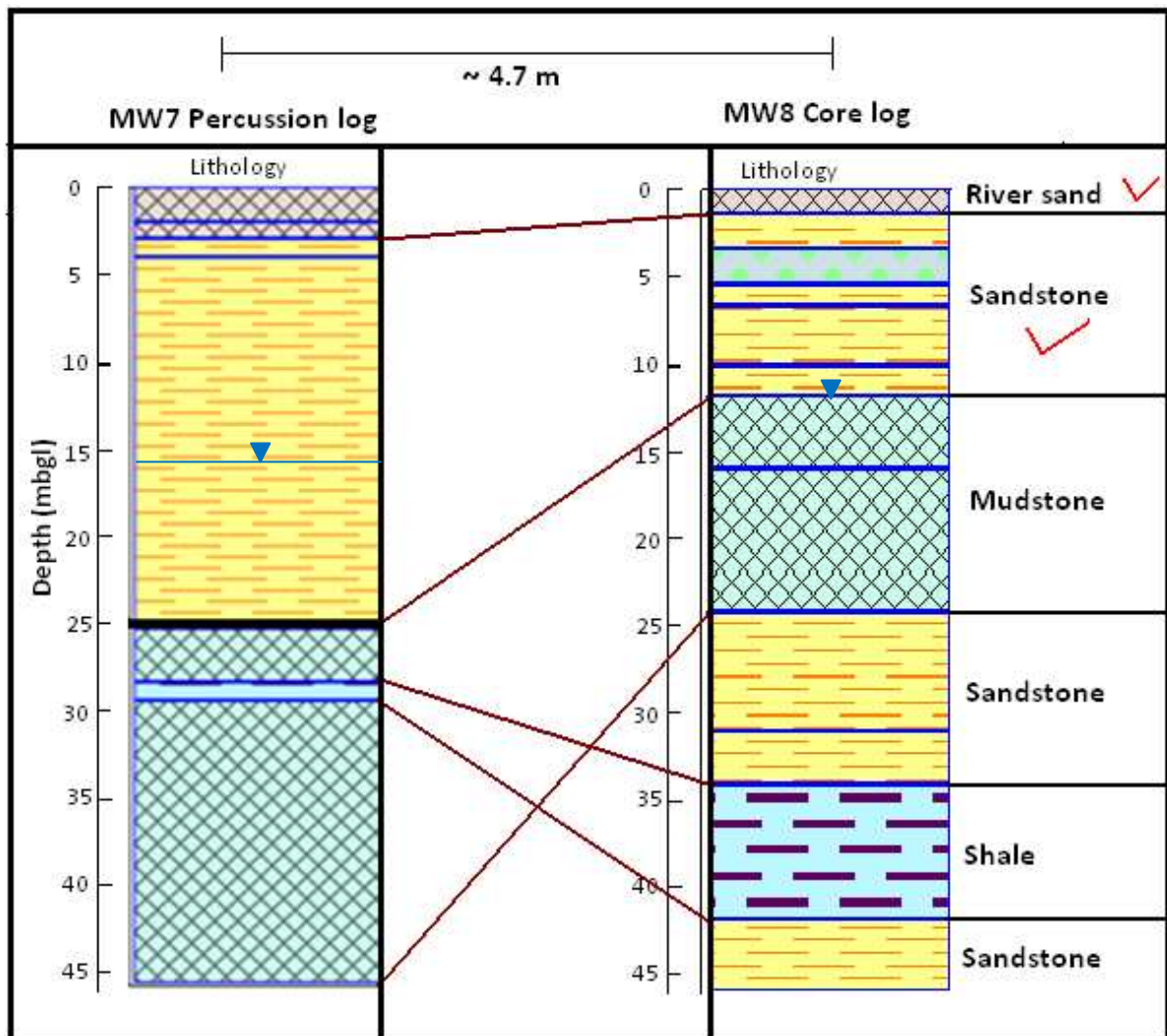


Figure 4-16 Geological log correlations between MW8 (Core) and MW7 (Percussion) boreholes.

The first two layers (top river sand and sandstone) can only be related in their order of layering and depth of location between the two boreholes logs (Figure 4-16) and would get a 50 % (2/4) rating. For the second layer (3 - 23 mbgl), MW7 percussion drilling log (Figure 4-16) only managed to identify sandstone which is the main formation, but missed mudstone interlayering. The percussion geological log also missed the majority of shale formation which is evident in MW8 core log between 23 - 42 mbgl. The positive and encouraging aspect is that percussion geology logs at least managed to identify the dominance of sandstone formation.

As highlighted in the first correlation analysis, the success rate achieved with percussion drilling in the first few top layers is due to the presence of less drilling cuttings. In most cases the drilling cuttings will be dry, making it easier to identify and relate to rocks of origin. It is a

fact that geological logging results (core or percussion) is largely depended on the capability and experience of personnel doing the logging. This fact might also have contributed on the results of this exercise considering that the logging was done by MSc students without much experience. The other important factor most likely to have contributed to the failure of percussion drilling to completely characterise the geological subsurface is the nature of sedimentary rocks in the study area in which the major constituent sandstone is interlayered with shale and mudstone. The existence of sandstone interlayered with shale and mudstone, can make it possible to interchange the formations during interpretation especially considering that a lot of mixing occurs during air percussion drilling.

It is an undeniable fact that crushed and pulverized drilling cuttings (Figure 4-17) are difficult to analyse and important information can be missed. Pulverization of drilling cuttings occurs after hitting the water strike and this was the case with the two percussion drilled boreholes at the study site. It important to highlight that in the next chapters only the core geological logs have been used for cross correlations and comparisons with borehole geophysics given their proved ability and reliability in subsurface characterisation. In other words, core geological logs formed the basis of the geology component for the study area's conceptual model.

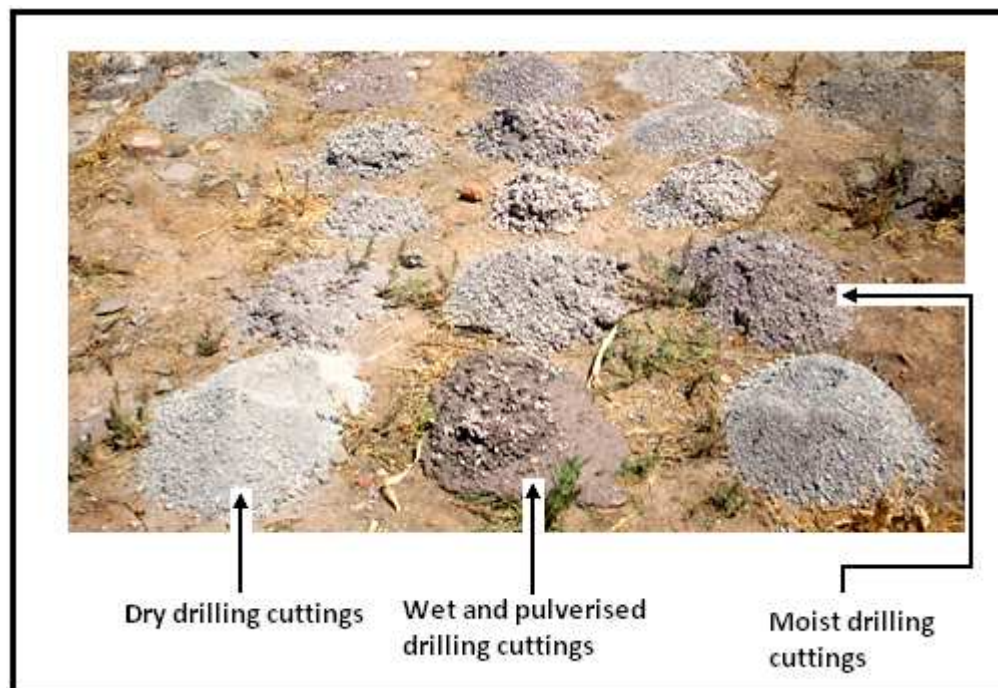


Figure 4-17 Typical drilling cuttings from the Beaufort West study area (Taken during the field work).

Table 4-1 gives a summary of the achievements and some flops of the two drilling methods used to characterise the geological subsurface of the Beaufort study area.

Table 4-1 Drilling achievements and failures at the Beaufort West study area.

Core drilling	Percussion drilling
Achievements	Achievements
1. In situ view of logs.	1. Water strikes identification.
2. Identification of fracture positions.	2. Soil samples collected for organic analyses.
3. Estimation fracture orientation.	3. VOC measurements were taken during drilling.
4. Physical core sampling for laboratory matrix and porosity experiments.	4. Bore diameter big enough to accommodate the downhole geophysics equipment.
Failures	Failures
1. Three core boreholes collapsed 2 days after drilling, could not be used for other tests.	1. Could not completely characterise the lithology.
2. Diameter of core hole too small to accommodate test equipment e.g. camera,	2. Did not identify any features, except after EC logging and cross correlation.

4.4 Summary of Chapter 4

In summary, Chapter 4 gives a detailed description of the subsurface geological characterisation, in particular the identification of fractures. This was achieved through drilling log analysis and visual observations made during the core and percussion drilling. As expected, core geological logs proved to be more superior in compared to percussion geological logs for characterising the geological subsurface. Vertical and subvertical fractures most likely responsible for facilitating the downward migration of LNAPL contamination towards the water table were identified on the Beaufort West study area. The drilling explorations however failed to locate the bedding plane fractures at shale/sandstone and

mudstone/sandstone weathered contact areas because the weathered material was washed away by the drilling mud. The next Chapter gives details on the borehole geophysics characterisation that was conducted at the Beaufort West study area with the objective of identifying preferential flow paths to groundwater and LNAPLs.

5 Borehole Geophysics Characterisation

Borehole geophysics logs can provide unbiased continuous and in - situ data. It also allows sampling of a larger volume than core and drill cuttings samples (Williams, 1998). Unlike the drilling geological log analysis that relies on the visual observation and the individuals' technical skills which may be biased, borehole geophysics logging has the potential to look beyond sidewalls which drilling logs usually depend on. Borehole geophysics investigations provide a cost - effective supplement to drilling due to the following factors:

- Relatively low cost.
- The ability of geophysics methods to look beyond the sidewalls of the borehole.
- The collection of in - situ data not available from a standard drilling program.

It is however important to note that borehole geophysics log interpretation is more of an art rather than a science because different phenomena can cause similar log responses (Welenco, 1996). In other words, there is no unique analysis and interpretation of borehole geophysics logs; there will always be various possible explanations for a single exhibited anomaly. It is that non - uniqueness property which brings the need to compare borehole geophysics to geological logs in trying to explain the observed anomalies. Borehole geophysics characterisation was conducted at the study area with the objective identifying preferential flow paths to groundwater and LNAPL contamination. Borehole geophysics equipment used on the Beaufort West study area consisted of; AV, FWS imaging, EC and Conventional logging [Resistivity, SP and Gamma].

5.1 Electrical Conductivity (EC) Logging

Contaminated groundwater is characterised by high electrical conductivity, thus it is possible to identify and infer zones associated with high electrical conductivity as preferential flow path to contaminants. According to Atekwana *et al* (1998) groundwater hydraulically conductive zones associated with the biodegradation of LNAPLs in the subsurface can provide a window into the biogeochemical processes ongoing at such sites. In such a situation, EC profiling would be more applicable considering that LNAPLs biodegradation by - products in form of organic and carbonic acid contribute to enhanced mineral dissolution leading to an increase in the amount of total dissolved solids. Hence the prevalence of elevated EC in the LNAPL contaminated aquifers is not unusual. EC logging as a borehole geophysics tool worked well on the study

area. Previous monitoring results by Gilbert (2006), suggested that LNAPL biodegradation is highly active.

5.1.1 EC Logging in Contaminated Private Boreholes

Electrical conductivity profiling was conducted on some of the contaminated private boreholes, during the process of selecting boreholes to use for the aquifer test. No geological logs or any drilling information is available about the private boreholes. EC logging proved to be of great value in revealing possible high hydraulic conductivity zones where elevated anomalies were recorded. The identified zones of high hydraulic conductivity were related to the location of possible water bearing fractures. Hydraulic conductive zones were targeted in tracer and pump testing, for pump positioning and tracer injection respectively.

For instance EC logging in PW5 (Figure 5-1) revealed an elevated EC at 23 mbgl. The observed anomaly at 23 mbgl was linked to a high hydraulic flow zone conveying degraded diesel product which according to (Hiebert *et al*, 1995) has the potential to generate carbonic acid during the biodegradation process. Electrical conductivity logging in PW2 private borehole (Figure 5-1) also indicated elevated EC values between 19 - 28 mbgl and the zone was targeted for the tracer tests.

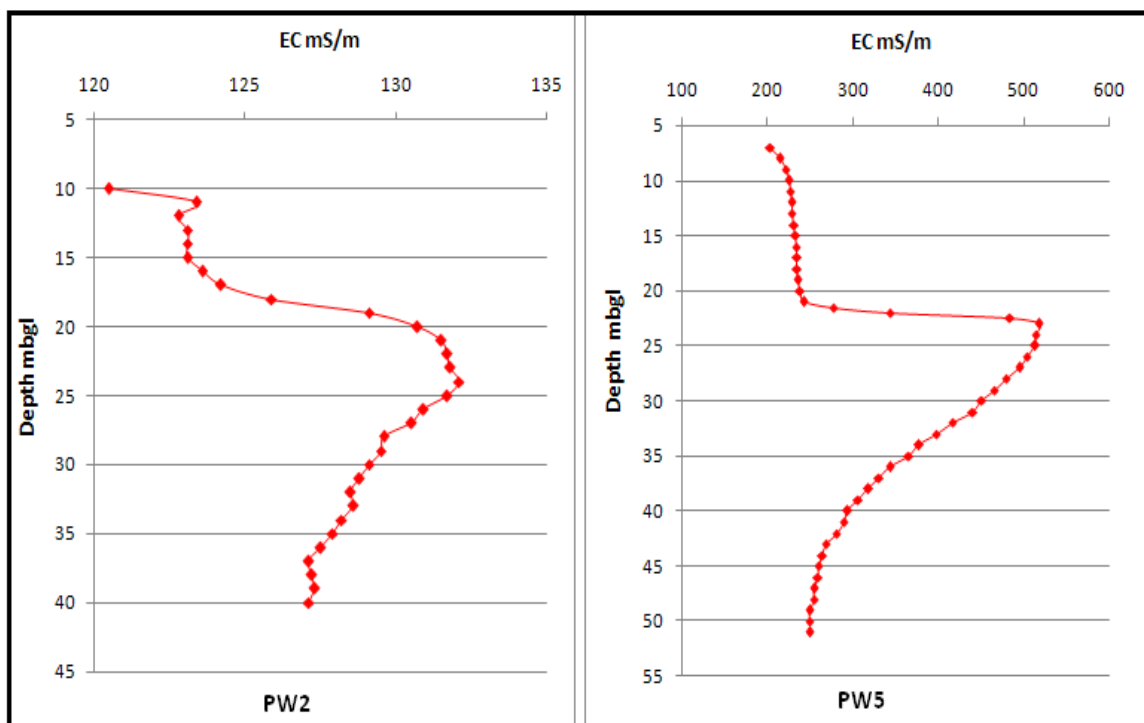


Figure 5-1 EC profile in PW2 and PW5 private boreholes.

5.1.2 EC Logging in newly Drilled Boreholes

Electrical conductivity profiling was conducted in newly drilled core and percussion boreholes prior to the aquifer testing and borehole geophysics logging. Identification of hydraulically conductive zones to contaminant and groundwater flow was the core objective. Electrical conductivity logging results were correlated to geological logs. The correlation presented an opportunity to test the concurrent applicability of geological and borehole geophysics logging site characterisation tools.

5.1.2.1 EC Logging in MW5 and MW6 Boreholes

Figure 5-2 shows the EC profile in core borehole MW6 and percussion borehole MW5 which are only 4.7 m apart. The profiles depict anomalies at 27.5 mbgl and 31.5 mbgl in MW5 and MW6 respectively. The EC anomaly in MW5 is attributed to the existence of a preferential flow path conveying LNAPL - contaminated groundwater. The preferential flow path being intersected in MW5 is most likely to be part of the fracturing system detected in MW6 core borehole which is evident on the core log at 31.5 mbgl (Figure 4-5, Section 4.1.1.1). It can be concluded from the two EC profiles that the two boreholes intersect the same fracture preferential flow path but at different depths. This conclusion however needed to be verified through the use of other complimentary tools for optimum subsurface understanding.

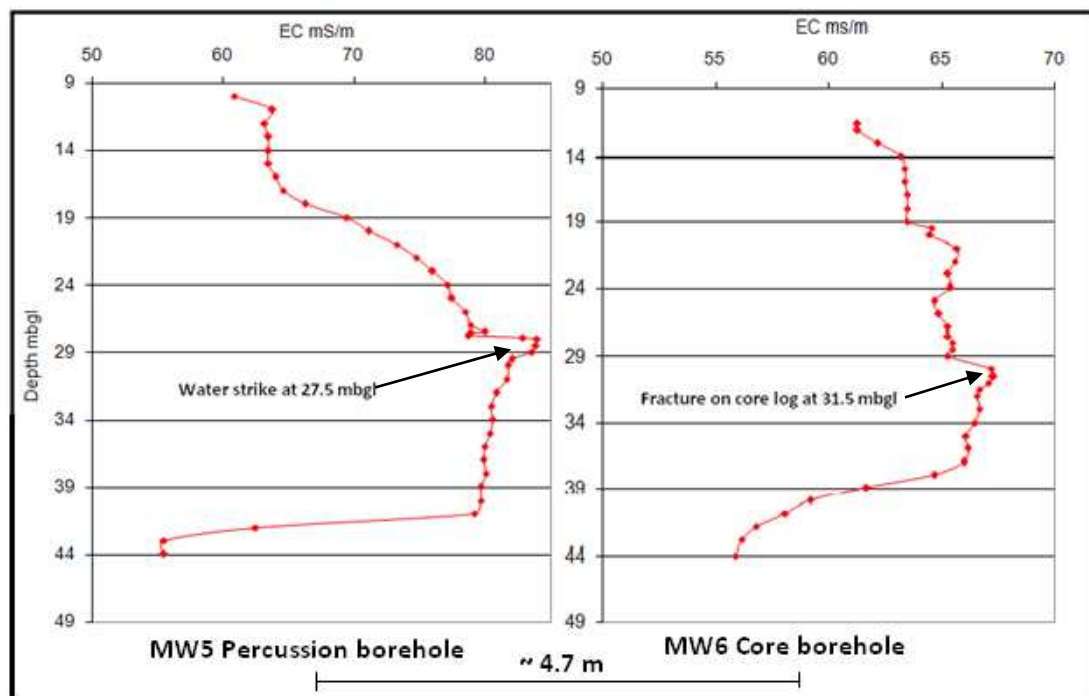


Figure 5-2 EC profiling in MW5 (Percussion) and MW6 (Core) boreholes.

5.1.2.2 EC Logging in MW7 and MW8 Boreholes

Figure 5-3 shows EC profiles in MW7 percussion and MW8 core boreholes. Displayed in both profiles are EC anomalies at 24 - 25 mbgl and 34 - 35 mbgl. The anomalies are most likely due to the weathering on the shale and sandstone contact areas, leading to the formation of a bedding plane fracture preferential flow path. MW8 geological core log also confirms the existence of shale and sandstone contact area as shown besides MW8 EC profile (Figure 5-3). It is most likely that that the two boreholes are intersecting the inferred bedding plane fractures at 24 - 25 mbgl and 34 - 35 mbgl. FWS, AV and conventional borehole geophysics logs (Section 5.2.2 and 5.2.3 respectively) also indicated clearly the existence of bedding plane fracture feature at those depths.

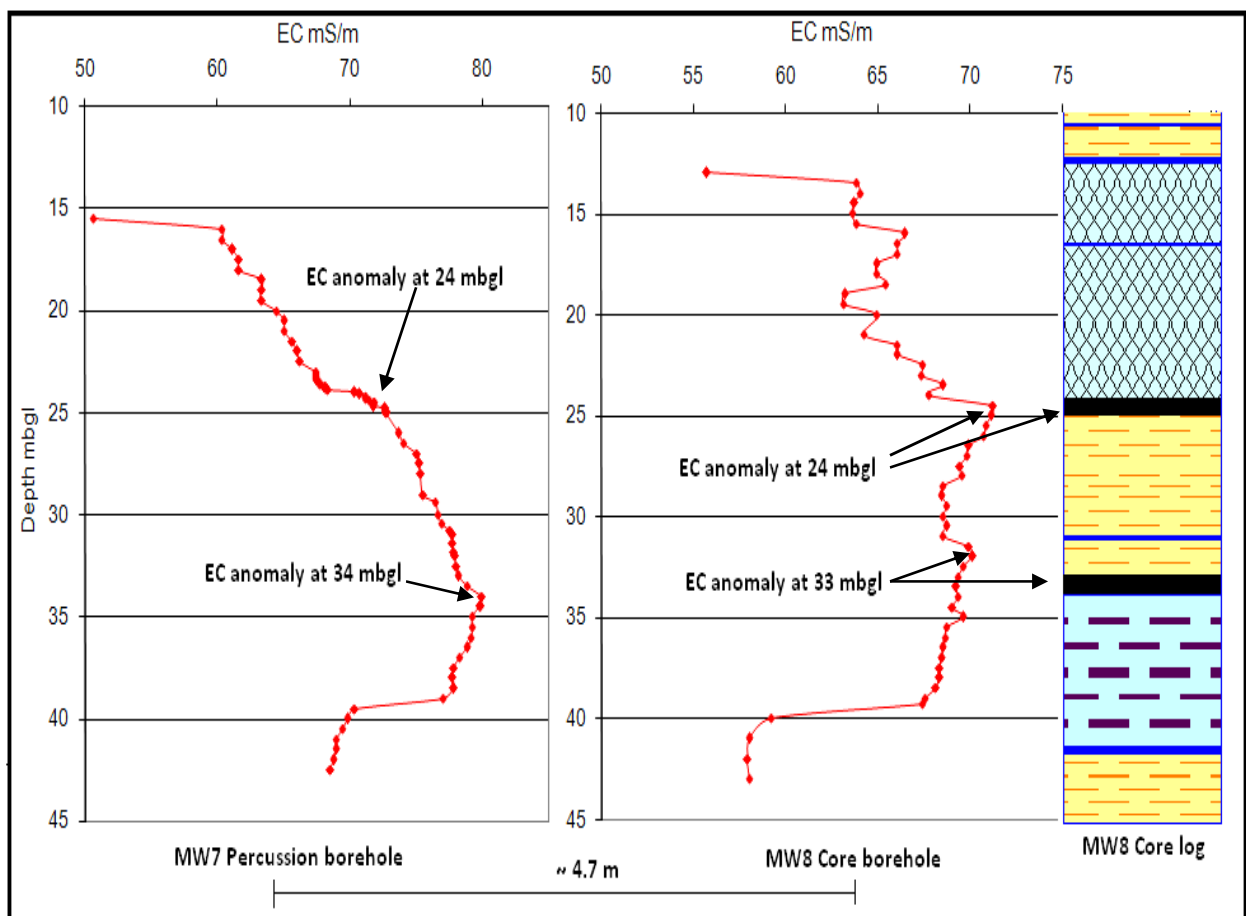


Figure 5-3 EC profiling in MW7 and MW8 boreholes and MW8 core geological log.

5.2 Combined Borehole Geophysics

Combined borehole geophysics toolbox used on the study area consisted of AV and FWS imaging and Conventional logging tools [SP, Gamma and Resistivity]. The results from borehole geophysics were correlated and also cross correlated to geological logs, with the objective of assessing the applicability and merits of using complimentary tools for characterising an LNAPL contaminated fractured rock aquifer. A short description about each tool is given in Section 5.2.1 before the presentation and discussion of results. Combined borehole geophysics logging was successfully conducted in MW6, MW7 and MW8 boreholes. Borehole camera was not used because its resolution was significantly affected by muddy colour of the borehole water.

5.2.1 Brief Description of the used Boreholes Geophysics Tools

1. Acoustic Viewer (AV)

Is a borehole geophysics tool that uses ultrasonic waves to scan the borehole wall. AV logs provide images of the acoustic reflectivity of an open fluid filled borehole wall. Fracture signatures are also observable and the tool enables measurement of fracture depth, orientation, dip, and apparent aperture where possible.

2. Full Wave Sonic (FWS)

Is a geophysical measurement of sound properties in an open hole in fluid filled formations. In general, formations could be filled by either fresh or contaminated groundwater. FWS logs can be used for fracture identification, lithologic and waveform analysis. The tool can also be used for rock property analysis such as porosity, permeability, competency, and rock strength.

3. Conventional Logging

3.1 Natural Gamma

The tool measures naturally occurring gamma emissions due to the decay of radioactive materials in the subsurface. Sodium - iodide crystal is used to detect gamma rays and the crystal produces a flash of light in response to a gamma ray collision within the detector (Keyes, 1989, Telford *et al*, 1990).

3.2 Resistivity

This tool measures the material's resistance to electrical flow. In a saturated porous material, the bulk resistivity is a combined electrical conductivity of earth materials and the pore fluid. Generally, in fresh pore water conditions, high resistivities are associated with coarse grained materials (sand and gravel), and low resistivities are associated with silt and clay. The decreasing resistivity in clay and silt is attributed to the increase of clay rich minerals with high electrical conductivity properties.

3.3 Spontaneous Potential (SP)

It measures the natural potential between the borehole fluid and the surrounding rocks. If the surrounding rocks are filled with water, the natural potential is a function of the geological formations. Differences in ion concentration exist between the borehole water and the water filling the surrounding rock formation and as a result a charge differences develops between the two. The charge difference is detected between the reference and measuring electrode and it gives a measure of the SP. It is useful for the identification and location of porous and permeable beds.

5.2.2 MW6 Logging

Figure 5-4 and 5-5 shows conventional logging, FWS and AV imaging in MW6 borehole from 15 - 20 mbgl. Of importance is an anomaly displayed in both logs between 18.5 - 19 mbgl. It is important to note that emphasis has only been placed on the depths with geophysics and geological features of interest. Complete borehole geophysics logs have been placed in Appendix 2. It is important to highlight that the radius of MW6 borehole was not big enough to accommodate the borehole camera with required flexibility for maximum performance. Furthermore the borehole water was too dirty for the camera to obtain clear pictures; hence video logging was not performed.

5.2.2.1 Bedding Plane Fracture Feature between 18.5 - 19 mbgl

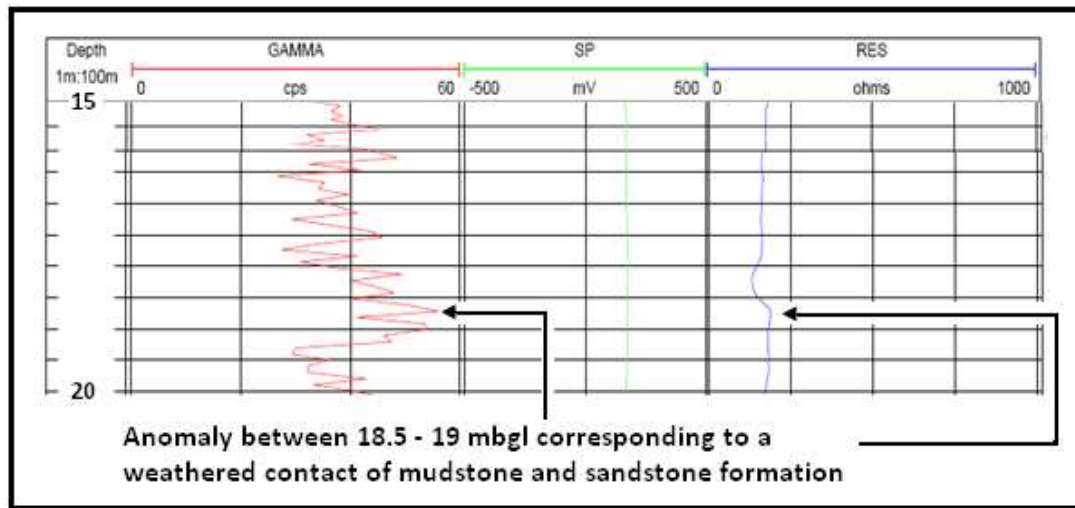


Figure 5-4 Gamma, Resistivity and SP logs from 15 - 20 mbgl in MW6 core borehole.

Gamma and Resistivity logs also show the same anomaly between 18.5 - 19 m depth (Figure 5-4). The elevated gamma and resistivity values at 18.5 - 19 mbgl, (mudstone/sandstone contact area) are most likely due to the existence of arkosic (feldspathic) minerals from weathered sandstone. In such a situation the high percentage of potassium feldspar is associated with increased amounts of potassium isotope (K_{40}). Potassium isotope is the most natural abundant radioactive isotope recorded on the natural gamma which results in higher gamma counts associated with increases in resistivity (Keyes, 1989). Resistivity follows the same increasing trend as influenced by quartz minerals of low electrical conductivity in the sandstone formation of the Beaufort group. Figure 5-5 shows AV and FWS logs from 15 - 20 mbgl.

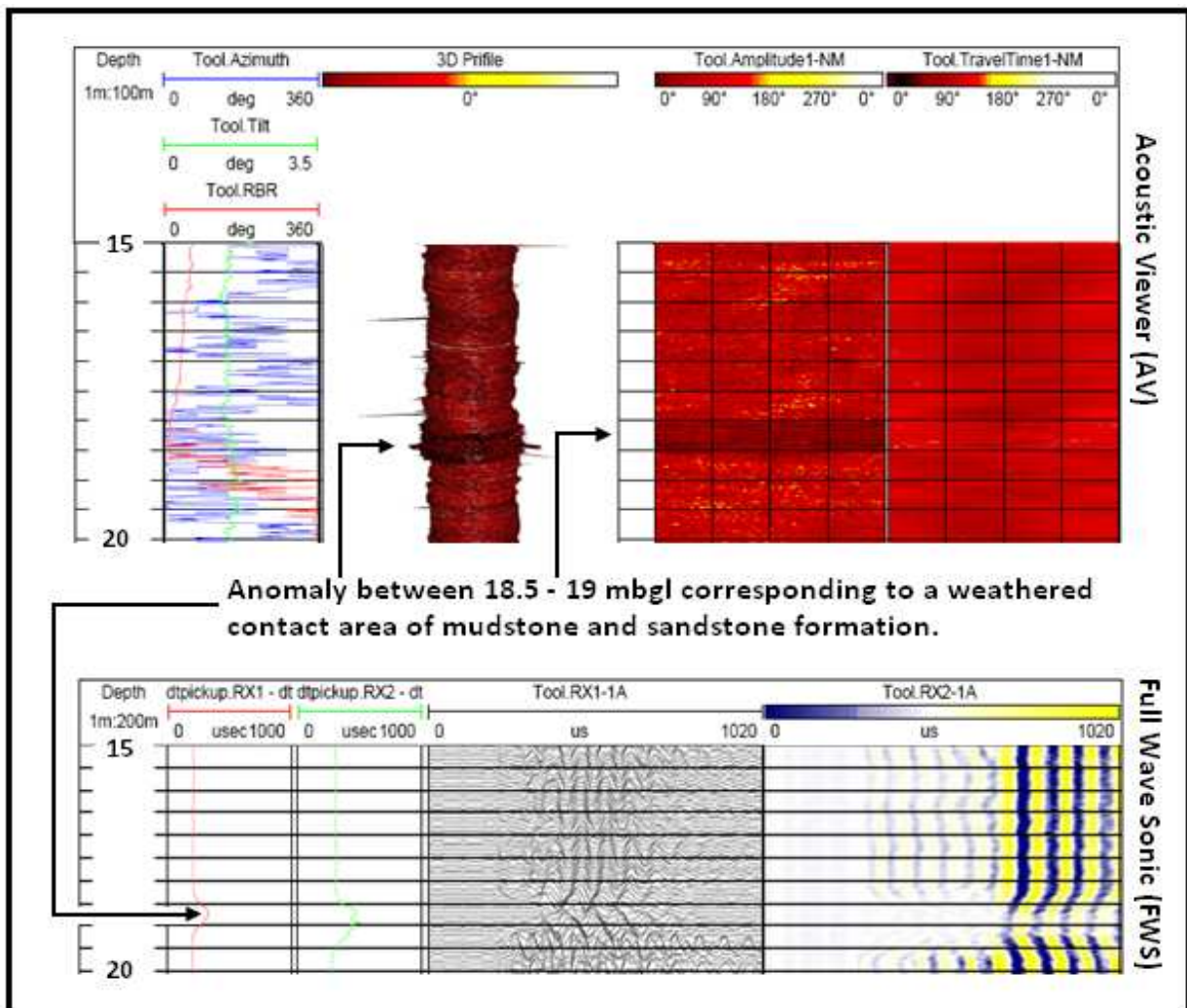


Figure 5-5 AV and FWS images from 15 - 20 mbgl in MW6 core borehole.

From AV (Figure 5-5), the existence of a horizontal oriented fracture feature is evident on the 3D view image between 18 - 19 mbgl. The displayed feature is characterised by a high travelling time and low amplitude. The FWS (Figure 5-5) further shows the horizontal fracture feature (18 - 19 mbgl) being associated with low wave amplitude and increased travelling time which is an indication of reduced wave velocity in the formation. A cross correlation to core geological logs closely suggest the presence of a bedding plane fracture feature at the mudstone and sandstone contact area (see MW6 geology log on Figure 4-3 in Section 4.1.1). It was also evident during the visualization of core geological logs that the contact area is heavily weathered, thus sonic waves were attenuated as shown by the reduced wave velocity leading to increased travelling time (Figure 5-5).

5.2.2.2 Fracture Feature in Sandstone Formation at 31.5 mbgl

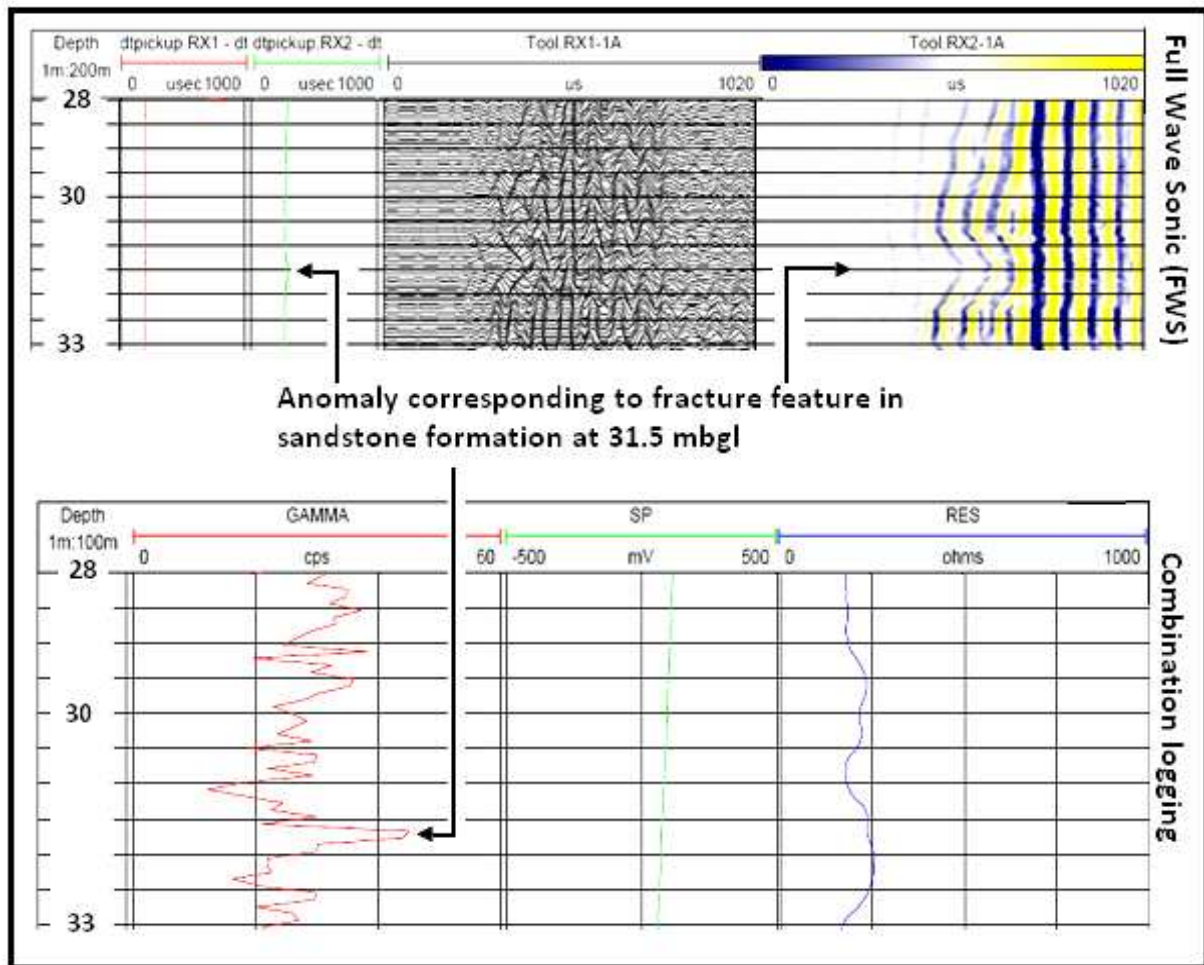


Figure 5-6 FWS and conventional logs from 28 - 33 mbgl in MW5 borehole.

The existence of a fracture feature anomaly at 31.5 mbgl is evident on both FWS and conventional logging (Gamma and Resistivity) (Figure 5-6). On the FWS image the fracture feature at 31.5 mbgl is characterised by a low amplitude sinusoidal wave at high travelling time, an indication of reduced wave velocity. The reduced wave velocity is most likely due to the attenuative effects of feldspathic clay (sandstone weathering product) filling the fracture feature at 31.5 mbgl. Acoustic viewer imaging could not detect the fracture feature at 31.5 mbgl and for that reason the log is not presented.

Gamma and Resistivity logs also confirmed the existence of a fracture feature at 31.5 mbgl with elevated values (Figure 5-6). The most likely reason for the Gamma log displaying an increase of natural gamma emissions in a sandstone formation is the presence of arkosic (feldspathic) clay minerals from sandstone filling the fracture. A closer look at Resistivity log

anomaly (Figure 5-6) fully supports the suggestion of arkosic (feldspathic) clay minerals from sandstone filling the fracture, because the anomaly take a small dip at 31.5 mbgl distinguishing from the high resistivity surrounding solid sandstone.

5.2.3 MW7 Logging

5.2.3.1 Horizontal Bedding Plane Fracture Feature at 24.5 mbgl

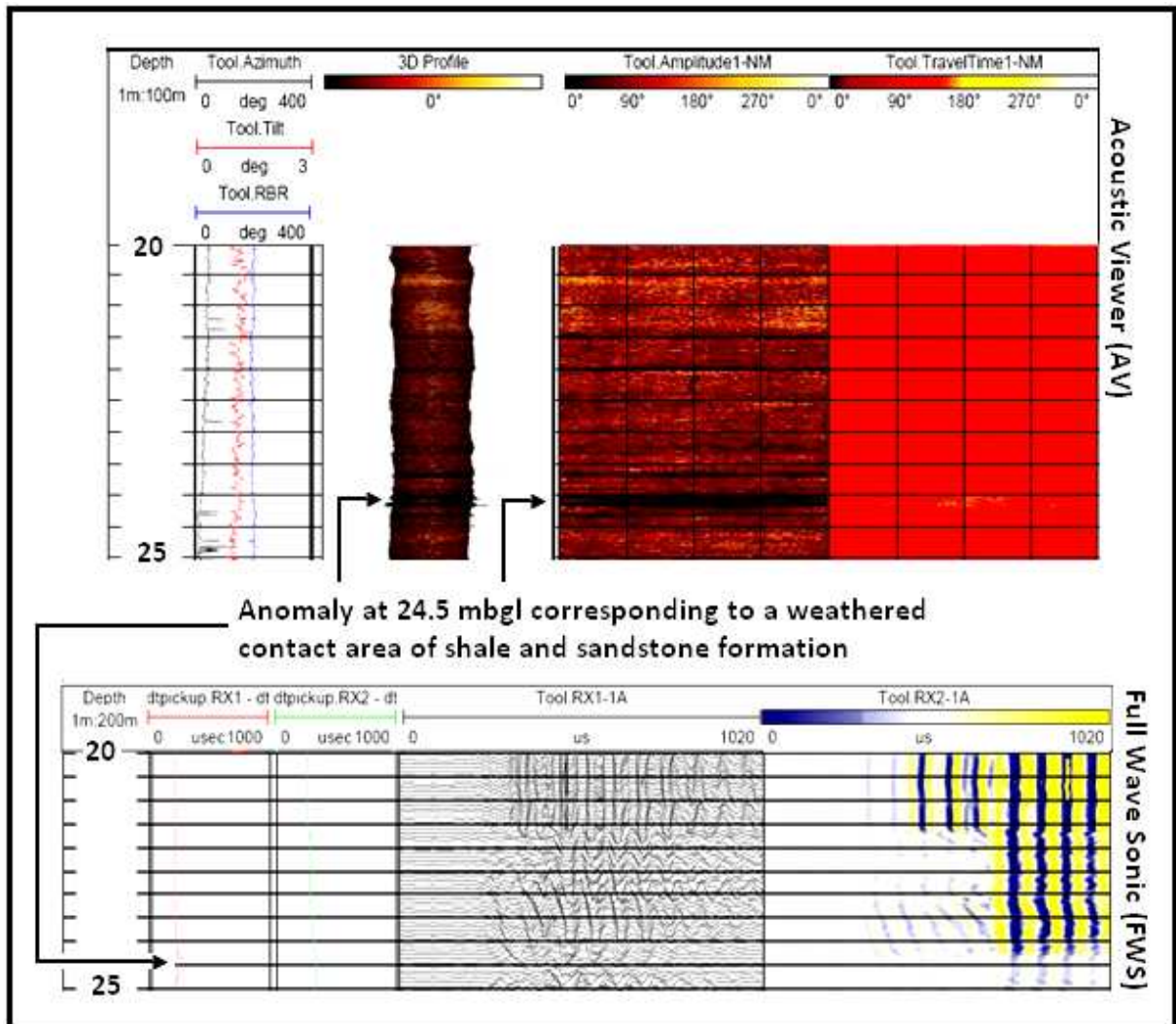


Figure 5-7 FWS and AV images from 20 - 25 mbgl in MW7 borehole.

Figure 5-7 shows AV and FWS borehole geophysics logging from 20 - 25 mbgl in MW7 borehole. Acoustic Viewer log displays the horizontal bedding fracture feature on the 3D image. The observation on the AV log is supported by an anomaly on the FWS log which shows an increase of wave travelling time at 24.5 mbgl which is associated with a reduction in

wave amplitude (Figure 5-7). Cross correlation to MW7 geological log (Figure 4-12, Section 4.2.1) shows the presence of a sandstone and shale contact area between 24 - 25 mbgl. It was also evident during core log visualization that the contact area is heavily weathered and is the most probable reason for the anomaly. Sonic waves are retarded and attenuated in loose weathered formations, resulting in an increased wave travelling time and low wave amplitude. Gamma log on Figure 5-8 also confirmed the presence of a bedding plane fracture displayed on AV and FWS images (Figure 5-7) at 24.5 mbgl.

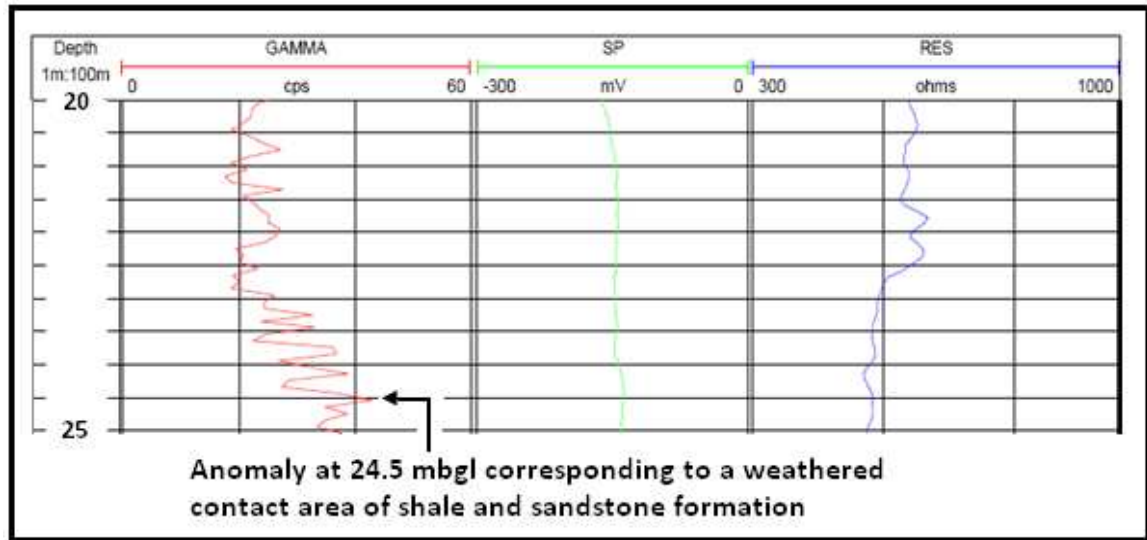


Figure 5-8 Gamma, Resistivity and SP logs from 20 -25 mbgl in MW7 borehole.

5.2.3.2 Horizontal Bedding Plane Fracture Feature at 33 - 34 mbgl

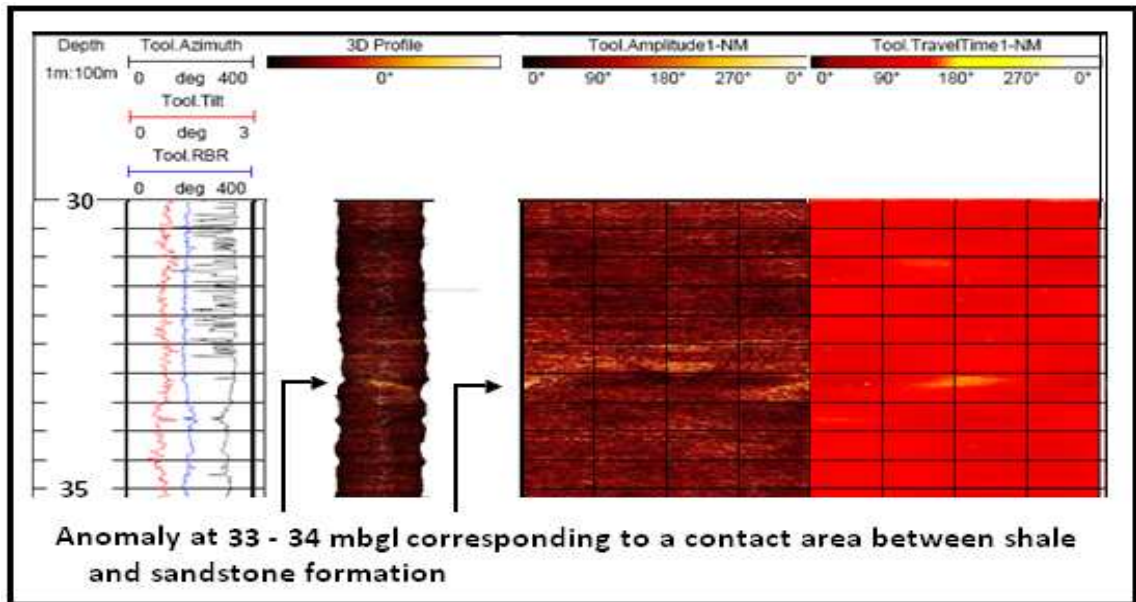


Figure 5-9 AV image from 30 - 35 mbgl in MW7 borehole.

The existence of a horizontal bedding plane fracture feature is evident on the AV imaging (Figure 5-9). The displayed anomaly is attributed to weathering at the contact area of sandstone and shale formation (see MW7 geological log on Figure 4-12 in Section 4.2.1). Weathering on the sedimentary layer contacts areas or interphase has great potential to create preferential flow path for groundwater movement at the same time enhancing LNAPL contamination migration. Conventional logging (Figure 5-10) and FWS could not detect the horizontal fracture feature at 33 - 34 mbgl, as indicated by absence of distinguishable anomaly between 30 - 35 mbgl.

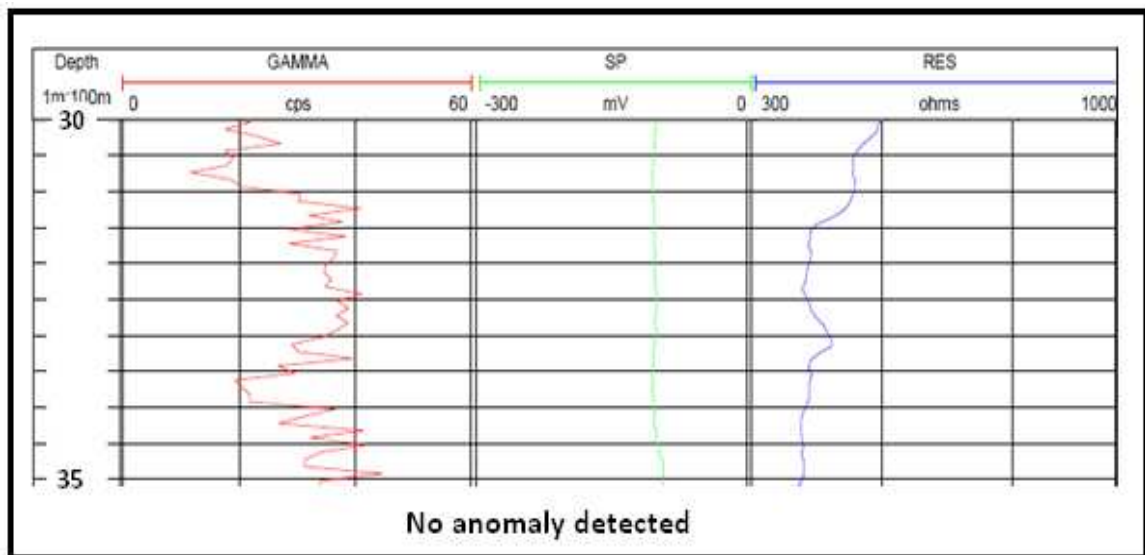


Figure 5-10 Gamma, SP and Resistivity logs from 30 -35 mbgl in MW7 borehole.

5.2.4 MW8 Logging

5.2.4.1 Horizontal Bedding Plane Fracture Feature at 24.5 mbgl

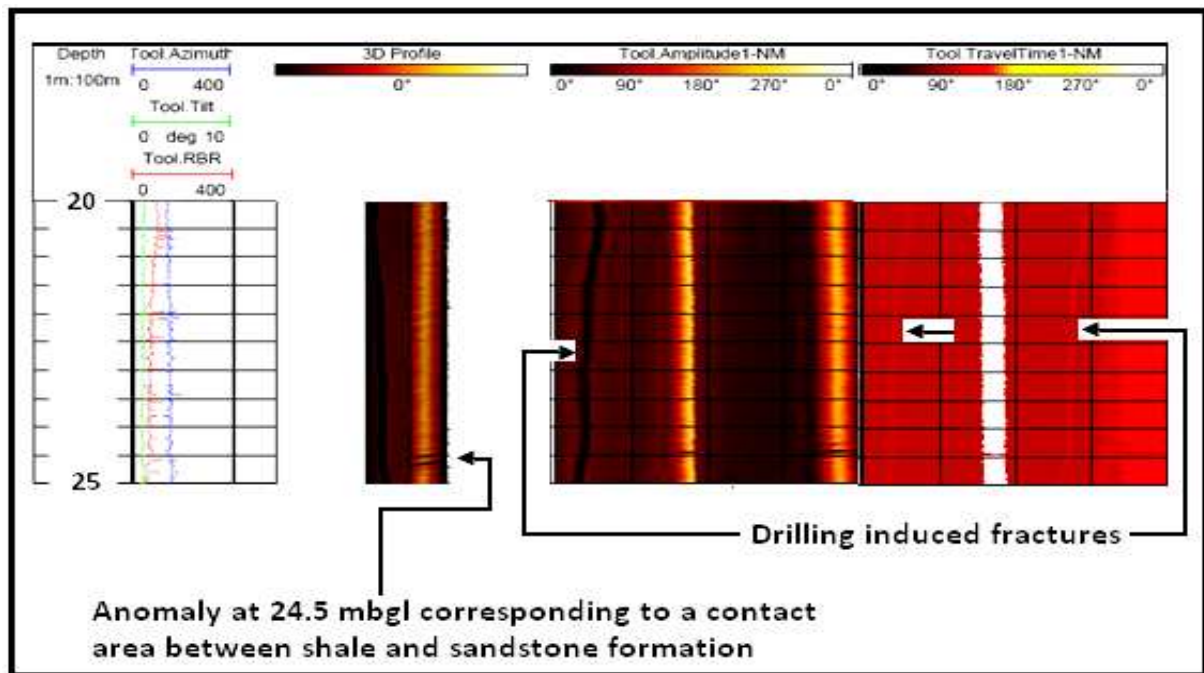


Figure 5-11 AV image between 20 - 25 mbgl in MW8 core borehole.

The AV image (Figure 5-11) shows an anomaly on the 3D profile at 24.5 mbgl. The anomaly corresponds to a contact area of sandstone and shale (see the MW8 geological log in Section

4.1.1.2). Weathering at sedimentary contact areas can lead to the formation of a bedding plane fractures. It is also important to note the presence of drilling induced fractures on the acoustic viewer's 3D profile between 20 - 25 mbgl as evidenced by breakouts separated by almost 180° (Figure 5-11). Both natural and drilling induced fractures are poor reflectors of acoustic waves and this result in the waves having to take too much time to travel in those features.

It is not surprising that AV and FWS images displays similar bedding plane fracture feature at the contact area of sandstone and shale in both MW7 (Figure 5-7, Section 5.2.3) and MW8 (Figure 5-11 and Figure 5-12) at 24.5 mbgl considering that they are only 4.7 m apart. This is expected considering the horizontal continuity in nature of sedimentary deposited layers unless they are offset by intrusion or faulting processes which are not highly active at the study area. The FWS imaging (Figure 5-12) indicates a wave of low amplitude and high travelling time at 24.5 mbgl and is most likely due to the attenuative property of the weathered materials at the sandstone/shale contact area.

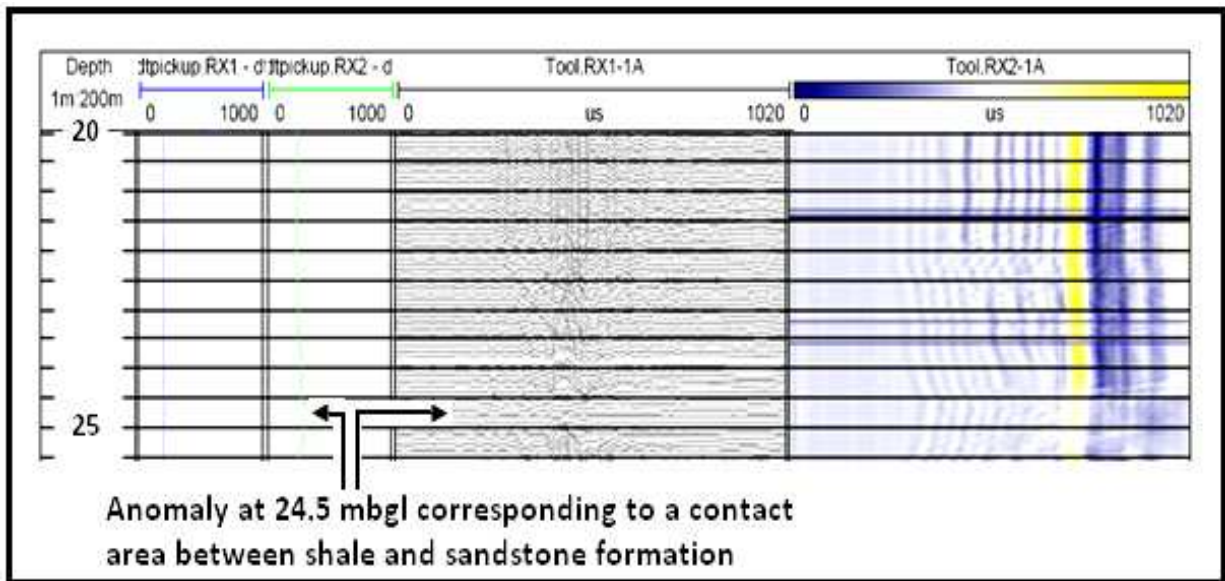


Figure 5-12 FWS image between 20 - 25 mbgl in MW8 core borehole.

It is evident based on the borehole geophysics results that AV, FWS and conventional logging cannot be used as standalone tools. Correlation to geological logs coupled with EC profiling enables maximum output and better understanding of the subsurface. For instance, AV imaging could not pick any fracture feature at 31.5 mbgl in MW6 borehole which conventional logging, FWS and core logs exhibited clearly. It is important to highlight that correlation of

results among borehole geophysics tools, further demonstrates the merit for the application of various geohydrological tools to complement one another considering the existence of a non - unique interpretation.

5.3 Summary of Chapter 5

The Chapter gives details on borehole geophysics characterisation conducted at the study area with the objective of identifying preferential flow paths to groundwater and LNAPL contamination. Borehole geophysics equipment used on the Beaufort West study area consisted of AV, FWS, EC and Conventional logging (Resistivity, SP and Gamma). Borehole geophysics characterisation proved important for determining tracer injection depth in private boreholes (PW5 and PW2) and newly drilled boreholes (MW8 and MW7). An important finding of this chapter is the identification of two bedding plane fractures at 24 - 25 mbgl and 34 - 35 mbgl. These bedding plane fractures form preferential flow paths to groundwater and LNAPL migration. The bedding plane fractures were identified at shale/sandstone and mudstone/sandstone weathered contact areas. The next Chapter gives a detailed description of hydraulic characterisation of the study area which was achieved through aquifer testing.

6 Hydraulic Characterisation

A total of 8 slug, 3 pump and 4 tracer tests were conducted during hydraulic characterisation of the LNAPL contaminated fractured rock aquifer in the Beaufort West study area. The map on Figure 6-1 shows the location of all boreholes used for the aquifer testing in relation to the identified potential LNAPL sources.

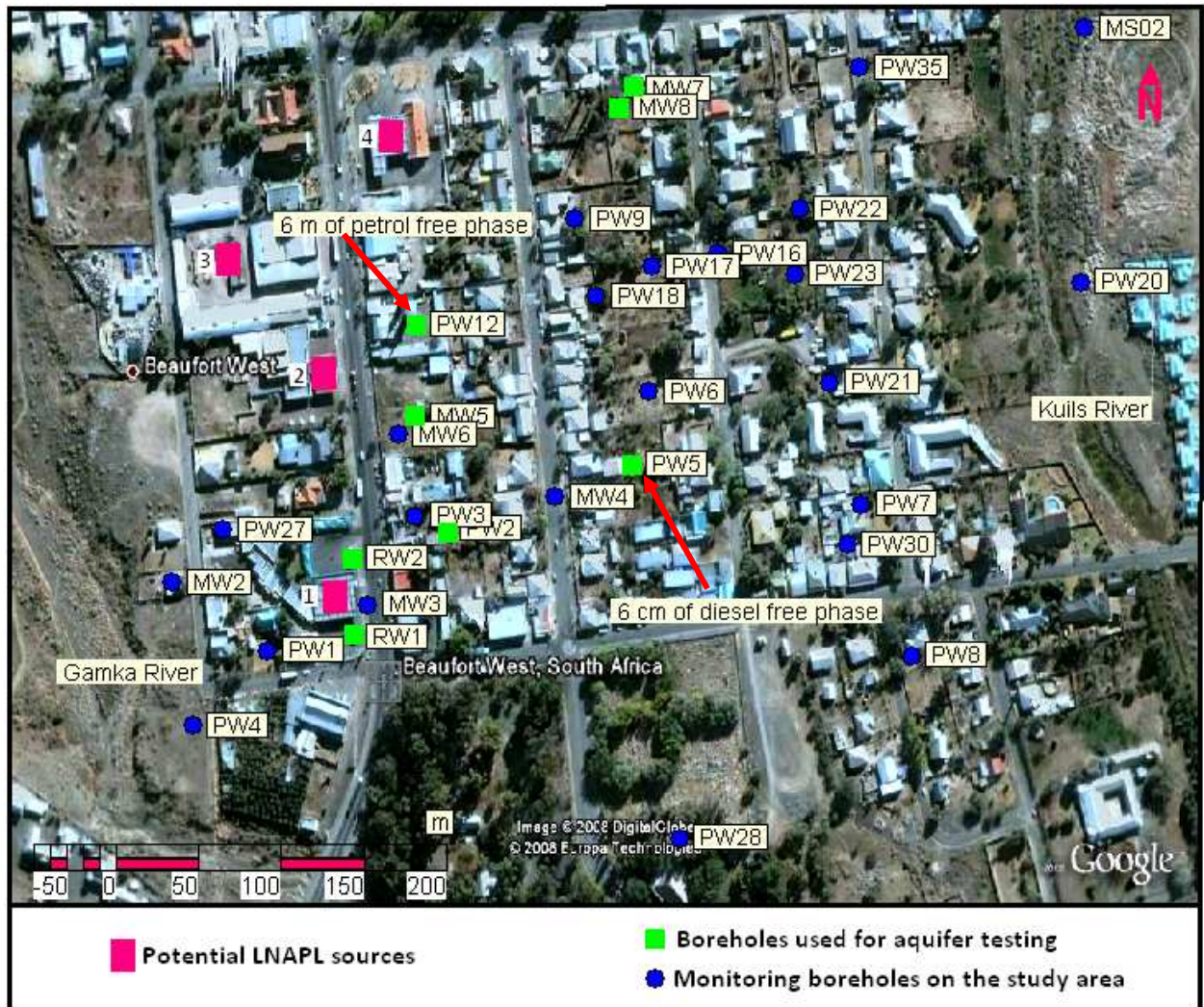


Figure 6-1 Location of the boreholes used for aquifer testing in the Beaufort West study area.

6.1 Challenges faced during Aquifer Testing

A number of constraints were faced during the aquifer testing and this is worth to mention so as to give readers an understanding of the operating environment. Understanding of the challenges faced during the test due to external factors is essential for interpreting and

analysing the observed trends. Three of the four tracer tests and two of the three pump tests were conducted on private boreholes without any idea of the drilling details such as; water strikes, geology logs, bore depth and date of drilling. The missing geohydrological information is important for aquifer testing preparation. The relevance and value of such information goes even beyond the aquifer testing exercise to data analysis and interpretation of the observed drawdown trends.

It is important to highlight that for hydraulic connectivity investigation between contamination source and receptors (private boreholes in this case), the use of contaminated boreholes during aquifer testing is ideal. It has great potential to provide insights on the pathways taken by the contaminants to reach the receptors. However the use the contaminated private boreholes presented us with a routine constrain of cleaning and decontaminating the equipment. Cleaning and decontamination of the equipment would mean downtime for at least an hour. Consider for instance, the time it would take to clean a pump which has been pumping water contaminated with both free and dissolved phase of diesel. Figure 6-2 shows the nature of the contaminants which we had to frequently clean.



Figure 6-2 Contaminated pumping equipment on PW5 private borehole (Taken during the fieldwork).

Bearing in mind that the Beaufort West area is characterised by arid to semi - arid climate with long periods of dry weather; the community relies much on groundwater with most of the houses having boreholes. The extent of the reliance on groundwater by the Beaufort West community has been partially reflected by the hydrocensus. Figure 3-11 in Section 3.5 shows the distribution of the boreholes identified during the hydrocensus on the Beaufort West study area. However observations made during the field work, shows that many boreholes than identified are present on the study area, putting on high the need for another hydrocensus. Such a big number of boreholes in use almost equate the Beaufort West study area to a well field and this had great implications during aquifer tests. Difficulties were faced in distinguishing between drawdown responds due the pump test itself and that due to abstractions on the surrounding boreholes.

In one instance after conducting a slug test in RW1 borehole, the respond was actually contrasting to the expected. Instead of the water receding back to its static water level, it was observed to be rising (Figure 6-3). The observations suggest that the borehole had been under the influence of some local abstractions before performing the test. Conducting aquifer tests on private boreholes would also mean asking for the permission and keys each time one has to enter into the private property which is very much time consuming.

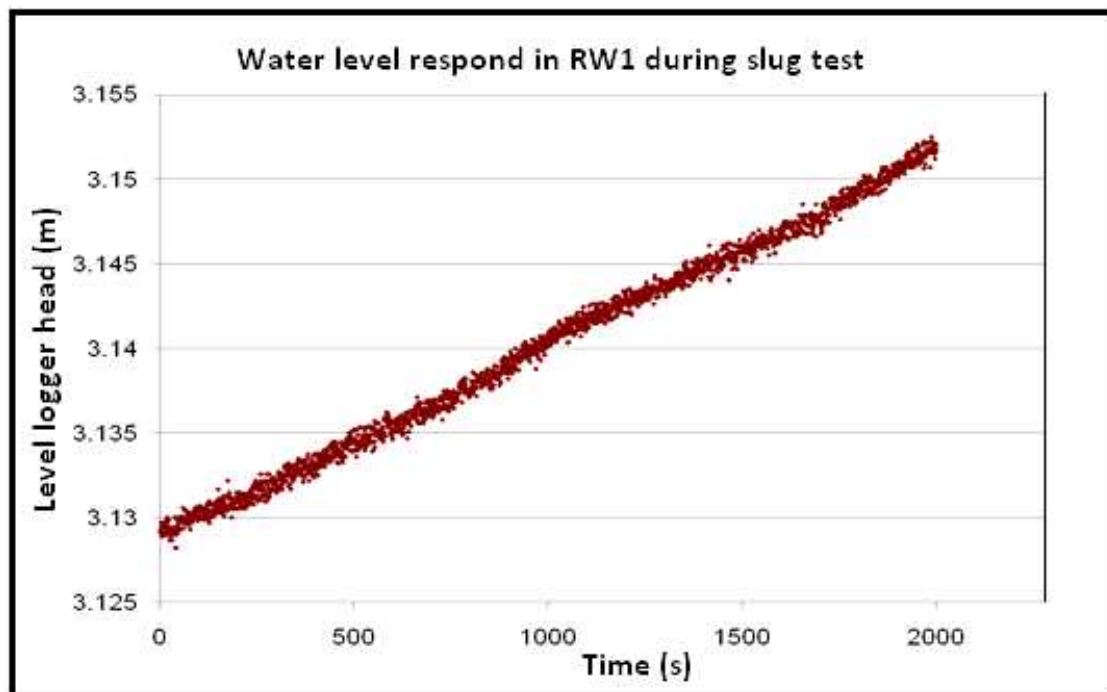


Figure 6-3 Recovering water level during slug test in RW1 (Instead of receding).

Some of the private contaminated boreholes are still equipped with submersible pumps which had to be taken out in order to use the boreholes for aquifer testing. The investigation team had to deal with the hassles involved in taking out contaminated pumps. Figure 6-4 shows a typical example on PW5, where extra man power had to be hired to remove the installed pump. Returning of the pumps after the tests was also another piece of time consuming and rigorous activity. The other challenge posed by working in a contaminated environment where people have been affected is; different questions pertaining to their plight. Unfortunately it happens that most of the questions will be directed at the inappropriate personnel as they would require legal experts or a social scientist.



Figure 6-4 Taking out a pump from PW5 borehole prior to the aquifer tests (Taken during the field work).

6.2 Aquifer Test Borehole Selection

Borehole selection for aquifer testing is critical, because the output of the test mainly depends on the degree to which test boreholes are connected among other hydraulic factors. In other words boreholes intersecting a closely connected fractured zone would be worth to use for both pump and tracer tests. The use of such boreholes would enable quick observation of a considerable drawdown and tracer breakthrough. Observation of considerable drawdown and tracer breakthrough is essential for aquifer and mass transport parameter estimation. It is upon such aquifer test requirements that test boreholes had to be selected from the newly drilled and existing private boreholes.

From an LNAPL contamination point of view, it was also essential to include boreholes contaminated with free phase LNAPLs, because it was important to note their drawdown responds during the test. Such a drawdown response can be related to the existence of a preferential flow path between the pumping well located at one of the conceptualised LNAPL source. This would be a major step in determining the existence of preferential flow paths for LNAPL migration.

Having highlighted some of the borehole selection requirements, private boreholes posed a challenge during the selection process as there was no geological and any geohydrological data. This was however not a surprise considering that most of these boreholes were drilled in the early 1980s. In the wake of such an adversity it was decided to EC profile all accessible private boreholes in order have an idea of flow zone location, borehole depth and any other observable anomalies. Also considered during the selection of test boreholes was access and easiness of removing installed pumps. Selection of test boreholes from newly drilled boreholes was done with some confidence given the availability of geological logs, geohydrological and borehole geophysics data. Detailed selection procedures have been outlined in each test Section.

6.3 Slug Tests

A slug test provides a rapid means of assessing the potential yield of especially low yielding (< 1 l/s) boreholes (Vivier *et al*, 1995). To perform a slug test, the static water level in a borehole is suddenly lowered or raised. To raise the water level, in this test was done by lowering a closed cylinder into the borehole. According to (Krusemann and De Ridder, 1999), measurement of the rate of recovery or recession of the water level allows the borehole's transmissivity or hydraulic conductivity to be determined. The slug test is also useful in estimating the borehole potential yield, which is used to select the pump size prior to pump testing.

Slug tests are usually single - well tests that give estimates of hydraulic conductivity near the bore or screen of the test borehole. However studies by (Belitz and Weston, 1999) revealed that in a porous media, water levels can also be monitored in observation wells during a slug test. This has the potential to improve aquifer parameter estimates because groundwater flow during the slug test is closer to natural conditions as compared pumping. Gonther and Mayer (2003) also highlighted the value of performing slug tests in contaminated boreholes during the initial site characterisation, before pumping tests. This is important because it prevent the risk

associated with lowering expensive equipment into contaminated boreholes. The above mentioned fact is not suggesting that the slug test should replace pump testing. But where the risk of placing equipment in contaminated boreholes is high, then a slug test can be of great value. A total of 8 slug tests were conducted on existing private and newly drilled boreholes with the objective of obtaining the contaminated site aquifer parameters. The slug test procedure (IGS, 2008) has been placed in appendix 3.

Bouwer and Rice (1976) method was used to estimate aquifer transmissivity. Table 6-1 shows the slug test results, borehole and aquifer configurations used during calculations, where:

- d is the estimated flow thickness (m) (Estimated from EC profiling).
- b is the aquifer thickness (m) (Equivalent to saturated thickness).
- r_w is the horizontal distance from the borehole centre to the undisturbed aquifer (m).

Table 6-1 Slug test results.

Site Name	Static Water Level (mbgl)	d (m)	b (m)	r_w (m)	T (m ² /d)	K (m/d)
MW5	10.9	3	34.1	0.08	0.068	0.002
MW8	11.8	8	33.2	0.06	0.033	0.001
MW7	14.4	15	30.5	0.08	0.031	0.001
RW2	11.9	8	30.0	0.08	3.14	0.104
Geometric mean					0.12	0.004

The estimated transmissivity for RW2 is high in comparison to the rest of the boreholes. The difference is mainly attributed to the fact that RW2 borehole has been under abstraction since 2002 as part of the LNAPL containment system installed at one of the petroleum service stations. In other words, RW2 borehole should be by now fully developed with very little skin effects, thus high transmissivity is expected in the vicinity of the borehole. As for MW5, MW8 and MW7, they are newly drilled boreholes which are still to be developed. The low transmissivity values observed in these boreholes is most likely a reflection of high skin effects

in the vicinity of the boreholes. Slug tests were also performed on RW1, PW2, PW5 boreholes, but the results were affected due to the recovery effects from previous abstraction on other boreholes in the study area.

6.4 Pump Test

Aquifer pump testing is essential for determining aquifer parameters. Aquifer parameters have great influence on the groundwater flow, contaminant transportation and fate. With regard to contaminant transportation and fate, pump test can yield important information such as the existence of hydraulic connectivity between contaminant source and receptors. This is the situation on the Beaufort West study area, where there was need to investigate the existence of fracture preferential flow paths between abstracting boreholes(RW1 and RW2) located at one of the conceptualised LNAPL source and contaminated private boreholes PW2, PW5 and PW12 (Figure 6-1). Aquifer parameters; hydraulic conductivities, transmissivity and storage properties are also important inputs of groundwater flow models. As guidelines the following procedure by Van Tonder *et al*/(2001a) was used to conduct the 3 constant rate pump tests:

- Choosing of pump size, possibly with high discharge rate.
- Calibration test.
- Determining length of constant rate test.
- Measuring of drawdown during the pumping period.
- Measuring of recovery on stopping the pump until 95 % of the recovery has been achieved.

6.4.1 Pump Test 1

During the test, RW1 borehole was used as the pumping well at an average abstraction rate of 0.78 l/s. PW2, RW2 and PW5 were used as the observation boreholes. Figure 6-5 shows the location of the boreholes used in pump test 1. It is important to highlight that RW1 and RW2 are boreholes drilled at conceptualised LNAPL source number 1 (Figure 6-5) and they are being used as part of the LNAPL containment system. PW2 and PW5 are private boreholes which are contaminated with both free and dissolved phases of diesel and petrol products respectively.

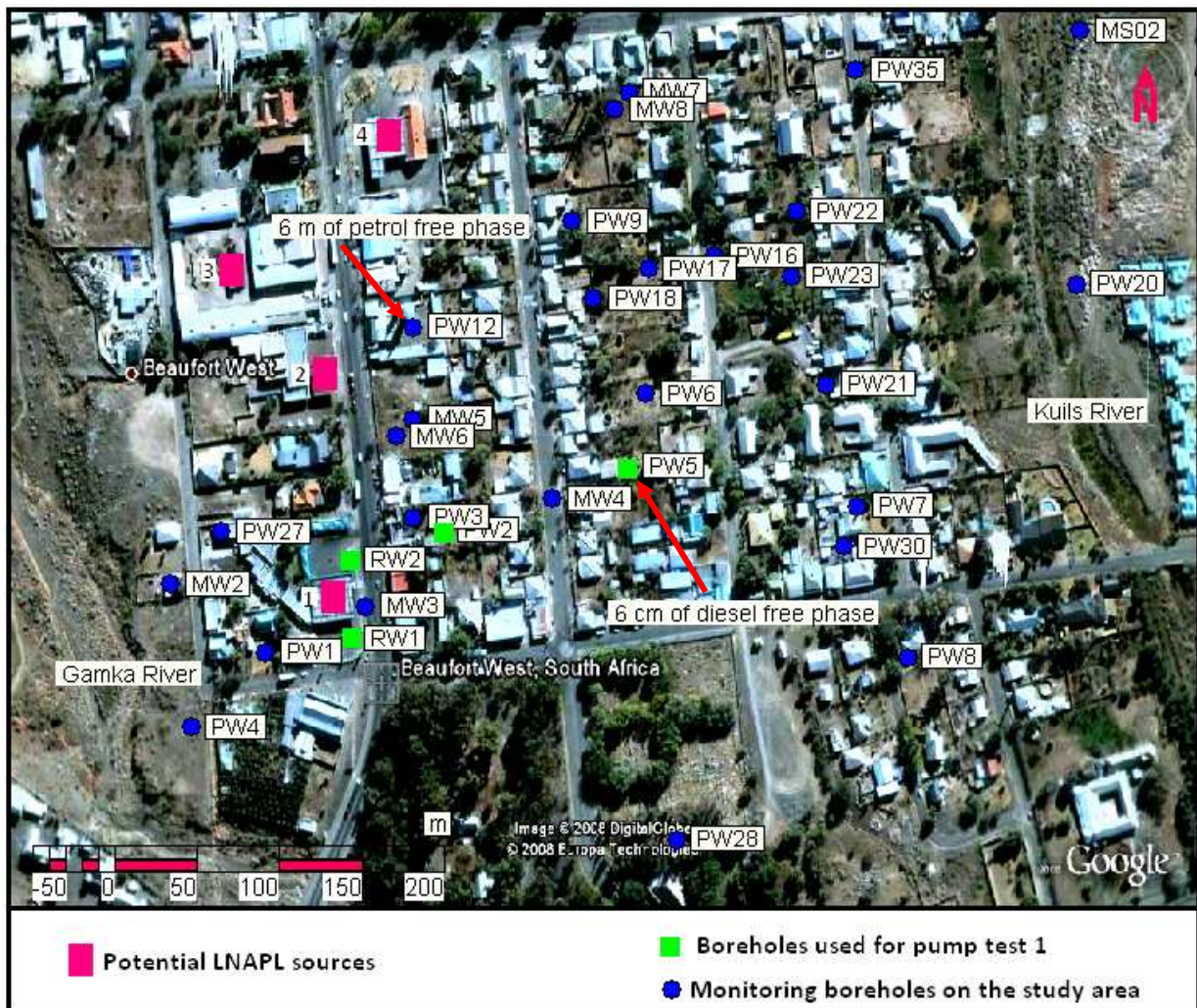


Figure 6-5 Location of boreholes used for pump test 1 in the Beaufort West study area.

On switching off the pump, all boreholes were allowed to fully recover during a 12 hour monitored recovery period. Transducers were installed in each well about 3 hours before the pumping test to monitor the water levels prior, during and after stopping of the pump (recovery). It is important to monitor water level behavior prior and after pumping so as to establish external effects on water level. Examples of the main external effects include artificial abstraction and barometric pressure due to changes in atmospheric pressure. Establishing and understanding of the external influence on water level has an important value when analyzing drawdown behavior and making corrections for water level changes. The FC program by Van Tonder *et al* (2001b) was used to estimate the transmissivity of the aquifer formation. Figure 6-6 shows the Copper Jacob fit at late time on the pumping well RW1 drawdown plot. Cooper Jacob yielded a transmissivity value of $3.4 \text{ m}^2/\text{day}$.

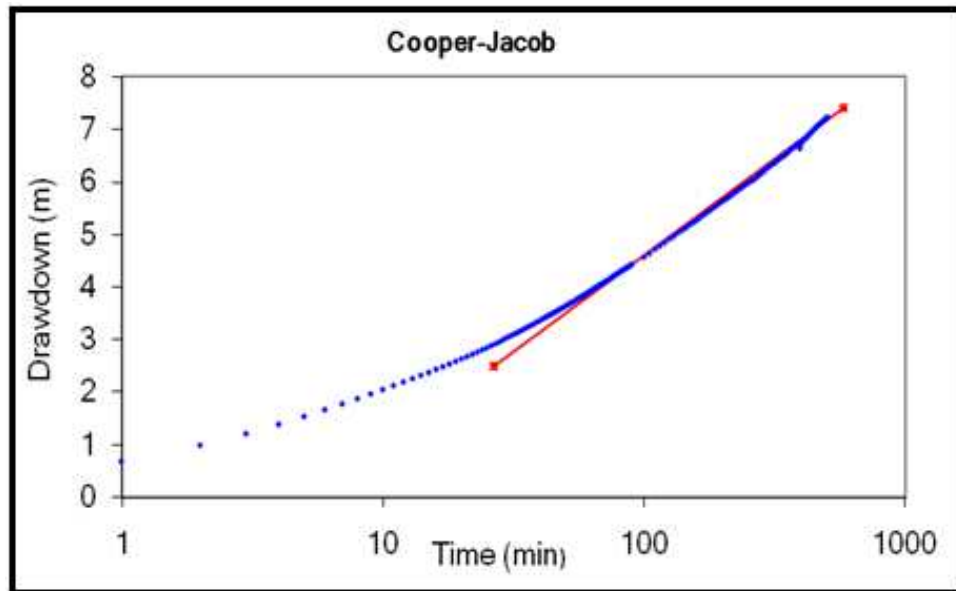


Figure 6-6 Late time Cooper Jacob fit on RW1 pumping well drawdown.

It is important to monitor the recovery on switching off the pump considering that the data is just valuable as pumping drawdown. Using the recovery data, a water level rise against t' plot on Figure 6-7 yielded a transmissivity estimate of $3.5 \text{ m}^2/\text{day}$.

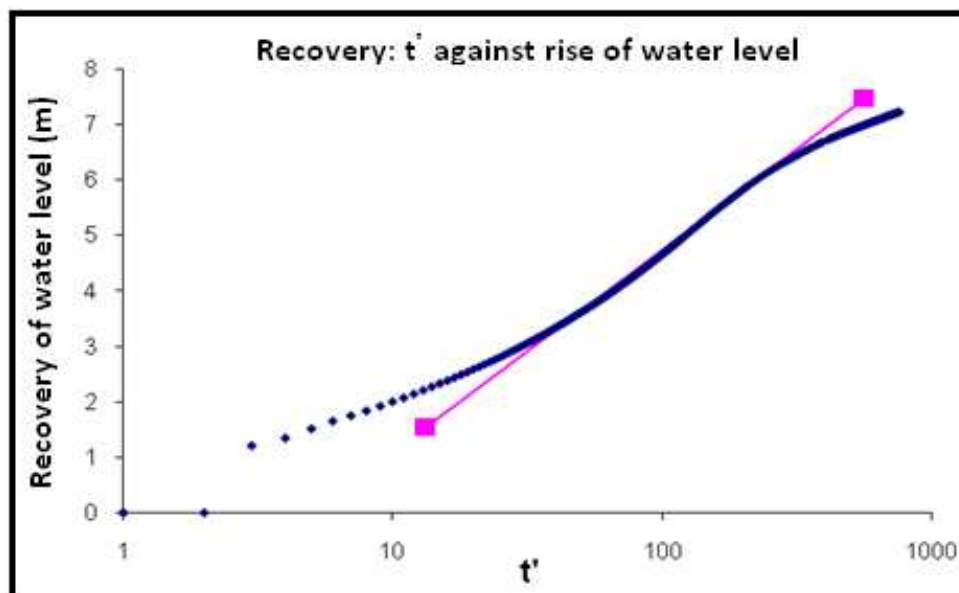


Figure 6-7 Water level rise during recovery against t' in RW1 borehole.

The transmissivity obtained from the recovery drawdown ($3.5 \text{ m}^2/\text{day}$), concurs with a value of $3.4 \text{ m}^2/\text{day}$ obtained above using the Cooper Jacob method. RPTSOLV program (Verwey *et al*, 1995) which avoids the dependency of storativity on distance was also used to estimate

aquifer parameters using RW1 drawdown. Observation wells PW2 and RW2 were affected by the abstraction effects from surrounding private boreholes; as a result the data could not be used for parameter estimation. In the RPTSOLV program, the pump was assumed to be set at matrix and fracture position. The fracture was taken as the observation position. Considering that RW1 is a pumping well, an observation distance of 0.065 m was used in the RPTSOLV program. Table 6-2 shows aquifer parameters estimated from the first pump test using the RPTSOLV program.

Table 6-2 Aquifer parameters estimated using RPTSOLV from pump test 1.

Site Name	T - Formation (m²/d)	S - Matrix
RW1	5.8	3.e-4

6.4.2 Pump Test 2

During the second pump test, RW2 was the pumping well at an average abstraction rate of 0.78 l/s. PW2, PW12 and PW5 were used as observation boreholes. Pump test 2 was conducted over a 5 hour period. Figure 6-8 shows the location of boreholes used in the second and third pump tests.

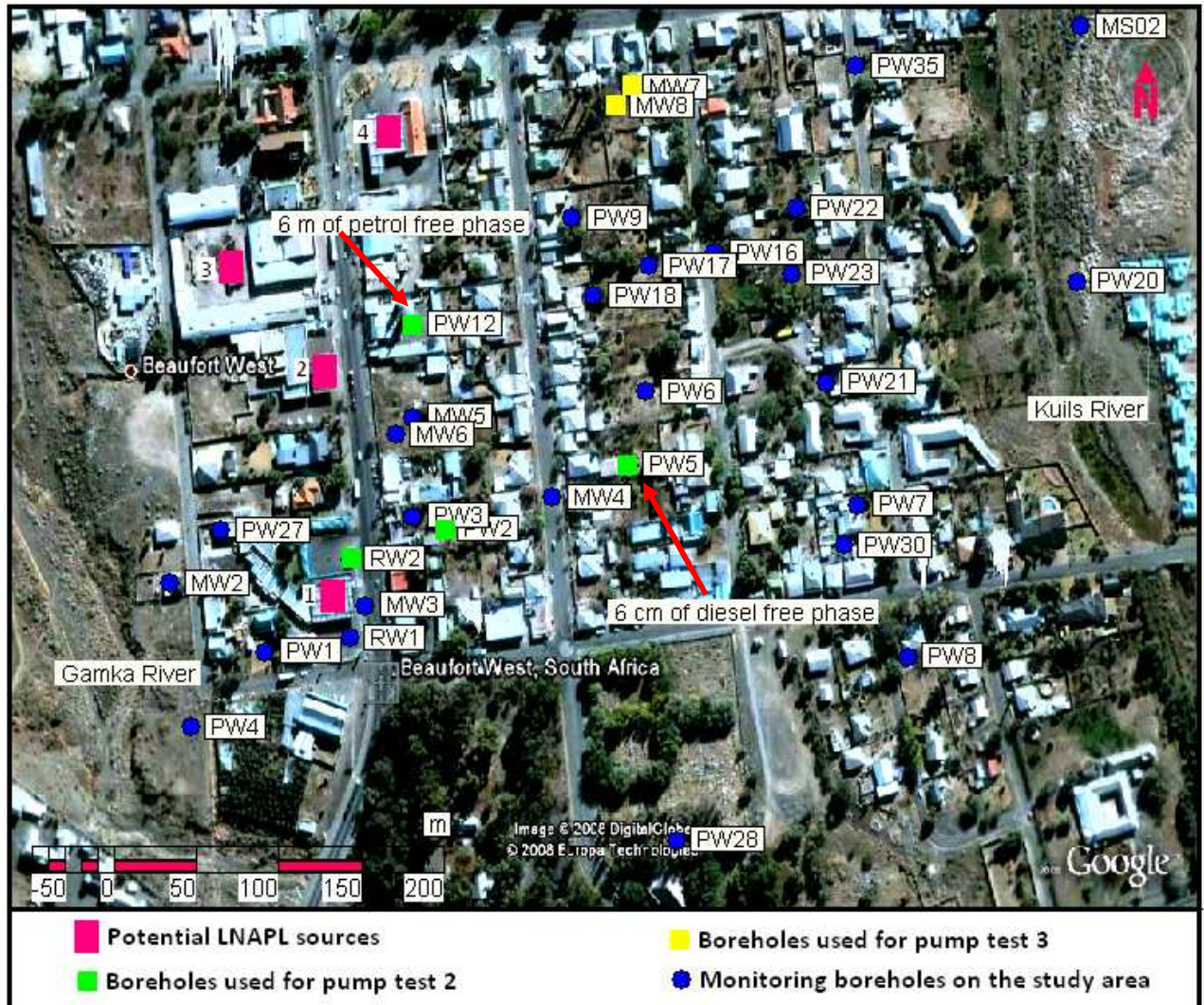


Figure 6-8 Location of the boreholes used for pump test 2 and 3 in the Beaufort West study area.

It is important to highlight that PW12 and PW5 boreholes are contaminated with both free and dissolved phase (6 m petrol and 6 cm diesel respectively). The inclusion of PW12 and PW5 contaminated boreholes as observation boreholes was essential in order to see their drawdown behaviors. Table 6-3 shows the aquifer parameters obtained from pump test 2 using the RPTSOLV program.

Table 6-3 Aquifer parameters estimated using RPTSOLV from pump test 2.

Site Name	T - Formation (m ² /d)	S - Matrix
RW2	5.8	8.e-4
PW5	4.7	8.e-4
PW12	6.0	5.e-4

6.4.3 Pump Test 3

During the third pump test, MW8 was used as the abstraction well and observations were made in MW7 which is located 4.7 m away (Figure 6-8). MW8 and MW7 are newly drilled core and percussion boreholes respectively. Initially a tracer test was only scheduled between the two boreholes, but it was later decided to place transducers and monitor drawdown changes during the five hour tracer test period. The data had to be smoothened by discarding the first 98 minutes points due to the interference during the calibration process. The calibration process was conducted to determine a suitable abstraction rate that would enable reaching a steady state flow without the borehole running dry.

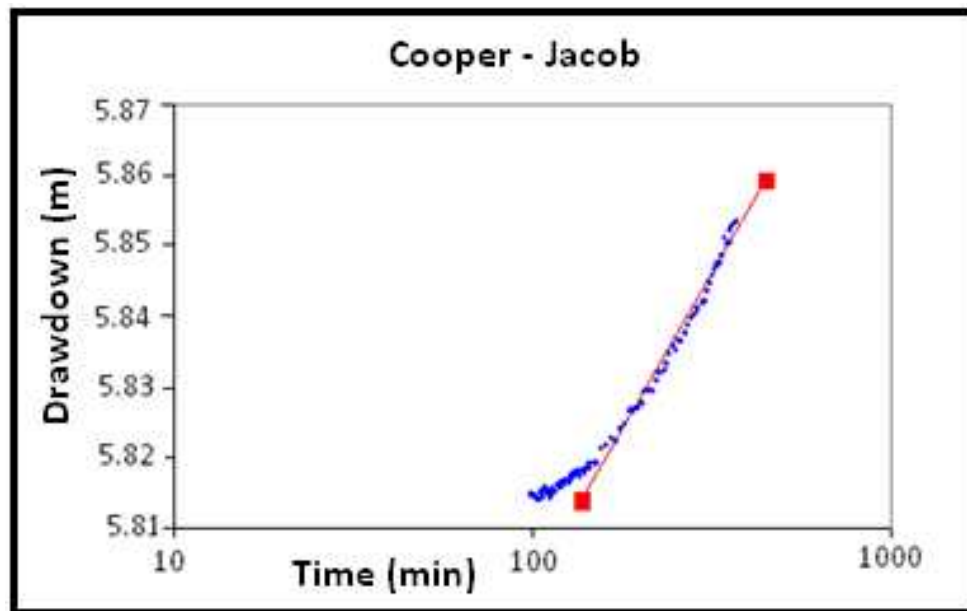


Figure 6-9 Late time Cooper Jacob fit on MW8 pumping borehole drawdown.

From the Cooper Jacob plot on Figure 6-9, a formation transmissivity of 15.4 m²/day was estimated using the pumping well (MW8) drawdown. It was not possible to monitor the water

level recovery because the abstraction core borehole MW8 collapsed towards the end of the test and all equipment had to be removed.

6.5 Tracer Tests

Tracer tests were carried out with the objective of determining mass transport parameters in particular; Darcy velocity, seepage velocity and effective porosity. Mass transport parameters are important for understanding the contaminant migration processes and also used as input in contaminant models. Figure 6-10 shows the location of boreholes used in the tracer tests. The following tracer tests were conducted; injection test, 1 point dilution test and 2 radial convergent tests.



Figure 6-10 Location of the boreholes used for tracer testing in the Beaufort West study area.

6.5.1 Tracer Injection Test

The tracer injection test was performed in order to investigate the hydraulic connectivity between the pumping and observation boreholes. Tracer injection test was performed concurrently with pump testing. About 200 mS/m equivalence of iodated salt was injected in PW5 borehole during the pump test. The breakthrough was monitored for 8 hours through the measurement of EC in RW2 (abstraction borehole) and PW2 (observation borehole) located between the injection (PW5) and pumping borehole (RW1). PW5 borehole is located about 125 m from PW2 and 225 from RW2 (Figure 6-10). Figure 6-11 shows the measured EC with time in PW2 (observation borehole) and RW1 (abstraction borehole). It is important to highlight that in PW2 the EC was measured at 23 mbgl, this depth was identified as the main flow zone through EC profiling (Figure 5-1, Section 5.1.1).

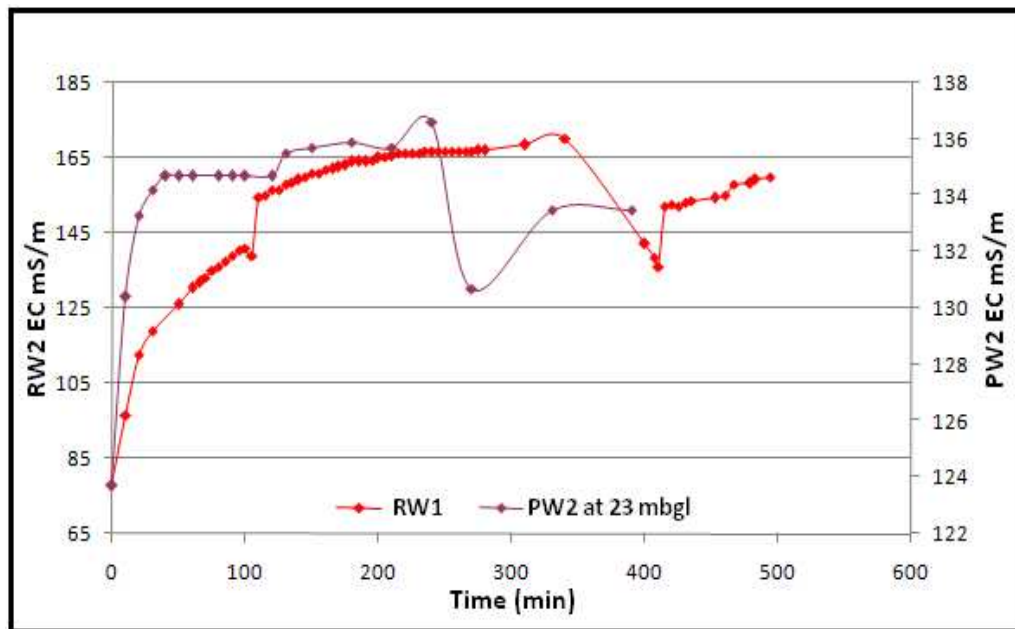


Figure 6-11 EC tracer breakthrough measurements in pumping RW2 borehole.

Despite having a few data points, an increase in the EC is evident in both boreholes with time (Figure 6-11). More interesting is the similarities displayed by the two curves which cannot be by coincidence. However from a practical point of view it is difficult to relate the displayed EC trend to the tracer breakthrough. This would translate into a forced groundwater velocity of 4.5 m/min during the first 50 minutes after injection over a distance of 225 m. Such a forced groundwater velocity is extremely too high in the context of groundwater flow.

On the other hand what is causing the EC trend remains a big of concern. One of the possible explanations for such a trend could be the mobilization of sediment containing clay minerals during pumping. Such an effect can result in increased total dissolved solids in the groundwater and consequently the EC. There might be need to just monitor EC trends in those boreholes without injecting any tracer. It is even more important to separate the causative effects of such a trend from the injected tracer effects. It is possible that the observed EC trend maybe partially related to tracer breakthrough.

6.5.2 Point Dilution Test

A point dilution test was performed in PW5 contaminated borehole to estimate Darcy velocity. A single - well point dilution test aims to relate the observed rate of tracer dilution in a borehole or the isolated borehole segment to the groundwater velocity. The estimated groundwater flow can be natural or forced. The test section of the borehole should be intersecting the fracture preferential flow path of interest. In this investigation a test section of 2 m (22 - 24 mbgl) was used. The test section was selected based on the EC profiling performed in PW5 borehole where an elevated EC was observed at 23 mbgl (Figure 5-1 in Section 5.1.1). The elevated EC at 23 mbgl was inferred to be the main preferential flow path to LNAPL and groundwater. Figure 6-12 shows the point dilution test equipment set up in PW5.

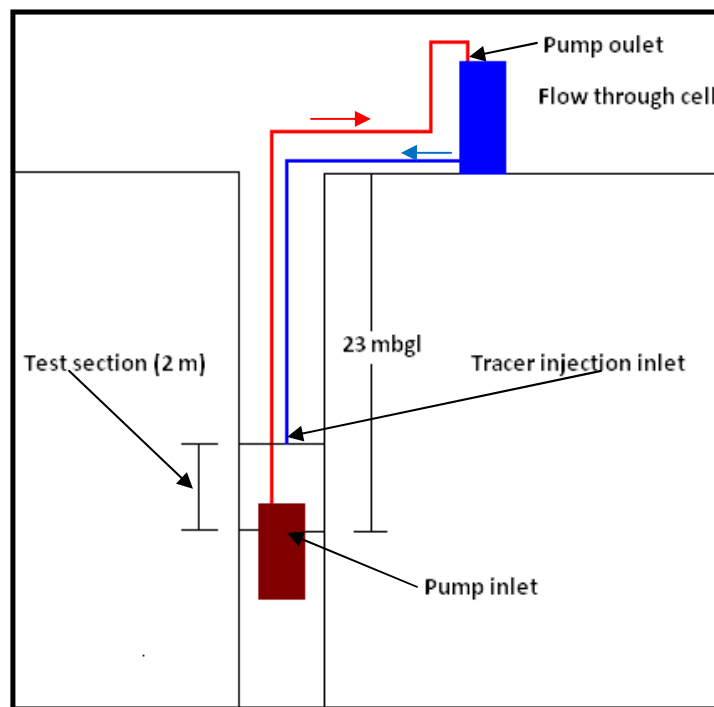


Figure 6-12 Set up of point dilution tracer test equipment on PW5 private borehole.

Sodium bromide (NaBr) (50 g), fluorescein (0.5 g) and sodium chloride (NaCl) (200 g) were used as tracers. The tracer quantities were selected based on the previous studies conducted in typical Karoo fractured rock aquifers (Riemann *et al*, 2002). The point dilution test was performed using the procedure by Riemann (2002) (Appendix 4). Before data analysis the measured EC (tracer concentration) was standardised (Figure 6-14) using equation 3 such that:

$C = 1$ at t_0 and $C = 0$ at $EC = EC$ (background)

$$C_t^* = \frac{C_t - C_b}{C_o - C_b}$$

Equation 3

Where: C_t^* = Standardized concentration

C_t = Equivalent concentration at different times after tracer injection

C_b = Background concentration in groundwater

C_o = Concentration in the borehole at t_0

Figure 6-13 shows the measured EC with respect to time. The tracer concentration decrease is evident in Figure 6-13 as indicated by an exponential decay of the measured EC.

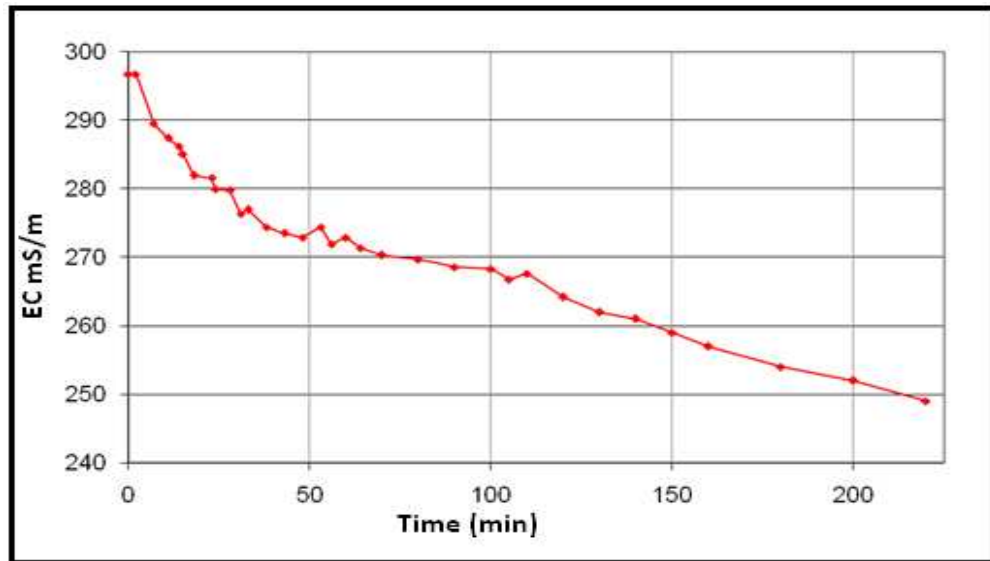


Figure 6-13 EC measurements for point dilution tracer test in PW5 borehole.

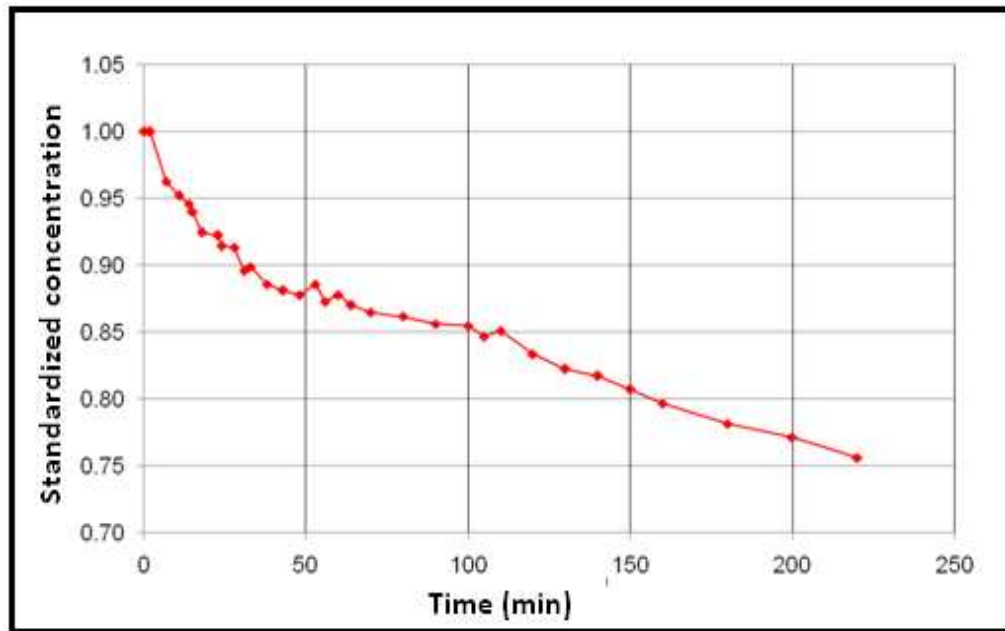


Figure 6-14 Standardized EC concentration for point dilution tracer test in PW5 borehole.

It is important to highlight that, due to limited time and the private working environment's constraints, it was not possible to measure the tracer concentration until 90 % of the initial EC had been depleted as stated by (Riemann, 2002). Darcy velocity (m/d) was calculated using equation 4 (Drost *et al*, 1968) using the standardized concentration.

$$q = \frac{W}{\alpha A t} \ln\left(\frac{C_0}{C}\right)$$

Equation 4

Where:

- | | | |
|----------------|---|--|
| W | = | volume of fluid contained in the test section (m ³) |
| A | = | cross sectional area normal to the direction of flow (evaluated from $\pi r L$, assuming a radial flow model with $n = 2$) (m ²) |
| C ₀ | = | tracer concentration at t = 0 |
| C | = | tracer concentration at time = t |

α = borehole distortion factor (between 0.5 and 4; = 2 for an open well) (note that $q\alpha = v^*$, where v^* = apparent velocity inside well)

t = time when concentration is equal to C (days)

L = test section length (m)

Darcy velocity was determined at different time intervals during the tracer decay and a geometric mean of 0.1 m/d (36 m/a) was estimated (Table 6-4).

Table 6-4 Darcy velocity estimated from point dilution test 1.

Time (min)	C (at time = t)	q (m/d)
58	0.87	0.138
100	0.85	0.092
150	0.81	0.081
200	0.77	0.075
Geometric mean		0.1

6.5.3 Radial Convergent Tests

Two radial convergent tests were conducted as part of the hydraulic characterisation, to determine effective porosity and seepage velocity for the fracture preferential flow path. It is also possible to determine dispersion parameters from field tracer tests, but in this study the level of technology and resources available only allowed for the estimation of effective porosity and seepage velocity. From an LNAPL contaminated site characterisation point of view, it was considered very important to use boreholes contaminated with free phase for the first radial convergent test. The second radial convergent test was performed in the newly drilled MW8 and MW7 boreholes. Refer to Figure 6-10 in Section 6.4.2 for the location of test boreholes.

6.5.3.1 Radial Convergent Test 1

In radial convergent test 1, private borehole PW5 which is contaminated by diesel product was used as the injection borehole. The tracer breakthrough was monitored for 5 hours by measuring EC in RW2 (abstraction borehole) and PW2 (observation borehole). PW2 observation borehole is located between the injection borehole (PW5) and pumping borehole RW2. PW5 is located about 125 m from PW2 and 225m from RW2.

The choice of tracer test boreholes was based on premise that; RW2 (abstraction borehole) is located on the conceptualised LNAPL source number 1 (Figure 6-10, section 6.5) while PW2 (observation borehole) and PW5 (injection borehole) are both contaminated with free and dissolved phases. Thus their inclusion would ideally replicate the contamination movement but in reverse direction from receptors to the source. The reverse replication of contamination movement was a deliberate move so as to avoid contaminant mobilization toward private boreholes. In this set up, RW2 which has a pump already installed as part of the LNAPL containment system was used for the tracer abstraction. This was also economical because instead of having an extra pump and the time consumed in installing and cleaning, an existing one was used. The inclusion of contaminated boreholes has important implications for the fracture preferential pathway characterisation, because by so doing, the hydraulic properties of preferential flow path to contamination can be estimated. The test was conducted using the procedure and guidelines from Riemann (2002) (Appendix 5).

6.5.3.1.1 Tracer Decay Measurements in PW5 Injection Borehole

The measured EC in PW5 injection borehole during the 5 hour monitoring period is displayed on Figure 6-15. Different tracer depletion rates are evident on the EC - time graph. Of particular interest on Figure 6-15 is the elevated rate of tracer decay from about 210 - 300 minutes. The most likely reason for the elevated rate of tracer decay (Figure 6-15), could be another groundwater user switching on a borehole in the vicinity of PW5 for almost one and half hours (210 - 300 minutes). This can be the most likely cause because after 300 min the tracer decay rate started to decrease. The suggestion is strongly supported by high number of groundwater users; most of households are having boreholes as revealed by the hydrocensus. In other words, the boreholes located in the study area constitute a well field and external effects on aquifer tests are highly possible. It is also important to note that from 100 - 200 minutes, the tracer decay rate almost reach a constant value which is low enough to relate to natural groundwater flow conditions.

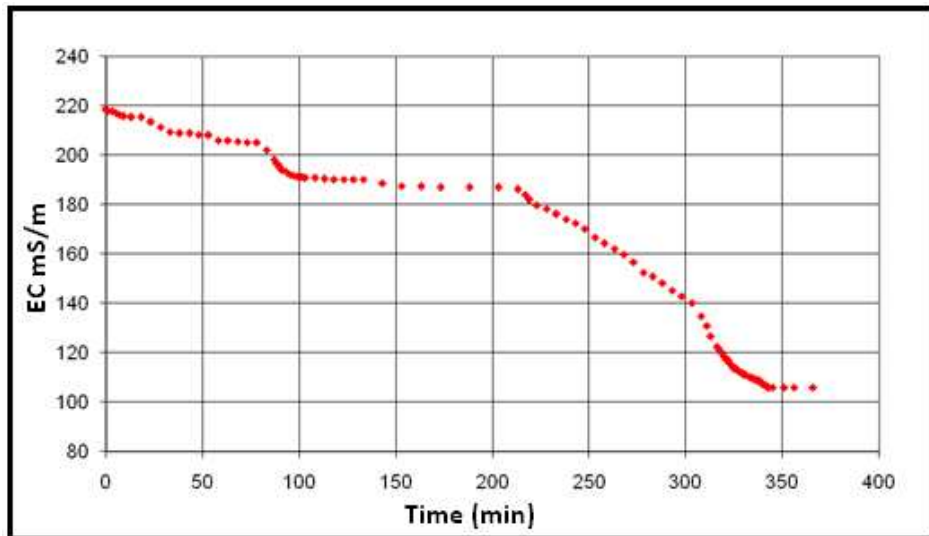


Figure 6-15 EC measurements for radial convergent tracer test in PW5 injection borehole.

It is also possible that exhibited different rates of tracer depletion/decay are a reflection of the nature of preferential fractured flow pathways linking the injection borehole (PW5) to the abstraction borehole RW2 and other private boreholes. Geohydrologic features possibly contributing to the fluctuating rate of tracer decay include; heterogeneities in the aquifer, fracture orientation and networks constituting the preferential pathways. Thus the estimated forced groundwater velocity is more of an average for different pathways with flow lines converging at PW5. Before data analysis, the measured EC was standardized (Figure 6-16) using equation 3 (Section 6.5.2).

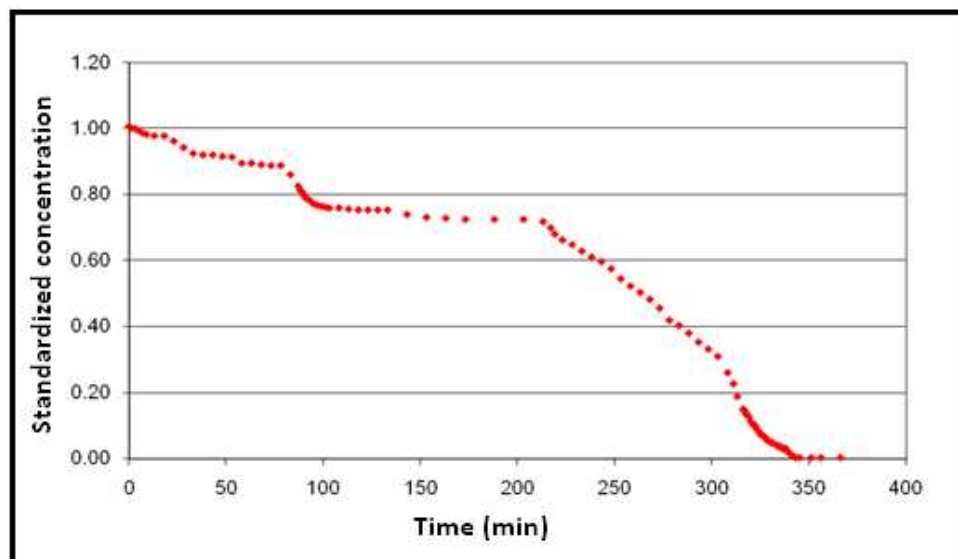


Figure 6-16 Standardized EC concentration for radial convergent tracer test in PW5 borehole.

Darcy velocity under forced gradient (Table 6-5) was calculated for different time intervals by taking into consideration various tracer depletion rates as displayed in Figure 6-15. Using a geometric mean, Darcy velocity of 0.2 m/d (72 m/a) was estimated for the inferred fracture preferential flow path at 34 - 35 mbgl. Table 6-5 shows the calculated Darcy velocities under forced gradient for different time intervals corresponding to different rates of tracer decay.

Table 6-5 Estimated Darcy velocity under forced gradient from radial convergent tracer test 1.

Time (min)	C_t^* (at time = t)	q (m/d)
58	0.89	0.12
153	0.73	0.12
253	0.54	0.14
303	0.31	0.22
Geometric mean		0.15

The observed different rates of tracer depletion (Figure 6-15) is an indication that the surrounding well field should also have had some strong implications in mobilizing the LNAPLs, thus accelerating the contamination movement as evidenced by the abstraction effects on rate of tracer decay from 210 - 300 minutes. In such a situation, contamination mobilization from the abstraction effects on private and municipal boreholes is more likely to be the dominant contamination driving factor as compared to natural groundwater flow. This observation in conjunction with fracture orientations are conceptually the mostly likely reasons why the LNAPL contaminant is observed to be migrating up and across gradient.

If pumping effects from private the boreholes could have such an implication on contaminant mobilization, the need to investigate the well field's capture zone cannot be overemphasized. Such an investigation would require a complete analysis of the stressed Beaufort West study area aquifer, through detailed hydrocensus about abstraction rates and water level responds during abstraction on private and municipal boreholes. It is also worth mentioning that the estimated Darcy velocity under forced gradient (72 m/a) is greater than the Darcy velocity under natural conditions (36 m/a) by a factor of two.

6.5.3.1.2 Tracer Breakthrough Measurements in PW2 Observation Borehole

From the EC profiling in the observation well PW2 (Figure 6-17) during the tracer breakthrough monitoring, a zone between 21 - 24 mbgl was identified to be conveying a high electrically conductive fluid. This is evidenced by the increase in EC) between 21 - 24 mbgl during the 5 hour tracer test (Figure 6-17).

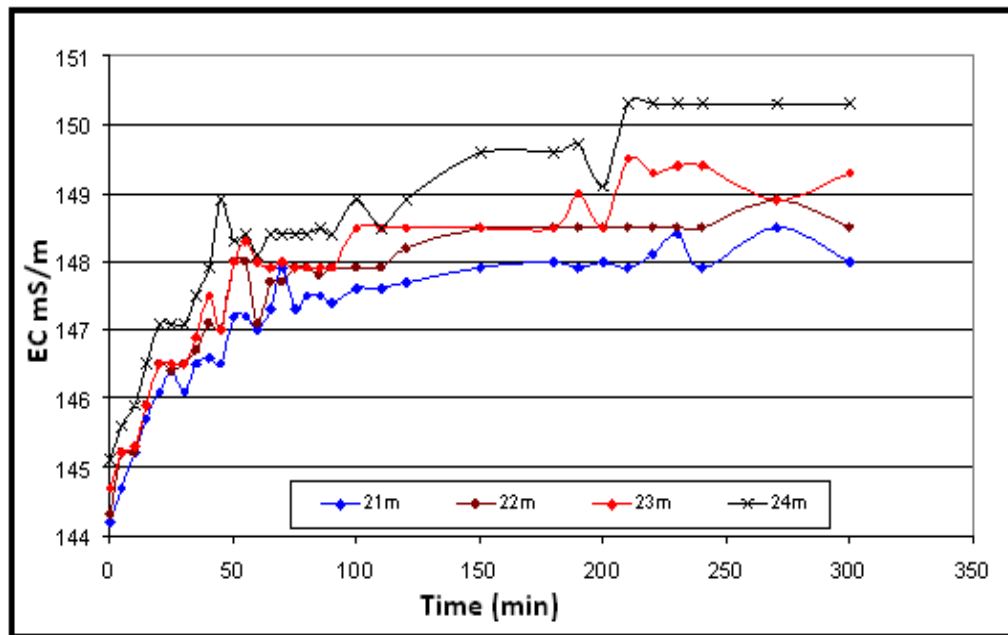


Figure 6-17 EC tracer breakthrough measurements in PW2 observation borehole.

The exhibited similar EC trend between 21 - 24 mbgl (Figure 6-17) is most likely an indication of a similar fluid being conveyed. It is however difficult to relate this high electrically conductive fluid to the injected tracer in PW5. Strictly speaking the fastest tracer would have taken only about 5 minutes to travel over 125 m which is not practical in the context of groundwater flow. The possible explanation for the observed EC trend could be the dilution within the borehole as a result of natural inflow and mobilization of salt rich sediments. From a geological perspective, it is possible that the zone between 21 - 24 mbgl is highly fractured as observed on the core drilling results. The result indicates the existence of a hydraulically conductive flow zone between 21 - 24 mbgl and is not necessarily linked to the tracer movement.

6.5.3.1.3 Tracer Breakthrough Measurements in RW2 Abstraction Borehole

Electrical conductivity was monitored in the abstraction borehole RW2 during the five hour tracer period. Figure 6-18 shows a flow through cell which was utilized to take EC

measurements using a temperature level conductivity meter (TLC). The flow through cell was more convenient for taking EC readings and tracer sampling.

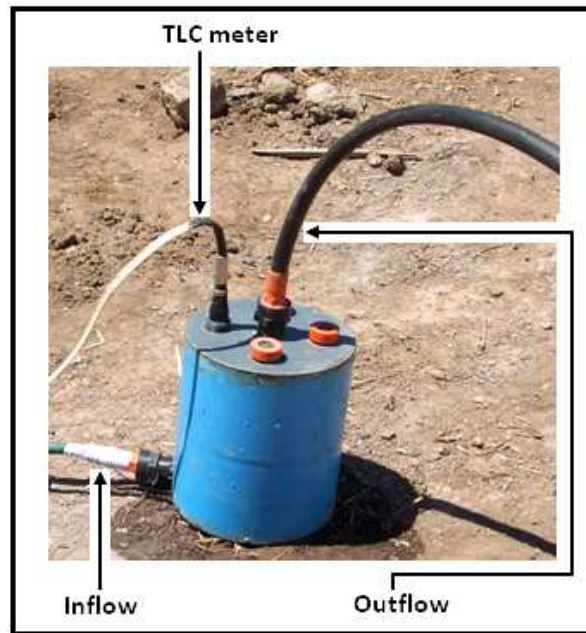


Figure 6-18 Small flow through cell used for EC measurement at abstraction boreholes during radial convergent tracer tests at the Beaufort West study area (Taken during the field work).

Figure 6-19 shows the measured EC against time at RW2 (abstraction borehole). Contrary to the trend in PW2 (observation borehole), the observed EC in RW2 shows a decreasing trend for at least three hours after the start of the test (Figure 6-19). The observed trend can be possibly attributed to the pumping of low EC water from the aquifer. Initially, stagnant water from the borehole column characterised by a high EC was being pumped. As the time progresses, water characterised by low EC or TDS was being pumped from the aquifer.

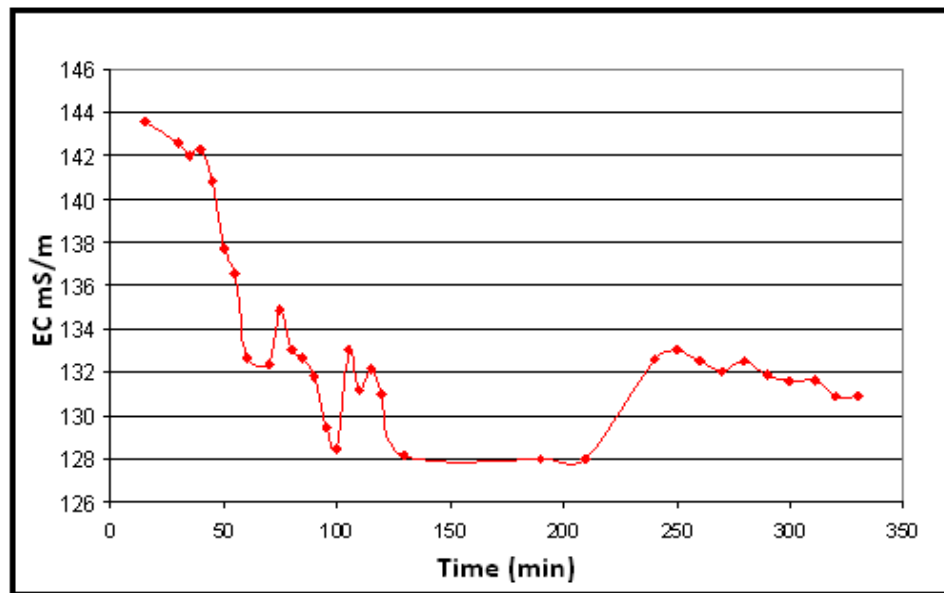


Figure 6-19 EC tracer breakthrough measurements in abstraction borehole RW2.

Based on the measured EC trend in the abstraction borehole RW2 (Figure 6-19), it is thus possible to conclude that no tracer breakthrough was observed over the 225 m distance. Only data from the injection borehole (PW5) was successfully used as point dilution test to estimate the forced groundwater velocity. Possible reasons to explain the breakthrough failure include; the existence of other well defined and connected preferential flow paths converging at PW5. In other words, the tracer might have moved easily to other boreholes, bearing in mind the different tracer decay rates observed in the injection well (PW5) which strongly suggest the influence of the well field on the tests. Considering that a 225 m distance is expected to be traveled by the tracer under advection, the effects of dispersion and matrix diffusion depleting some of the tracer before breakthrough observation cannot be ruled out.

6.5.3.2 Radial Convergent Test 2

The second radial convergent test was performed between the newly drilled MW7 and MW8 boreholes which are only 4.7 m apart (Figure 6-10, Section 6.5). It was important in this test to use the newly drilled boreholes with all the geological logs and borehole information present. There was also a privilege of using borehole geophysics results in conjunction with the core geological logs for identifying and selection of the test section. The equipment set up and procedure is the same as used in radial convergent test 1. MW7 was the injection borehole and the tracer was injected at 34 mbgl in a 2 m test section (33 - 35 mbgl). The selection of tracer injection depth (34 mbgl) was based on following observations:

- EC profiling on MW7 showed an elevated anomaly at 34 - 35 mbgl (Figure 5-3, Section 5.1).
- Multiple water strikes were identified between 28 - 35 mbgl in MW7 during the drilling (Figure 4-12, Section 4.2.1.2).
- Combination logging in particular gamma indicate the existence of a fracture existence feature at 24 - 25 mbgl and 34 - 35 mbgl in MW7 (Figure 5-8, Section 5.2.2.1).
- FWS and AV images also shows bedding plane fracture positions at 24 - 25 and 34 - 35 mbgl in both MW7 and MW8 boreholes (Figure 5-7, Section 5.2.2.1).

MW8 core borehole could only accommodate a small pump, thus it was used for tracer abstraction. The pump was set at 34 mbgl depth giving an initial allowable drawdown of about 21 m. Just as with the first radial test convergent 200 g of iodated salt (NaCl), 50 g NaBr and 0.5 g of fluorescein were used as tracers. It was not possible to attain steady state flow between the 2 boreholes. This was mainly attributed to slow hydraulic responds because the boreholes had not been developed. Sticking drilling mud on the borehole side walls has great potential to increase the resistance to groundwater flow close to the borehole column. It was therefore decided to inject the tracer after one hour of pumping at an average rate of 0.08 l/s.

Figure 6-20 shows the schematic equipment set up for the radial convergent test between MW7 and MW8 boreholes.

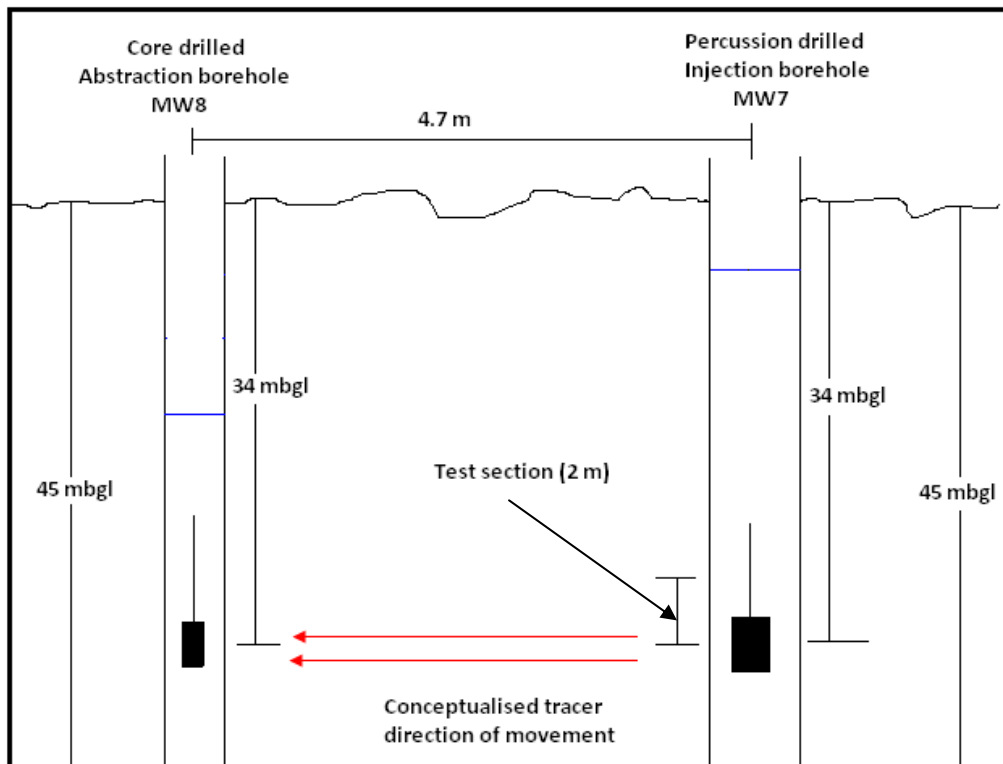


Figure 6-20 Schematic equipment set up for radial convergent test 2 between MW7 and MW8 boreholes.

6.5.3.2.1 Tracer Decay Measurements in MW7 Injection Borehole

Electrical conductivity was measured by a TLC meter fixed at 34 mbgl. Figure 6-21 shows the measured EC in the MW7 injection borehole.

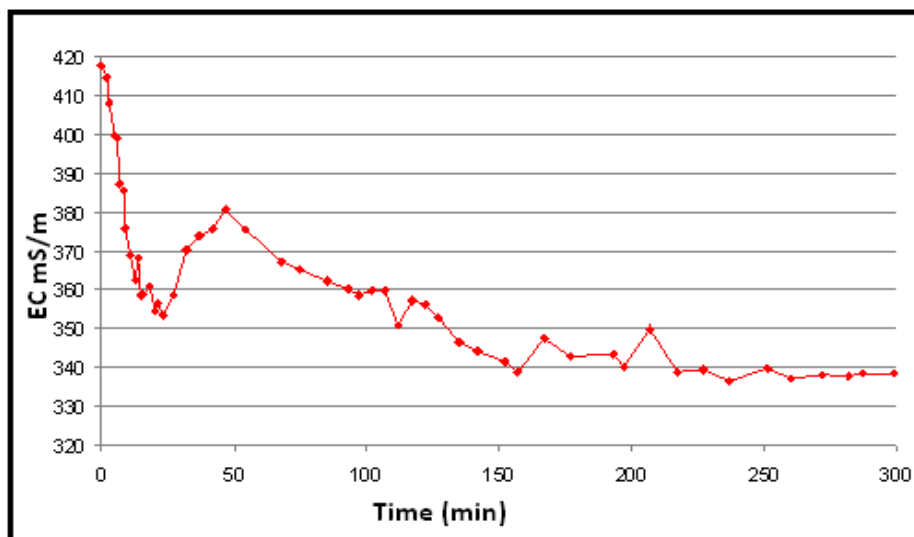


Figure 6-21 EC measurements for radial convergent tracer test in MW7 injection borehole.

The decay curve (Figure 6-21) is initially characterised by high rate of EC decrease (about 2.57 mS/min) for the first 23 minutes. This was followed by a slight EC increase up to 47 min before receding at a reduced rate of about 0.17 mS/min up to the end of test. Possible reasons for the decreased tracer decay rate have been discussed in the next paragraph. The measured EC was standardized using equation 3 (Section 6.5.2) and Figure 6-22 shows the standardized tracer concentration.

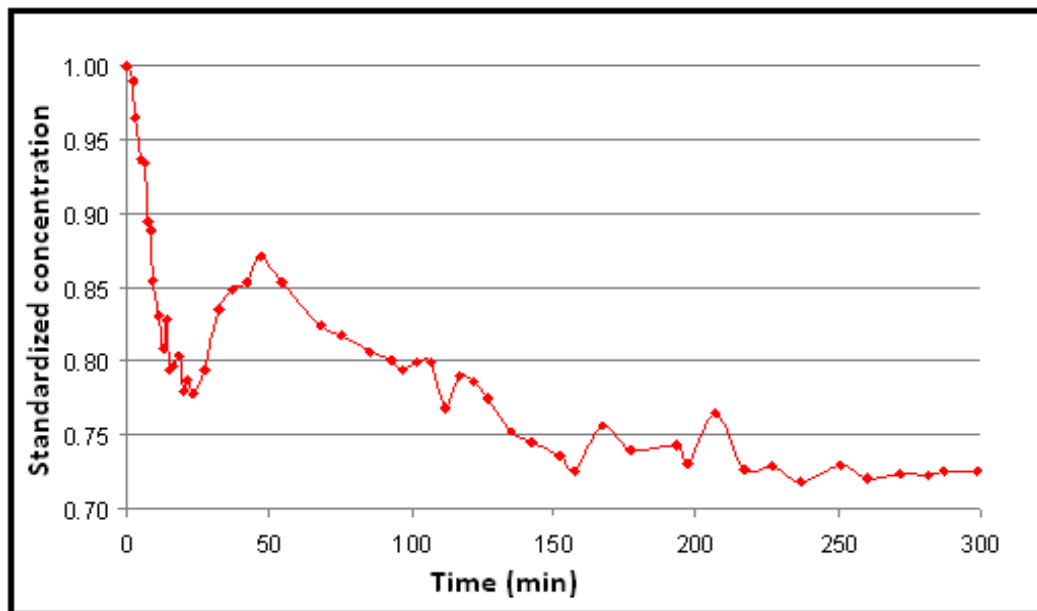


Figure 6-22 Standardized EC concentration for radial convergent tracer test in MW7 injection borehole.

Darcy velocity of 0.62 m/day under forced gradient was estimated using equation 4 (Section 6.5.2) (Drost *et al*, 1968). The estimation was conducted using the EC tracer decay during the first 23 minutes (Figure 6-21). The remainder of the data was believed to have been affected by noise effect, most likely because some of the tracer initially displaced upstream, by dispersion would later re - enter the borehole by advection. Thus a plateau is evident after 23 to 47 minutes (Figure 6-21) before receding due to the advective groundwater flux across the borehole.

In other words, the tracer concentration (EC) decay from 47 minutes most likely occurred at lower rate than expected as some of the upstream advected groundwater would be already containing some tracer (Lamontange *et al*, 2002) with a low diluting capacity on tracer in the injection borehole. Considering that another test had been conducted the previous day with PW5 located about 110 m away as the injection borehole, chances of the advected

groundwater containing the tracer cannot be ruled out. As part of evidence for the possible hydraulic interaction between the current injection well MW7 and previous (PW5), diesel fumes were smelled from the water samples collected from MW7 borehole. This suggests the existence of a hydraulic connectivity between the current injection well (MW7) and some of the contaminated boreholes with PW5 being no exception.

6.5.3.2.2 Tracer Breakthrough Measurements in MW8 Abstraction Borehole

6.5.3.2.2.1 EC Tracer Breakthrough Measurements in MW8 Abstraction Borehole

Electrical conductivity was measured in the abstraction well (MW8) during the five hour test period. Measurements were obtained from a TLC meter placed directly into a flow cell placed outside the borehole (Figure 6-18, Section 6.5.3.1.3). Figure 6-23 shows the measured EC against time in MW8 tracer abstraction borehole. The EC breakthrough measurements were obtained for comparison purposes with the selective conservative bromide anion breakthrough (Section 6.5.3.2.2.3). Bromide breakthrough measurements have been used for calculating groundwater velocity and dispersion parameters (Section 6.5.3.2.2.2).

Two tracer peaks that are displayed on the EC measured breakthrough (Figure 6-23) can be attributed to the existence of at least two preferential flow pathways conveying the tracer. EC profiling in MW8 borehole had earlier displayed another anomaly at 24 - 25 mbgl, suggesting the possible existence of at least two fracture preferential flow pathways.

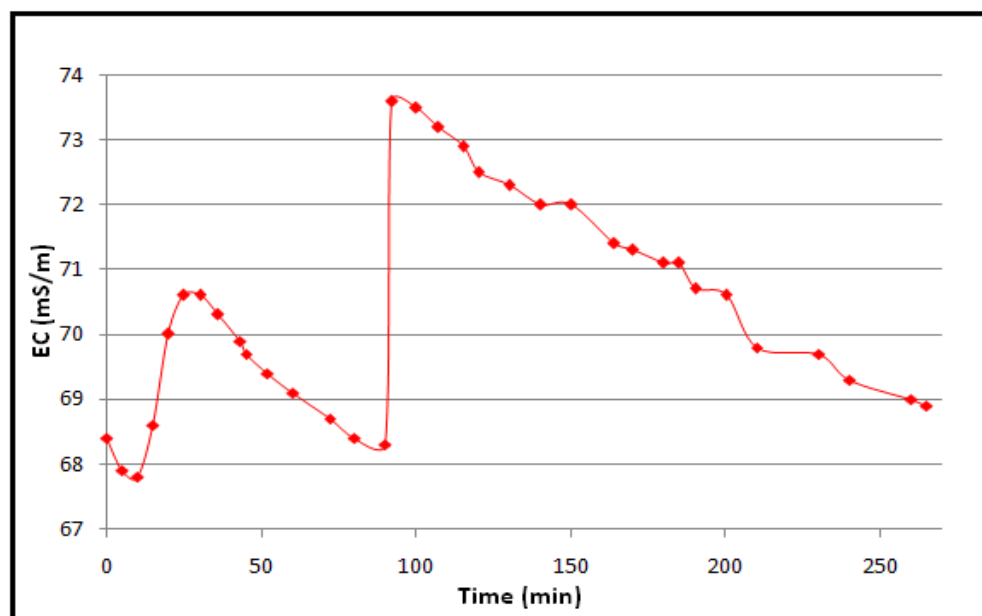


Figure 6-23 EC tracer breakthrough measurements in MW8 observation borehole.

6.5.3.2.2.2 Bromide Tracer Breakthrough Measurements in MW8 Abstraction Borehole

Eight tracer water samples were collected at unequal time intervals during the five hour tracer period for bromide concentration analyses. Samples were collected directly from the abstraction pipe outlet into 100 ml brown bottles. The samples were stored under refrigerated conditions (4 °C) through the use of ice packs and a field cooler box. Laboratory analyses for bromide concentration were performed courteously of IGS chemical laboratory. Figure 6-24 shows the measured bromide concentration with time in MW8 tracer abstraction borehole.

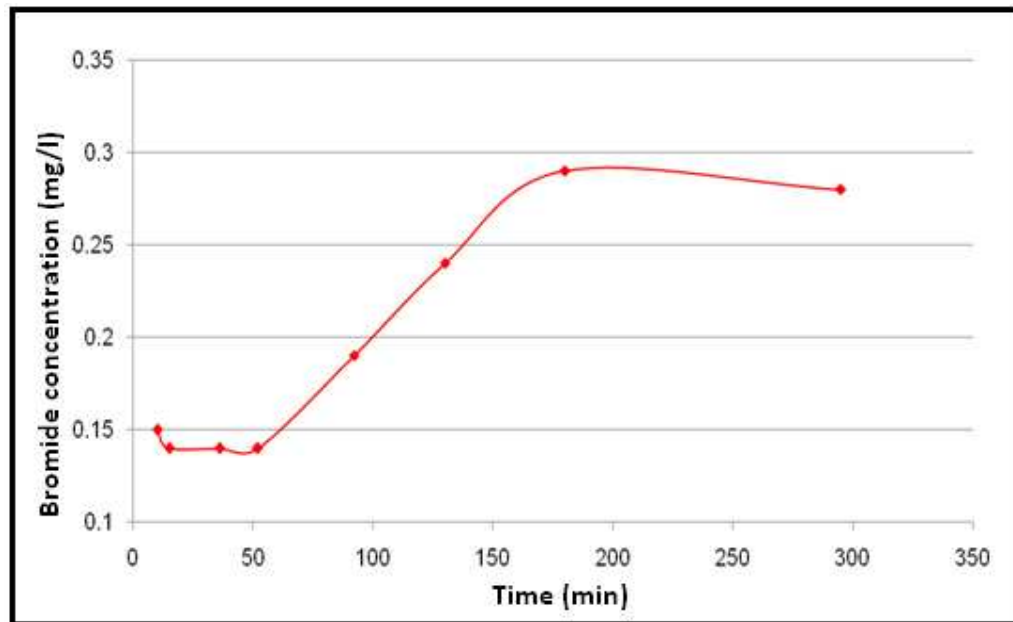


Figure 6-24 Bromide tracer breakthrough measurements in MW8 abstraction borehole.

The bromide tracer breakthrough (Figure 6-24) displays a constant rate of tracer concentration increase (about 8.3×10^{-3} mg/min) from 50 min until the tracer peak passed after 180 min. Groundwater velocity is established from the radial convergent test between the tracer injection borehole (dilution borehole) and the tracer detection borehole (abstraction borehole). The velocity is derived from fitting the model data through the measured field data on the TRACER programme (Riemann, 2002). According to Riemann (2002), manually changing the values for the flow thickness, dispersion and groundwater velocity until the measured data and the simulated data shows a good fit, will yield the estimates of the fitting parameters (Table 6-6). Figure 6-25 shows the best fit between the model and measured field data obtained at a Root Mean Square Error (RMSE) of $7.22E - 02$.

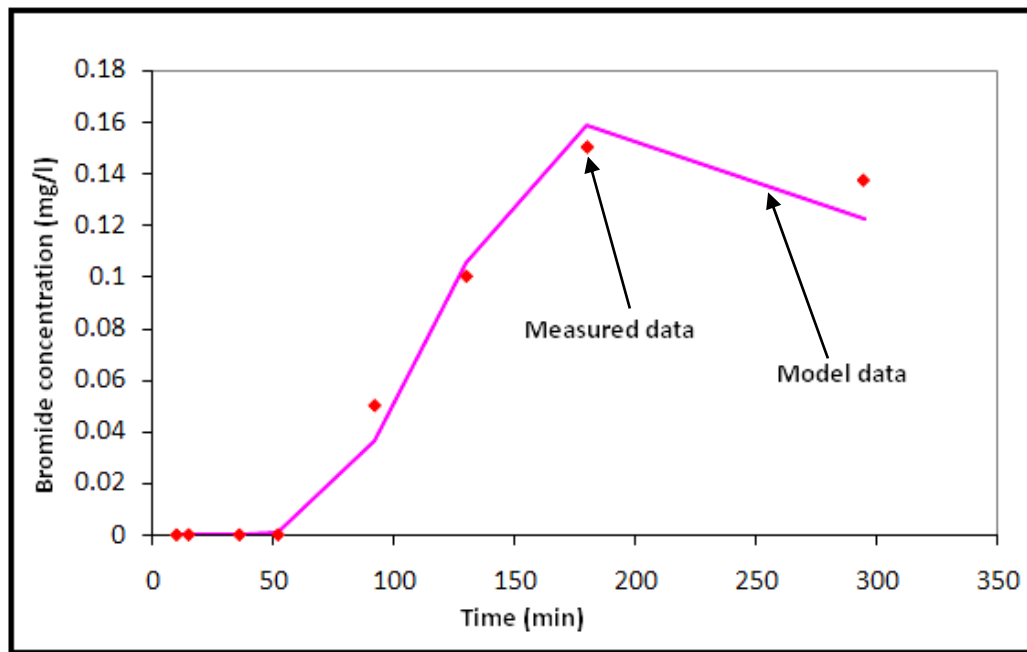


Figure 6-25 Best fit between the model and measured bromide tracer breakthrough concentration in MW8 abstraction borehole.

Table 6-6 Mass transport parameter estimates from the TRACER programme (Riemann, 2002).

Distance between boreholes (m)	Abstraction rate (l/s)	Mass of injected tracer (kg)	Dispersion (m)	Groundwater velocity (m/day)	Kinematic porosity
4.7	0.08	0.05	0.6	23	0.02

It is expected that the kinematic porosity of the Beaufort West formations could be between 0.03 - 0.07, obtained from a large number of tracer tests conducted by IGS in Karoo Formations (Van Tonder, 2009). From these range of possible kinematic porosity values, estimated seepage velocities ranges between 1 and 3 m/a [using a flow zone thickness of 2 m and a gradient of 0.005]. High estimated seepage values (23 m/day, Table 6-6) can only be attributed to the existence of fracture preferential flow path between the two boreholes.

6.5.3.2.2.3 Comparison between EC and Bromide Tracer Breakthrough

Figure 6-26 shows a comparison of bromide and EC measured breakthroughs. It is evident that the Br tracer peak arrived late by approximately 100 minutes after the arrival of the EC breakthrough peak. The EC measured tracer breakthrough suggests that a pulse of groundwater with high EC passed through the abstraction well MW8. The suggestion is supported by subsequent decrease of EC after 98 minutes indicating the passing of tracer peak. In other words, if there was no external influences contributing to the increase of electrical conductivity along the flow path, then theoretically the EC and bromide tracer peaks were suppose pass at the same time. Chances of Br being retarded cannot be ruled out.

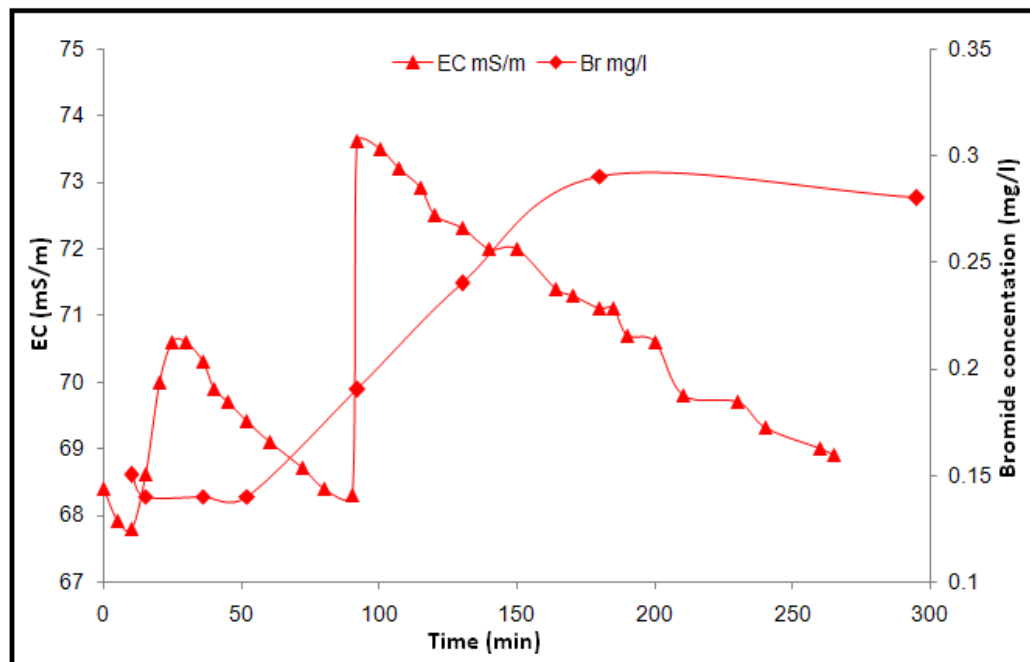


Figure 6-26 Comparison between EC and bromide tracer breakthrough measurements in MW 8 abstraction borehole.

It is possible for one to argue that, the measurement of selective conservative chloride (Cl) anion in mg/l could have done a better comparison to EC measurements. However in this case the measured EC was due to the addition of both the iodated salt (NaCl) and NaBr tracers. Besides what is more important in breakthrough measurements is the position of the tracer peak concentration with respect to time along the flow path. EC measurements do not necessarily detect and follow the tracer peak along the flow path. It is important to highlight that EC measurements does not detect only chloride tracers but anything which cause EC increases along the flow path. The use of EC measurement for tracer breakthrough

measurements is thus not reliable. In most cases it is not possible to distinguish between causes of EC changes along the flow path. Possible causes can include:

- Mobilization of the contaminated groundwater in the aquifer in this case it could be degraded LNAPL by - products or inorganic contaminants.
- Unknown activities can also result increase in groundwater EC increase, especially in stressed aquifer system.
- Mineral interactions in the vicinity of the abstraction borehole and along the flow path or other added tracers can also lead to increase in EC.

6.6 Summary of Chapter 6

In summary, Chapter 6 describes the slug, pump and tracer tests conducted on the Beaufort West study area to hydraulically characterise the LNAPL contaminated fractured rock aquifer. Hydraulic characterisation of the LNAPL contaminated fractured rock sandstone aquifer was important for determining aquifer and mass transport parameters which are essential for remediation exercises. Estimated formation transmissivity from pump testing ranges from 3.4 - 15.4 m²/day. Table 6-7 shows the estimated mass transport parameters from the tracer tests for different located preferential paths. Chemical characterisation which constitutes of organic, inorganic and volatile organics carbon analysis is covered in Chapter 7.

Table 6-7 Estimated mass transport parameters from the tracer tests.

Parameter	Value	Method
q (m/day) (Natural gradient in PW5)	0.1	Drost <i>et al</i> , 1968
q (m/day) (Forced gradient in PW5)	0.2	Drost <i>et al</i> , 1968
q (m/day) (Forced gradient in MW7)	0.6	Drost <i>et al</i> , 1968
v (m/day) (Between MW7 and MW8)	23	TRACER (Riemann, 2002)
Effective porosity, n_e (Between MW7 and MW8)	0.02	TRACER (Riemann, 2002)
Dispersion (m) (Between MW7 and MW8)	0.6	TRACER (Riemann, 2002)

7 Chemical Characterisation

Chemical characterisation aims to understand the nature and type of contamination on the study site, it could be in groundwater and or soil. Furthermore it can yield valuable clues to the chemical processes operating at the site. This stage of site characterisation is important for planning detailed field investigations, monitoring and establishing remediation requirements. Various aspects can be covered during the site chemical characterisation, but in this thesis focus has been placed on the organic hydrocarbon and inorganic compound analysis. Included in the organic constituent study is the VOC measurement and analysis during air percussion drilling using a PID meter.

7.1 Sampling

Groundwater sampling aims to obtain samples which are a representative of the in - situ groundwater conditions. The sampling process should ensure minimum chemical changes during sample collection and handling. On an LNAPL contaminated site, the objective of sampling is to identify and quantify the occurrence of contaminants in groundwater and to investigate processes around the contamination event(s). Weaver *et al* (2007) discusses in detail the sampling protocols for different sampling objectives and in some cases sampling protocols come from the analyzing laboratory. It is however important to note that there will always be some differences between theory and reality. In such cases a balance between theory and reality should be maintained during data interpretation. In this study, about 88 % of the boreholes are installed with pumps which are only accessible via tap outlets. Purging was conducted for 15 minutes before collection of samples from the tap outlet.

In total, 22 boreholes were sampled in order to chemically characterise the LNAPL contaminated fractured rock aquifer. It is important to highlight that of the 22 sampled wells, 7 were identified during the hydrocensus and these were initially analysed using the Site Lab kit. Fifteen of the sampled boreholes are part of a monitoring network used by the GPT consulting company working on the study area. It is important to highlight that MSO1 and MSO2 boreholes are part of the municipal water supply system serving the Beaufort West town community. It was therefore important to include them as part of the LNAPL sampling investigation considering the pivotal role they are playing. Figure 7-1 shows the location of sampled boreholes in relation to identified main potential LNAPL sources.

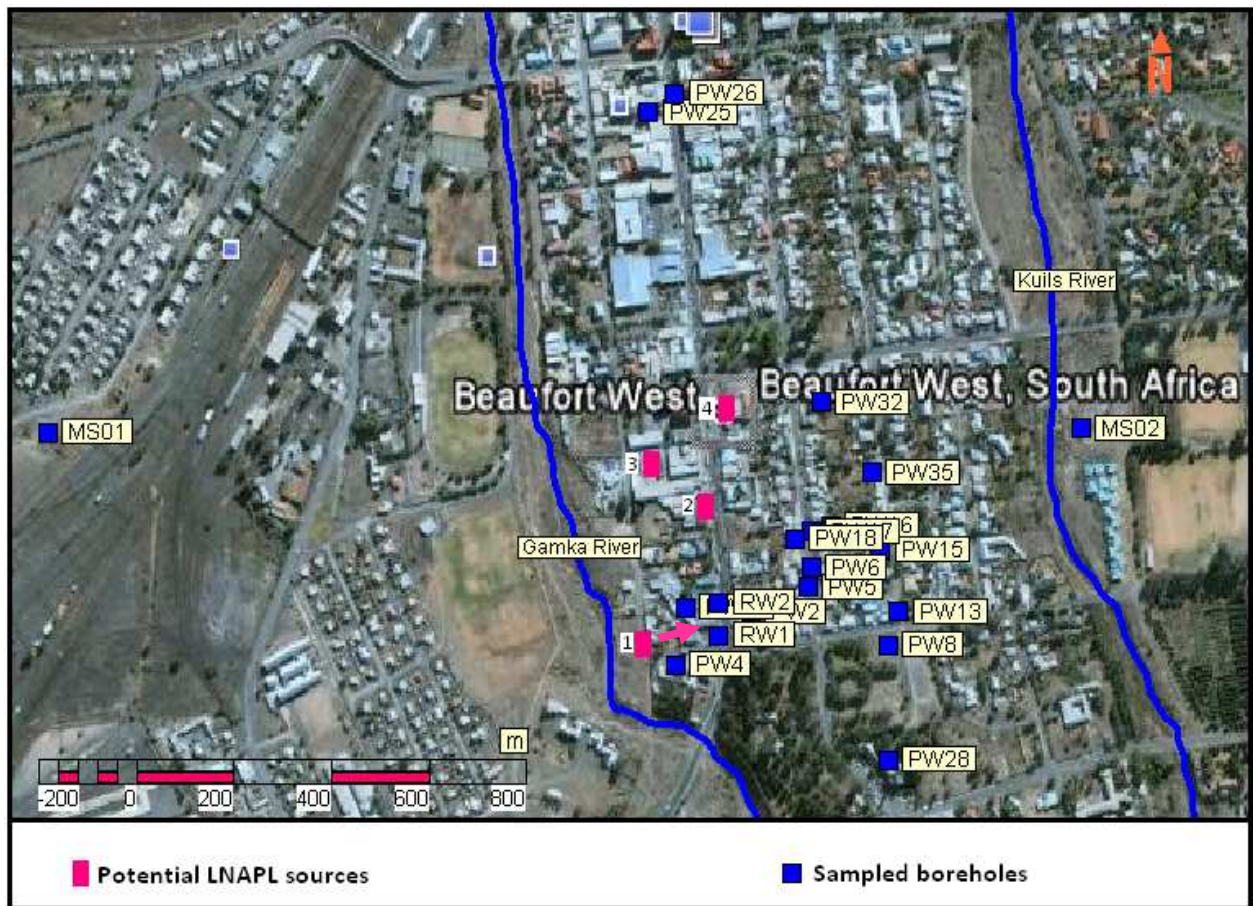


Figure 7-1 Location of sampled boreholes on the Beaufort West study area in relation to the potential LNAPL sources.

Only 4 of the existing monitoring private boreholes (PW2, PW5, RW1 and RW2) were sampled using a specific depth bailer (Figure 7-2). The sampling depth was determined through EC profiling (Appendix 6). Electrical conductivities anomalies were used to infer groundwater flow zones and these were targeted for sampling. Table 7-1 gives the sampling depth for the four boreholes. Samples from the rest of the boreholes were collected directly from the tap outlets.

Table 7-1 Sampling depths.

Borehole name	Sampling depth (mbgl)
RW1	24
PW5	23
PW2	24
RW2	23



Figure 7-2 Specific steel sampling bailer used for sampling in RW1, RW2, PW5 and PW2 boreholes (Taken during the field work).

To avoid cross contamination, the bailer was initially cleaned with a sunlight liquid detergent followed by deionized water and finally rinsed with methanol. Cleaning was conducted after the sampling on each borehole. Samples were collected into 100 ml and 500 ml petrol package containers as prescribed by the analyzing laboratory. Samples were then stored in cooler boxes and maintained at a temperature of 4 °C using ice packs. The cold chain was maintained until laboratory sample analysis.

7.2 Sample Analysis

Groundwater samples were analysed for inorganic constituents and for the following organic hydrocarbon carbon constituents:

- Benzene Toluene Ethylbenzene Xylenes (BTEX).
- Methyl Tert - Butyl Ether (MTBE).
- Tertiary Amyl Methyl Ether (TAME).
- Naphthalene.
- Total Petroleum Hydrocarbon (TPH) Volatile (C6 - C10).
- TPH (C10 - C40).
- VOCs (During air percussion drilling).

7.2.1 Organic Chemistry

Organic hydrocarbon chemical characterisation is important for understanding the nature and compounds of LNAPL, which is of great value in trying to identify the source of contamination. It also plays an important part in the delineation of LNAPL plume, assessment of Monitored Natural Attenuation (MNA) and contamination monitoring. The reliability of organic hydrocarbon analysis results is of great concern, because important and costly site characterisation decisions are made based on these results. Health risk assessments are also conducted based on the organic hydrocarbon results which in most cases indicate levels of various LNAPL compounds and VOCs in soil and groundwater. In this study, organic hydrocarbon analysis was performed by Eurofins Analytico (Netherlands based laboratory). These organic hydrocarbon analytical results have been referred to as “reference laboratory” throughout the thesis and have been used as the basis of comparison for assessing the applicability of the Site Lab kit as a preliminary field screening procedure. It is important to highlight that during the analysis and discussion of the present results, reference has been made to previous chemical results from the work performed by GPT from 2002 - 2007.

7.2.1.1 Distribution of LNAPL Contaminants at the Study Area

Out of the 22 sampled boreholes, 11 were found to be contaminated with LNAPL petroleum hydrocarbon. Figure 7-3 shows the percentage proportions of the LNAPL detected in the contaminated boreholes. Uncontaminated boreholes (MSO1, PW26, PW25, PW3 and PW27) have been excluded from Figure 7-3 in order ensure a clear view of the map.

Transverse and longitudinal mass transportation processes are highly active at the study area as evidenced by LNAPL detections across and in the downgradient boreholes of the four potential LNAPL sources (Figure 7-3). The fact that the study area's fractured sandstone aquifer serves as a well field implies that; LNAPL contaminant mobilization due to abstraction effects is highly possible. Abstraction effects from private and municipal boreholes might induce an artificial gradient that has the potential to mobilize both dissolved and free phase LNAPL towards pumping boreholes. This would be a significant contributing factor to the observed LNAPL migration across gradient towards the easterly direction (See the direction of inferred groundwater flow under assumed natural conditions in Figure 7-5).

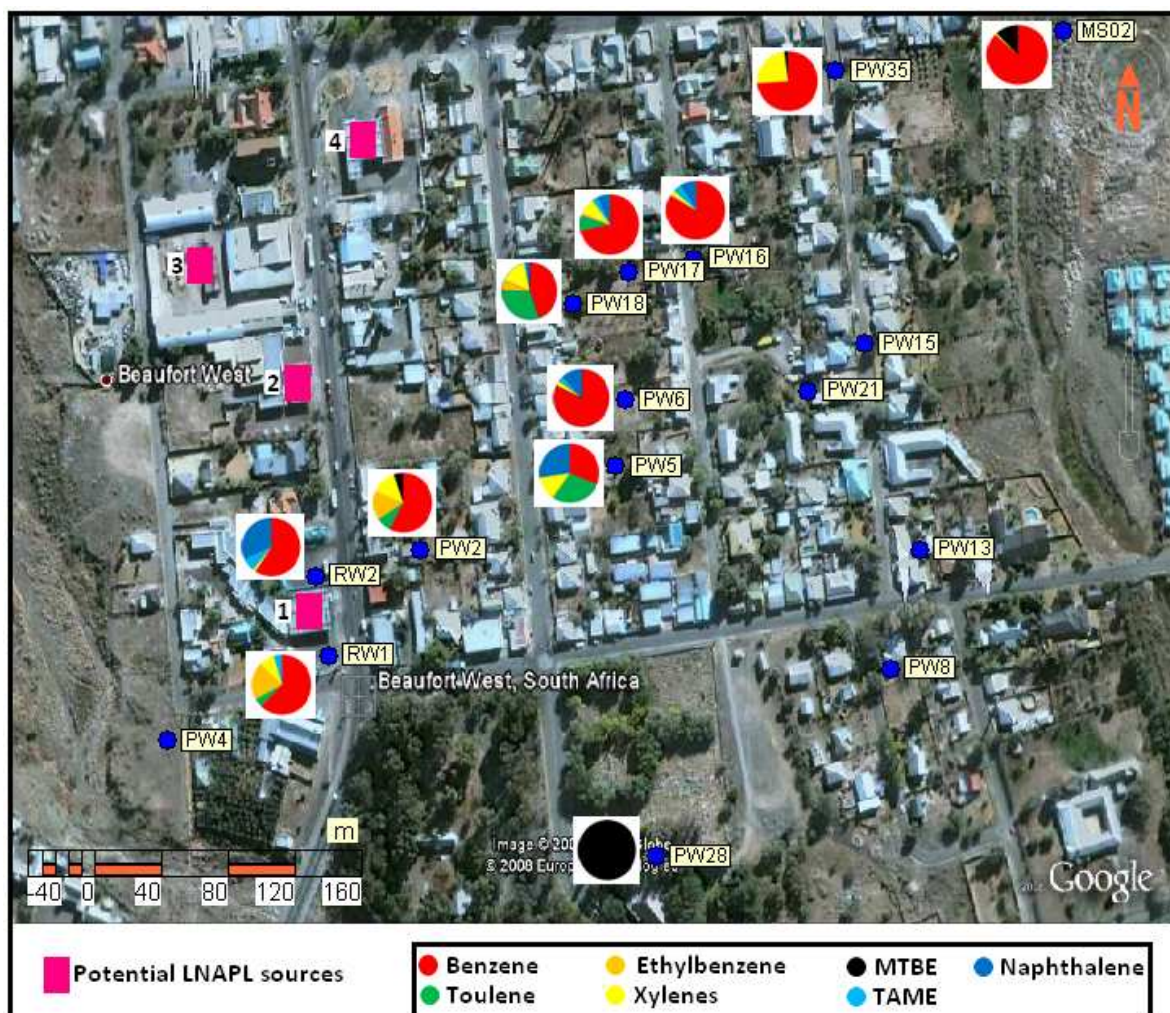


Figure 7-3 Percentage proportions of LNAPLs detected in contaminated boreholes at the Beaufort West study area.

According to Williams *et al* (2006), benzene is often the main groundwater contaminant of concern at petroleum release sites because of its high toxicity and mobility in comparison to other BTEX compounds. As evident in Figure 7-3, benzene dominates the LNAPL contaminants at the study area after being detected in 10 out of the 11 contaminated boreholes. In other words, benzene is the most water soluble component of the BTEX compounds (Table 7-2); its occurrence in most of the contaminated boreholes is thus expected. Specific concentrations of BTEX compounds are presented in Figure 7-4.

MSO2 had the highest benzene and MTBE detectable concentrations of 48 µg/l and 6.7 µg/l respectively (Figure 7-4 and 7-6). It is important to highlight that MSO2 is a municipal borehole located at least 400 m east of the four potential LNAPL sources. The detection of high

benzene concentrations at such a distance from the potential LNAPL sources is a major cause of concern; theoretically benzene is expected to be within the vicinity of the source due to low mobility as compared to MTBE. Another contrasting observation is the presence of MTBE oxygenates in the upgradient MS02 and PW35 boreholes (Figure 7-5 shows the inferred groundwater flow direction). The most possible reason for the two contrasting observations is the mobilization of LNAPL contaminants from other unidentified LNAPL sources. Considering that MS02 borehole is part of the municipal water supply system, it is most likely being operated at a high abstraction rate in comparison to other individual household boreholes. This would effectively create an artificial gradient that can transport the LNAPL contaminants towards the pumping borehole.

Ethylbenzene had the lowest detected concentrations (mg/l) in all contaminated boreholes (Figure 7-4) as compared to other BTEX compounds. This observation is expected considering that ethylbenzene has the lowest solubility of all the BTEX components (Table 7-2). The measured BTEX concentration in PW18 borehole confirms to their theoretical solubility (Table 7-2) in the order of benzene, toluene, ethylbenzene and xylenes. However the BTEX concentrations measured in PW35 borehole (Figure 7-4) shows a sharp contrast to the expected based on the solubility theory. In PW35 borehole, benzene compound tops the concentration followed by xylenes and toluene. Possible reasons for the elevated xylenes as compared to toluene concentration in PW35 include:

- Other LNAPL sources having a high initial concentration (mg/l) of xylenes.
- Cross contamination of sample during the sampling process.

Table 7-2 Vapor pressure and solubility of selected LNAPL compounds

Compound	Vapor pressure (mmHg) at 30 °C	Solubility in water (mg/l) at 20 °C
Benzene	100	1200
Toluene	30	800
Ethylbenzene	13	105
Xylenes	11	110
MTBE	30 000	643

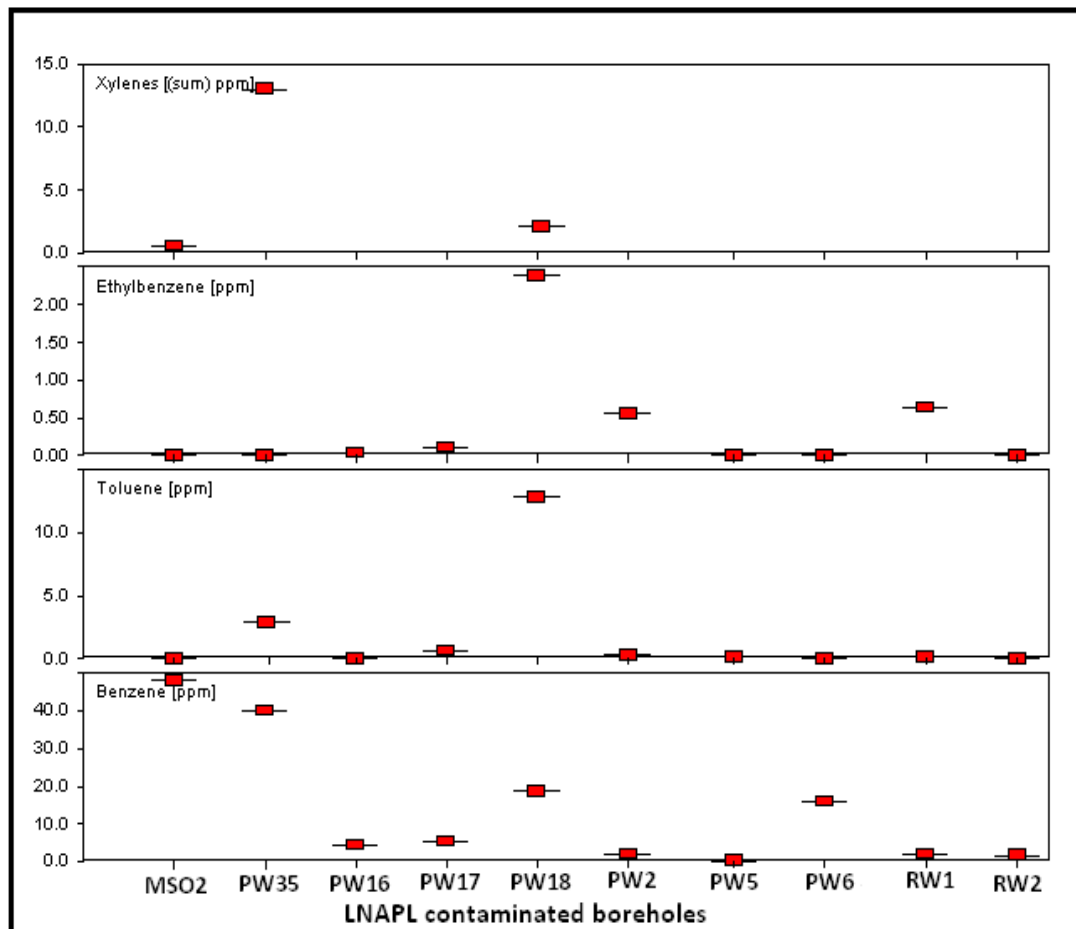


Figure 7-4: BTEX concentration in LNAPL contaminated boreholes.

PW5 has the least benzene concentration of 0.17 $\mu\text{g/l}$ and the most likely reason for that is the enhanced biodegradation due to additional sulphate (1 kg) which was injected into that borehole (Nabee, 2007). Possible evidence and results to infer LNAPL biodegradation has been discussed in Section 7.2.1.2. Of all the LNAPL contaminated boreholes, PW18 had the highest BTEX proportion (Figure 7-4). It is interesting to note that in the 2007 sampling run by GPT (2002 - 2007) an elevated concentration of 16.3 $\mu\text{g/l}$ benzene was measured in PW2 as compared to 2.03 $\mu\text{g/l}$ recorded in the present sampling run. Based on the observed substantial decrease of BTEX concentration in some of the private boreholes, it is possible to infer shrinking of the dissolved plume at the site. Five of the contaminated boreholes (PW17, PW18, PW6, PW35 and MSO2) had benzene concentration exceeding the Maximum Contamination Level (MCL) of 5 $\mu\text{g/l}$ based on the US EPA (2002) advisory regulations.

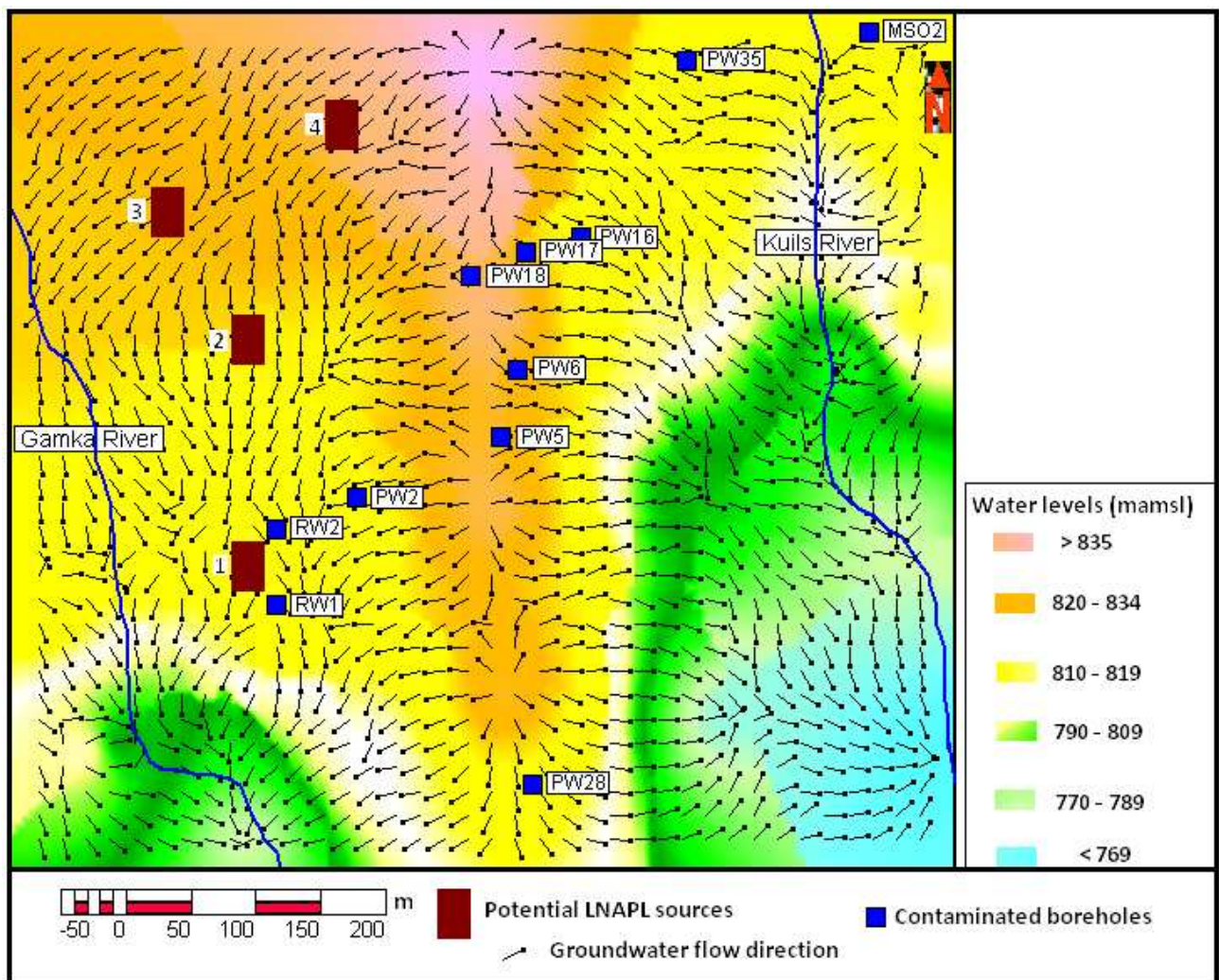


Figure 7-5 Inferred groundwater flow direction under assumed natural conditions in the Beaufort West study area.

A closer look at the detected LNAPL contaminants indicate low concentrations in $\mu\text{g/l}$ of MTBE relative to benzene and this is most likely caused by the natural attenuation processes of dilution and dispersion. MTBE is more prone to dilution because it is highly soluble in water (Table 7-2). In MSO2 borehole, the maximum detected concentrations of benzene and MTBE are $48 \mu\text{g/l}$ (MSO2) and $6.7 \mu\text{g/l}$ (MSO2) respectively. MTBE was the only LNAPL compound detected in PW28 borehole located to the downgradient of potential LNAPL sources. The detection of MTBE as the only LNAPL compound in the downgradient borehole PW28 (Figure 7-5) is expected because of its high solubility and low retardation properties.

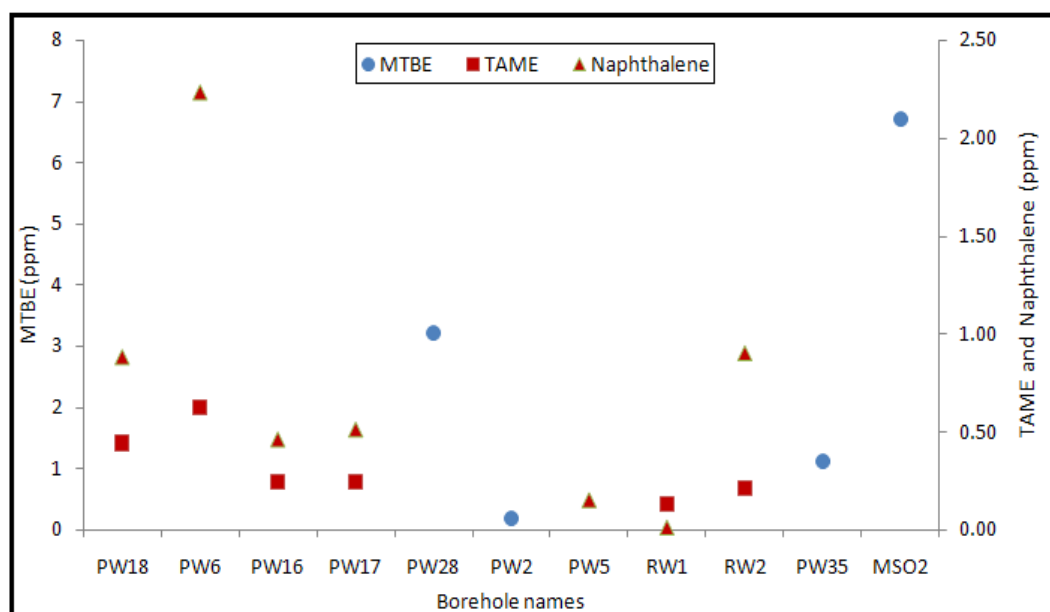


Figure 7-6 MTBE, TAME and Naphthalene concentrations in LNAPL contaminated boreholes.

The high solubility of MTBE in water, coupled with its low sorption characteristics, implies that MTBE plumes have the potential to move on the scale of kilometers away from the source of contamination as compared to BTEX compounds. The observation of benzene transportation being retarded with respect to advective groundwater flow and MTBE can only be attributed to the higher solubility, lower adsorption and lower biodegradation potential of MTBE as compared to benzene (Landmeyer *et al*, 1998). This is the most likely possible reason why only MTBE was detected in PW28 borehole downgradient of the potential sources. With respect to US EPA (1997a), the MTBE concentrations of 1.1 to 6.7 µg/l detected at the site during this investigation are still below the MCL of 20 to 40 µg/l. TAME and Naphthalene contaminants were also detected in the contaminated boreholes at the study area (Figure 7-6).

7.2.1.2 Evidence of LNAPL Biodegradation at the Study Area

In aquifers contaminated with LNAPL petroleum hydrocarbon, reduction of the contaminant mass by microbes is often determined by the presence of microbes capable of degrading the hydrocarbon, terminal electron acceptor processes, production of hydrocarbon degradation by-products such as organic acids (Cozzarelli *et al*, 2001), ferrous iron [Fe(II)], manganese (Mn) and production of carbon dioxides. Microbes need terminal electron acceptors in order for them to consume organic hydrocarbon from the LNAPL contaminant. In other words, the diminishing supply of oxygen (O₂), nitrates (N) and sulphates (SO₄) can be attributed to LNAPL hydrocarbon biodegradation. It is evident based on the organic hydrocarbon results (Section

7.2.1.1) that the study area's aquifer is contaminated by LNAPL petroleum hydrocarbon. Indigenous microorganisms are therefore expected to utilize the LNAPLs as a carbon source in the presence of electron acceptors (Lee *et al*, 2001). In order to understand possible biodegradation effects at the study area, uncontaminated boreholes (Figure 7-7 and Table 7-3) has been used as the background chemistry.

According to the National Research Council (1993) multiple lines of evidence are generally required to demonstrate the existence of biodegradation processes at LNAPL contaminated sites. The lines of evidence used to examine biodegradation of petroleum hydrocarbons include (US EPA, 1997b):

- Chemical data that indicate decreasing concentrations of LNAPLs.
- Geochemical data that indicate the depletion of electron acceptors.
- Laboratory or field microbiological data indicating that the bacteria present at a site can degrade LNAPL petroleum hydrocarbons.

In this study, the LNAPL biodegradation analysis was based on the comparison of nitrates as nitrogen ($\text{NO}_3 - \text{N}$) and SO_4 as available electron acceptors between contaminated and uncontaminated boreholes. A comparison of detected Fe (II) and Mn concentrations as reduced species between the contaminated and uncontaminated boreholes were also conducted.

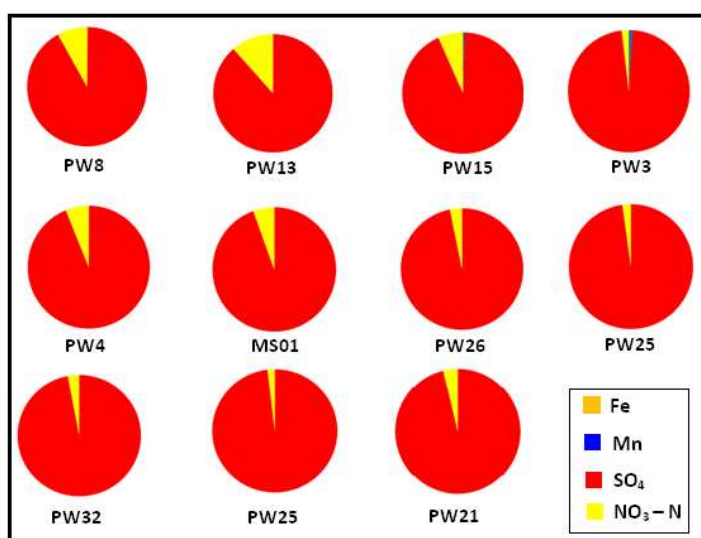


Figure 7-7 Percentage proportions of Fe (II), Mn, $\text{NO}_3 - \text{N}$ and SO_4 in uncontaminated boreholes.

Table 7-3 Concentration of Fe (II), Mn, NO₃ - N and SO₄ in uncontaminated boreholes.

Borehole number	Fe (II) (mg/l)	Mn (mg/l)	SO₄ (mg/l)	NO₃ - N (mg/l)
PW8	0.19	0.09	118	10.4
PW13	0.00	0.00	166	21.6
PW15	0.00	0.48	117	8.4
PW4	0.00	0.00	144	9.4
MS01	0.00	0.00	315	18.4
PW32	0.00	0.00	111	3.4
PW26	0.00	0.00	70	2.3
PW3	0.00	1.39	142	2.8
PW25	0.00	0.00	78	1.5
PW27	0.00	0.00	141	3.2
PW21	0.00	0.00	120	4.7
Average			138	7.8

The biodegradation processes yield various depleted electron acceptors, which produce reduced species. The presence of ferrous iron and dissolved manganese (Figure 7-8) in contaminated boreholes relative to the background chemistry (Figure 7-7 and Table 7-3) indicate that iron and manganese reduction is occurring in contaminated boreholes. Dissolved manganese was detected in all contaminated boreholes with the exception of PW28 (Figure 7-8 below) that is only contaminated by MTBE which is less susceptible to biodegradation as compared to benzene. It is important to note that no Fe (II) and Mn were detected in uncontaminated boreholes with the exception of PW15 and PW3 where only a Mn concentration of 0.5 mg/l and 1.9 mg/l were detected respectively.

Ferrous iron as a by - product of LNAPL biodegradation was detected in PW5, PW18, PW17, PW2 and RW1 contaminated boreholes (Figure 7-8). In PW5, evidence of reduced species indicating biodegradation includes elevated concentrations of both Fe (II) and Mn of 13.9 mg/l and 2.87 mg/l respectively. Fe (II) and Mn were not detectable in PW28; this is however possible because the borehole is only contaminated with MTBE which is less susceptible to biodegradation as compared to benzene (Landmeyer *et al*, 1998). In other words biodegradation is expected in PW28 borehole but at a slower rate as compared to other LNAPL contaminated boreholes. The argument is further supported by the presence of nitrate electron acceptor in PW28 which is completely depleted in other contaminated boreholes

(Figure 7-8 and Table 7-4). For specific concentrations of Fe (II), Mn, NO₃ - N and SO₄ in LNAPL contaminated borehole refer to Table 7-4.

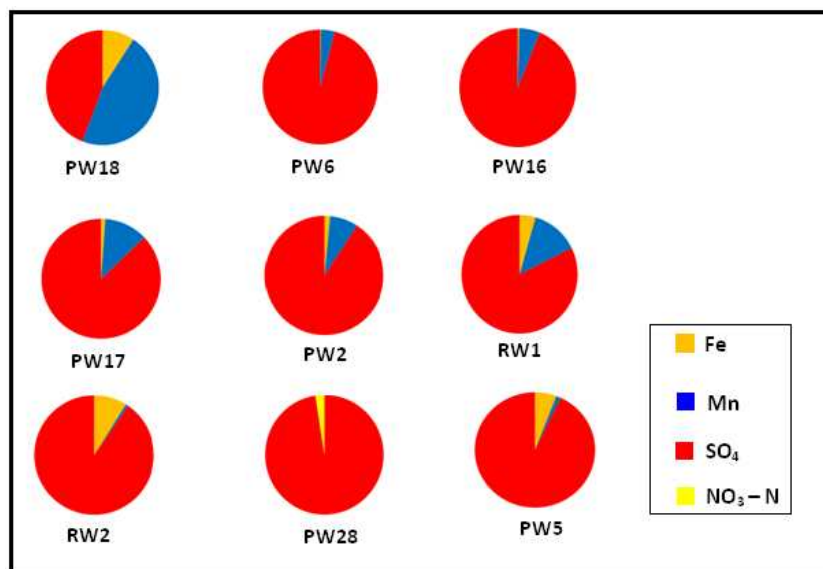


Figure 7-8 Percentage proportions of Fe (II), Mn, NO₃ - N and SO₄ in contaminated boreholes.

Table 7-4 Concentration of Fe (II), Mn, NO₃ - N and SO₄ in contaminated boreholes.

Borehole number	Fe (II) (mg/l)	Mn (mg/l)	SO ₄ (mg/l)	NO ₃ - N (mg/l)
PW18	1.21	6.16	5.84	0
PW6	0.18	3.26	80.10	0
PW16	0.27	4.54	73.40	0
PW17	0.54	5.60	41.70	0
PW2	0.43	2.18	25.90	0
RW1	0.87	2.57	16.00	0
PW28	0.00	0.00	133.00	3.35
PW5	13.90	2.87	222.00	0
RW2	11.20	0.90	114.00	0
Average	3.18	3.12	79.10	

Considering the sampling exercise for this investigation as a snapshot, it is difficult to base the biodegradation argument on the detected sulphate concentration. Monitoring of SO₄ concentration over a number of years is required to ascertain whether sulphate reduction is active on the site. It is however worth to mention that PW5 had the highest SO₄ concentration of 222 mg/l (Table 7-4) and this is despite having the least concentration of BTEX compounds (Figure 7-4). From an LNAPL biodegradation point of view, this is not expected considering

that most of the SO_4 should have been consumed during petroleum hydrocarbon degradation. The presence of elevated Fe (II) concentration of 13.9 mg/l in PW5 is enough evidence to show that biodegradation has been occurring in this contaminated borehole, hence low SO_4 concentration were expected. The most likely reason for high sulphate concentration in PW5 is that an additional amount of 1 kg SO_4 was added in the borehole to enhance biodegradation by the consulting company working on the site (Gilbert, 2006). PW18 (Table 7-4) is a good example of the expected from the perspective of LNAPL biodegradation in the sense that low SO_4 concentration of 5.84 mg/l which was detected corresponds closely to the elevated concentration of Fe (II) and Mn reduced species in the borehole.

Lowered redox potential in contaminated boreholes (Figure 7-9) indicate the highly reduced groundwater environment with respect to the contaminated boreholes. The reduced groundwater environment is further evidence to infer LNAPL biodegradation at the Beaufort West study site.

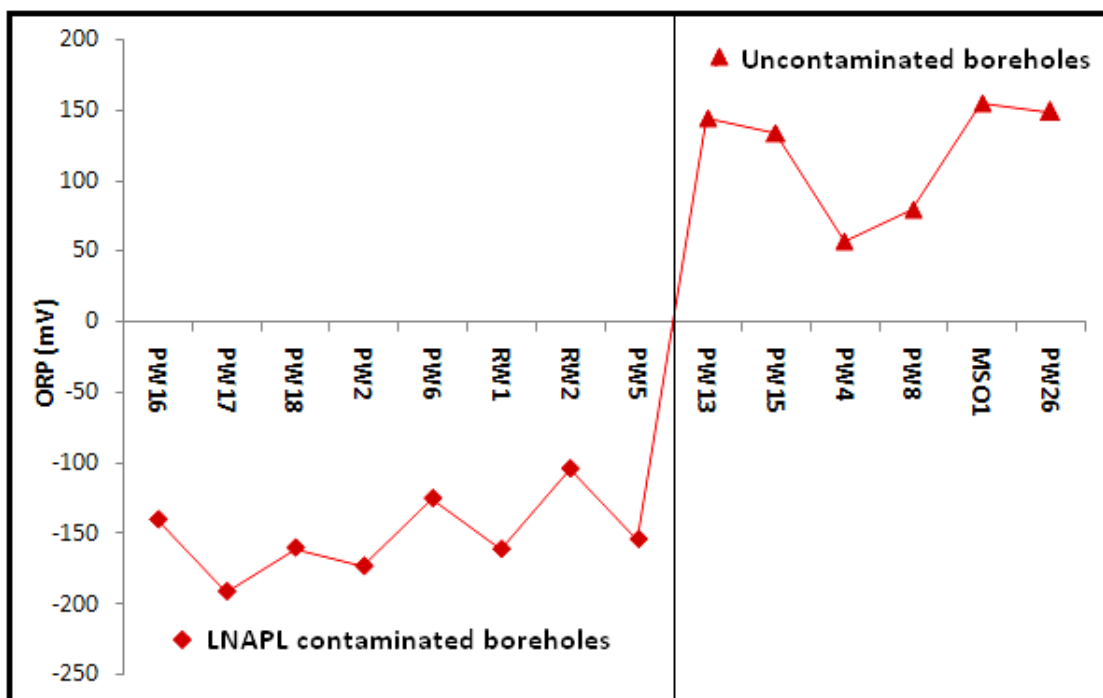


Figure 7-9 Oxidation Reduction Potential in contaminated and uncontaminated boreholes.

There is a need to investigate why some of the boreholes in the study area are not contaminated. Considering that the study area is characterised by Karoo fractured rock aquifer system, a possibility exist that the boreholes intersect different fracture networks. In other words contaminated and uncontaminated boreholes may not be hydraulically connected. The other possible reason could be that the boreholes are abstracting from different aquifers with

the uncontaminated boreholes being situated in a deep confined aquifer protected from contamination. The existence of a leaky aquifer cannot be ruled out as it can also allow movement of contaminants between different aquifer layers due to fluctuating of the abstraction regimes.

7.2.1.3 Soil Vapor Surveys

A soil vapor survey is a rapid and relatively inexpensive method of detecting VOCs contaminants in the vadose zone. Volatile organic carbons diffuse through unsaturated soils to the surface, achieving equilibrium with other soil gases. Presented in this section is the VOC measured during the air percussion drilling of MW5 borehole (Figure 7-10). This was important considering the potential volatilization of LNAPLs in the subsurface during air percussion drilling. It is important to highlight that no VOCs were detected during core drilling. High soil VOC gases in excess of 100 ppm are regarded as dangerous for health and are also a potential source of combustion. Elevated VOC concentrations are an indication of LNAPLs in the vadose zone near the sample location. This might require excavation to remove the LNAPL contaminated soil in the vadose zone if large enough volumes are present.

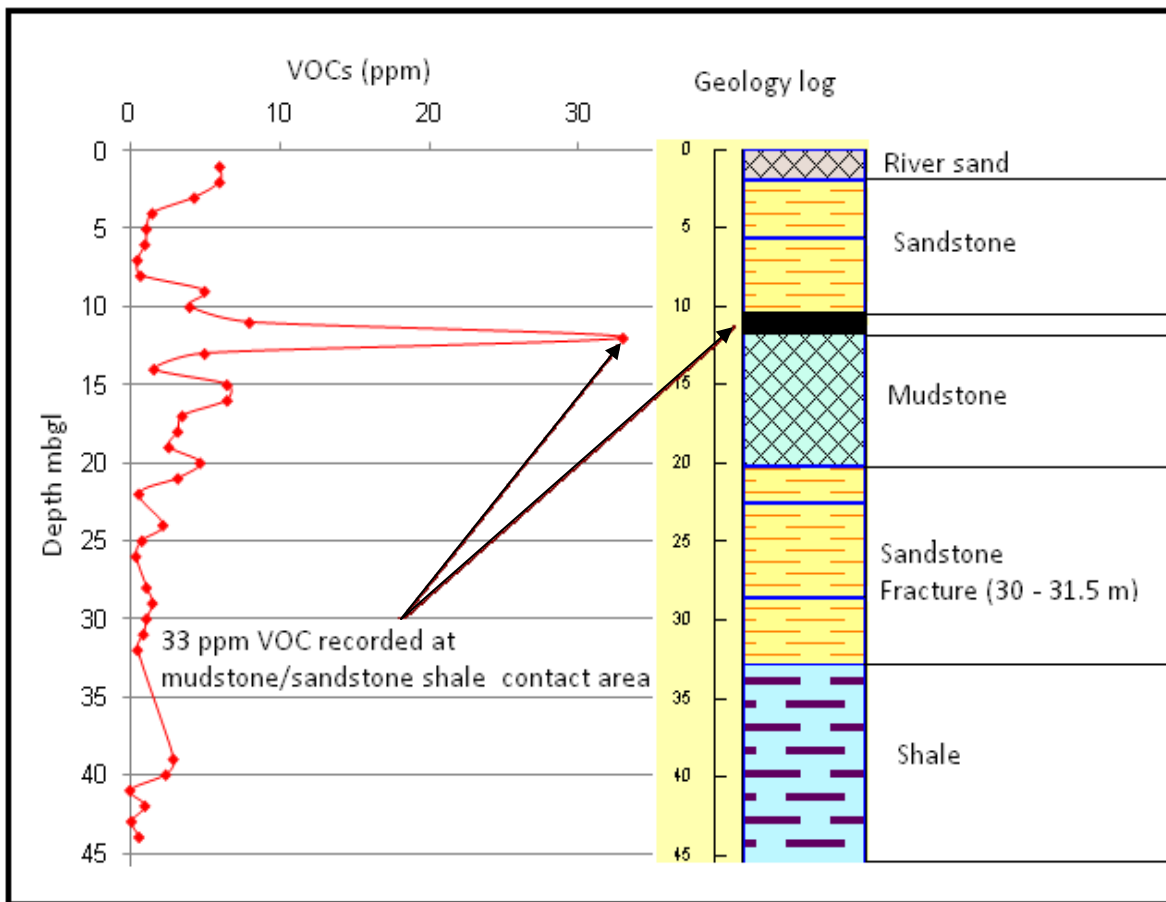


Figure 7-10 VOC concentration measured during the drilling of MW5 percussion borehole and geological log for MW5.

A peak VOC of 33 ppm was measured between 11 - 12 mbgl during the percussion drilling of MW5 borehole. Cross correlation to geological logs revealed the existence of a sandstone and shale contact area (Figure 7-10) between 11 - 12 m depth just below the water level (10.5 mbgl). Weathered loose materials are most likely to be occupying the interface facilitating easier diffusion of VOCs into the unsaturated zone as compared to the solid rock formation. Despite the accumulation of VOCs through diffusion processes, LNAPL smearing during the rising and falling of water levels might also have contributed to spreading of VOCs in the aquifer system. Residual LNAPL entrapment is also highly possible at this zone considering that it can be enhanced by loose and fine weathered materials.

7.2.1.4 Site Laboratory (Lab) Kit

The site lab instrument uses the Ultraviolet Fluorescence (UVF) selective detection method and it is useful for testing many types of organic environmental contaminants. The principle of

operation relies on the electronic configuration of the molecular structure for each contaminant. Aromatic hydrocarbons, which include double - bonded carcinogenic compounds, like benzene and toluene, both excite and emit energy at specific wavelengths under the effects of UVF. The amount of excited and emitted energy gives a measure of aromatic hydrocarbon present in the contaminated groundwater or soil sample. The Ultraviolet Fluorescence UVF-3100 analytical test kit (Figure 7-11) was used in this investigation as a field screening device for the measurement of petroleum hydrocarbon concentrations in groundwater. The investigation seeks to assess the applicability of the site lab kit as a preliminary screening procedure prior for reference laboratory sampling. Screening would substantially reduce sampling work and analysing cost by only targeting contaminated boreholes.



Figure 7-11 UVF-3100 Site Lab analytical test kit (Taken from *site-lab*, 2009)

7.2.1.4.1 Site Laboratory Analysis for Hydrocensus Boreholes

The hydrocensus groundwater samples were analysed for Extended Diesel Range Organics (EDRO) - Total Petroleum Hydrocarbon (TPH) and Gasoline Range Organics (GRO) - BTEX using the site laboratory kit. Figure 7-12 shows the site laboratory TPH and BTEX concentration in sampled hydrocensus boreholes.

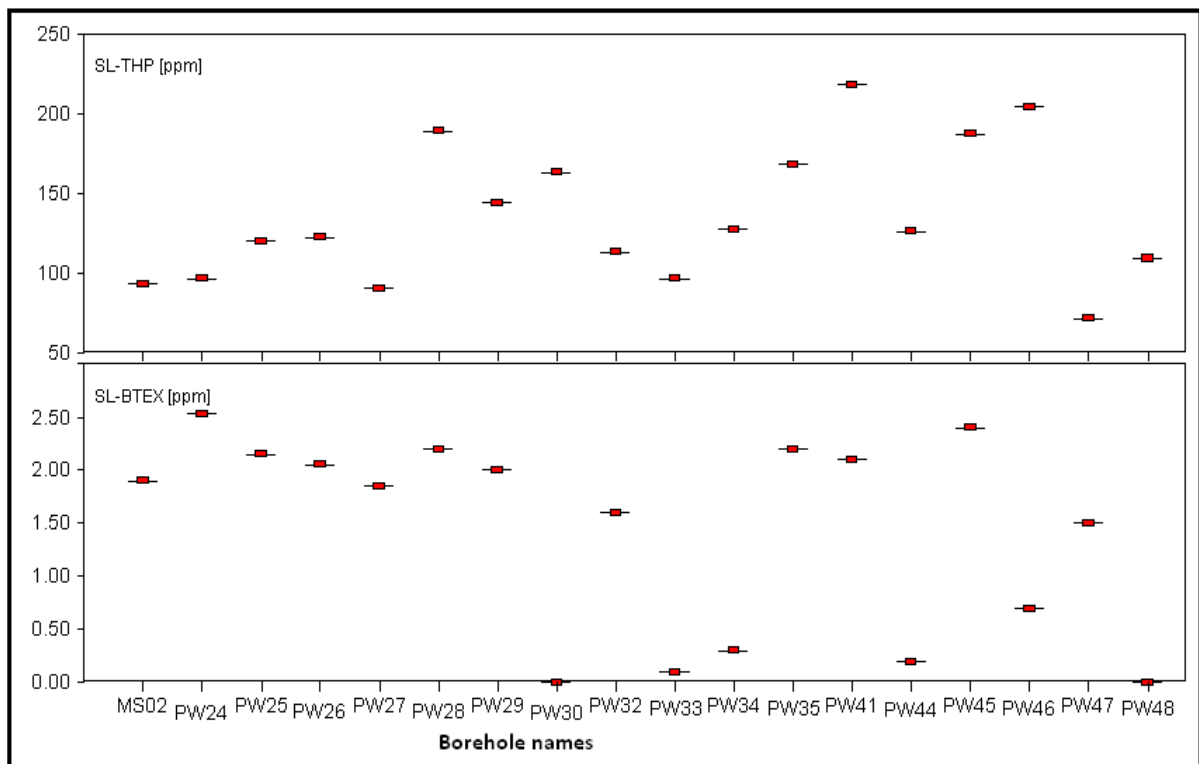


Figure 7-12 Site Lab TPH and BTEX concentrations detected in hydrocensus boreholes.

During the first phase of the project, site laboratory kit was used during the hydrocensus exercise as a field screening procedure to determine which private boreholes could be sampled for reference laboratory analysis. Based on the site lab kit results (Figure 7-12) it appeared that all sampled boreholes had at least some traces of petroleum hydrocarbon contamination. Based on preliminary site lab results the following 10 private boreholes had to be selected for sampling:

- PW 25, PW26, PW27, PW28, PW29, PW32, PW35, PW41, PW45 and MSO2

The selection was firmly based on BTEX results, the reason being that most of the private wells under monitoring by GPT indicated elevated levels of BTEX. Ten private boreholes were initially planned to be sampled for the reference laboratory analysis, but only 7 boreholes were accessible. Figure 7-13 shows the location of the boreholes which were sampled during assessment of the site lab kit.

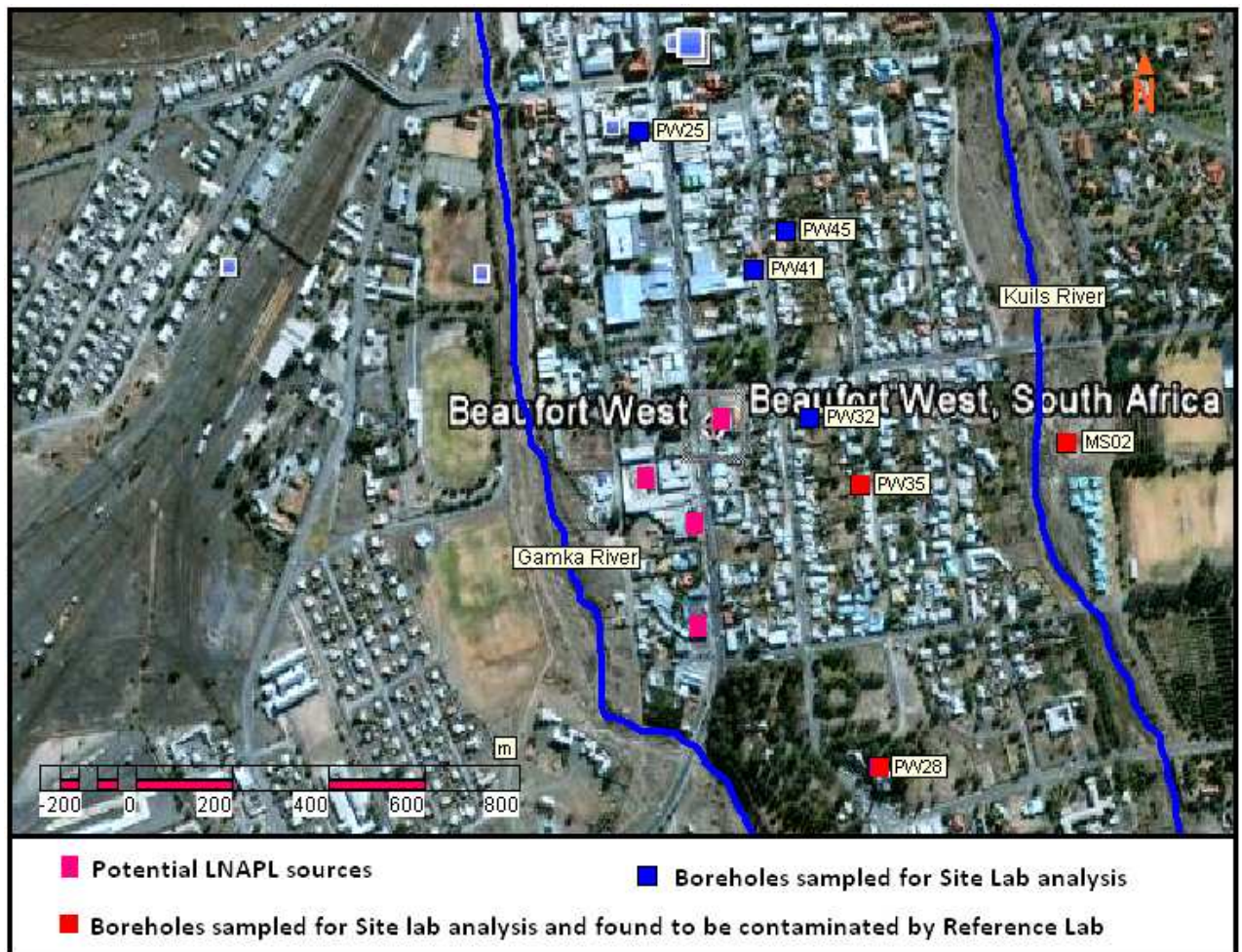


Figure 7-13 Boreholes sampled for assessing the applicability of the Site lab kit.

7.2.1.4.2 Correlation between Site and Reference Laboratory results

As part of chemical characterisation, site lab results from already existing monitoring boreholes were measured and compared to reference laboratory analytical results with the objective of establishing a relationship and basis for future use of the site lab kit. However, data from only four sampling points were available and had to be used for linear correlation analysis.

A linear correlation of 85 % existed between site and reference laboratory analysis for TPH (Figure 7-14). There was no linear correlation established for BTEX between site and reference laboratory analysis (Figure 7-15). Considering that only four points have been used to perform the correlation analysis, such results cannot be conclusive and the need for a large number of samples remains critical.

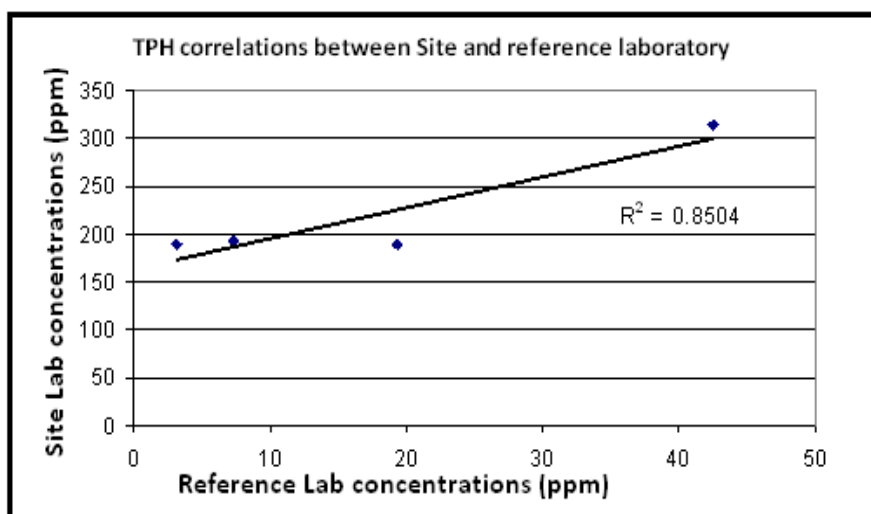


Figure 7-14 TPH correlation between Site and Reference laboratory concentrations.

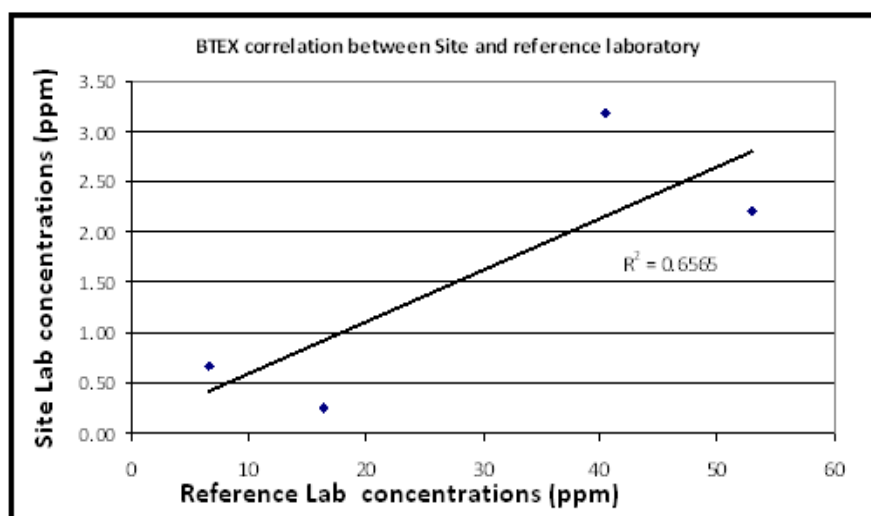


Figure 7-15 BTEX correlation between Site and Reference laboratory concentrations.

It is important to note that TPH site lab concentrations are extremely high in comparison to reference laboratory concentration (Figure 7-14). Possible reasons that might have contributed to elevated site lab concentrations especially during the sample analysis include the use of methanol from different sources during sample extraction. This is more important considering that unclean methanol has the ability to emit energy when exposed to UVF light, implying that it can also be detected as TPH contaminant. The other possible source of variation could be that the petroleum hydrocarbon product volatilization as a result of different sampling containers and storage conditions between reference and site lab samples before analysis. The lag time between sampling and sample analysis can also contribute to such a concentration differences

between site and reference laboratory results. The site lab kit worked successfully as a field screening procedure only on 3 of the 7 sampled boreholes (Figure 7-13) and can be given a 43 % success rate. In other words only 3 of the 7 groundwater samples which had been screened using the Site Lab kit were actually found to be contaminated.

Such a success rate is however too low to recommend for the use of site lab kit as a field screening procedure considering that, the objective is to reduce sampling cost by only targeting contaminated wells. This success rate would mean only 43 % of the screened samples are most likely to be found contaminated by costly reference laboratory. The situation will be even more compounded if one is working with a large number of samples because chances of failure increases and the possibility of missing the actual contaminated samples increase. Based on this finding, the only recommendation is further trials to establish good correlations and high success rate. This should enable the use site lab kit to reduce cost of sending uncontaminated samples to reference analytical laboratories.

7.2.2 Inorganic Chemistry

Inorganic chemical characterisation was important for groundwater classification in terms of South African Water Quality Guidelines (SAWQG) (2006) and also to assess potential for LNAPL degradation. Figure 7-16 displays the water quality of the Beaufort West study area on a Piper diagram.

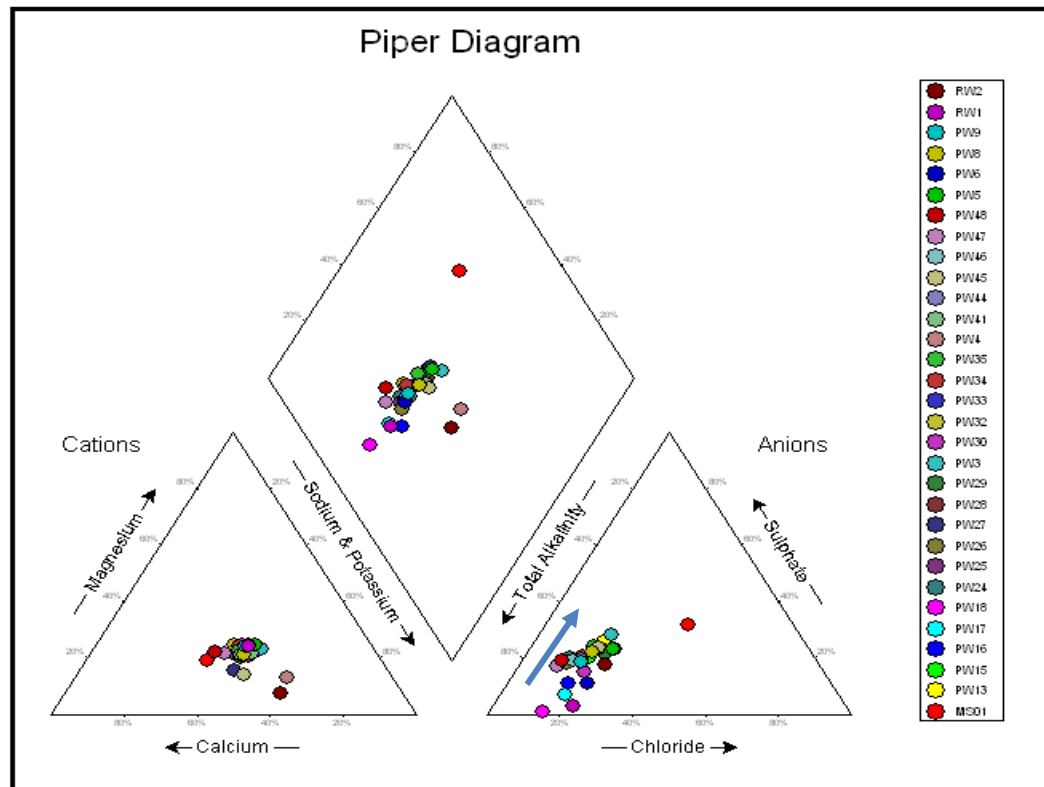


Figure 7-16 Piper diagram showing the study area water chemistry.

The groundwater chemistry appears to evolve along two lines one from calcium (Ca) towards sodium (Na) and potassium (K) rich type; the other one evolves from carbonate (CO_3)/bicarbonate (HCO_3) to sulphates (SO_4) (Figure 7-16). However as depicted on the piper diagram, the groundwater evolving from CO_3/HCO_3 system to SO_4 is more dominant. The Piper diagram also shows the presence of old water in MSO1 municipality borehole as evidenced by elevated chloride values. The rest of the boreholes are characterised by recently recharged groundwater as indicated by high bicarbonate concentrations (Figure 7-16).

The groundwater can be classified as calcium (Ca)-(Na+K)-(HCO_3). The presence of Ca and HCO_3 recharge waters in the near surface environment result most likely from two closely

related processes; carbonate dissolution and plagioclase weathering. The study area is bounded by dolerite intrusions which have plagioclase minerals (Albite and anorthite) as one of its main constituents. Plagioclase weathering produces calcite that precipitates mostly in the fractures and cavities, resulting in a source of $\text{Ca}+\text{HCO}_3$ waters. Total dissolved solids ranged from 195.8 - 1090.8 mg/l, and this concentration according to SAWQG (1996) does not have any likely negative health effects. The alkalinity dominance is also evidenced by the slightly high pH range varying between 6.8 - 8.07. Consequently the electrical conductivity follows the same trend ranging from 45.9 - 190 mS/m (Figure 7-17).

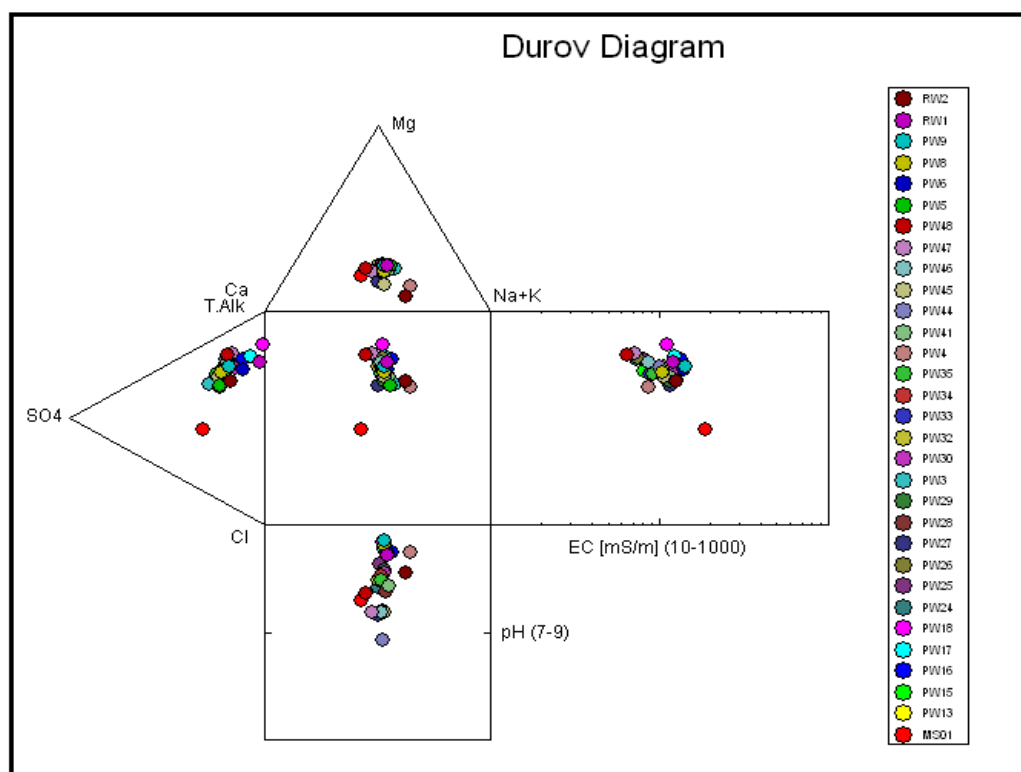


Figure 7-17 Durov diagram showing the study area water chemistry.

Elevated Na concentrations in the range of 44.8 - 212 mg/l can be mainly attributed to the cation exchange of Ca and magnesium (Mg) ions in aqueous solution with sodium ions on clay laminating the shale geological formation in the study area. It is also important to highlight that the water sample from municipal well MSO1 plotted differently from the rest, this sample is characterised by high EC and high TDS values. The Stiff diagram (Figure 7-18) further confirms the dominance of CO_3/HCO_3 groundwater system which contributes to the total alkalinity of the aquifer system. In contrast, the Stiff diagram (Figure 7-18) also depicts the municipal well (MSO1) water quality which is depleted in alkalinity. Considering that MSO1

municipal borehole is located in the far east (Figure 7-1, Section 7.1), further away from the rest of the boreholes and such a contrast in water quality cannot be unique and is most likely a reflection of different water type evolving as function of the underlying geology. However as the Piper diagram (Figure 7-16) has indicated, the most likely reason for that difference is the presence of old waters in MSO1 municipal borehole.

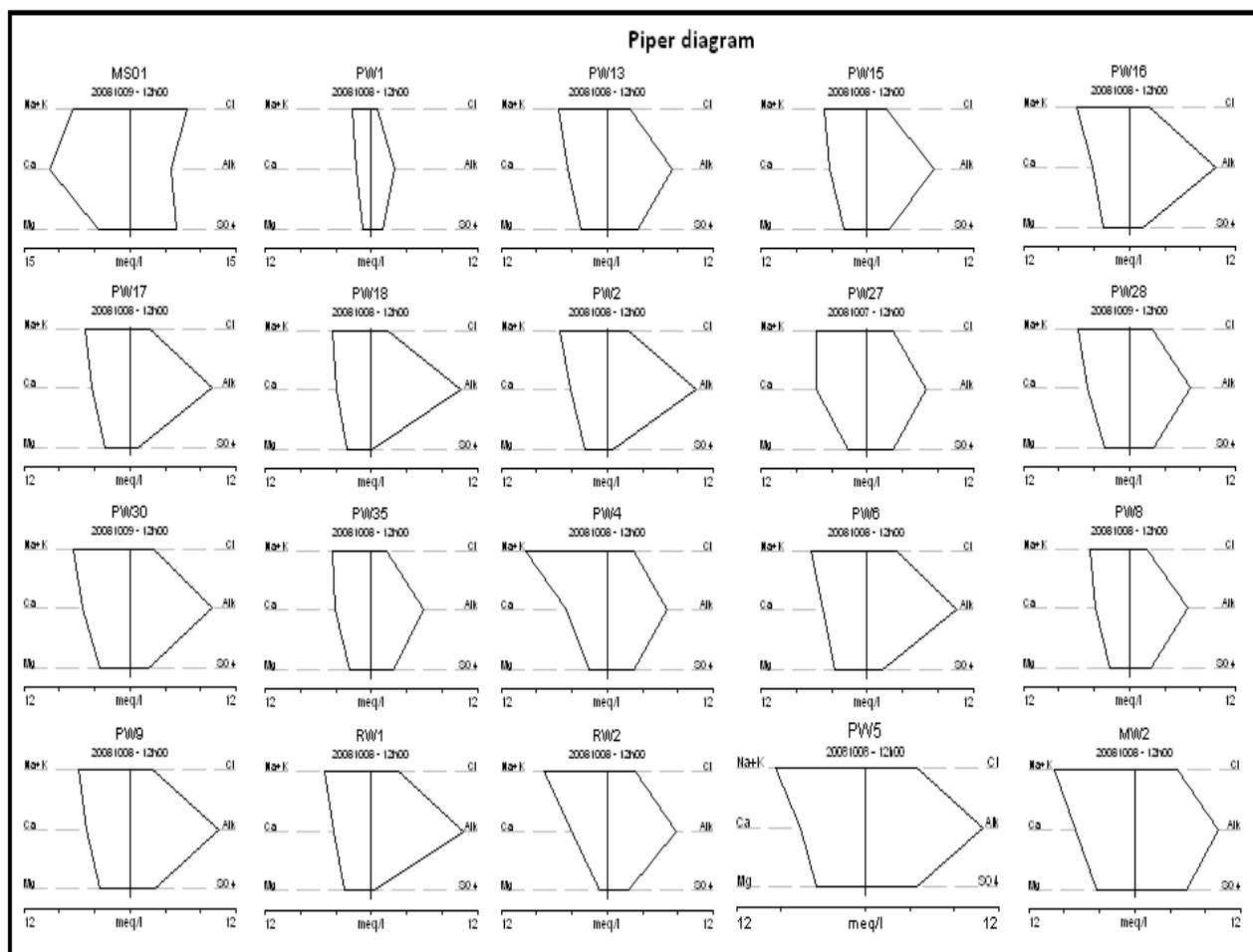


Figure 7-18 Stiff diagrams showing the study area water chemistry.

Sulphates range from 5.84 - 315 mg/l with the highest concentration being also recorded in the municipal boreholes (MSO1). The contrast displayed by municipal MSO1 water quality as characterised by elevated NO_3^- - N and SO_4 concentration (Table 7-2, Section 7.2.1.2) could also be as a result of groundwater ageing. It is possible to infer that water in MSO1 originated from the nitrogen redox based zone (Danish EPA, 2000). In such zones, high SO_4 content is a sign of possible nitrate reduction with pyrite in the sediment as this reaction among other things produces SO_4 .

The presence of SO_4 ions in all boreholes, though in low concentrations is most likely due to oxidation of sulphide minerals contained in the shale formation underlying the study area. The relatively low SO_4 concentrations in LNAPL contaminated boreholes can also be attributed to microbial hydrocarbon degradation which utilizes electron acceptors including SO_4 . Silicon (Si) concentration ranges from 2.74 - 20.2 mg/l. The presence Si is explained by the quartz minerals in the sandstone formation underlying the study area.

Ferrous iron and Mn are the only trace metals present. Ferrous iron is relatively low in all samples except for RW2 and PW5 in which 11.2 mg/l and 13.9 mg/l were measured respectively, exceeding the SAWQG (2006) of 2 mg/l. Compared with the SAWQG, Mn concentrations exceeded the guidelines of 1 mg/l in 9 LNAPL contaminated boreholes (Table 7-4, Section 1.2.1.2). Besides LNAPL biodegradation, the occurrence of elevated concentrations of Fe (II) and Mn can be attributed to industrial effluent and sewage. It is important to point out that Fe (II) and Mn are only aesthetic parameters which contribute significantly to water taste, smell and colour. Nitrates as nitrogen concentrations are generally low, except in the municipal borehole MSO1 where 18.4 mg/l was measured and is above the SAWQG (2006) of 10 mg/l. Total hardness as calcium carbonate ranges from 240 mg/l - 790 mg/l (Figure 7-19). The Beaufort West study area's groundwater can be classified as hard.

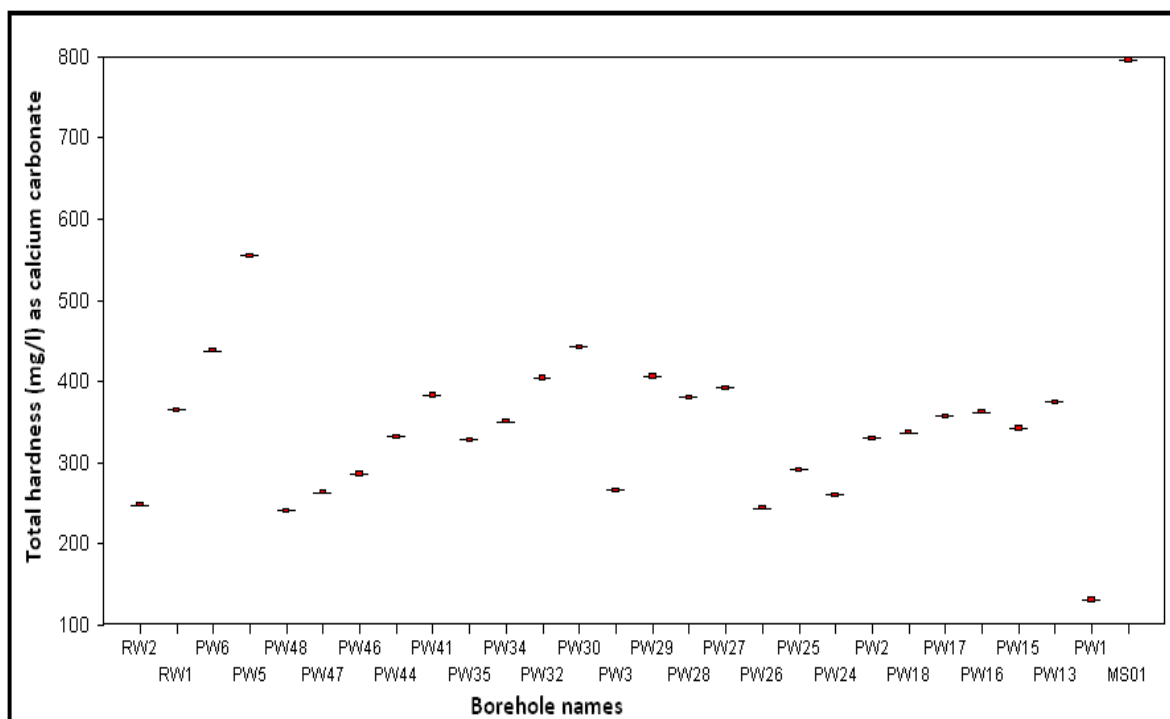


Figure 7-19 Total hardness for the Beaufort West study area groundwater.

As part of this academic study, one cannot be conclusive about the organic hydrocarbon site status based on a single sampling run conducted during the field work. Chemical results from which conclusions can be made about plume migration, shrinking or expanding requires long term chemical site monitoring data. The need for time chemistry organic and inorganic data in order to achieve a detailed chemical characterisation for LNAPL contaminated aquifers cannot be overemphasized.

7.3 Summary of Chapter 7

In summary, Chapter 7 documents the chemical status of the Beaufort West study area achieved through the analyses of organic and inorganic groundwater and volatile organic carbon sampling. The overall output of the chapter is the concentration levels of LNAPL petroleum hydrocarbon on the Beaufort West study area and the existing chemical processes. Benzene is the most dominant LNAPL compound after being detected in 10 of the 11 contaminated boreholes. Benzene concentration exceeded the Maximum Concentration Levels (MCL) of 5 µg/l (US EPA, 2002) in 5 of the contaminated boreholes (PW17, PW18, PW6, PW35 and MSO2). MTBE concentration detected in all contaminated boreholes is below MCL of between 20 - 40 µg/l (US EPA, 1997a). LNAPL biodegradation is inferred to be taking place at the study area as evidenced by the reducing environment. The reducing environment

is characterised by elevated concentrations of Fe (II) and Mn species and depleted SO_4 and NO_3 - N electron acceptors. The chapter also highlights the failure of the Site Lab kit as a preliminary field screening procedure before sending LNAPL contaminated groundwater samples for reference laboratory analysis.

8 Site Conceptual Model

A geohydrological conceptual model is a description and visual representation of the predicted relationships between geohydrological components or attributes. In other words, it is a representation of the geohydrological system based on observations made during field investigations. This conceptual model is based on the integration of all the work conducted at the Beaufort West study area by upgrading of the initial conceptual model. The study area's geohydrological system is defined by the following main components:

- Geology.
- Hydraulic parameters.
- LNAPL source location and loading, migration and movement.

8.1 Geological Component

The geology underlying the Beaufort West study area is typical of South African Karoo formations. Based on core drilling results, the subsurface lithology of the study area was conceptualised to be occupied by river sand and sandstone inter - layered with mudstone and shale formations (Figure 8-1).

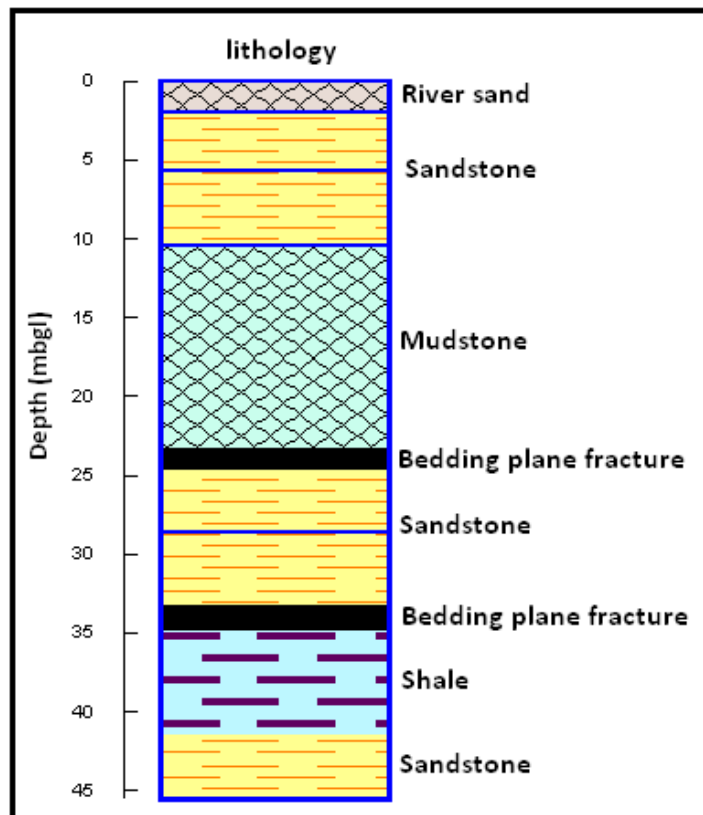


Figure 8-1 Beaufort West study area geological conceptualization.

Bedding plane fracture features located at the sandstone/shale and sandstone/mudstone contact areas forms the main preferential flow pathways to groundwater and LNAPLs (Figure 8-1). Two bedding plane fractures have been located at the study area between 24 - 25 mbgl and 34 - 35 mbgl respectively. The location was based on the comparison and cross correlations between geological logs and borehole geophysics characterisation results.

Other important structures underlying the study area include:

- Vertical and subvertical fractures intersected by the drilled boreholes in the vadose and saturated zones. These are important for groundwater flow but also serve as conduits for downward migration of LNAPL contamination.
- Dolerite intrusions which present good opportunities for water strikes at shale and dolerite contact areas were also identified.

8.2 Hydraulic Parameters

8.2.1 Groundwater Levels

Groundwater levels in the study area range between 8 - 15 mbgl. A very good correlation of 99.5 % exists between topography and water levels (Figure 8-2). In a natural groundwater system under ambient conditions, the water table would follow the topography in the study area. A good correlation implies that Bayesian interpolation method can be used to construct a groundwater contour map and infer the groundwater flow direction.

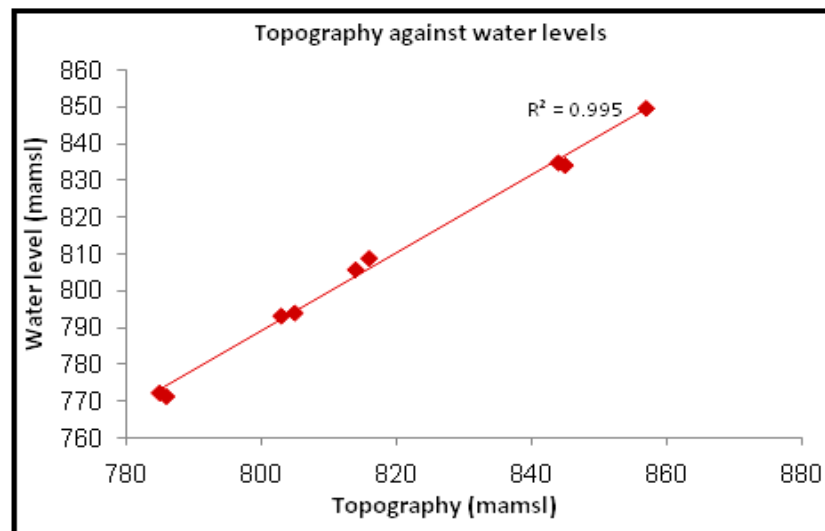


Figure 8-2 Correlation between topography and water level on the Beaufort West study area.

Figure 8-3 below shows the inferred groundwater flow direction under assumed natural conditions on the Beaufort West study area.

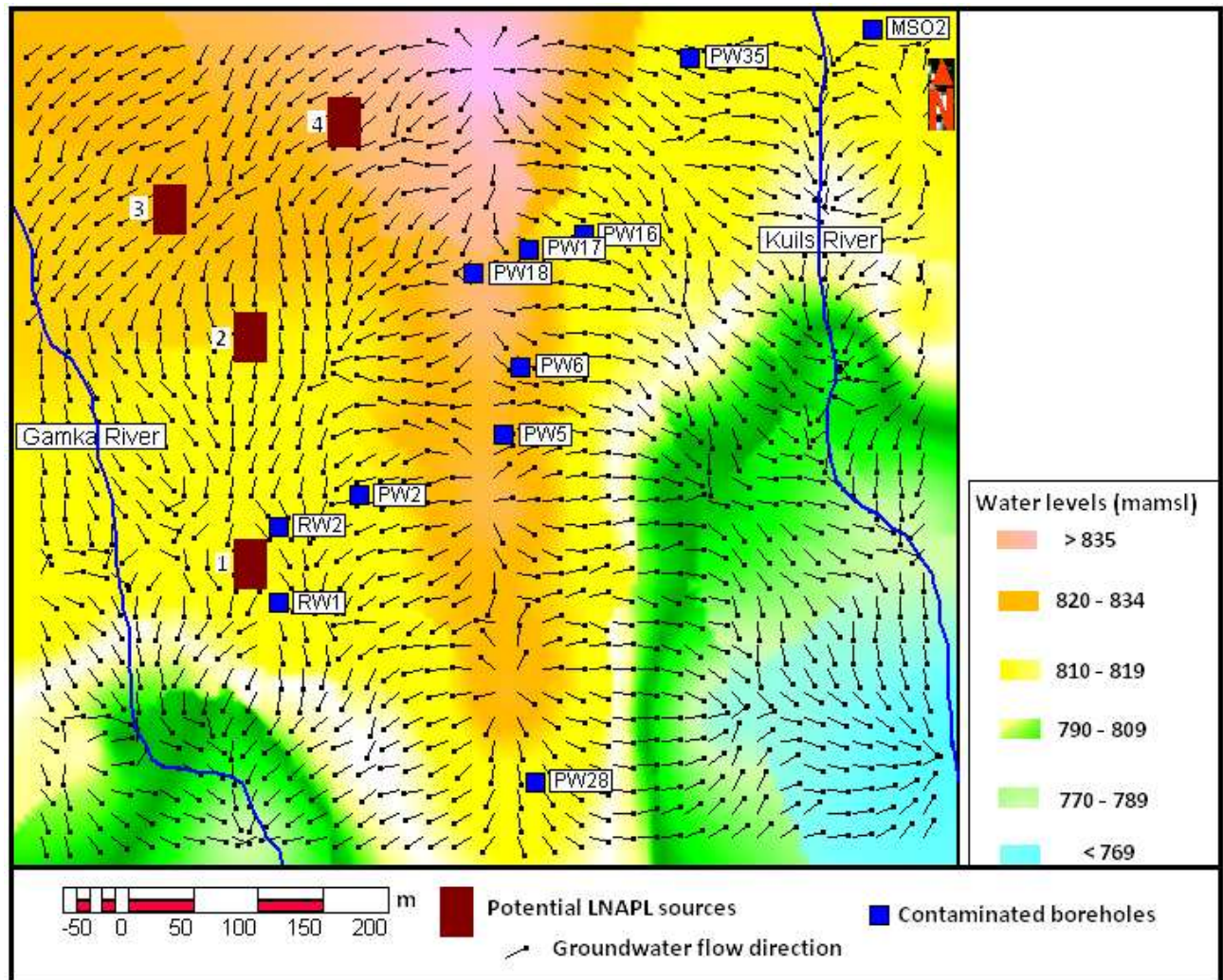


Figure 8-3 Inferred groundwater flow direction under assumed natural conditions in the Beaufort West study area.

8.2.2 Recharge

Recharge is mainly important to replenish groundwater resources for abstraction purposes. From a contamination point of view, recharge has the following implications for LNAPL migration, distribution and fate:

- Enhanced contaminant migration especially in fractures where groundwater flow velocity can be extremely high.

- Dilution of contaminants, leading to physical natural attenuation.
- Replenishment of groundwater oxygen which is an important electron acceptor for LNAPL biodegradation to occur.

The study site aquifer was conceptualised to be a two layer system; an unconfined aquifer underlain by semi - confined/confined. The volume of water in unconfined aquifers is dependent on seasonal precipitations considering that these aquifers are directly exposed to the atmosphere through soil pores. A recharge value of 1.4 % was estimated using the Chloride Mass Balance method after making an assumption of 1 mg/l Cl concentration in the precipitation (Appendix 7). The estimated recharge is conceptually too low to have significant effects on the migration, distribution and fate of LNAPLs at the study area as compared to abstraction effects. It is also important to highlight again that Beaufort West is a dry area with less than 230 mm of rainfall per year (*weathersa*, 2008), hence extremely low recharge are expected.

8.2.3 Aquifer and Transport Parameters

Estimated aquifer transmissivities for the study area ranges from 3.4 - 15.4 m²/day. It is expected that the kinematic porosity of the formations in Beaufort West area could be between 0.03 - 0.07, as obtained from a large number of tracer tests conducted by IGS in typical Karoo Formations (Van Tonder, 2009). From these range of kinematic porosity, seepage velocities would range between 1 and 3 m/a (using a flow zone thickness of 2 m and a gradient of 0.005). Using a forced gradient tracer tests between the two boreholes which are 4.7 m apart on the study area, a seepage velocity of 23 m/day was obtained. This estimated seepage velocity is significantly higher than the expected natural seepage velocity of the area and can only be attributed to the existence of fracture connectivity between the two boreholes.

8.3 LNAPL Migration and Distribution

Leaking USTs are the conceptualised LNAPLs sources at the Beaufort West study area. The USTs are installed below the four retail service stations identified as the main potential LNAPL sources (Figure 8-3) at the study area. The underground storage tanks are assumed to be continuously leaking thus creating a constant loading point source of LNAPL. The exact date and quantities of lost petroleum products could not be established.

After release, the free phase LNAPL moves through the vadose zone using vertical and subvertical fracture preferential flow paths towards the water table as shown in Figure 8-4. The migration of the LNAPL free phase in the vadose zone occurs under the influence of gravity until it reaches the water table. It is also important to highlight the existence of gaseous and entrapped LNAPL phases in the unsaturated zone; this is facilitated by the thin top layer of the unconsolidated fine river sand which promotes diffusion and entrapment of LNAPLs in the soil pore spaces.

Though it was not possible to determine and measure the amount of diffused LNAPLs in the core matrix samples, matrix diffusion is also conceptualised to be an important process at the study area. Matrix diffusion's prevalence is promoted by the presence of a sandstone aquifer which has naturally high porosity as compared to shale and mudstone formations. Matrix diffusion occurs in both saturated and unsaturated zones.

On reaching the water table, free phase LNAPL accumulates on top and the petroleum hydrocarbon start to dissolve into the aquifer system (Figure 8-4). In the saturated zone, downward migration of the dissolved LNAPL occurs through subvertical and vertical fractures. Lateral migration of both the dissolved and free phase LNAPL occurs due to groundwater advection under natural and forced gradient due to abstraction effects. The horizontal bedding plane fractures at 24 - 25 mbgl and 34 - 35 mbgl conveys mainly dissolved LNAPL which are indicted by horizontal blue arrows in Figure 8-4. Groundwater abstraction at private and municipal boreholes assists in mobilizing the LNAPL contamination. The LNAPL plume is thus conceptualised to be migrating both down (towards low hydraulic gradient) and across the hydraulic gradient (Figure 8-3).

It is important as part of contaminated site characterisation to define the extent of a plume. The LNAPL contaminants at the Beaufort West study area are conceptually migrating through bedding plane fracture and thus it can only be observed in boreholes which are connected to the fracture pathway. The contribution of abstraction effects on contamination migration also makes it difficult to delineate the plume extend considering that not all boreholes were identified during the hydrocensus. The abstraction rates and pattern also have an important role in contamination migration and these could not be determined. In this fractured rock aquifer, defining the plume extent is a difficult and complicated process; the LNAPL plume extent can only be linked to the existence of fracture preferential pathway between potential sources and receptors and abstraction activities.

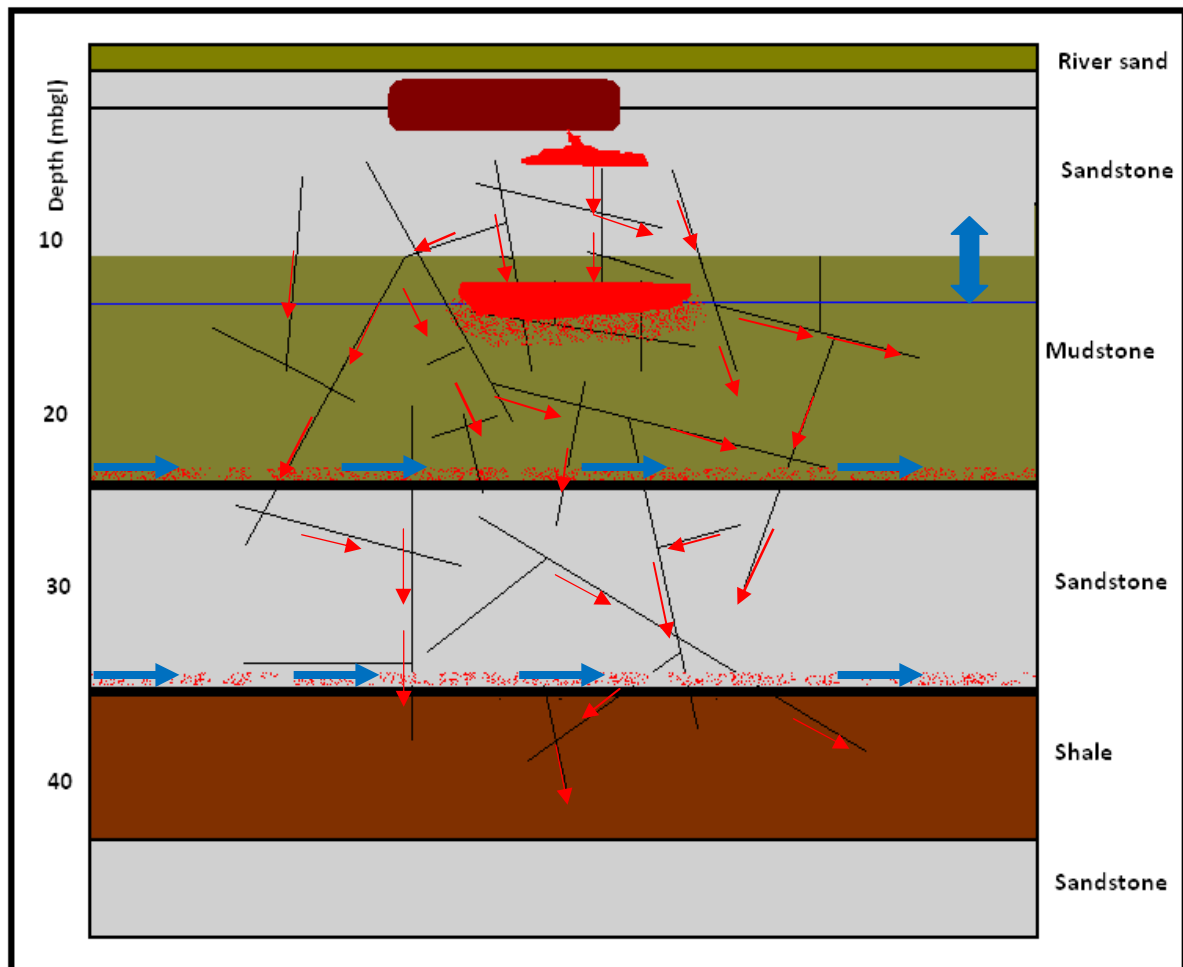


Figure 8-4 Conceptual model of LNAPL source loading, movement and migration at the Beaufort West study area. Red arrows indicate the downward migration of both free and dissolved LNAPL phases through vertical and subvertical fractures in the vadose and saturated zones. Blue arrows indicate the conceptualised movement of dissolved LNAPL along the bedding plane fractures at sandstone/mudstone and sandstone/shale contact areas

8.4 Summary of Chapter 8

In summary, Chapter 8 gives the Beaufort West study area's conceptual model which was developed based on all the field work conducted at the site. The conceptual model was constructed by encompassing geological and hydraulic components of the fractured sandstone aquifer system. Emphasis was also placed on conceptualizing the LNAPL migration at the study area which is governed by vertical, subvertical fractures and horizontal bedding plane fractures. Conclusions and recommendations from the study are given in the next Chapter.

9 Conclusions and Recommendations

9.1 Conclusions

Several important findings about the Beaufort West study area and for the site characterisation of LNAPL contaminated fractured rock aquifers were obtained during the study and are summarized as follows:

9.1.1 Findings about the Study Area

- The Beaufort West study area is conceptualised to be underlain by at least two aquifer systems; the finding is based on the fact that some boreholes in the vicinity of potential LNAPL sources are free of contaminants, i.e. PW4 and PW3.
- Vertical and subvertical fractures most likely responsible for facilitating the downward migration of LNAPL contamination in the aquifer were identified on the Beaufort West study area. The vertical and subvertical fractures were located through core drilling and borehole geophysics logging.
- Two bedding plane fractures were located between 24 - 25 mbgl and 34 - 35 mbgl and these are preferential flow paths to groundwater and LNAPL contaminants. The bedding plane fractures were identified at shale/sandstone, mudstone/sandstone weathered contact areas.
- The method of SP borehole geophysics did not manage to detect any preferential fracture flow path; hence its applicability is limited in the Beaufort West study area. The most likely reason for the failure by SP logging to detect anomalies is the absence of a strong solute contrast between the borehole fluid and fluid filling the surrounding rock formation.
- Benzene concentrations exceeded the MCL of 5 µg/l (US EPA, 2000) in 5 of the contaminated boreholes (PW17, PW18, PW6, PW35 and MSO2).
- MTBE concentration detected in all contaminated boreholes is below MCL of between 20 - 40 µg/l (US EPA, 1997a).

- LNAPLs biodegradation is inferred to be taking place at the study area as evidenced by the reducing environment which is characterised by elevated concentrations of Fe (II) and Mn species and depleted concentration of electron acceptors.
- Since no long chemical term data is available, one cannot be conclusive about the LNAPL plume extent and distribution on the Beaufort West study area. The extent of the LNAPL plume can only be linked to the existence of fracture preferential flow paths between potential sources and receptors and abstraction activities.

9.1.2 Conclusions for Site Characterisation of LNAPL - Contaminated Fractured - Rock Aquifers

These are general conclusions with respect to site characterisation of LNAPL contaminated fractured rock aquifers and contaminated site in general. It is important to highlight that these are not new findings but a confirmation on the applicability of the already existing geohydrological tools in the Beaufort West study area.

- The hydrocensus proved useful in revealing other contaminated private boreholes, this was important for understanding the plume migration and the extent of the contamination problem. Information obtained from the hydrocensus played an important role for field test planning.
- It is important to use contaminated boreholes as part of aquifer testing when characterizing LNAPL contaminated fractured rock aquifers. Contaminated boreholes most likely intercept fractured preferential flow paths to both groundwater and contamination. The inclusion of such boreholes in aquifer testing can yield important aquifer and mass transport parameters for the preferential flow paths.
- Pumping effects from private boreholes can have a pronounced influence on the LNAPL direction of migration in comparison to natural groundwater flow. In stressed aquifers abstraction, contamination migration and distribution is also a function of various flow regimes created during pumping.
- Site lab field kit had a 40 % success rate as a field screening procedure before sampling for costly reference laboratory analysis. The success rate is too low and may not be able to save time and resources as expected. Furthermore the magnitude of

difference between Site Lab and reference laboratory concentrations is extremely above the manufacturer's set threshold of 3.4 ppm (*site-lab*, 2009).

- Borehole geophysical characterisation proved important for determining fracture preferential flow paths depths, these were used for tracer testing in private boreholes (PW5 and PW2) and newly drilled boreholes (MW8 and MW7).
- The use of EC measurement to monitor tracer breakthrough is not reliable, because in most cases it is not possible to distinguish between EC increase due to the tracer and other external effects. In the context of an LNAPL contaminated fractured rock aquifer, the EC increase could be due to the mobilization of LNAPL biodegradation by - products [Fe (II) and Mn].
- It is evident based on the results that AV, FWS or Conventional logging cannot be used as standalone tools. Correlation of AV, FWS and Conventional borehole geophysics to geological logs coupled with EC profiling enables maximum output and better understanding of the site.

9.2 Recommendations

Based on the study findings, the following recommendations have been made:

- Delineation of the Beaufort West study area aquifer system is recommended. This should help to provide insights into why some of boreholes located in the vicinity of the 4 main potential LNAPL sources are not contaminated. This could assist in the development of new boreholes for the affected people, whose boreholes are contaminated and unsafe for use.
- Monitored natural attenuation (MNA) is recommended for the Beaufort West study area to assess the existing microbial environment for LNAPL biodegradation. This is more important taking into consideration that some evidence to infer biodegradation were found on the study area during the snap shot chemical characterisation. MNA would require specific sampling and monitoring of all biodegradation lines of evidence and analysis of the existing microorganism environment.
- The need for a social scientist to talk with affected people when conducting groundwater investigations in contaminated communities cannot be underestimated.

This was evident during the hydrocensus and field investigations when some affected residents were eager to know the solution to their plight.

- The superiority of core drilling for subsurface geological characterisation over percussion drilling cannot be overemphasized, thus at least one core borehole is recommended for improved geological characterisation of a site.
- Borehole development is recommended prior to borehole geophysics because drilling fluid has the ability to cause alteration of minerals (especially clay) near the borehole. Such an effect can create a zone with lower velocity than in the virgin formation giving a wrong picture about the actual formation.
- Conducting EC profiling as part of the borehole selection prior to the aquifer test in order to identify hydraulically conductive zones is also highly recommended especially in contaminated boreholes and where no geological and or geohydrological information is available.
- When conducting tracer test, measurement of a conservative selective anion concentration is recommended for tracer breakthrough analysis and parameter estimation in comparison to EC measurements. EC measurements should be used just for breakthrough monitoring purpose. It can also be used in point dilution tracer test during concentration decay measurements considering that what is mainly important is the decay in concentration (EC) attributed to groundwater flow.
- Based on the site lab field screening kit trial results, there is no enough evidence to suggest its usage in field environment. What can only be recommended are further trials to establish good correlations and a higher success rate.
- Flow logging can also be used to compliment the used geophysics tools.

9.2.1 Basic steps to follow after site characterisation

Listed below are general basic steps that can be followed after the site characterisation process:

- Review and update of the initial conceptual model.

- Risk assessment by comparing the site LNAPL concentrations to MCL (US EPA, 2000 and 1997a). Development of site-specific targets levels (SSTL).
- Selection of remediation measure(s) based on risk, available technological capacity, social and economic factors.
- Planning, designing and implementation of the appropriate remediation system(s).
- Monitoring of the implemented remedial system.
- Evaluation of the remediation based on SSTL.

9.2.2 Recommended Remedial Options

Some of the recommended remedial options for the Beaufort West study site include:

- Enhanced natural attenuation (bioremediation) through direct injection of electron acceptors e.g. Oxygen release compounds.
- Removal of free petroleum phase in PW6 and PW5 boreholes.
- Air sparging which can remove volatile organic compounds from groundwater into the unsaturated zone.
- Pumping and treat as a hydraulic containment system to slow down the plume migration.
- Monitored natural attenuation can also be used in conjunction with selected remedial active remedial options.

9.2.3 Challenges encountered with Site Characterisation Tools

Despite the witnessed success from the LNAPL contaminated fractured rock aquifer site characterisation, the following challenges were encountered with some of the tools:

- Three of the four core drilled boreholes collapsed 2 days after drilling and they could not be used for further testing and monitoring exercises. The collapse was mainly attributed to the nature of the sedimentary deposits underlying the study area.

- Acoustic view imaging in the core drilled borehole (MW8) could not detect any anomaly at 24 - 25 mbgl and 34 - 35 mbgl. This is despite the FWS, AV, EC and conventional borehole geophysics results indicating the existence of fracture features at those depths. AV image only showed some breakouts caused by drilling induced fractures from the water level to the bottom of the hole. The observation raises a big question on the post drilling usefulness of core holes to obtain complimentary information which can be used to correlate with geological logs.
- Due to core losses, it was not possible to observe and identify the weathered shale and sandstone contact areas associated with bedding plane preferential flow paths at 24 - 25 mbgl and 34 - 35 mbgl depth in MW8 core hole. The weathered material was washed out during drilling. However the limitation also helps to bring into picture the idea behind the use of complimentary site characterisation tools in the sense that if drilling logs cannot pick the weathered material then borehole geophysics will help to locate the weathered depth.
- The method of SP borehole geophysics was not useful as a complementary tool because it failed to display anomalies where gamma and resistivity indicated contrasting features.

10 References

- Abriola, L.M., 1989.** Modeling multiphase migration of organic chemicals in groundwater systems - A review and assessment. *Environmental Health Perspectives*: vol. 83, pp 117- 143.
- API (American Petroleum Institute), 1989.** Phase separated hydrocarbon contaminant modeling for corrective action, Publ. 4474, pp 125.
- Atekwana, E.A, Sauck, A., Douglas, D and Werkema, Jr., 1998.** Investigations of geoelectrical signatures at a hydrocarbon contaminated site. *J. Applied Geophysics*: vol. 44, pp 167 - 180.
- Aquifer Mechanics (GHR611) Lecture notes, 2008.** Institute of Groundwater Studies, University of the Free State - South Africa.
- Bear, J., 1972.** Dynamics of Fluids in Porous Media. American Elsevier Publishing Co., New York, pp 763.
- Belitz, K and Weston, D., 1999.** Cross - well slug testing in unconfined aquifers: A case study from the Sleepers River Watershed, Vermont. *Groundwater*: vol. 37, no. 3, pp 438 - 447.
- Brost, E.J and DeVaul, G.E., 2000.** Non-aqueous phase liquid (NAPL) mobility limits in soil and Groundwater. *American Petroleum Institute (API)*: Research Bulletin, No. 9.
- Botha, J.F., Verwey, J.P., Van der Voot, I., Vivier, J.J.P., Buys, J., Colliston and Loock, J.C., 1998.** Karoo Aquifers: Their Geology, Geometry and Physical Properties. Water Research Commission, South Africa.
- Bouwer, H and Rice, R.C., 1976.** A Slug Test for Determining Hydraulic Conductivity of Unconfined Aquifers with Completely or Partially Penetrating Wells. U.S.A Department of Agriculture, Phoenix, USA.
- Bunker, J.P.G., 1998.** Application of the oriented core drilling/sampling methods. Environ International Corporation, Los Angeles, California, USA.
- Campbell, G.D.M., 1980.** Beaufort West groundwater investigation (1975 - 1977). *Unpublished* Technical Report GH 3155, Department of Water Affairs. South Africa.
- Charman, N.E. 2003.** Sleeping giants - What's the deal with USTs and Corrosion? IMIESA.

Cohen, R.M and Mercer, J.W., 1993. DNAPL Site Evaluation, CRC Press, Boca Raton, FL, pp 314.

Cohen, A.J. B., Karasaki, K., Benson, S., Bodvarsson, Gudmundur, K., Freifeld, B., Benito, P., Cook, P., Clyde., J, Grossenbacher, K., Peterson, J., Solbau, R., Thapa, B., Vasco, D and Zawislanski, P., 1996. Hydrogeologic Characterization of fractured Rock Formations: A Guide for Groundwater Remediators. EPA/600/S-96/001 USA.

Cozzarelli, I.M., Bekins, B.A., Baedecker, M.J., Aiken, G.R., Eganhouse, R.P., Tuccillo, M.E., 2001. Progression of natural attenuation processes at a crude oil spill site: Geochemical evolution of the plume. *J. Contam. Hydrol.* vol. 53, pp 369 - 385.

Danish EPA, 2000. Groundwater zoning. Guide no. 3. Danish EPA, Ministry of Environment, Copenhagen. Denmark.

Drost, W., Klotz, D., Koch, A., Moser, H., Neumaier, F., Rauert, W., 1968. Point dilution methods of investigating groundwater flow by means of isotopes. *Water Resour: Res* vol. 4, no. 1, pp 125 -146.

Feenstra, S., Cherry, J.A and Sudicky, E.A., 1984. Matrix diffusion effects on contaminant migration from and injection well in fractured sandstone. *Groundwater:* vol. 22, pp 307 - 316.

Fetter, C.W., 2001. Applied hydrogeology (4th Edition). Prentice Hall, New Jersey.

Gebrekrastos, R.A., Pretorius, J.A and Usher, B. H., 2008. Manual for site assessment at DNALP contaminated sites in South Africa. WRC Report No. 1501/2/08, South Africa.

Gilbert, C., 2006. Monitoring of Hydrocarbon Plume at Donkin Motors - Beaufort West. Unpublished consulting report of GPT. Cape Town, South Africa.

Gonthier, G. J and Mayer G.C., 2003. Slug - test results from a well completed in fractured crystalline rock, U.S Air Force Plant 6, Marietta, Georgia. Proceedings of the 2003 Georgia Water Resources Conference, University of Georgia, Athens, Georgia.

GWS114, 2008. Introduction to general Geosciences part 1 *geology lecture notes*. Geology department. University of the Free State. Bloemfontein, South Africa.

Hardisty, P.E., Roher, J and Dottridge, J., 2004. LNAPL Behavior in Fractured Rock: Implications for Characterization and Remediation. *Unpublished*.

Hardisty, P.E., Wheeler, H.S., Johnson, P.M., and Bracken, R.A. 1998. Behaviour of Light Immiscible Liquid Contaminants in Fractured Aquifers. *Geotechnique*: vol. 48, no. 6, pp 747 - 760.

Hiebert, F.K., Bennet, P.C., Folk, R.L and Pope, S.R., 1995. Enhanced mineral alteration by petroleum biodegradation in a freshwater aquifer in Microbial process for bioremediation, Hinchee et al., (Eds), Ballete Press. Columbus, pp 297 - 308.

Huling, S.G and Weaver, J.W., 1991. Dense non - aqueous phase liquids, Ground Water Issue, EPA/540/4-91-002, U.S.EPA, pp 21.

IGS, 2008. Aquifer Mechanics Lecture notes. Institute for Groundwater Studies, University of the Free State. Bloemfontein, South Africa.

Keyes, W.S., 1989. Borehole Geophysics Applied to Ground-Water Investigations, National Water Well Association, Dublin, OH, pp 313.

Kruseman, G. P. and de Ridder, N.A., 1999. Analysis and evaluation of pumping test data (2nd Edition). International Institute for Land Reclamation and Improvement. Wageningen, Netherlands, pp 237.

Kueper, B.H. and McWhorter, D.B. 1991. The Behaviour of Dense Non Aqueous Phase Liquids in Fractured Clay and Rock. *Groundwater*: vol. 29, no 5, pp 716 - 728.

Lee, J., Cheon, J., Lee, K., Lee, S and Lee, M., 2001. Factors affecting the distribution of hydrocarbon contaminants and hydrogeochemical parameters in a shallow sand aquifer. *Journal of Contaminant Hydrology*: vol. 50, pp 139 - 158.

Lamontange, S., Dighton, J and Ullman, W., 2002. Estimation of groundwater velocities in riparian zones using point dilution tests. CSIRO Land and Water. Technical Report 14/04. USA.

Landmeyer, E. J., Chapelle, H. F., Bradley, M. P., Pankow, F. J., Church, D. C and Tratnvek, G. P., 1998. Fate of MTBE relative to benzene in a Gasoline contaminated aquifer (1993 - 98). *Ground Water Monitoring and Remediation (GWMMR)*: vol. 18, no. 4, pp 93 - 102.

McMahon. P.B., Vroblesky, D.A., Bradley, P.M., Chapelle, F.H and Gutter, C.D., 1995. Evidence of enhanced mineral dissolution in shallow groundwater. *Groundwater*: vol. 33, pp 207 - 216.

- Mercer, J.W., and R.M. Cohen, 1990.** A review of immiscible fluids in the subsurface: Properties, models, characterization, and remediation. *J. Contam. Hydrol.*: vol. 6, pp 107 - 163.
- Nabee, R., 2007.** Monitoring of Hydrocarbon Plume at Donkin Motors - Beaufort West. Unpublished consulting report of GPT. Cape Town, South Africa.
- National Research Council, 1993.** In situ bioremediation: when does it work?, National Academy Press, pp 207. Washington, DC, USA.
- Newell, J.C, Acree, D.S and Ross, R. R and Huling, G.S., 1995.** Light Non - Aqueous Phase Liquids. EPA/540/S-95/500, USA.
- Riemann, K., Van Tonder Gerrit, J and Dzanga, P., 2002.** Interpretation of single - well tracer tests using fractional-flow dimensions. Part 2: A case study. *Hydrogeology*: vol. 10, no. 3, pp 357 - 367.
- Riemann, K., 2002.** New Developments in Conducting and Analysing Tracer Tests in Fractured Rock Aquifers. *Unpublished* PhD Thesis at the Institute for Groundwater Studies, University of the Free State, South Africa.
- Sasol Facts, 2007.** Sasol group corporate affairs department. Johannesburg, South Africa.
- South African Water Quality Guidelines (SAWQG) 1996.** Volume 1: Domestic Water Use (2nd Edition). Department of Water Affairs & Forestry. Pretoria, South Africa.
- Telford, W.M., Geldart, L.P and Sheriff, R.E., 1990.** Applied Geophysics (2nd Edition). Cambridge University Press, United Kingdom, pp 770.
- Tire'n, S.A., Askling, P and Wa'nstedt, S., 1999.** Geologic site characterization for deep nuclear waste disposal in fractured rock based on 3D data visualization. *Elsevier Engineering Geology*: vol. 52, pp 319 - 346.
- US EPA, 2004.** Site Characterisation Technologies for DNAPL Investigations. Publication EPA 542-R-04-017. USA. Washington DC, USA.
- US EPA, 2003.** Guidelines on the design, installation and management requirements for underground petroleum storage systems (UPSS). Publication: 888. Washington DC, USA.
- US EPA, 2002.** National Recommended Water Quality Criteria. Washington DC, USA. Publication: EPA-822-R-02-047. Washington DC, USA.

US EPA, 2001. The State - of - the Practice of Characterisation and Remediation of Contaminated Ground Water at Fractured Rock Sites, Publication: 542-R-01-010. Washington DC, USA.

US EPA, 1997a. Drinking Water Advisory: Consumer Acceptability Advice and Health Effects Analysis on Methyl Tertiary - Butyl Ether (MTBE). Publication: 822-F-97-009. Washington DC, USA.

US EPA, 1997b. Use of monitored natural attenuation at Superfund, RCRA corrective action, and underground storage tank sites. Publication 9200: Washington DC, USA.

US EPA, 1991. Site Characterisation for Subsurface Remediation. Publication: 625/4-91/026. Washington DC, USA.

Vandoolaeghe, M.A.C., 1978. Report on Geophysical interpretation of Geohydrological investigation at Beaufort west. *Unpublished* Technical Report 2970, Department of Water Affairs and Forestry. South Africa.

Van Biljon, W, 2002. Soil Vapor Survey. Unpublished consulting report of GPT. Cape Town, South Africa.

Van Biljon, W and Hassan, L., 2003. Sampling Report. Unpublished consulting report of GPT. Cape Town, South Africa.

Van Tonder, G. J., Bardenhagen, I., Riemann, K., Van Bosch, J., Dzanga, P. And Xu, Y., 2001a. Manual on Pumping Test, Analysis in fractured - Rock Aquifers. Institute of Groundwater Studies, University of the Free State. South Africa.

Van Tonder, G.J., Kunstmann, H., Xu, Y., 2001b. FC program, software developed for DWAF by the Institute of Groundwater Studies. Institute of Groundwater Studies, University of the Free State, South Africa.

Van Tonder, G. J, 2009. *Personal communication on 11 March.* Institute of Groundwater Studies, University of the Free State, South Africa.

Verwey, J., Kinzelbach and Van Tonder, G.J., 1995. Interpretation of pumping test from fractured porous aquifers with a numerical model. Institute of Groundwater Studies, University of the Free State, South Africa.

Vegter, J. R and Foster, B. J., 1992. Hydrology of dolomitic formations in the Southern and Western Transvaal. *Int. Contribution to Hydrogeology*: vol. 13, pp 355 - 376.

Visser, J.N.J., 1989. Course notes on Geology 216: Sedimentology. Lecture delivered at of the Orange Free University, Bloemfontein, Republic of South Africa.

Vivier, J. P. J., Van Tonder, G. J and Botha, J. F., 1995. The use of Slug tests to predict borehole yields: correlation between the regression time of slug and borehole yields. Institute of groundwater Studies, University of the Free State. South Africa.

Weaver J M C, Cave L and Talma A. S., 2007. Groundwater Sciences, CSIR, South Africa.

Welenco, 1996. Water and Environmental Geophysical Well Logs, Volume 1, Technical Information and Data (8th Edition), Welenco, INC, Bakersfield, CA, pp 153.

Williams, D.E and Wilder, D.G., 1971. Gasoline pollution of a ground-water reservoir - A case history. *Groundwater*: vol. 9, no. 6, pp 50 - 54.

Williams, S. D., Ladd, D. E and Farmer, J. J., 2006. Fate and Transport of Petroleum Hydrocarbons in Soil and Ground Water at Big South Fork National River and Recreation Area, Tennessee and Kentucky (2002 - 2003). USSG, Scientific Investigations Report 2005 - 5104.

Woodford, A and Chevallier, L., 2002. Hydrogeology of the main Karoo Basin: Current Knowledge and Research Needs. Water Research Commission, Report No TT 179/02, pp 466.

Websites referenced in this study

www.earthscienceworld.org/images (March, 2009).

www.eia.doe.gov/emeu/safrica.html (November, 2007).

www.engen.co.za (December, 2007).

www.geoscience.org.za (March, 2009).

www.maps.google.co.za (December, 2009).

www.pacificenvironment.org/img/original/sakh_pipeline.jpg (June, 2009).

www.sabcnews.com (February, 2003).

www.saflii.org (November, 2007).

www.sapref.co.za (November, 2007).

www.science.jrank.org/.../joints-and-jointing.1.jpg (February, 2010).

www.shell.co.za (December, 2007).

www.site-lab.com (February, 2009).

www.total.com (December, 2007).

www.total.co.za (December, 2007).

www.weathersa.co.za (October, 2007).

Williams, J. H., 1998. Introduction to Borehole Geophysics, United States Geological Survey,
In: *http://ny.usgs.gov/projects/bgag/intro.text.htm*s, pp 4.

11 Appendices

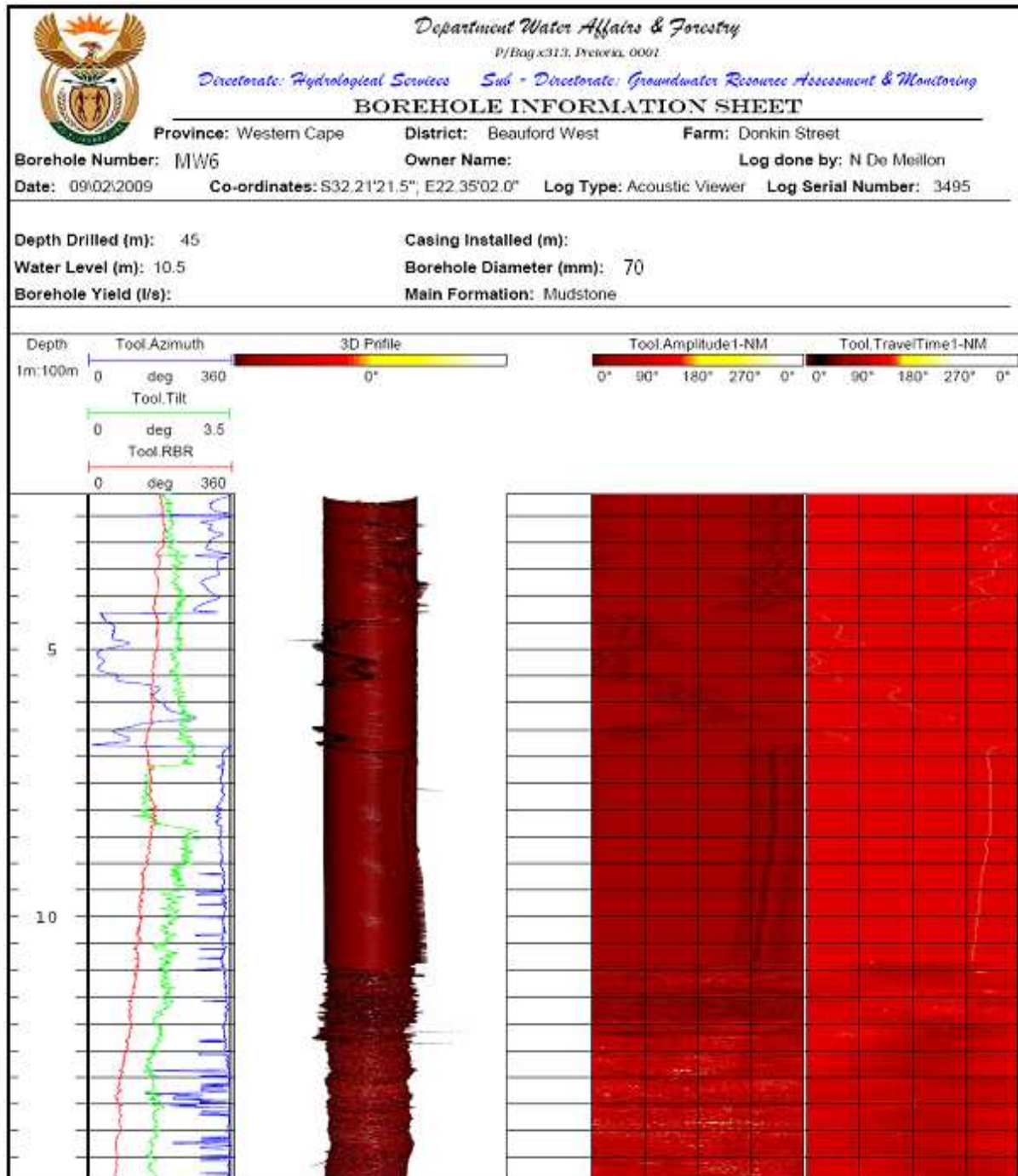
Appendix 1 Geohydrological Information obtained from the Hydrocensus carried out in the Beaufort West Study Area.

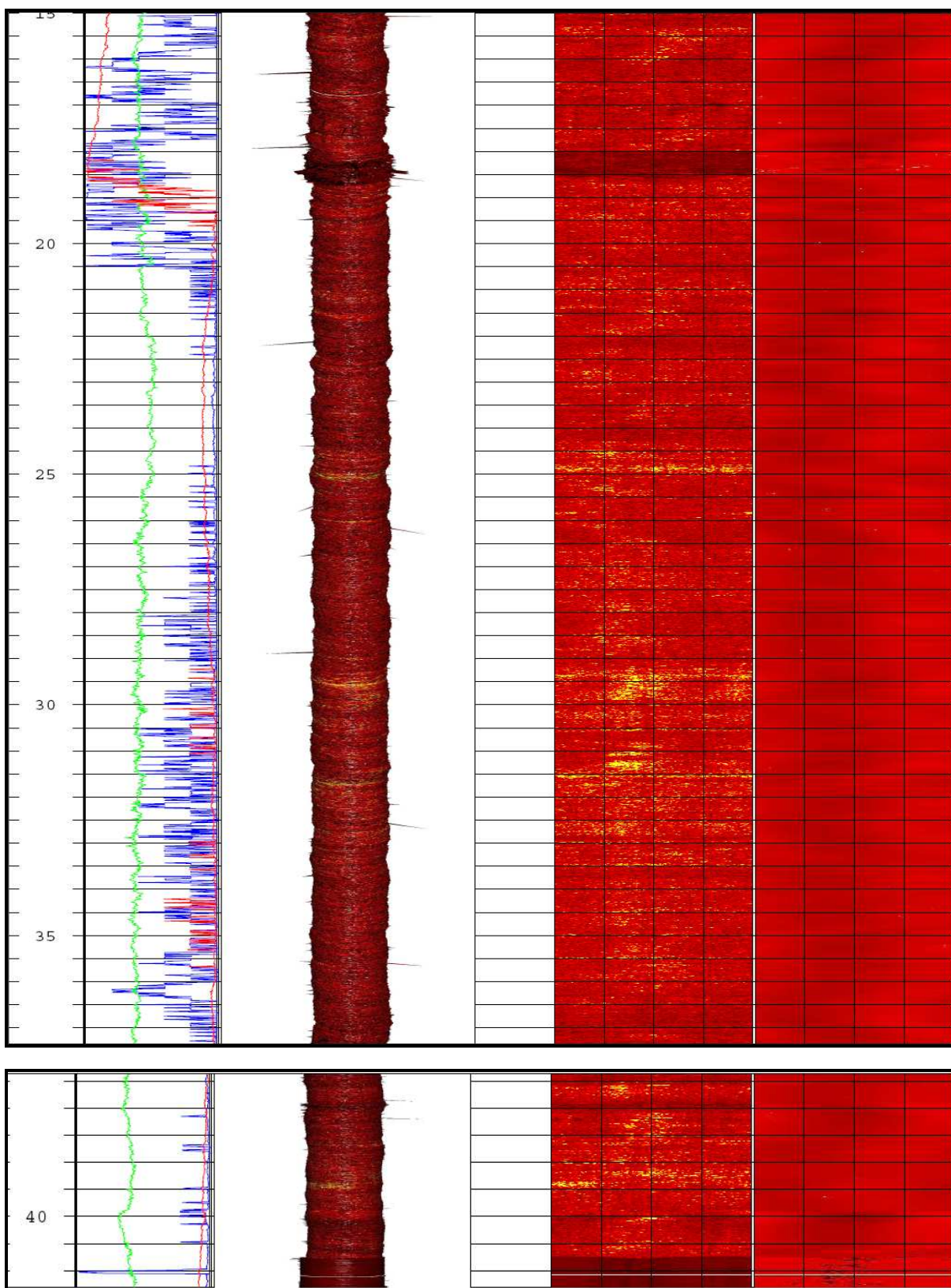
Borehole Name	Borehole Location	Depth mbgl	Date Drilled	Sample Depth	PH	EC mS/m	Groundwater use activity
MS01	Municipal pools			tap	7.85	245.5	Municipal use
PW24	Donkin 38	56	1985	tap	7.57	75.3	Garden
PW25	Donkin 16			tap	7.5	84.5	Garden and domestic
PW26	Devinish 13			tap	7.47	77.7	Garden only
PW27	Donkin 162	70		tap	7.85	124.7	Garden only
PW28	4 Herman Street	60			7.27	134	Garden
PW29	Herman 11				7.27	106.7	Garden and swimming pool
PW30	61 De Villers			tap	7.22		Garden
PW31	15 De Villers					112.1	Garden and domestic
PW32	19 De Villers			tap	7.16	98.3	Garden only
PW33	14 De Villers			tap	7.2	93.6	Garden
PW34	Skol in De Villers			tap	7.21	53.5	Garden
PW35	26 Brand			tap	7.34	85	Garden use
PW41				pumped	7.02	110.4	Irrigation and drinking
PW42							Irrigation and swimming pool
PW43	Guest house			pumped	7.49	76.7	Irrigation
PW45	Beaufort Mannar			tape	7.35	106.9	Irrigation
PW44	Beaufort Mannar			tape	7.33	98.9	Irrigation
PW46				tap	7.55	84.1	
PW47					7.45	70.4	Irrigation and drinking
PW48					7.37	62	Irrigation
MS02	Kuils River bank			tap			Municipal borehole

Appendix 2 Borehole Geophysics Logs

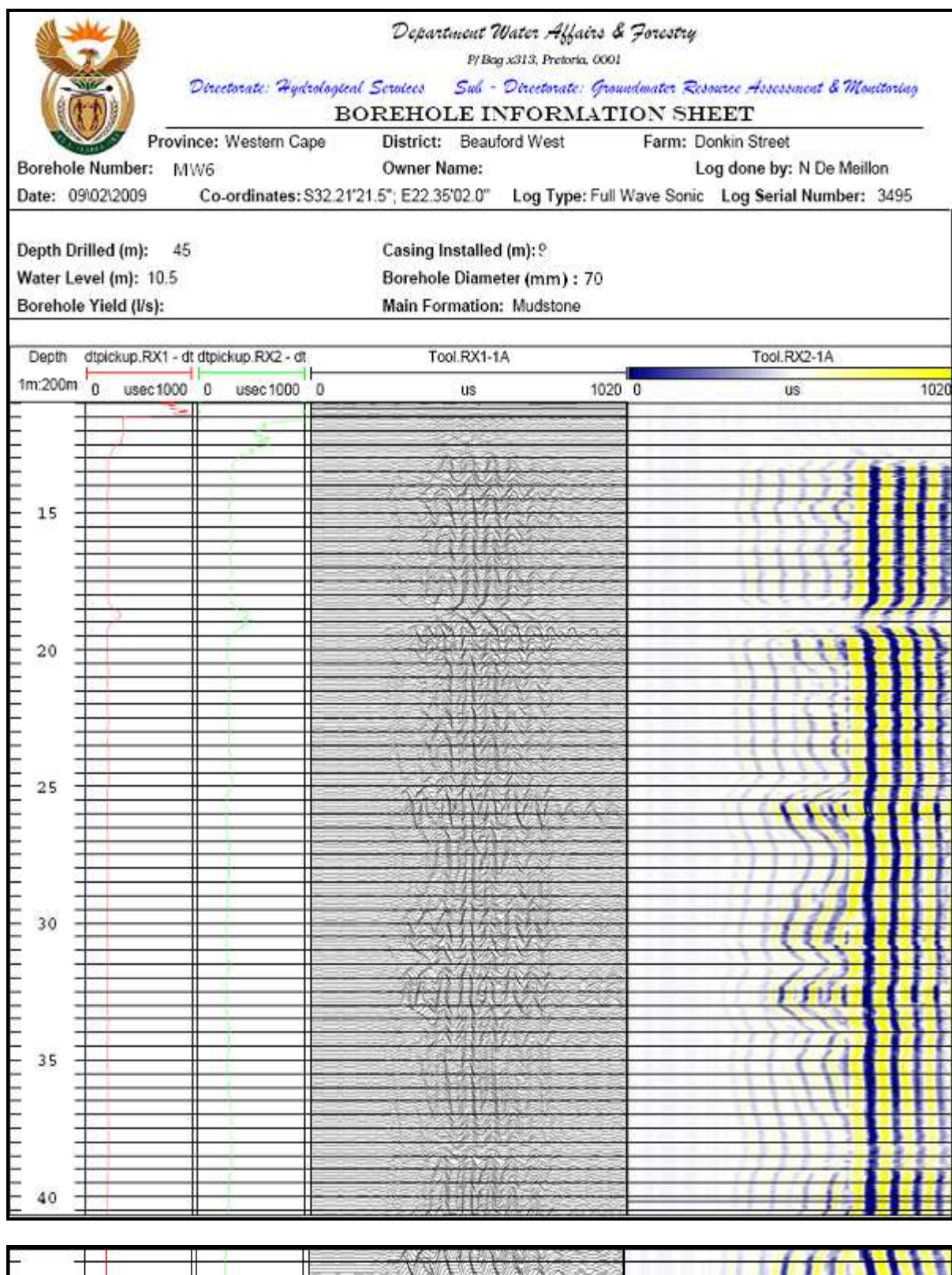
MW6 Logging

Acoustic Viewer (AV)

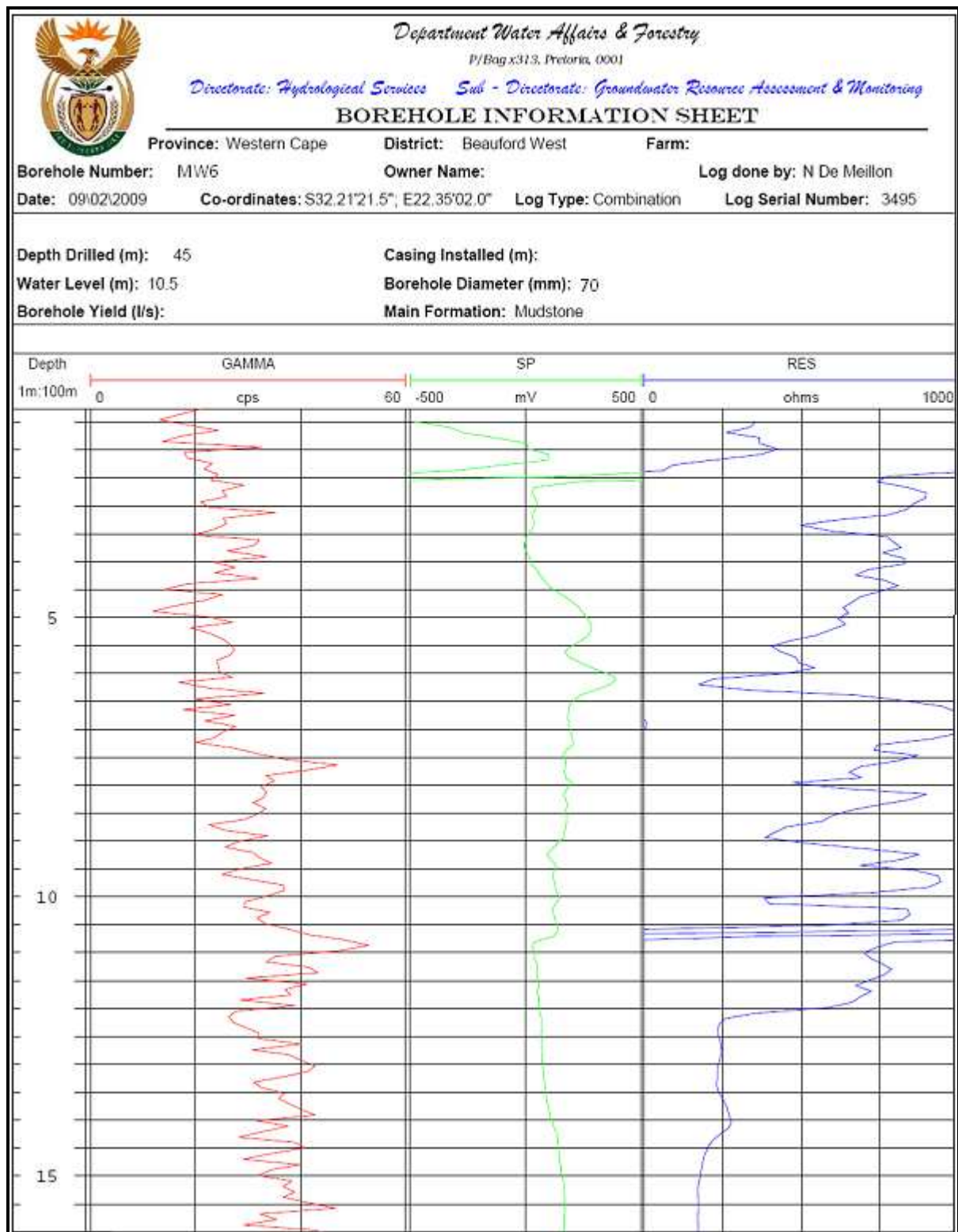


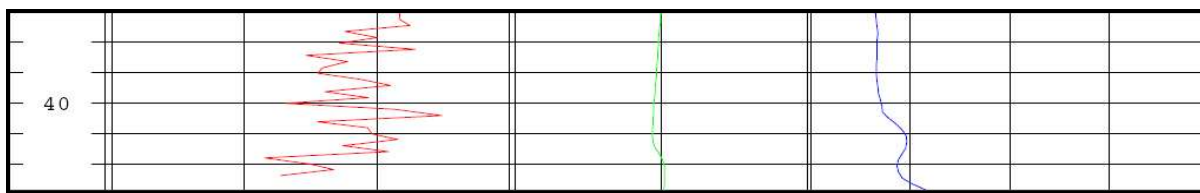
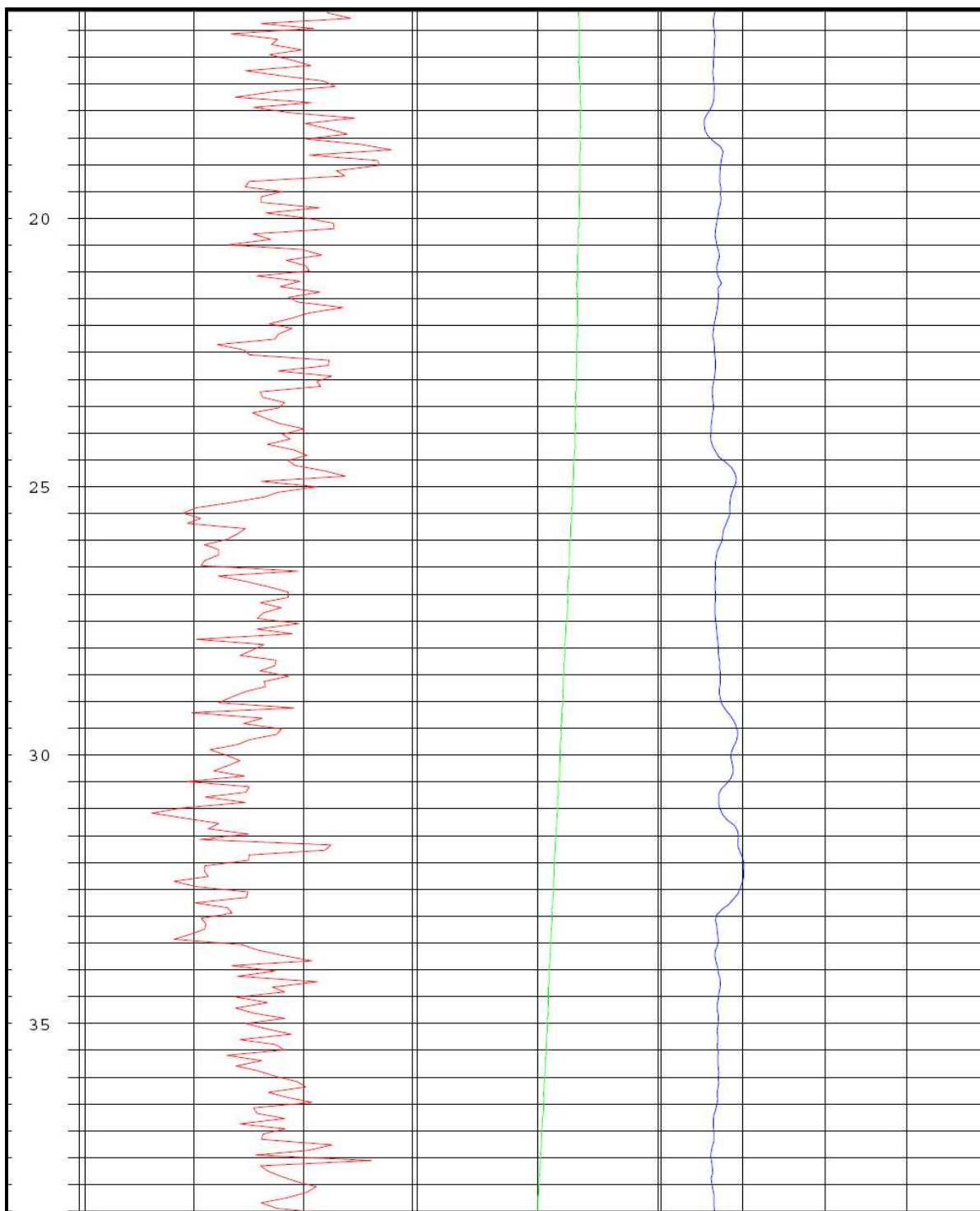


Full Wave Sonic (FWS)



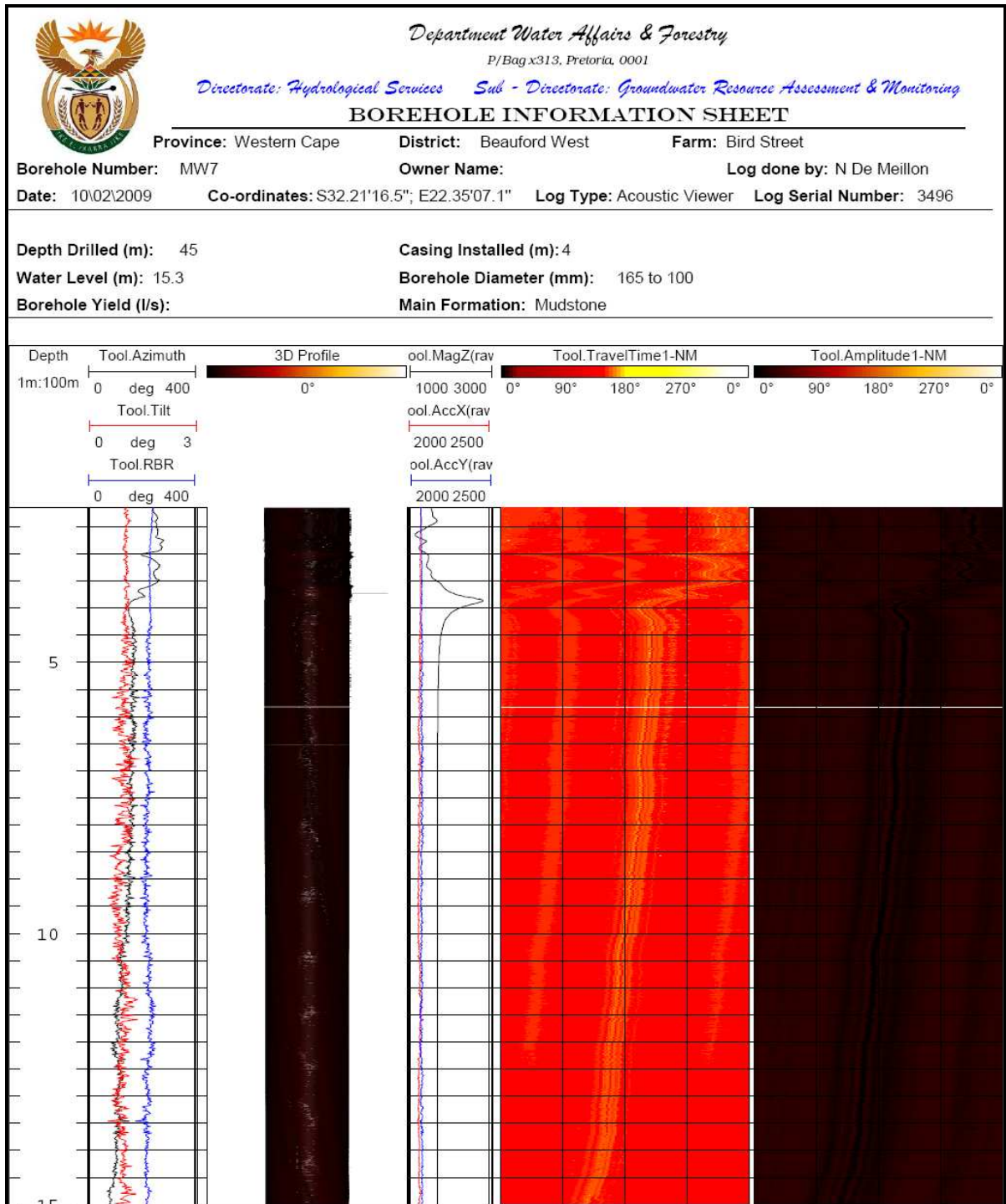
Conventional Logging (Gamma, Resistivity and Spontaneous Potential)

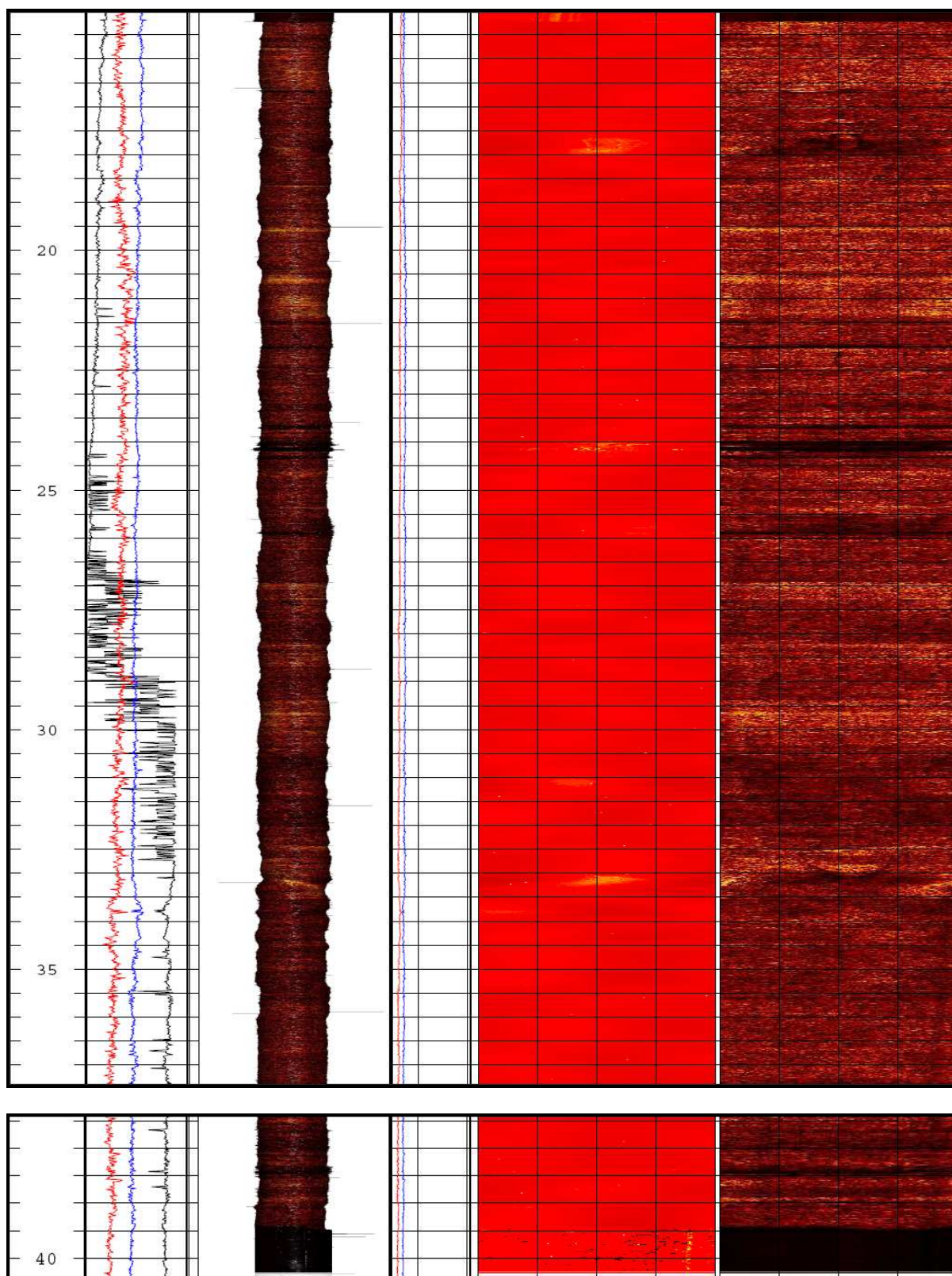




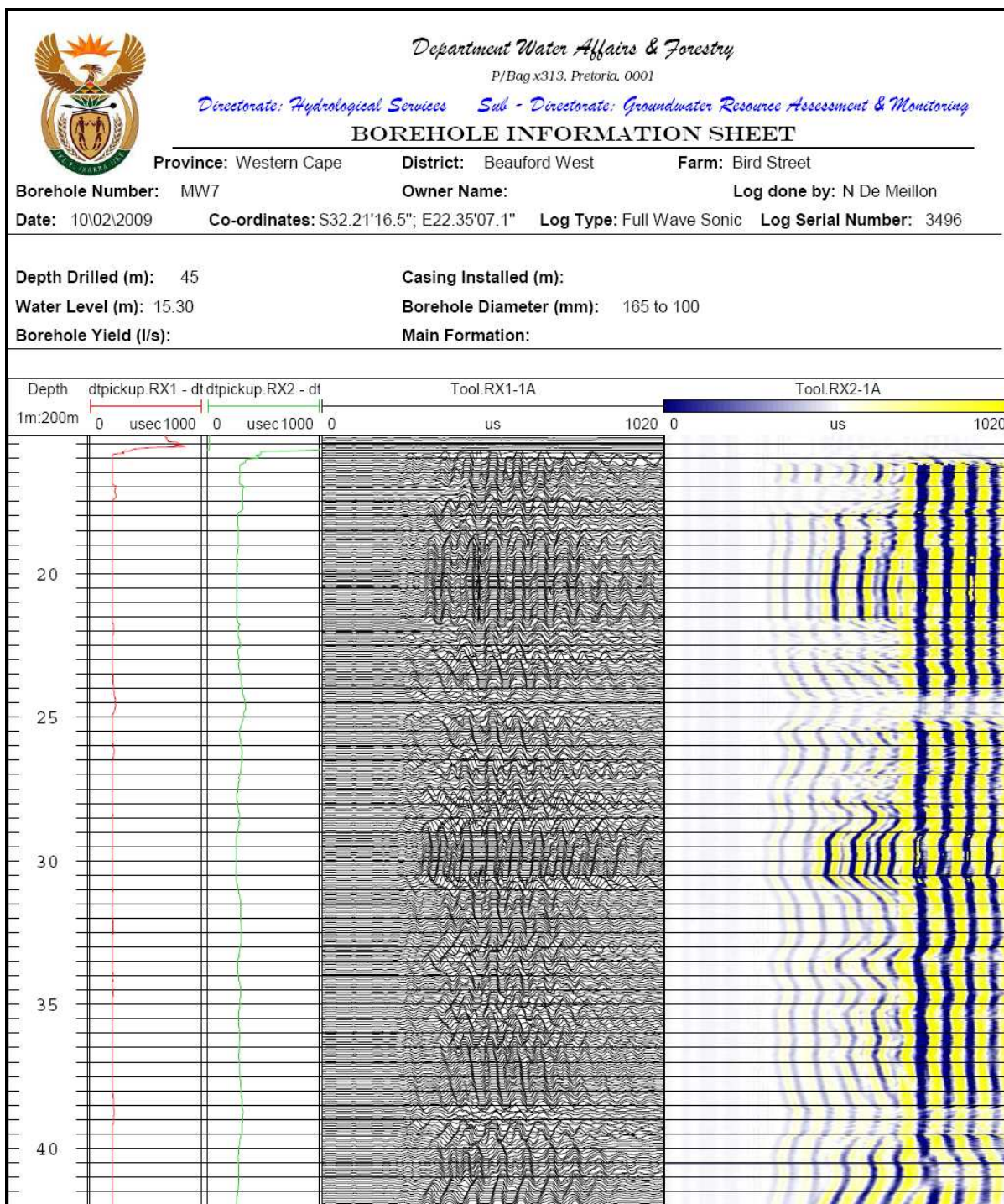
MW7 Logging

Acoustic Viewer (AV)

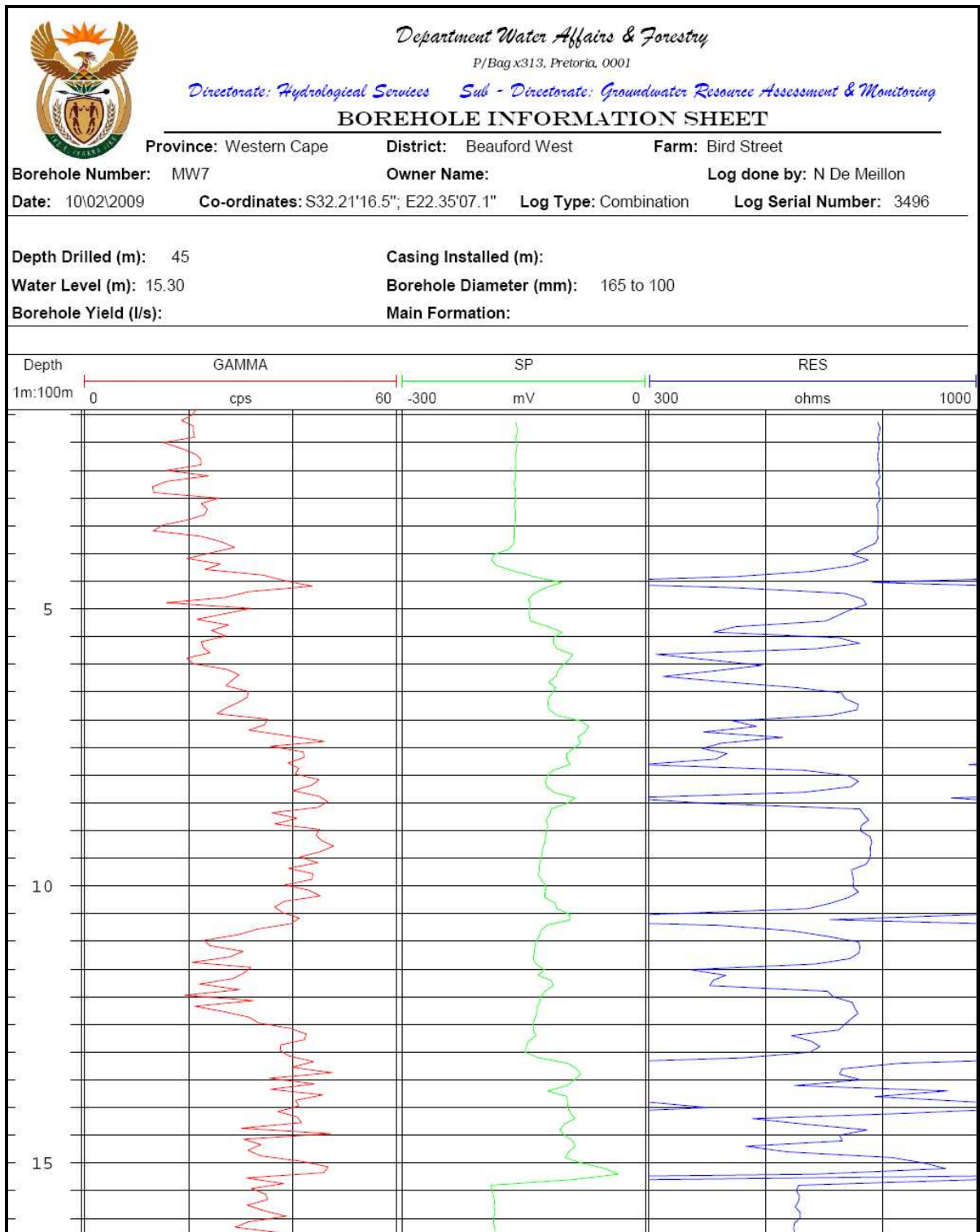


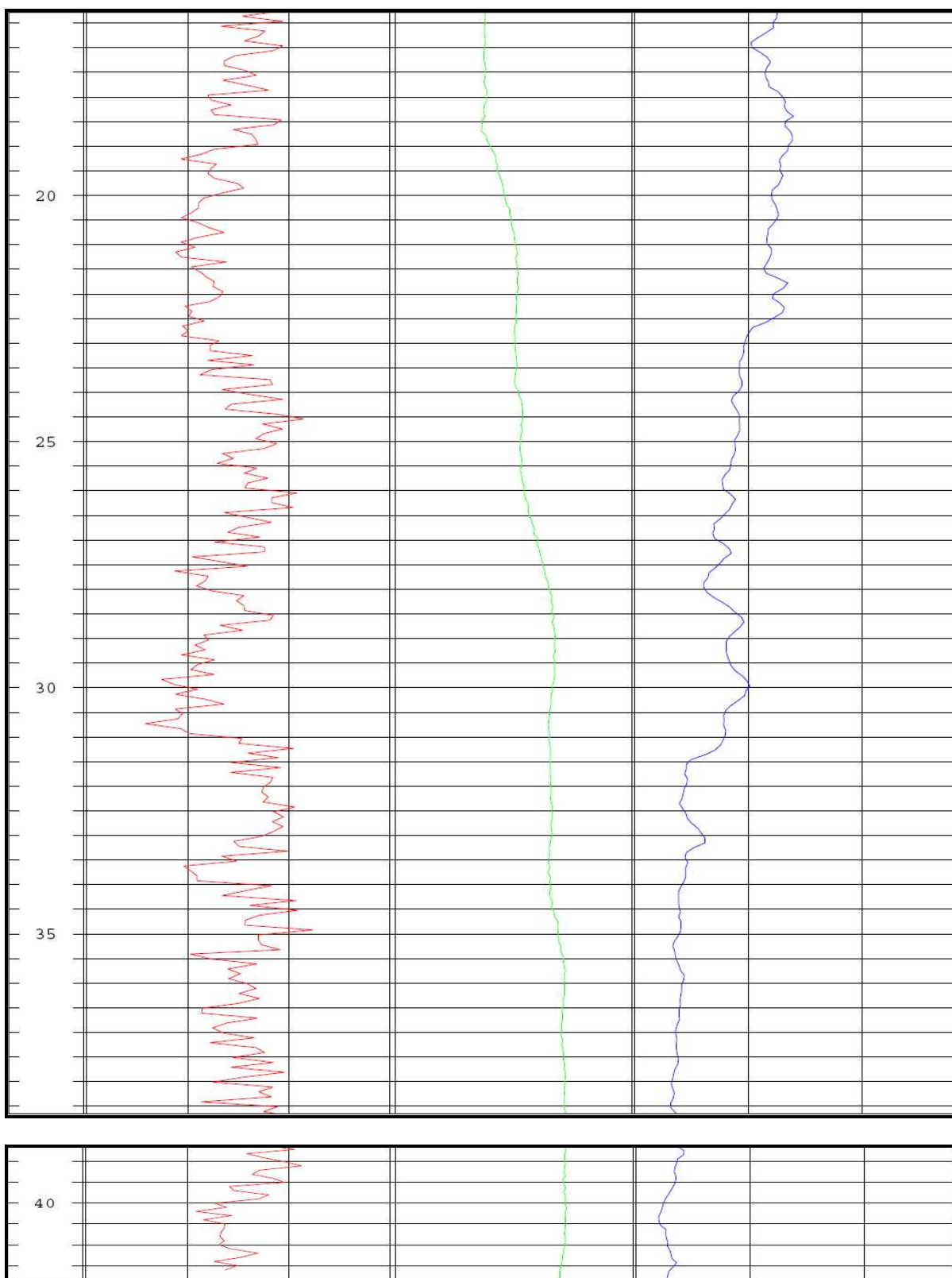


Full Wave Sonic (FWS)



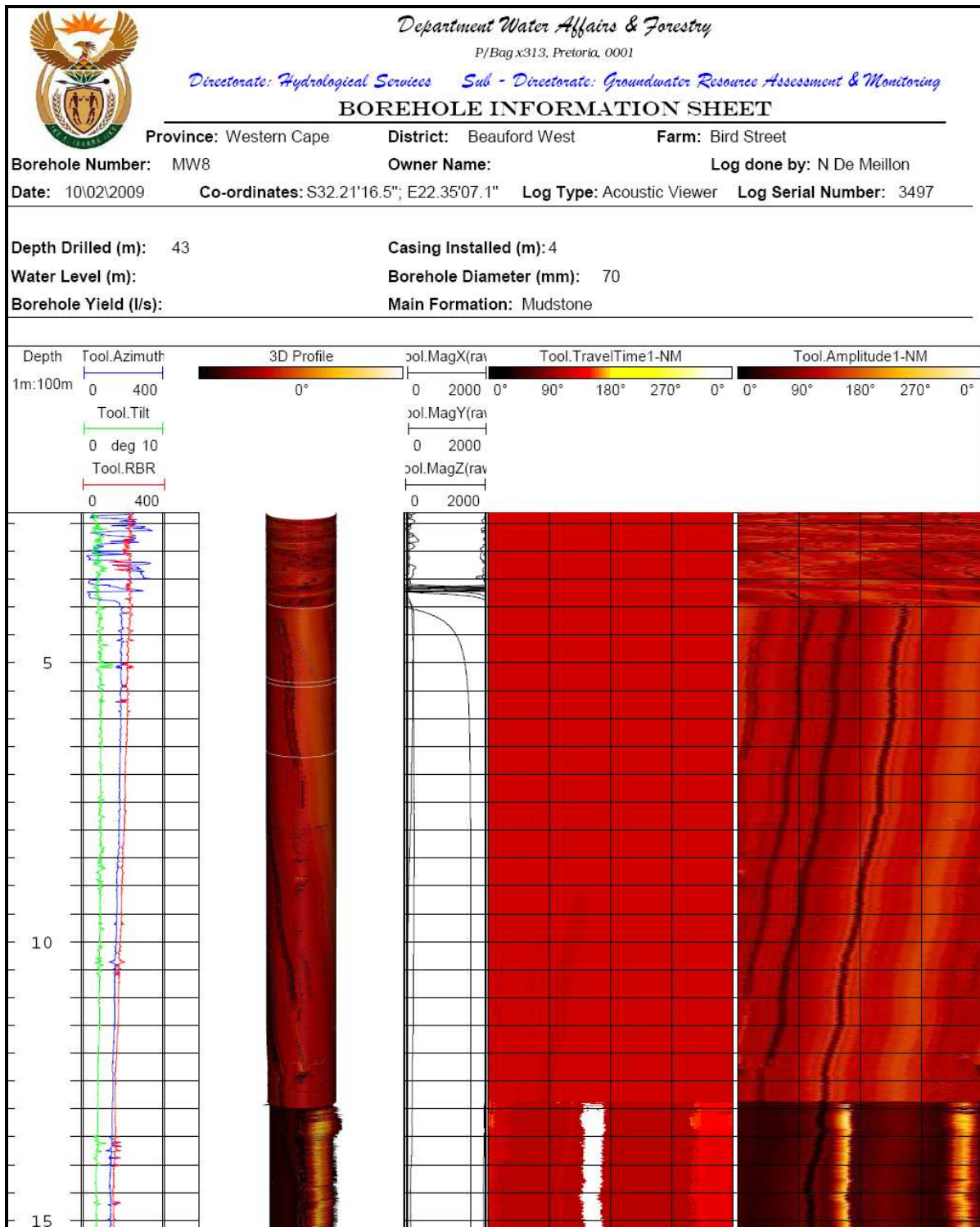
Conventional Logging (Gamma, Resistivity and Spontaneous Potential)

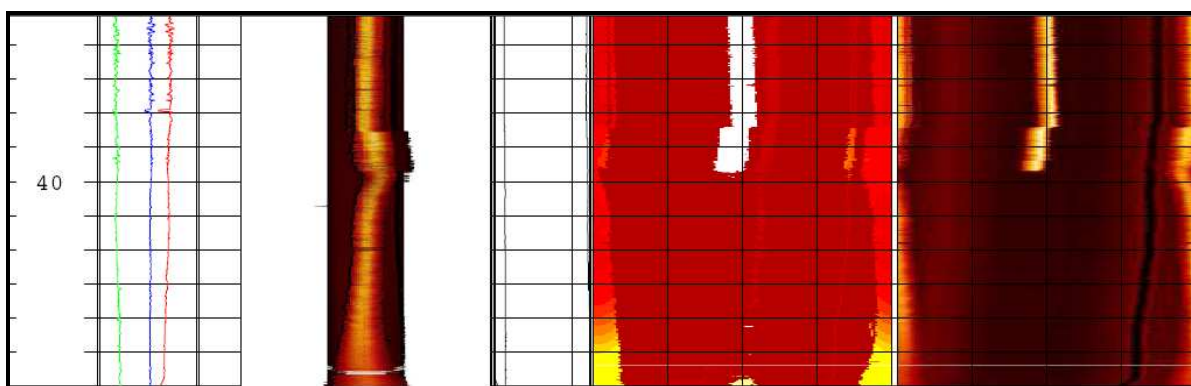
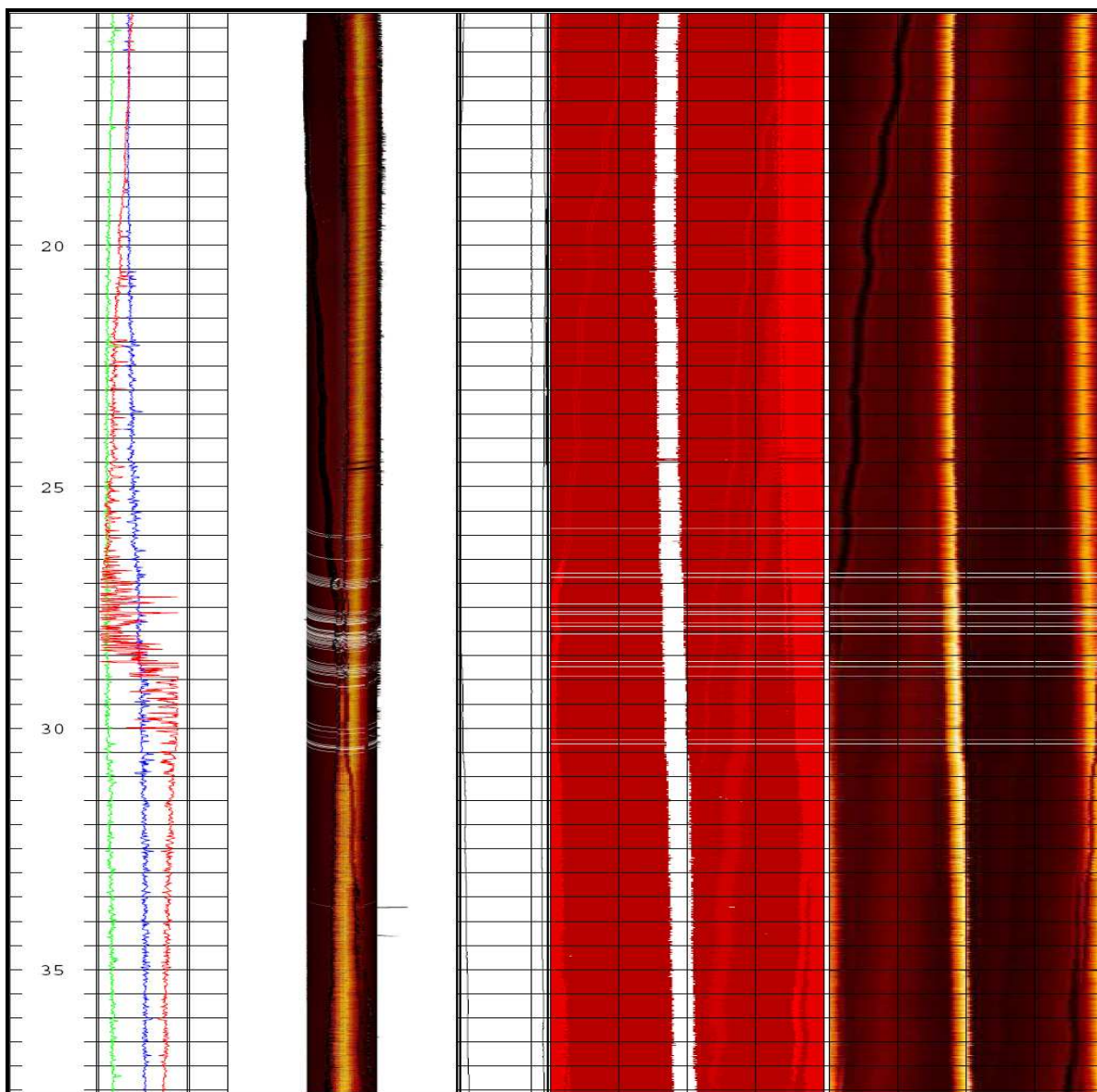




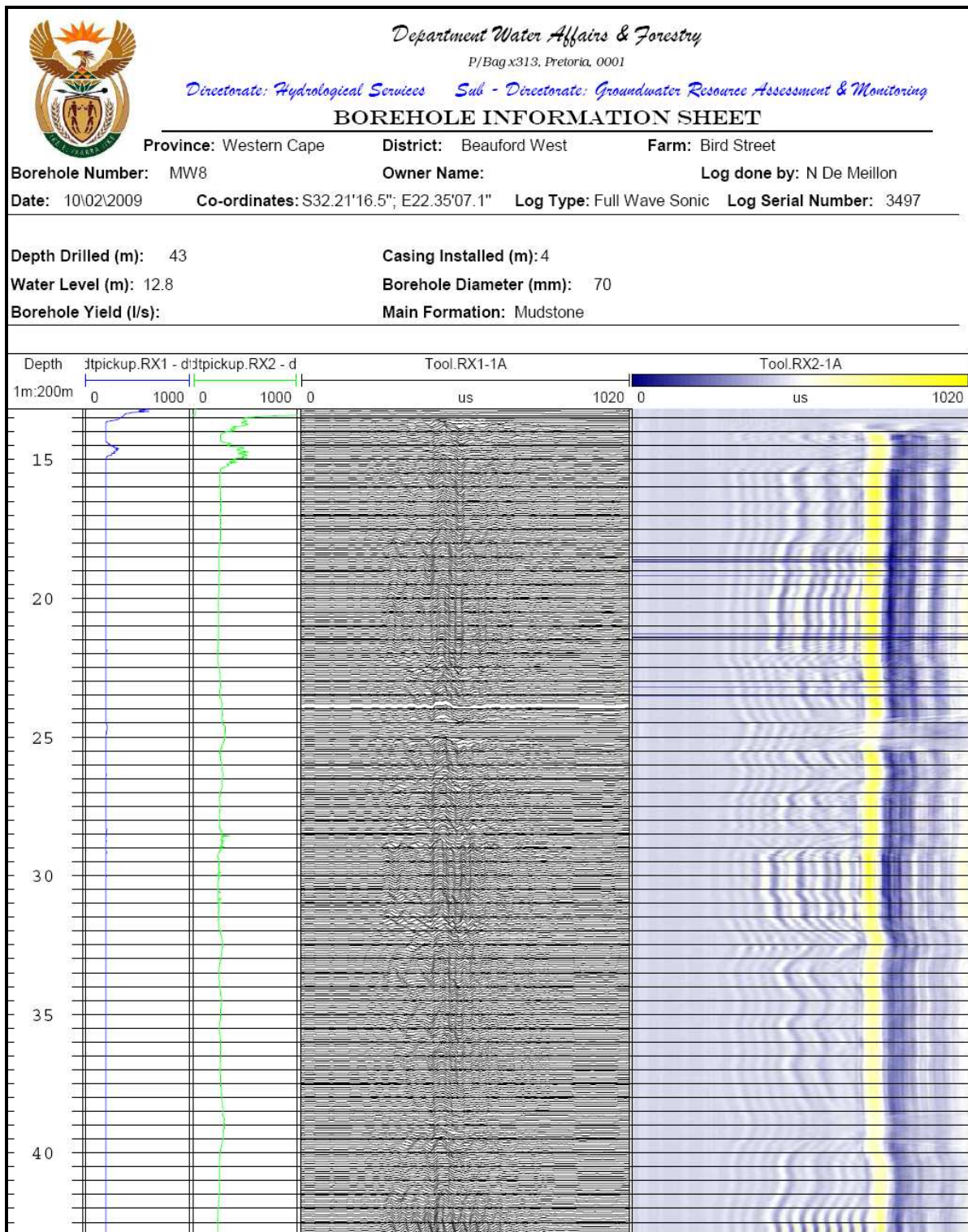
MW8 Logging

Acoustic Viewer (AV)





Full Wave Sonic (FWS)



Appendix 3 Slug Test Procedure

The following procedure was used to conduct the slug test (IGS, 2008)

- Measurement of static water level.
- Level logger setting and installment.
- Inserting the slug into the borehole to displace a well volume equivalent to the slug volume.
- Manually measure the rate of water level recession where possible using a Temperature Level Conductivity (TLC) meter until at least 90 % of the recession is achieved.
- For this study an automatic level logger was also used in conjunction with a manual TLC meter to measure the water level recession.

Appendix 4 Point dilution Tracer Test Procedure

The following procedure by Riemann (2002) was used as guidelines to conduct point dilution tracer tests:

- Setting the equipment as shown in Figure 6-12 (Section 6.5.2) and using a test section of 2 m, the pump was placed at 23 mbgl which had been identified as the main flow depth from EC profiling.
- Mixing and circulating the tracer with water in the tested section. Mixing and circulation was achieved by using a submersible pump installed at the bottom of the test section. Mixing and circulation was carried out until an average uniform EC reading was obtained to signal complete dilution. A flow through cell (Figure 0-1) was used to aid the mixing and circulation process.
- Injecting the tracer into the test section and continuously measuring the tracer concentration in the test section until at least 90 % of the injected concentration has been depleted. In this point dilution test, a TLC meter (Figure 6-20, Section 6.5.3.1.3) was used to measure the EC at 23 mbgl in PW5 during the 4 hour test.



Figure 11-1 Flow through cell used for tracer injection at the study area (Taken during the field Photos).

The flow through cell proved to be more effective in circulating and mixing the tracer with water at minimum spillage. However the need for maintaining a balance between the inflow and out flow of the flow through cell remains high. Overflow can still occur in some instances, due to turbulence and pressure build - ups within the flow through cell.

Appendix 5 Radial Convergence Tracer Test Procedure

The following procedure according to Riemann (2002) was used as guidelines conduct the radial convergent test:

- The injection borehole set up remains the same as in the point dilution test (Figure 6-12, Section 6.5.2). Still using the 2 m test section located at 23 mbgl, measuring and mixing 200 g of iodated salt (NaCl), 50 g of NaBr and 0.5 g of fluorescein with the water.
- Riemann (2002), further highlight the need for a point dilution test to continue until dilution in the source borehole is complete and the background concentration of the tracer is reached. Minimum time recommended for measurements is 1 hour.
- The withdrawal part of an injection - withdrawal tracer test should start only after a minimum of 50 % of the dilution has been achieved. It is encouraged to wait with the pump back until the dilution is complete.
- The duration of the withdrawal part should last at least until the tracer is abstracted (i.e. breakthrough curve is observed) and the background concentration is reached.
- The injection of the tracer for a radial convergent test should start only, when a steady state flow field is established. Steady state flow is indicated either by a constant hydraulic gradient between the injection and abstraction borehole or by a constant drawdown in both the abstraction and observation boreholes.
- The duration of the radial convergent test depends on the occurrence of the breakthrough curve and should last at least until the background concentration of the tracer is reached.

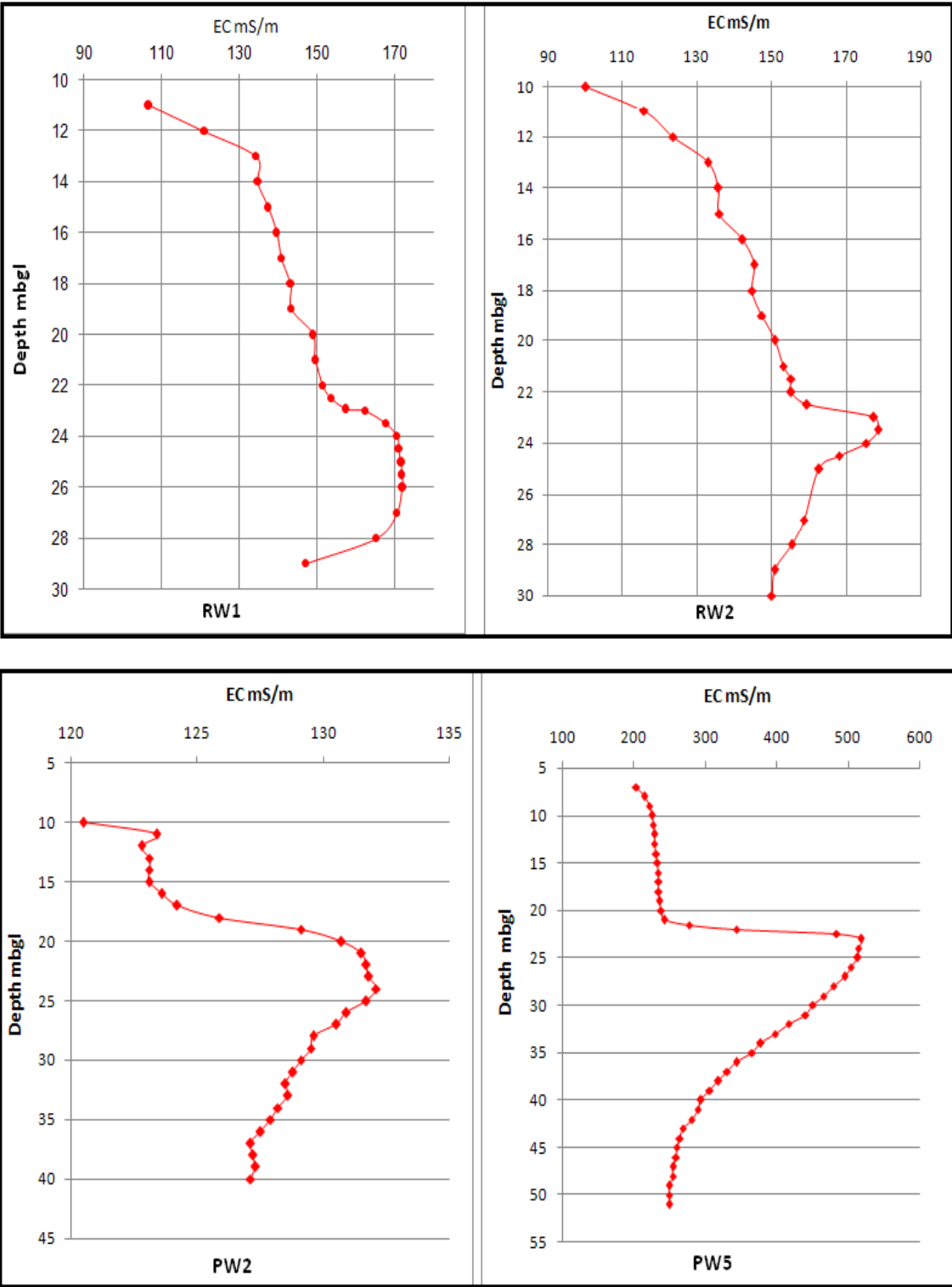
The abstraction borehole RW2 was pumped at an average abstraction rate of at 0.78 l/s for about 1 hour, while monitoring the drawdown in RW2, PW2 and PW5. However there was no observed drawdown in the observation boreholes (PW2 and PW5). Considering the time constrain associated with the private working environment, it was decided to inject the tracer before achieving the steady state flow. The EC decay in PW5 injection well was monitored and treated as point dilution test under forced gradient. Electrical conductivity measurements were taken at PW2 (observation borehole) and RW2 (abstraction borehole) to monitor the tracer

breakthrough. Due to the time constrain, it was not possible to monitor the breakthrough during the night, hence the test had was stopped after 5 hours. After stopping the test, pumping was carried for about 30 minutes to clear out the injected tracer in the injection borehole (PW5). Figure 0-2 below shows the tracer which had to be pumped out after the tests.



Figure 11-2 Pumping out injected tracer after the tracer tests (Taken during the field work).

Appendix 6 EC profiles for RW1, RW2, PW2 and PW5 Boreholes



Appendix 7 Recharge Estimation

The recharge was estimated using the Chloride Mass Balance method:

$$Recharge = \frac{Cl_p}{Cl_{gw}}$$

Equation 5

Where: Cl_p = Chloride concentration (mg/l) in the precipitation
(assumed to be 1 mg/l).

Cl_{gw} = Chloride concentration (mg/l) in the concentration (measured in
the boreholes).

Borehole name	Cl mg/l	Recharge (%)	Borehole name	Cl mg/l	Recharge (%)
MW2	168.00	0.6	PW25	41.86	2.4
PW1	25.80	3.9	PW26	37.53	2.7
PW13	92.30	1.1	PW27	105.00	1.0
PW15	77.80	1.3	PW28	91.00	1.1
PW16	80.80	1.2	PW29	100.00	1.0
PW17	79.60	1.3	PW30	96.00	1.0
PW18	64.20	1.6	PW32	67.00	1.5
PW2	86.50	1.2	PW33	60.00	1.7
PW3	75.10	1.3	PW34	63.00	1.6
PW4	108.00	0.9	PW35	62.00	1.6
PW5	164.00	0.6	PW41	86.00	1.2
PW6	118.00	0.8	PW43	42.06	2.4
PW8	69.90	1.4	PW44	66.00	1.5
PW9	93.00	1.1	PW45	78.00	1.3
RW1	110.00	0.9	PW46	47.68	2.1
RW2	113.00	0.9	PW47	31.22	3.2
PW24	36.36	2.8	PW48	27.85	3.6
Geometric mean					1.4

Abstract

Site characterisation aims to obtain fundamental data needed to describe the subsurface flow pathways and distribution of contaminants. The study describes the application of various geohydrological techniques as complimentary tools to characterise an LNAPL contaminated fractured - rock aquifer on the Beaufort West study area in South Africa. Field investigations were designed to define and determine the properties of the fracture preferential flow paths responsible for LNAPL transportation in a typical Karoo fractured - rock aquifer system. The research places emphasis on the integration of results to maximise the subsurface geological understanding in particular location of fracture features chiefly responsible for facilitating LNAPL migration and distribution.

The core and percussion drilling explorations, cross - correlated with borehole geophysics, were valuable for geological subsurface investigations in particular locations of bedding fractures, which are often associated with high hydraulic conductive flow zones. Tracer and pump tests were conducted to determine hydraulic and mass transport parameters respectively. Hydraulically conductive bedding plane fracture flow zones were identified by integrating results from the geological core logs, borehole geophysics and aquifer tests. The chemical characterisation of the study area was conducted by means of organic hydrocarbon, inorganic water analyses and volatile organic carbon measurements in the soil during air percussion drilling.

Based on the findings, the hydrogeological structure of the formation was conceptualised as a fractured sandstone aquifer, characterised by bedding plane fracture preferential flow paths at contact areas, with shale and mudstone formations. The study findings demonstrate the merit and value in the application of various geohydrological tools to complement one another for optimised site understanding. The findings and recommendations of the case study are not necessarily confined to LNAPL contaminated fractured - rock aquifers, but may also be applicable to other types of contaminants in fractured - rock aquifer formations.

Opsomming

Die doel van terrein karakterisering is om fundamentele data te verkry wat nodig word om die ondergrondse vloei rigtings en verspreiding van kontaminasie te beskryf. Die studie beskryf die toepassing van verskeie geohidrologiese tegnieke as komplimenterende middele vir die karakterisering van 'n LNWW (ligte nie-wateroplosbare vloeistowwe) besoedelde fraktuur-klip akwifer in die Beaufort-Wes studie area in Suid-Afrika. Veldondersoek is ontwerp om die eienskappe van fraktuur voorkeur vloei rigtings te definieer en bepaal. Hierdie vloei rigtings is verantwoordelik vir LNWW vervoer in 'n tipiese Karoo fraktuur-klip akwifer stelsel. Die ondersoek plaas klem op die integrasie van resultate om die begrip van ondergrondse geologie te maksimeer, veral in terme van die ligging van frakture wat verantwoordelik is vir LNWW migrasie en verspreiding.

Die kern- en slagboorgat ondersoek gebruik 'n kruis-vergelyking met boorgat geofisika. Dit was waardevol in terme van ondergrondse geologiese ondersoek, spesifiek met betrekking tot die ligging van stratifikasie frakture, wat dikwels geassosieer word met hoë hidroliese en massavervoer parameters. Hidroliese geleidende stratifikasie vlak fraktuur vloei sones is geïdentifiseer deur die integrasie van resultate vanaf die kern-aantekeninge, geofisiese en akwifer toetse. Die chemiese karakterisering van die studieterrrein is voltooi deur middel van organiese hidro-koolstof, anorganiese water analiese en deur die meting van vlugtige organiese koolstof in die grond gedurende lug slagboorwerk.

Die bevindinge dui aan dat die hidrogeologiese struktuur van die formasie as 'n fraktuur sandsteen akwifer gekonseptualiseer is. Dit word gekenmerk deur stratifikasie vlak fraktuur voorkeur vloei roetes in kontakareas, met leiklip en modderlip formasies. Hiermee word die meriete en waarde van die bevindinge gedemonstreer in terme van die toepassing van verskeie geohidrologiese middels vir optimale terrein bepaling. Die bevindinge en aanbevelings van die studie is nie noodwendig beperk tot LNWW besoedelde fraktuur-klip akwifere nie; dit kan ook toepaslik gemaak word op ander tipes kontaminasie in fraktuur-klip akwifer formasies.